Studies on Catalysis by Ordered Mesoporous SBA-15 Materials Modified with Transition Metals

Thesis Submitted to the
Cochin University of Science and Technology
in partial fulfillment of the requirements
for the award of the degree of
Doctor of Philosophy
in Chemistry
Under the Faculty of Science

By

Ambili V. K.

Department of Applied Chemistry
Cochin University of Science and Technology
Cochin-682 022, Kerala, India.

April 2011

Department of Applied Chemistry
Cochin University of Science and Technology
Cochin – 682 022, Kerala, India.

Dr. S. Sugunan
Professor

Date :.....

Certificate

This is to certify that the research work presented in the thesis entitled **"Studies on Catalysis by Ordered Mesoporous SBA-15 Materials Modified with Transition Metals"** is an authentic record of research work carried out by Ms. Ambili V. K. under my supervision at the Department of Chemistry, Cochin University of Science and Technology, in partial fulfillment of the requirements for the degree of Doctor of Philosophy in Chemistry and that no part thereof has been included for the award of any other degree.

Dr. S. Sugunan
(Supervising Guide)

Declaration

I hereby declare that the thesis entitled **"Studies on Catalysis by Ordered Mesoporous SBA-15 Materials Modified with Transition Metals"** is the bonafide report of the original work carried out by me under the supervision of Dr. S. Sugunan at the Department of Applied Chemistry, Cochin University of Science and Technology, and no part thereof has been included in any other thesis submitted previously for the award of any degree.

30-04-2011 **Ambili V. K.**

Cochin-22

To My Family…

Acknowledgement

I wish to express my sincere gratitude to the people who helped and encouraged me for the successful completion of the work. Before that let me thank God almighty, for the blessings showered upon me in my life.

I am extremely happy to express my deep sense of gratitude to my supervising guide Dr. S. Sugunan, Professor, Department of Applied Chemistry, CUSAT for his proper guidance, suggestions and motivations throughout my research work.

I would like to thank Prof. K. Sreekumar and Prof. K. Girishkumar, present and former heads of the department for their timely help and support. I express my gratitude to all teaching and non teaching staffs of the department for their help and wishes.

I am very happy to extend my acknowledgement to my lovable labmates Ajithamiss, Joyesmiss, Reshmi, Bolie, Rajesh, Dhanya, Reni, Cimi, Sandhya, Rosemiss, Soumini, Mothi and Nissam for their help and support. I express my sincere thanks to my friends Satheesh, Jofrin and Temi for their support. I am very much thankful to all seniors of physical lab for the suggestions and advices provided. I extend my thanks to friends of other labs and other departments of cusat.

My sincere thanks to my roommates and all other inmates of Athulya hostel for their love and care during my hostel stay. I extend my gratitude to the Matron and mess workers of Athulya hostel.

My special thanks to staff of SAIF, STIC, CUSAT, IIT Madras, NCL Pune for their help during various analysis.

This acknowledgement would be incomplete without mentioning my family members who loved me a lot.

The financial support granted by CSIR- New Delhi is herewith acknowledged with great pleasure.

Ambili V K

PREFACE

Nanosciences will be one of the fields that will contribute to a high level of scientific and technological development along the 21st century. Nanostructured inorganic, organic or hybrid organic inorganic nanocomposites present paramount advantages to facilitate integration and miniaturization of the devices thus affording a direct connection between the inorganic, organic, and biological worlds. The ability to assemble and organize inorganic, organic, and biological components in a single material represents an exciting direction for developing novel multifunctional materials presenting a wide range of novel properties. The growth of soft chemistry derived inorganic or hybrid networks templated by organized surfactant assemblies (structure directing agents) allowed construction of a new family of nanostructured materials in the mesoscopic scale (2-100 nm), the best example is the ever-growing family of mesoporous inorganic materials.

Regardless of the great amount of work dedicated to zeolites and related crystalline molecular sieves, the dimensions and accessibility of pores were restrained to the sub-nanometer scale. This limited the application of these micro pore systems to small molecules. During the past decade, an important effort has been focused on obtaining molecular sieves showing larger pore size and a permanent effort is made to develop textured inorganic or hybrid phases. Because these materials are potential candidates for a variety of applications, in the fields of catalysis, optics, photonics, sensors, separation, drug delivery, etc. The design and development of heterogeneous catalysts having high surface area is one of the major objectives in the current research area.

After the discovery of mesoporous silicates in early 1990's various kinds of mesoporous materials with different pore geometries, compositions, and attached functionalities have been developed. Their excellent textural characteristics such as large surface area, pore volume, and uniform pore size

distribution allow the easy diffusion of reactants in mesoporous materials. This characteristic makes them highly advantageous for catalytic applications. However, the presence of the neutral framework and the lack of any acidic or redox properties in the mesoporous silica materials limit their use as catalysts for many catalytic reactions involving bulky molecules. The mesoporous silica materials with interesting chemical, acidic and redox properties can be generated by the isomorphous substitution of silicon with transition metals, which can replace zeolites and zeotypes as catalysts for several catalytic reactions concerning bulky molecules. In order to introduce catalytically active and redox sites in the mesoporous silica materials, a direct synthesis was adopted in the present work to incorporate heteroatoms such as W, Ti, Zr,V, Mo, Cr, and Co into the framework of the SBA-15 silica. Mesoporous SBA-15 materials with hetero atoms on the frame work of silica walls, can offer high density of active sites at the channel surface and enhance the catalytic activity. From the activity studies done using the prepared catalysts it was found that the catalysts are highly effective for various industrially important reactions such as oxidations, acetalization, alkylations etc.

CONTENTS

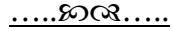

PAPERS PRESENTED IN INTERNATIONAL/NATIONAL CONFERENCES

- *Oxidation of alkenes over transition metal supported SBA15 materials* - AMBILI V. K. AND S. SUGUNAN* (20th National Symposium on Catalysis: Catalysis for Sustainable Energy and Chemicals- IIT Madras).
- *Surface properties and catalytic activity of pure and modified mesoporous SBA15 materials* - AMBILI V. K. AND S. SUGUNAN* (International Congress on Analytical Science 2010 ISAS and CUSAT).
- *Heterogeneous Catalysts Obtained by Incorporation of Tungsten into SBA15 Used in Oxidation Reactions* - AMBILI V. K. AND S. SUGUNAN* (5th Mid-Year Chemical Research Society of India – Symposium in Chemistry – NIIST and IISER Thiruvananthapuram).
- *Ti and V containing mesoporous SBA15 materials as catalysts for oxidation of cyclohexene with H_2O_2 as oxidant*- AMBILI V.K. AND S. SUGUNAN* (22nd Kerala Science Congress-KFRI Peechi).
- *Synthesis, Characterization and Catalytic Activity of Transition metal Incorporated SBA 15 Nanostructured Catalytic Materials*-V.K.AMBILI AND S.SUGUNAN* (International Conference on Material for The New Millennium-Dept of Applied Chemistry, CUSAT).
- *Tungsten Incorporated Mesoporous SBA 15 Materials-Preparation, Characterization and Catalytic Activity*- AMBILI V.K. AND S. SUGUNAN* (National Conference on Advances in Physical and Theoretical Chemistry- Dept of Chemistry, University of Calicut).
- *Tungsten containing mesoporous SBA15 materials as catalysts for oxidation of cyclohexene with H_2O_2 as oxidant*-AMBILI V.K. AND S. SUGUNAN* (19th National Symposium on Catalysis: Catalysis for Sustainable Energy and Chemicals- National Chemical Laboratory, Pune).

WORKSHOP ATTENDED

- *Orientation Programme in Catalysis Research* held at National Centre for Catalysis Research, IIT Madras, 17th November to 8th December 2008.

PAPERS PUBLISHED

- N.N. Binitha, Z. Yaakob, M.R. Reshmi, S. Sugunan, V.K. Ambili, A.A. Zetty,, *Catalysis Today 147S (2009) S76–S80.*

…..ꕥ…..

Chapter 1

Mesoporous SBA–15: Introduction and Literature Survey

Contents

Recently explored periodic mesoporous silica (PMS) samples have a very promising range of future applications. The development of PMS materials such as mesostructured MCM-41, HMS, and SBA-15 molecular sieves, has opened up a vast field of research with respect to both their structural properties and their many technological applications as molecular sieves, catalysts, and sensors and in nanoelectronics. In the field of catalysis, these silica materials offer new opportunities for creating highly disperse and more-accessible catalytic sites in which metal ions are grafted into the silica framework. The mesoporous materials have attracted considerable attention due to their high surface area, uniform pore size distribution, large pore size, and potential application in the fields of catalysis and separation. Many kinds of mesoporous materials, such as MCM family, SBA family, HMS etc have been synthesized by using different templating agents. Among the mesoporous silica materials, SBA-15 has one of the large pore size and high surface area siliceous mesostructured materials. Because of its easy synthesis, adjustable pore size, thick pore wall, and remarkable hydrothermal stability, the hexagonally ordered SBA-15 is currently the most prominent member of the family of triblock copolymer-templated materials. Many applications of SBA-15 materials in the fields of catalysis, sorption, and advanced material design can be envisioned. However, the pure silica mesoporous molecular sieves are poor in catalytic activity, so a number of transition metal incorporated mesoporous materials were synthesized and applied to various catalytic reactions.

1.1 Mesoporous Materials

In chemical catalysis, environmentally benign technologies are always been sought due to the strict environmental regulations. Many industrially important acid catalyzed processes were carried out usually using conventional liquid acids such as HF, H_2SO_4, $AlCl_3$, and BF_3. Such reactions have unavoidable drawbacks due to the corrosive nature and environmental problems. Solid acid seems to be a suitable substitute to the present liquid acid based technologies and significant efforts have been made to develop solid acid catalysts for various applications [1]. Catalytic transformation of hydrocarbons generally provides routes for the formation of wide range of important functionalized molecules such as alcohols, ketones, epoxides, carboxylic acids etc. [2]. Homogeneous catalysis systems of lower oxidation state transition metals have been successfully applied in many industrial processes in acetic acid media [3]. Promoters or additives were needed to improve the activities of such catalysts. For the oxidation of p-xylene to terephthalic acid using Co/Mn catalyst system bromide is employed as a promoter [4]. Co(II) and Mn(II) salts combined with a radical promoter were found to be effective catalysts for oxidation of various hydrocarbons in acetic acid media [5–7]. It was investigated that the addition of promoters or additives is very efficient for oxidation of hydrocarbons but it may cause more cost. Moreover, these homogeneous systems have several disadvantages in separation of products and the disposal of toxic solids and liquid wastes [3]. One way to resolve the problems related with homogeneous catalysis is to heterogenize the active catalytic moieties on porous supports.

In recent years porous materials attract the attention of researchers and material scientists due to commercial interest in their applications in various fields especially in heterogeneous catalysis [8-12]. During the past decade substantial progress has been made in the field of porous materials and several

mesoporous materials have been introduced successfully [13, 14]. There were a huge range of structurally different porous materials reported in various literatures including patents. The design and functionalization of porous materials suitable for specific application is still a challenge for the chemist [15]. After the discovery of zeolitic materials as catalysts, several reactions of organic substrates using dilute solution of hydrogen peroxide were studied in mild reaction conditions [16, 17]. But these zeolitic catalysts have some limitations in the case of bulky reactant molecules, whose kinetic diameters are higher than 0.55 nm, since they are not accessible to the internal pore system of these materials [18].

To overcome the limitations of microporous zeolite type materials, studies have been conducted in the field of mesoporous molecular sieves, beginning with the M41S family [19]. The pore diameters of these newly developed solids have been tuned in the mesoporous range (2-50 nm), which make them suitable for processes involving diffusion of bulky molecules to internal active sites. Then the mesostructured materials like MCM-41 under the M41S family and exhibiting a large variety of structures and pore sizes [20– 23] have been developed. The Stucky group introduced the Santa Barbara Amorphous (SBA) materials in 1998 and SBA-15 is the well-known candidate in that family. The synthesis of SBA-15 materials by Zhao et al. in 1998 becomes one of the most promising developments in the research field of this century. They synthesized SBA-15 material using nonionic triblock-copolymer as structure-directing agent in acidic medium [24, 25]. Compared with MCM-41, the first reported member of mesoporous family, the SBA-15 mesoporous silica shows enhanced hydrothermal stability with thicker silica walls [26, 27] and possesses larger pores. The amorphous silica walls associated with the mesoporous molecular sieves generally limits their application in catalysis [28, 29].

Since pure silica SBA-15 showed very limited catalytic activities due to the lack of lattice defect, redox properties, basicity and acidity considerable interest has been made to introduce guests into the framework of SBA-15 to increase the active sites and thus improve the catalytic activity [30, 31]. It was proved that a proper selection of preparation procedure is essential to obtain a homogeneous metal dispersion on the carrier. This generates effective catalysts for various applications in the field of catalysis [32]. The interesting features such as high pore volumes, large surface areas and a high volume fraction of active metal sites render modified mesoporous SBA-15 materials as very interesting heterogeneous catalysts for driving reactions at mild conditions.

1.2 Mesoporous SBA-15

Periodic mesoporous silicates, which possess uniform channels with large pore size (1.5-40 nm), high surface area (up to 2000 m^2/g), and tunable structure, have received much attention in recent years [19, 24]. The ordered mesoporous materials have been widely used as supports in various catalytic applications, including acidic/basic catalysis, hydrogenation, desulfurization, oxidation, asymmetric synthesis, or enzyme catalysis [29, 30, 33-37]. The surface of the mesoporous silicates can be modified by the incorporation of different groups, [38-40] through which it can greatly adjust surface functionality and change textural properties. The surface hydrophobic/ hydrophilic properties of the solid catalysts may influence the catalytic activity of the mesoporous catalysts [41].

A remarkable contribution in the synthesis of ordered mesoporous materials was made by Zhao et al. [24, 25] in 1998, which used triblock copolymer surfactants to template the formation of ordered large-pore mesoporous silica with different structures under strongly acidic conditions. They synthesized mesoporous SBA-15 material with interesting features like

large specific surface area, high porosity, controllable and narrowly distributed pore sizes, good mechanical and thermal stability etc [42].

A large number of studies have been dedicated to SBA-15 mesoporous silica after its discovery [24]. Its characteristics features make this material very attractive for many applications, such as catalysis [43-45], biosensing [46, 47], and controlled drug release [48, 49]. The majority of the surface groups of dry SBA-15 are isolated silanols, and a smaller part consists of geminal and hydrogen-bonded silanols [50].

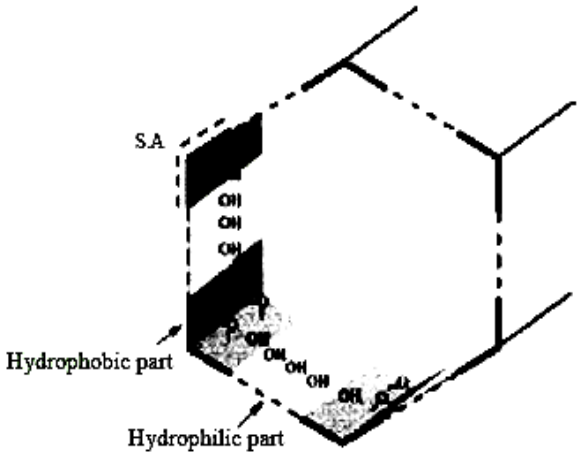

The following features contributed to the strong popularity of SBA-15 silica: (i) it can be easily and reproducibly prepared within a wide range of temperatures (35–130^{0}C) using tetra ethylene ortho silicate or sodium silicate; (ii) it is a hexagonally ordered silica material with tailorable uniform mesopores [51, 52] and micropores in the mesopore walls; (iii) it has thick pore walls (2–6 nm), leading to improved thermal and hydrothermal stability; and (iv) it may exhibit a large variety of morphologies depending on the synthesis conditions [51, 53]. The frameworks of mesoporous silica materials are neutral and, the applicability is limited. Modification of the surfaces of

these materials, or introduction of nanoparticles in the cavities of mesoporous silicates are ways to stabilize highly dispersed metals and oxides in uniform porous matrices. Such incorporated nanomaterials are of interest in the nanotechnology field, gas absorption, separation, and catalysis since they combine unique physicochemical characteristics of nanoparticles with the well ordered structure found in mesoporous molecular sieves [52, 54, 55]. The introduction of precursors in to the mesoporous SBA-15 is facilitated by the large amount of Si–OH inside the mesopores. The high surface area allows high dispersion of the precursors in to the silica framework.

SBA-15 is a promising support material for synthesis of novel catalytic materials due to its uniform hexagonally arrayed channels with a narrow pore size distribution. The thicker amorphous silica walls of SBA-15 provide higher hydrothermal stability than those of the thinner-walled MCM-41 materials. Its tunable large pore openings (5–30 nm) have the advantage over the microporous zeolite counterparts in reactions involving bulky molecules [56].

Mesoporous materials [24, 57, 58] present an interesting substitute for preparing nanoparticles in-situ. It is possible to control the size and the shape of the particles, and to optimize the volume fraction of nanoparticles and preserving good mechanical resistance. These materials are of fundamental interests, since they enable us to study certain metals under confinement and facilitate the synthesis of arrays with high density nanoparticles [59]. The high hydroxyl content of mesoporous silicates makes it suitable support for the attachment of transition-metal species [60].

1.3 Mechanism of formation of SBA-15

There are three main synthetic approaches proposed to explain the formation of mesoporous materials. All these models are proposed on the basis of surfactants or templates in solution guiding the structure. Surfactants

contain hydrophilic head groups and hydrophobic tail within the same molecule and will self organize so as to minimize the contact with incompatible ends. Among the various synthetic routes, the main difference is the way in which the surfactants interact with inorganic species. In all proposed mechanisms condensation followed by polymerization of silica leads to the mesostructure. In liquid crystal templating route (A) the molecular or supramolecular templates are present in the synthesis media from the beginning and the self assembly process of the templates results the formation of liquid crystal mesophase , which is followed by the formation of mineral network deposited around the self assembled substrate. In many cases a "cooperative self-assembly" can take place in situ between the templates and the mineral network precursors yielding the organized architectures (route B). A third approach was also proposed in which a nanometric inorganic component (nanometric building block) is present and can be subsequently assembled and linked by the organic connectors.

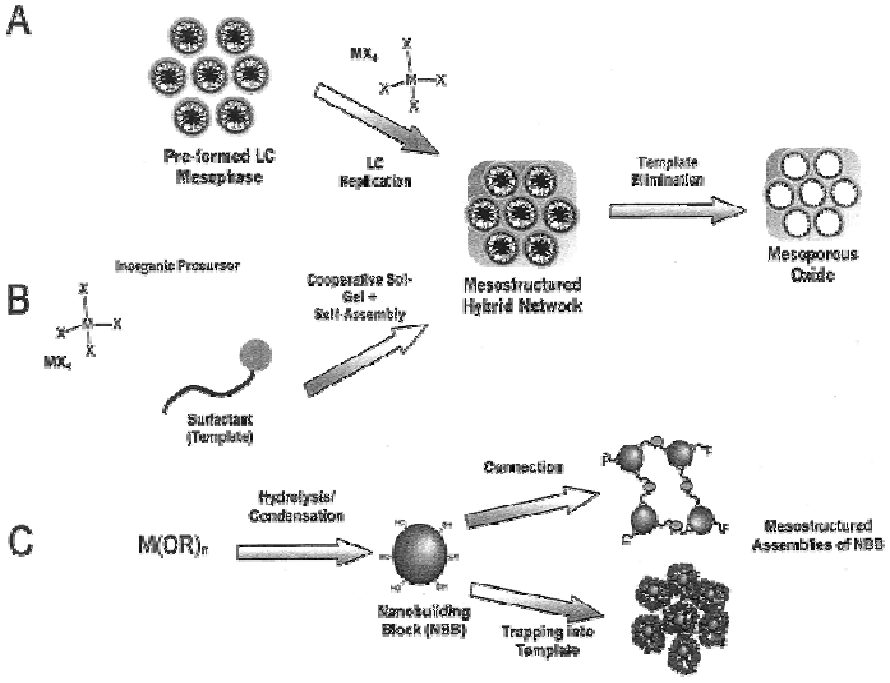

Main synthetic approaches for mesostructured materials.

Among the different approaches for the formation of mesostructure the most popular mechanism adopted for the formation of SBA-15 is the cooperative self assembly route. Here the mesoporous material formation was explained in terms of self assembled surfactants in a solution to guide the formation of material from the inorganic precursor through condensation reactions. There is a cooperative sol gel self assembly can take place insitu between the inorganic precursor and surfactant and thus results the formation of a mesostructured hybrid network.

Both surfactant and inorganic soluble species direct the synthesis of mesostructured materials. The hybrid solids thus formed are strongly dependent on the interaction between surfactants and the inorganic precursors. In the case of ionic surfactants, the formation of the mesostructured material is mainly governed by electrostatic interactions. In the simplest case, the charges of the surfactant (S) and the mineral species (I) are opposite, in the synthesis conditions (pH). Two direct synthesis routes have been proposed and represented as S^+I^- and S^-I^+. (96, 97) Two indirect synthesis paths also lead to hybrid mesophases from the self-assembly of inorganic and surfactant species bearing the same charge. In this case counterions get involved as charge compensating species. In acidic conditions The $S^+X^-I^+$ path takes place in the presence of halogenide anions (X^- = Cl^-, Br^-) and the $S^-M^+I^-$ route is characteristic of basic media is also identified in the presence of alkaline cations (M^+ = Na^+, K^+). The different possible hybrid inorganic organic interfaces are schematized in Figure 10. Some other synthesis routes called neutral path were proposed on nonionic surfactants, where the main interactions between the template and the inorganic species are H-bonding or dipolar and are denoted as [S^0I^0 and $S^0(IX)^0$].

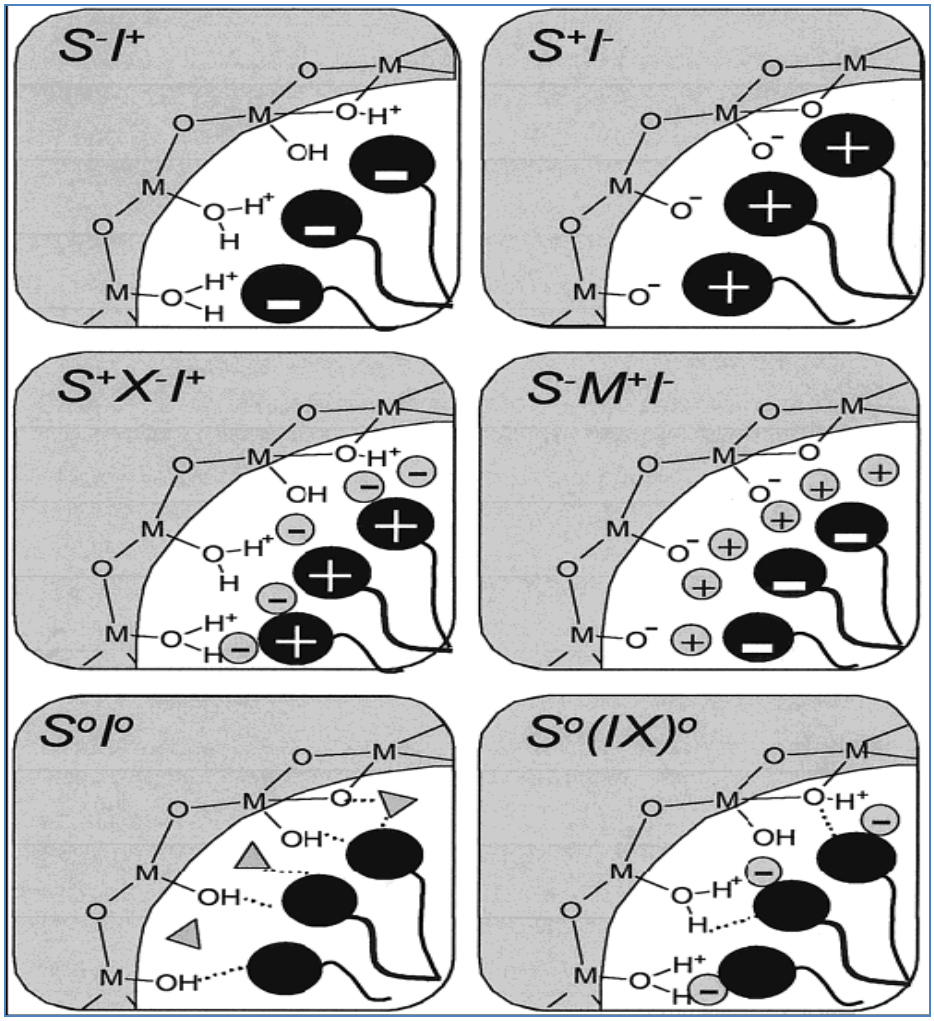

Schematic representation of the different types of precursor-surfactant interfaces.

The neutral templating mechanism ($S^0H^+X^-I^+$) based on hydrogen bonding interactrions has been proposed to synthesize mesoporous SBA-15 materials, in which the randomly ordered rod like micelles (formed from the self organized surfactants) interact with the silica species to yield tubular silica deposited around the external surface of the micelle rods. The spontaneous ordering of these composite species resulted in the formation of hexagonal structure.

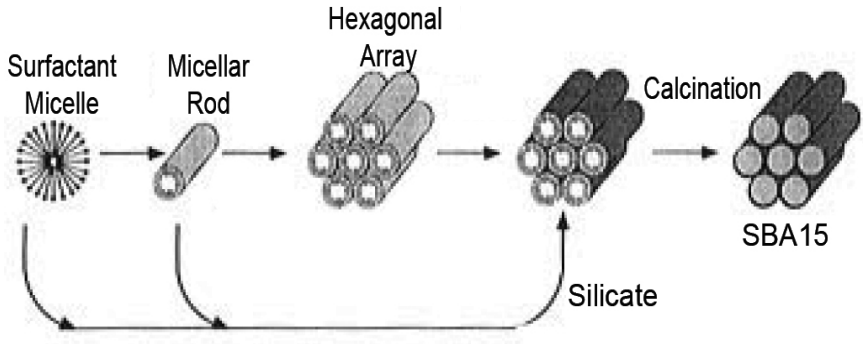

- EO moieties of the surfactant in strong acid media associated with hydronium ions.

  $REO_m + yHX \rightarrow REO_{m-y}[(EO).H_3O^+]y.....YX^-$

- Alkoxy silane species are hydrolyzed.

  $Si(OEt)_4 + nH_3O^+ \rightarrow Si(OEt)_{4-n}(OH_2^+)_n + nEtOH$

Organic inorganic self-assembly is driven by weak non covalent bonds such as H- bonds, Vander Waals forces and electrovalent bonds between the surfactants and inorganic species.

$REO_{m-y}[(EO).H_3O^+]y\ldots YX^-...I^+ \equiv S^0H^+X^-I^+$

1.4 Synthesis of SBA-15 and Transition Metal incorporated SBA-15 materials

The synthesis of mesoporous materials were carried out employing cationic surfactant, mixture of cationic and anionic surfactant [61] and neutral surfactant molecules [62, 63] as templates. Among all the synthesis pathways, the one in which neutral surfactant molecules are used as templates, is very attractive, since hydrogen bonding is responsible for the cohesiveness between the surfactant molecule and the inorganic precursor. Due to the relatively weak interaction between the entities the extraction of surfactant molecule can easily be achieved by simple methods like solvent extraction using ethanol or calcinations under mild conditions [64]. Using a triblock copolymer as template, Zhao et al. [24] generated firstly the mesoporous SBA-15, which possess more

regular structures and thicker channel walls than those of MCM-41. The pore size can be controlled and the pores are well-defined in SBA-15 materials and the materials are thermally stable and possess high surface areas [65].

Formation of highly dispersed metallic nanoclusters in SBA-15, provide a significant and valuable contribution to the area of mesoporous material synthesis and the resulted catalysts have the advantage of higher stability (thicker pore wall) and the excellent control of the pore size and shape. Recently many efforts have been made to investigate the pore structure of SBA-15 and to utilize SBA-15 as templates to prepare a variety of nanostructured materials [66, 67]. SBA-15 can be used as a versatile catalyst support material or catalytic site via partial substitution of Si^{4+} by other cations, [33, 68]. The introduction of heteroatoms into the walls of mesoporous silica material is of great importance in catalysis field. But it is difficult to prepare SBA-15 containing heteroatoms in the framework by means of a condensation process because metals will exist only in the cationic form rather than their corresponding oxo species under strong acidic synthesis conditions [69].

Traditional strategies for the incorporation of transition metals into SBA-15, such as wetness impregnation or ion exchange method, diffuse metal salts easily to the outer surface of the host silica to form large metal aggregates during the reduction or thermal treatment process [70-72]. The incorporation of various transition metals into the SBA-15 silica framework is still a challenge in the field of mesoporous material synthesis and only a few successful reports were available to demonstrate the modification [72, 73-83]. In the present work highly ordered transition metals incorporated SBA-15 materials are prepared under mild conditions by direct synthesis. It is expected that this quick, convenient, and effective method will be a general technique and very promising for the synthesis of metal nanoparticles confined in the

host architectures. The prepared materials will be both fundamentally and technologically useful for catalytic, optical, electronic, magnetic, and energy-storage applications [84].

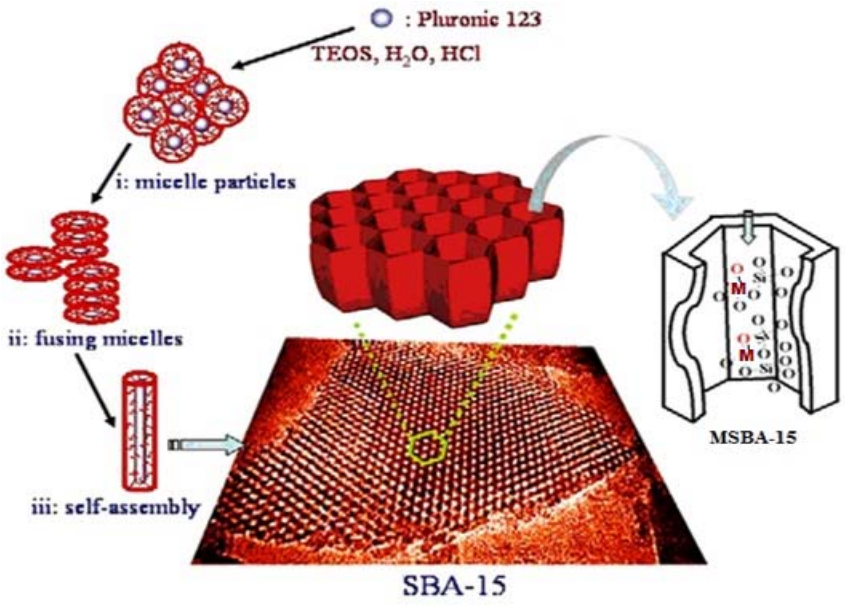

Scheme for the synthesis of periodically ordered mesoporous MSBA-15.

In the present work the insertion of metal cations into the silica framework can be attained by the mixing of the adequate precursors in the initial reacting systems. The synthesized materials maintain the hierarchical structure of the mesopores and improve the lifetime and reusability of the heterogeneous catalysts for various reactions.

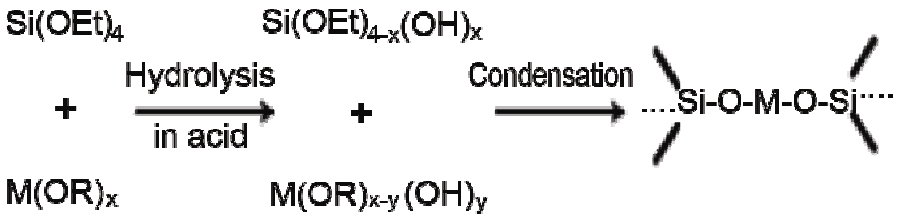

1.5 Transition metal incorporation in to Mesoporous Materials-Literature Review

Recently developed approaches in the preparation of catalysts have widely used homogeneous dispersion of metal species on the surface of porous high-surface area supports, like SBA-15 to achieve increased stability of active species on a support. In present days extensive efforts have been made to the synthesis and characterization of supported transition metal oxide species. Transition-metal-incorporated mesoporous molecular sieves are of current interest as catalysts for the transformation of a variety of organic compounds. The transition metal species incorporated in to SBA-15 have been proposed to be in a tetrahedral coordination environment through various characterization techniques [85].

The synthetic parameters greatly influence the substitution of metal in SBA-15 materials were investigated in several works [75, 86, 87]. The influences of hydrochloric acid concentration, silicon precursor concentration, and hydrothermal treatment temperature and time on the metal incorporation ratio and its chemical environment were systematically studied over a wide range of metal content [18, 86].

Several pathways are known for incorporating metal nanoparticles into mesoporous silica [27-29, 33, 88-93]. The most conventional method was impregnation of mesoporous silica with metal precursor solution. However, these post synthesis methods sometimes lead to the formation of metal oxides in the channels or on the external surface of the catalysts. Sonication-aided impregnation [94, 95] and chemical vapor deposition [96] were also reported for the preparation of metal nanoparticles in mesoporous silica. Somorjai and coworkers [97, 98] developed an effective step method for the synthesis of Pt nanoparticles encapsulated in SBA-15 by hydrothermal growth of mesoporous silica in the presence of pre-prepared polymer-stabilized metal

nanoparticles [99]. In the case of metal incorporated SBA15, only a small fraction of the metal precursor added was retained into the mesoporous structure, which might be due to the easy dissociation of metal–O–Si bonds under strongly acidic conditions. In the present work a direct synthesis method was adopted to prepare transition metal incorporated mesoporous SBA-15 materials.

Incorporation of transition-metal ions into the frameworks of molecular sieves was reported as a conventional method to introduce catalytic sites into zeolites [100] and mesoporous materials [33,101-103]. Yue et al. [104] reported a direct synthesis for the incorporation of aluminum into the frameworks of SBA-15 materials, but extra framework aluminum species were obtained. Xiao et al. [105] have suggested a complex method to synthesize Al and Ti substituted SBA-15 materials. Newalkar et al. [106] have tried to synthesise Ti-containing SBA-15 materials using a microwave-assisted method. However, the preparation of metal-substituted SBA-15 materials directly via the usual hydrothermal method remains still as a challenge due to the difficulties during the incorporation procedure. SBA-15 materials have generally been synthesized under strongly acidic hydrothermal conditions that easily induce the dissociation of the M-O-Si bonds. The large difference in the hydrolysis rate between the titanium and silicon precursors also contribute to the less incorporation of metals in to silica framework [107]. Several attempts have been made to incorporate titanium into the silica framework of mesostructured materials by direct one-pot synthesis [108-119]. Various optimization methods were used to increase loading of isolated Ti^{4+} into the silica framework, such as fluoride addition [74], microwave hydrothermal treatment [106], and pH adjustment of the synthesis solution [120] etc. Various studies have been made to prepare Al, V, and Ti substituted SBA-15 frameworks [121]. There are various reports including the incorporation of heteroatoms in SBA-15 [104, 86].

Recent reports investigated the preparation of several metal containing mesoporous silica such as Ti, Al, Zr, Au, Pt, and Ce [73, 104, 107, 122-126]. Zhang et al. [127] reported W-MCM-41 mesoporous silica in which tungsten was incorporated in the tetrahedrally coordinated positions of the MCM-41 framework. Klepel et al. [128] also studied tungsten-containing ordered MCM-41 by the incorporation of tungsten into the framework of MCM-41 without extra framework oxide species under basic conditions. Hu et al. [129, 130] reported the excellent catalytic performance of tungsten substituted SBA-15 in the metathesis of 1-butene to high-value olefins. Vanadium incorporated mesoporous materials are of significant importance both for the chemical industry and atmospheric purification and are widely applied in oxidative catalytic processes [131]. Kong et al. reported a simple and effective route of directly incorporating large quantities of vanadium into the SBA-15 framework by adjustment of the pH value of the gel mixtures [31].

Synthesis of mesoporous, titanosilicate molecular sieves containing Ti ions in lattice framework positions was reported [132]. Several Co(II) complexes have been reported as efficient oxygenation catalysts for alkane and alkene oxidations [133-136]. Incorporation of heteroatoms such as Al, Ti and Zr into the silica framework was investigated as the simplest way to enhance the surface acidity of ordered mesoporous materials. Acid properties of mesoporous materials containing transition metals have received much interest in view of their potential applications in heterogeneous catalysis. Benedicte Prelot and co-workers studied the influence of the porous structure of Zr-doped SBA-15 based materials on the heteroatom incorporation efficiency [137].

Zhang et al. reported the synthesis of catalytically active tungsten containing MCM-41 with good dispersion, but segregated crystalline WOx

was detected after mild thermal treatments [138]. Briot et al. adopted a method including oxoperoxometalate precursors to avoid crystalline phases but extensive leaching of the tungsten species was observed which results the poor stability of these materials [139]. Recently tungsten oxide species incorporated mesoporous silica materials were prepared by adopting an atomic layer deposition (ALD) method [140].

Landau and co-workers [141] used chemical solution decomposition (CSD) and internal hydrolysis method to synthesize Zr-doped mesoporous solids. Chen et al. [142] reported the preparation of Zr-incorporated mesoporous molecular sieves using zirconyl chloride as source of zirconium. Many elements such as B, Al, Ga, Mn, V, Nb, Cr, Sn, Zr, and Ti could be incorporated into the siliceous frameworks of mesoporous materials to create catalytic active sites [31, 101-103].

The ability to control the heteroatom insertion during the co-condensation stage and its amount remaining in the material after the template removal are the main challenges when preparing ordered mesoporous materials containing hetero atoms.

1.6 Catalysis by Mesoporous Materials-A Literature Review

Ordered mesoporous silicas like SBA-15 [24, 143-145] have received considerable attention in the field of heterogeneous catalysis and nanoscale materials because of their large surface areas and uniform pore structures [146-149]. In recent years, many highly active catalysts have been prepared by means of the introduction of transition metals and noble metals and their oxides into the channels of ordered mesoporous silica as well as by the direct incorporation of transition-metal ions into the framework of ordered mesoporous silica during the synthesis process. Wang et al. [150] found that Pt/TiO_2 (ZrO_2)/SBA-15 composite materials displayed high activity in ethyl

acetate combustion. Raja et al. [151] proposed a highly effective bimetallic catalyst for olefin hydrogenation by the incorporation of Pd-Ru nanoparticles in to MCM-41. Inumaru et al. [152] prepared crystalline TiO_2 -MCM-41and used as a highly active photocatalyst for decomposition of 4-nonylphenol.

There were some reports including titanium-substituted zeolites for selective oxidation reactions using aqueous hydrogen peroxide as the oxidant [107]. SBA-15 related materials were found to be the best candidates for a wide range of applications in catalysis. The gas and liquid phase oxidation of various organic compounds have been studied over niobium containing mesoporous molecular sieves of MCM-41 [153], SBA-3 [154], and SBA-15 [155, 156]. TS-1, titanosilicate molecular sieves have been found to be highly efficient catalysts for the oxidation of various organic substrates (i.e., alkanes, alkenes, alcohols, aromatics) with H_2O_2 as an oxidant under mild conditions [157]. Synthesis of mesoporous, titanosilicate molecular sieves containing Ti ions in lattice framework positions have been attracting much attention for selective oxidation of bulky molecules [132].

Chemical reactions such as the oxidation of sulfur dioxide to sulfur trioxide [158], oxidation of o-xylene to phthalic anhydride [159,160] and selective catalytic reduction of NOx [158, 161] were reported using supported vanadia catalysts. The surface concentration of redox, basic and acidic sites could be correlated to the product selectivity in the gas-phase partial oxidation of methanol to FA [158,160,162-164]. Silica-supported vanadia catalysts exhibit low activity in the oxidation of methanol to FA in comparison to a series of vanadia catalysts supported on titania [160, 163]. Recent studies examined the reactivity of vanadium oxide supported on mesoporous silica MCM-48 towards methanol oxidation and compared with the activity of (amorphous) silica supported vanadia [165].

More active sites could be generated by the dispersion of vanadia in mesoporous molecular sieves M41S. Solsona et al. [166] reported that the use of MCM-41 as support resulted in higher concentration of isolated tetrahedral vanadium species and greater density of active sites compared with amorphous silica. It was reported that the VOx/MCM-41 catalysts showed higher catalytic activity in the ODH of propane and ethane [65]. VOx/SBA-15 materials can be used as catalysts for the ODH of propane [167, 168]. Hess et al. [169] reported the preparation of the nanostructured SBA-15-supported vanadia catalysts and found that these materials exhibited high selectivity to acrylic acid in the partial oxidation of propane.

Supported vanadium catalysts consisting of a surface vanadium oxide phase on a high-surface area oxide support have received great attention for the partial oxidation of hydrocarbons, oxidative dehydrogenation of alkanes to alkenes, selective catalytic reduction of NO*x*, and oxidation of SO_2 [169-175]. Several studies suggested that the accessible catalytic sites for many reactions are isolated tetrahedral vanadium oxide species with terminal V=O group [176–178].The catalytic activity of such compounds largely depends on the dispersion of vanadium [179, 180], the metal–support interaction [174,181] and the nature of the vanadium active sites. First row transition metal incorporated MCM-41 catalysts were widely studied [182-184]. Co-MCM- 41 has been extensively reported as a catalyst for synthesizing single-walled carbon nanotubes (SWNTs) [185,186].

1.7 Reactions Catalyzed by Mesoporous Materials

The application of solid catalysts in both liquid and vapour phase reactions gives rise to the heterogeneous system with several advantages from many points of view. Recently the use of clean oxidants, such as hydrogen peroxide, makes the reactions environmentally-friendly compared to traditional processes, which need an inorganic oxidant in stoichiometric amounts [187].

In the field of research, the recent development of ordered mesoporous silica materials has opened new perspectives. The mesostructured metallosilicate catalysts have attracted great interest in view of their better activities as compared to microporous zeolites such as TS-1 for various organic reactions involving bulky molecules [188, 189]. Several features such as texture/structure parameters, pore diameters, defect holes etc influence the catalytic activity of heterogeneous catalysts. In recent years transition metal incorporated SBA-15 catalysts has gained considerable interest for the selective oxidation of organic compounds, especially of the bulky olefinic compounds.

The chemical properties of the surface play an important role in determining catalyst activity and selectivity of surface bound active sites. To overcome the issue of poor catalytic performance of mesoporous SBA-15 several researchers have studied the surface modification of the catalyst with a variety of reagents [190] and significant improvements in activity have been observed, but little research has addressed the inventions from a mechanistic standpoint to create a structure– reactivity relationship .

The catalytic properties of most of the molecular sieves depend on the presence of active sites in their frameworks. In the case of SBA-15, the incorporation of heteroatoms to the electrically neutral, purely siliceous framework may generate active sites. Thus, the introduction of transition metals in SBA-15 is of great interest in various reactions especially of large molecules which cannot diffuse in the pores of microporous materials [191-196]. Since in the industrial manufacturing of fine chemicals the selective oxidation transformations are widely performed in the presence of organic peroxides and are catalysed by metallosilicate-based heterogeneous catalysts. A good accessibility of reactant to the active sites and rapid departure of the desired products could be possible with anchoring of metal oxide species onto the inner walls of the mesopores.

Porous metallosilicate materials have been found to be highly effective catalysts in various oxidation reactions using hydrogen peroxide under mild conditions. The production of epoxides is of growing interest in the chemical and petrochemical industries because these compounds can serve as organic intermediates in pharmaceutical synthesis or as monomers in the production of various functional polymers.

A great effort has been devoted to the research and development of new catalysts for several industrial chemical reactions. In the present work, the catalytic activities of various transition metal incorporated SBA-15 catalysts were investigated in various reactions such as oxidations, acetalizations, and Friedel-Craft alkylations. The prepared mesoporous solid acid catalysts exhibit superior catalytic performance towards the chemical reactions of various organic substrates under the present study.

1.8 Scope of the work

Mesoporous silica materials with regular pore structure, such as MCM-41 and SBA-15, have recently attracted attention because of their applicability as model mesoporous materials in catalysis. The removal of volatile organic compounds from emissions is of considerable interest due to the harmful effects of these pollutants. Recently, strict regulations on the environmental standards in several countries have initiated concerns on the pollutants control requiring a 40% reduction in VOC emissions by 2010. Most of the VOCs are produced from the petrochemical, pressing, and printing industries. The catalytic oxidation is an alternative to the incineration process for the destruction of VOCs. The activity of the catalyst is an important factor for determining the effectiveness of this technique. The transition metal-modified mesoporous SBA-15 silicas are appropriate catalysts for various organic transformations. Mesoporous molecular sieves such as SBA-15 containing various transition metals were

effective, especially for the reaction of large organic compounds such as cycloalkene, cycloalkanes and branched alkanes due to their large pore sizes. The catalytic potential for this new class of materials, for example, in the preparation of fine chemicals, is now generating a great deal of interest in their synthesis and characterization.

1.9 Objectives of the present work

- To prepare mesoporous silica SBA-15 using amphiphilic surfactant following hydrothermal route having large surface area and pore size.
- To modify the mesoporous silica SBA-15 with transition metals W, Ti, V, Zr, Mo, Cr, and Co.
- To characterize the prepared catalysts via physico-chemical techniques like XRD, Nitrogen adsorption isotherm, Thermal analysis, FTIR spectroscopy, SEM, TEM , NMR and UV-Vis DRS.
- To study the catalytic activity of the systems towards liquid phase oxidation of cycloalkenes.
- To study the catalytic activity of the systems towards liquid phase oxidation of Benzyl alcohol.
- To study the catalytic activity of the systems towards liquid phase acetalization of carbonyl compounds.
- To study the catalytic activity of the systems towards vapour phase isopropylation of benzene and substituted benzenes.
- To study the catalytic activity of the systems towards liquid phase benzylation of isobutyl benzene.

References

[1] Platon, W.J. Thomson, Appl. Catal. A: Gen., 282 (1 and 2) (2005) 93.

[2] K. Suresh, M. M. Sharma, T. Sridhar, Ind. Eng. Chem. Res., 39 (2000) 3958.

[3] Hong Ma, Jie Xu, Chen Chen, Qiaohong Zhang, Jianbo Ning, Hong Miao, Lipeng Zhou, Xiaoqiang Li, Catal. Lett., 113 (2007) 104.

[4] K. Nair, D. P. Sawant, G. V. Shanbhag, S. B. Halligudi, Catal. Commun., 5 (2004) 9.

[5] Y. Ishii, S. Sakaguchi, T. Iwahama, Adv. Synth. Catal., 343 (2001) 393.

[6] R. A. Sheldon, I. W. C. E. Arends, Adv. Synth. Catal., 346 (2004) 1051.

[7] B. Wentzel, M. P. J. Donners, P. L. Alsters, M. C. Feiters, R. J. M. Nolte, Tetrahedron, 56 (2000) 7797.

[8] X. Zhao, B. Xiao, A. J. Fletcher, K. M. Thomas, D. Bradshaw, M. J. Rosseinsky, Science, 306 (2004) 1012.

[9] H. G. Schimmel, G. J. Kearley, M. G. Nijkamp, C. T. Visser, K. P. de Jong, F. M. Mulder, Chem. Eur. J., 9 (2003) 4764.

[10] E. Brunet, H. M. H. Alhendawi, C. Cerro, M. J. de la Mata, O. Juanes, J. C. Rodriguez-Ubis, Angew. Chem., 118 (2006) 7072.

[11] J. S. Seo, D. Whang, H. Lee, S. I. Jun, J. Oh, Y. J. Jeon, K. Kim, Nature, 404 (2000) 982.

[12] P. Feng, X. Bu, G. D. Stucky, Nature, 388 (1997) 735.

[13] L. Schlapbach, A. Züttel, Nature, 414 (2001)353.

[14] J. L. C. Rowsell, O. M. Yaghi, Angew. Chem., 117 (2005) 4748.

[15] Ying Lua, Markus Tonigolda, Björn Bredenköttera, Dirk Volkmera, Julia Hitzbleckb, Gerhard Langsteinb, Z. Anorg. Allg. Chem., 634 (2008) 2411.

[16] Notari, Adv Catal., 41 (1996) 253.

[17] J. E. Gallot, S. Kaliaguine, Can J Chem Eng., 76(1998) 833.

[18] Francois Berube, Freddy Kleitz, Serge Kaliaguine, J Mater Sci., 44 (2009) 6727.

[19] T. Kresge, M. E. Leonowicz, W. J. Roth, J. C. Vartuli, J. S. Beck, Nature, 359 (1992) 710.

[20] Q. S. Huo, D. I. Margolese, U. Ciesla, D. G. Demuth,P. Y. Feng, T. E.Gier, P. Sieger, A. Firouzi, B. F. Chmelka, F. Schuth, G. D. Stucky, Chem Mate., 6 (1994) 1176.

[21] Y. Wan, Y. F. Shi, D. Zhao, Chem. Commun., (2007) 897.

[22] Y. Wan, D. Zhao Chem. Rev., 107 (2007) 2821.

[23] G. J. J. A. Soler-Illi , C. Sanchez, B. Lebeau, J. Patarin, Chem. Rev., 102 (2002) 4093.

[24] Zhao, J. Feng, Q. Huo, N. Melosh, G. H. Fredrickson, B. F. Chmelka, G. D. Stucky, Science, 279 (1998) 548.

[25] D. Zhao, Q. Huo, J. Feng, B. F. Chmelka, G. D. Stucky, J. Am. Chem. Soc., 120 (1998) 6024.

[26] Y. Khodakov, V. L. Zholobenko, R. Bechara, D. Durant, Microporous and Mesoporous Materials, 79 (2005) 29.

[27] T. Linssen, K. Cassiers, P. Cool, E. F. Vansant, Adv. Colloid. Interface. Sci., 103 (2003) 121.

[28] D. T. On, D. Desplantier-Giscard, C. Danumah, S. Kaliaguine, Appl. Catal. A., 253 (2003) 543.

[29] Taguchi, F. Schuth, Microporous and Mesoporous Materials, 77 (2005) 1.

[30] S. Xiao, Top. Catal., 35 (2005) 9.

[31] Fei Gao, Yanhua Zhang, Haiqin Wan, Yan Kong, Xingcai Wu, Lin Dong, Baiqin Li, Yi Chen, Microporous and Mesoporous Materials, 110 (2008) 508.

[32] N. Perkas, Y. Koltypin, O. Palchik, A. Gedaken, S. Chandrasekaran, Appl. Catal. A., 209 (2001) 125.

[33] Corma, Chem. ReV., 97 (1997) 2373

[34] Li, Catal. ReV., 46 (2004) 419.

[35] X. S. Zhao, X. Y. Bao, W. P. Guo, F. Y. Lee, Materials Today, 9 (2006) 32.

[36] Y. J. Wang, F. Caruso, Chem. Mater., 17 (2005) 953.

[37] C. J. Liu, S. J. Li, W. Q. Pang, C. M. Che, Chem. Commun., (1997) 65.

[38] D. J. Macquarrie, Chem. Commun., (1996), 1961.

[39] X. S. Zhao, G. Q. Lu, J. Phys. Chem. B., 102 (1998) 1556.

[40] D. J. Macquarrie, D. B. Jackson, J. E. G. Mdoe, J. H. Clark, New J. Chem., 23 (1999) 539.

[41] Renyuan Zhang, Wei Ding, Bo Tu, and Dongyuan Zhao, Chem. Mater. Commun., (2007).

[42] Xiancai Li, Shaoxiang Huang, Qingrong Xu, Yifeng Yang, Transition Met Chem., 34 (2009) 943.

[43] Sayari, Chem. Mater., 8 (1996) 1840.

[44] Galarneau, D. Desplantier-Giscard, F. DiRenzo, F. Fajula, Catalysis Today, 68 (2001)191.

[45] T. Ressler, A. Walter, Z. D. Huang, W. Bensch, J. Catal., 254 (2008) 170.

[46] Z. Dai, J. Bao, X. Yang, H. Ju, Biosens. Bioelectron., 23 (2008) 1070.

[47] Liu, J. Zhang, W. Hou, J. J. Zhu, Nanotechnology, 19 (2008) 135707.

[48] M. Manzanoa, V. Aina, C. Arean, F. Balas, V. Cauda, M. Colilla, M. R. Delgado, M. Vallet-Regı, Chem. Eng. J., 137 (2008) 30.

[49] R. Mellaerts, R. Mols, J. A. G. Jammaer, C. Aerts, P. Annaert, J. van Humbeeck, G. van den Mooter, P. Augustijns, J. A. Martens, Eur. J. Pharm. Biopharm., 69 (2008) 223.

[50] Juliette van der Meer, Isabelle Bardez-Giboire, Cyrille Mercier, Bertrand Revel, Anne Davidson, Renaud Denoyel, J. Phys. Chem. C., 114 (2010) 3507.

[51] Sayari, Y. Yang, Chem Mater., 17 (2005) 6108.

[52] N. Chino, T. Okubo, Microporous and Mesoporous Materials, 87 (2005) 15.

[53] V. Meynen, P. Cool, E. F. Vansant, P. Kortunov, F. Grinberg, J. Karger, M. Mertens, O. I. Lebedev, G. Van Tendeloo, Microporous and Mesoporous Materials, 99 (2007) 14.

[54] Yuranov, L. Kiwi-Minsker, P. Buffat, A. Renken, Chem Mater., 16 (2004) 760.

[55] W. Zhu, Y. Han, L. An, Microporous and Mesoporous Materials, 80 (2005) 221.

[56] Volkan Degirmenci, Ozlen Ferruh Erdem, Orcun Ergun, Aysen Yilmaz, Dieter Michel, Deniz Uner, Top Catal., (2008).

[57] Lelong, S. Bhattacharyya, S. Kline, T. Cacciaguerra, M. A. Gonzalez, M. L. Saboungi, J. Phys. Chem. C., 112 (2008) 10674.

[58] S.A. Bagshaw, E. Prouzet, T.J. Pinnavaia, Science, 269 (1995) 1242.

[59] Roland Benoit, F. Warmont , V. Meynen , K. De Witte, P. Cool, M. Treguer-Delapierre, M. L. Saboungi, Microporous and Mesoporous Materials, 120 (2009) 2.

[60] Mark Morey, Anne Davidson, Hellmut Eckert, Galen Stucky, Chem. Mater., 8 (1996) 486.

[61] D. Chandra, A. Bhaumik, Ind. Eng. Chem. Res., 45 (2006) 4879.

[62] P.T. Tanev, M. Chibwe, T.J. Pinnavaia, Nature, 368 (1994) 321.

[63] Bhaumik, S. Samanta, N.K. Mal, Microporous and Mesoporous Materials, 68 (2004) 29.

[64] Mahasweta Nandi, Krishanu Sarkar, Asim Bhaumik, Materials Chemistry and Physics, 107 (2008) 499.

[65] Wei Liu, Suk Yin Lai, Hongxing Dai, Shuiju Wang, Haizhen Sun, Chak Tong Au, Catal. Lett., 113 (2007) 147.

[66] Y. Xia, Z. Yang, R. Mokaya, J. Phys. Chem. B., 108 (2004) 19293.

[67] Y. Xia, R. Mokaya, Chem. Mater., 17 (2005) 1553.

[68] Y. J. Ying, C. P. Mehnert, M. S. Wong, Angew. Chem., Int. Ed. 38 (1999) 56.

[69] Zhensong Lou, Ruiheng Wang, Hui Sun, Yuan Chen, Yanhui Yang, Microporous and Mesoporous Materials, 110 (2008) 347.

[70] L. Shi, Z. L. Hua, L. X. Zhang, J. Mater. Chem., 14 (2004) 795.

[71] Yamamoto, Y. Sunagawa, H. Takahashi, A. Muramatsu, Chem. Commun., (2005) 348.

[72] P. Han, X. Wang, X. Qiu, X. Ji, L. J. Gao, Mol. Catal. A: Chem., 272 (2007) 136.

[73] Vinu, V. Murugesan, W. Bohlmann, M. Hartmann, J. Phys. Chem. B., 108 (2004) 11496.

[74] W. H. Zhang, J. Lu, B. Han, M. Li, J. Xiu, P. Ying, C. Li, Chem. Mater., 14 (2002) 3413.

[75] Vinu, P. Srinivasu, M. Miyahara, K. Ariga, J. Phys. Chem. B., 110 (2006) 801.

[76] Y. Li, Z. C. Feng, Y. X. Lian, K. Q. Sun, L. Zhang, G. Q. Jia, Q. H. Yang, C. Li, Microporous and Mesoporous Materials, 84 (2005) 41.

[77] Nozaki, C. G. Lugmair, A. T. Bell, T. D. Tilley, J. Am. Chem. Soc., 124 (2002) 13194.

[78] Vinu, D. P. Sawant, K. Ariga, K.Z. Hossain, S.B. Halligudi, M. Hartmann, M. Nomura, Chem. Mater., 17 (2005) 5339.

[79] E. Berrichi, L. Cherif, O. Orsen, J. Fraissard, J.-P. Tessonnier, E. Vanhaecke, B. Louis, M.J. Ledoux, C.P. Huu, Appl. Catal. A., 298 (2006) 194.

[80] Luan, J.Y. Bae, L. Kevan, Chem. Mater., 12 (2000) 3202.

[81] S. Wu, Y. Han, Y.C. Zou, J.W. Song, L. Zhao, Y. Di, S.Z. Liu, F.S. Xiao, Chem. Mater., 16 (2004) 486.

[82] S. Y. Chen, L. Y. Jang, S. F. Cheng, Chem. Mater., 16 (2004) 4174.

[83] Vinu, M. Hartmann, Chem. Lett., 33 (2004) 588.

[84] Zhou-jun Wang, Yong-bing Xie, Chang-jun Liu, J. Phys. Chem. C., 112 (2008) 19818.

[85] Guoan Du, Sangyun Lim, Mathieu Pinault, ChuanWang, Fang Fang, Lisa Pfefferle, Gary L. Haller, J. Catal., 253 (2008) 74.

[86] F. Berube, F. Kleitz, S. Kaliaguine, J. Phys. Chem. C., 112 (2008) 14403.

[87] Y. Chen, Y. Huang, J. Xiu, X. Han, X. Bao, Appl. Catal. A., 273 (2004)185.

[88] Moller, T. Bein, Chem. Mater., 10 (1998) 2950.

[89] W. C. E. Arends, R. A. Sheldon, Appl. Catal. A., 212 (2001) 175.

[90] G. E. Fryxell, Inorg. Chem. Commun., 9 (2006) 1141.

[91] G. Oye, W. R. Glomm, T. Vralstad, S. Volden, H. Magnusson, M. Stocker, J. Sjoblom, Adv. Colloid. Interface. Sci., 123 (2003) 17.

[92] Ungureanu, D. T. On, E. Dimitriu, S. Kaliaguine, Appl. Catal. A., 254 (2003) 203.

[93] Dube, S. Royer, D. T. On, F. Beland, S. Kaliaguine, Microporous and Mesoporous Materials, 79 (2005) 137.

[94] S. M. Zhu, H. S. Zhou, M. Hibino, I. Honma, J. Mater. Chem., 23 (2003) 1115.

[95] Z. Konya, E. Molnar, G. Tasi, K. Niesz, G. A. Somorjai, I. Kiricsi, Catal. Lett., 113 (2007)19.

[96] S. Suvanto, J. Hukkamaki, T. T. Pakkanen, T. A.Pakkanen, Langmuir, 16 (2000) 4109.

[97] Z. Konya, V. F. Puntes, I. Kiricsi, J. Zhu, P. Alivisatos, G. A. Somorjai, Catal. Lett., 81(2002) 137.

[98] Song, R. M. Rioux, J. D. Hoefelmeyer, R. Komor, K. Niesz, M. Grass, P. Yang, G. A. Somorjai, J. Am. Chem. Soc., 128 (2006) 3027.

[99] Changli Li, Qinghong Zhang, Ye Wang, Huilin Wan, Catal. Lett., 120 (2008) 126.

[100] R. Szostak, Molecular Sieves: Principles of Synthesis and Identification; Van Nostrand Reinhold: New York, (1989) 211-238.

[101] K. Raman, M. T. Anderson, C. Brinker, J. Chem. Mater., 8 (1996) 1682.

[102] Moller, T. Bein, Chem. Mater., 10 (1998) 2950.

[103] Y. J. Ying, C. P. Mehnert, M. S. Wong, Angew. Chem., Int. Ed. Engl., 38 (1999) 56.

[104] Y. Yue, A. Gedeon, J. L. Bonardet, N. Melosh, J. B. DEspinose, J. Fraissard, Chem. Commun., (1999) 1967.

[105] Y. Han, F. S. Xiao, S. Wu, Y. Sun, X. Meng, D. Li, S. Lin, F. Deng, X. Ai, J. Phys. Chem. B., 105 (2001) 7963.

[106] B. Newalkar, J. Olanrewaju, S. Komarneni, Chem. Mater., 13 (2001) 552.

[107] Wen-Hua Zhang, Jiqing Lu, Bo Han, Meijun Li, Jinghai Xiu, Pinliang Ying, Can Li, Chem. Mater., 14 (2002) 3413.

[108] T. Blasco, A. Corma, M. T. Navarro, J. Perez Pariente, J. Catal., 156 (1995) 65.

[109] A. Koyano, T. Tatsumi, Microporous Materials., 10 (1997) 259.

[110] T.Maschmeyer, F. Rey, G. Sankar, J. M. Thomas, Nature, 387 (1995) 159.

[111] A. Koyano, T. Tatsumi, Chem. Commun., (1996) 145.

[112] Corma, Q. Kan, F. Rey, Chem. Commun., (1998) 579.

[113] Morey, A. Davidson, G. Stucky, Microporous Materials., 6 (1996) 99.

[114] S. Morey, S. O. Brien, S. Schwarz, G. D. Stucky, Chem. Mater., 12 (2000) 898.

[115] Zhang, M. Froba, J. Wang, P. T. Tanev, J. Wong, T. J. Pinnavaia , J. Am. Chem. Soc., 118 (1996) 9164.

[116] A.Tuel, Microporous and Mesoporous Materials, 27 (1999) 151.

[117] S. A. Bagshaw, E. Prouzet, T. J. Pinnavaia, Science, 269 (1995) 1242.

[118] S. A. Bagshaw, F. Di Renzo, F. Fajula, Chem. Commun., (1996) 2209.

[119] S. A. Bagshaw, T. Kemmitt, N. B.Milestone, Microporous and Mesoporous Materials, 22 (1998) 419.

[120] S. Wu, Y. Han,Y. C. Zou, J. W. Song, L. Zhao, Y. Di, S. Z. Liu, F. S. Xiao, Chem. Mater., 16 (2004) 486.

[121] Bharat L. Newalkar, Johnson Olanrewaju, and Sridhar Komarneni, J. Phys. Chem. B., 105 (2001) 8356.

[122] S. Wong, H. C. Huang, J. Y. Ying, Chem. Mater., 14 (2002) 1961.

[123] S. Chen, L. Jang, S. Cheng, Chem. Mater., 16 (2004) 4174.

[124] M. Yang, H. S. Sheu, K. J. Chao, Adv. Funct. Mater., 12 (2002)143.

[125] J. Zhu, Z. Konya, V. F. Puntes, I. Kiricsi, C. X. Miao, J. W. Ager, A. P. Alivisatos, G. A. Somorjai, Langmuir, 19 (2003) 4396.

[126] M. N. Timofeeva, S. H. Jhung, Y. K. Hwang, D. K. Kim, V. N. Panchenko, M. S. Melgunov, Yu. A. Chesalov, J. S. Chang, Appl. Catal. A: Gen., 317 (2007) 1

[127] Z. Zhang, J. Suo, X. Zhang, S. Li, Appl. Catal. A: Gen., 179 (1999) 11.

[128] Klepel, W. Bohlmann, E. B. Ivanov, V. Riede, H. Papp, Microporous and Mesoporous Materials, 76 (2004) 105.

[129] J. Hu, Y. Wang, L. Chen, R. Richards, W. Yang, Z. Liu, W. Xu, Microporous and Mesoporous Materials, 93 (2006) 158.

[130] Linhua Hu, Shengfu Ji, Zheng Jiang, Huanling Song, Pingyi Wu, and Qianqian Liu , J. Phys. Chem. C., 111 (42) (2007) 15173.

[131] Tanya Tsoncheva, Ljubomira Ivanova, Rayna Dimitrova, Jessica Rosenholm, Journal of Colloid and Interface Science, 321 (2008) 342.

[132] J. M. Thomas, G. Sankar, Acc. Chem. Res., 34 (2001) 571.

[133] A. Chavez, J. M. Rowland, M. M. Olmstead, P. K. Mascharak, J. Am. Chem. Soc.,120 (1998) 9015.

[134] A. Chavez, J. A. Briones, M. M. Olmstead, P. K. Mascharak, Inorg. Chem., 38 (1999) 1603.

[135] L. Saussine, E. Brazi, A. Robine, H. Mimoun, J. Fischer, R. Weiss, J. Am. Chem. Soc., 107 (1985) 3534.

[136] D. K. Chand, P. K. Bharadwaj, Inorg. Chem., 36 (1997) 5658.

[137] Karol Szczodrowski, Benedicte Prelot, Sebastien Lantenois, Jerzy Zajac, Marc Lindheimer, Deborah Jones, Anne Julbe, Arie van der Lee, Microporous and Mesoporous Materials, 110 (2008) 111.

[138] Z. Zhang, J. Suo, X. Zhang, S. Li, Appl. Catal. A., 179 (1999) 11.

[139] E. Briot, J.Y. Piquemal, M. Vennat, J. M. Bregeault, G. Chottard, J. M. Manoli, J. Mater. Chem., 10 (2000) 953.

[140] J. E. Herrera, J. H. Kwak, J. Z. Hua, Y. Wang, C. H. F. Peden, J. Macht, E. Iglesia, J. Catal., 239 (2006) 200.

[141] M.V. Landau, L. Vradman, X. Wang, L. Titelman, Microporous and Mesoporous Materials, 78 (2005) 117.

[142] Chen, L.Y. Jang, S. Cheng, Chem. Mater., 16 (2004) 4174.

[143] C. T. Kresge, M. E. Leonowicz, W. J. Roth, J. C. Vartuli, J. S. Beck, Nature, 359 (1992) 710.

[144] J. S. Beck, J. C. Vartuli, W. J. Roth, M. E. Leonowicz, C. T. Kresge, K. T. Schmitt, C. T. W. Chu, D. H. Olson, E. W. Sheppard, S. B. McCullen, J. B. Higgins, J. L. Schlenker, J. Am. Chem. Soc., 114 (1992) 10834.

[145] Zhao, Q. Huo, J. Feng, B. F. Chmelka, G. D. Stucky, J. Am. Chem. Soc.,120 (1998)6024.

[146] Schuth, W. Schmidt, Adv. Eng. Mater., 4 (2002) 269.

[147] P. Wight, M. E. Davis, Chem. Rev., 102 (2002) 3589.

[148] Stein, Adv. Mater., 15 (2003) 763.

[149] D. R. Rolison, Science, 299 (2003) 1698.

[150] Wang, M. V. Landau, H. Rotter, L. Vradman, A. Wolfson, A. Erenburg, J. Catal., 222 (2004) 565.

[151] R. Raja, G. Sankar, S. Hermans, D. S. Shephard, S. Bromley, J. M. Thomas, B. F. G Johnson, Chem. Commun., (1999) 1571.

[152] K. Inumaru, T. Kasahara, M. Yasui, S. Yamanaka, Chem. Commun., (2005) 2131.

[153] Kilos, M. Aouine, I. Nowak, M. Ziolek, J. C. Volta, J. Catal., 224 (2004) 314.

[154] Kilos, A. Tuel, M. Ziolek, J. C. Volta, Catalysis Today, 118 (2006) 416.

[155] B. Kilos, I. Nowak, M. Ziolek, A. Tuel, J. C. Volta, Stud. Surf. Sci. Catal., 158 (2005) 1461.

[156] M. Ziolek, Catalysis Today, 90 (2004) 145.

[157] Weibin Fan a, Peng Wu, Takashi Tatsumi, J. Catal., 256 (2008) 62.

[158] Deo, I.E. Wachs and J. Haber, Crit. Rev. Surf. Chem., 4 (1994) 141.

[159] [C.R. Dias, M.F. Portela and G.C. Bond, J. Catal., 157 (1995) 344.

[160] G.C. Bond and S.F. Tahir, Appl. Catal., 71 (1991) 1.

[161] E.T.V. Vogt, A. Boot, A.J. van Dillen, J.W. Geus, F.J.J.G. Janssen and F.M.G. van der Kerkhof, J. Catal., 114 (1988) 313.

[162] M. Baltes, P. Van der Voort, O. Collart and E.F. Vansant, J. Porous Mater., 5 (1998) 357.

[163] Deo and I.E. Wachs, J. Catal., 146 (1994) 323.

[164] Van der Voort, M. Baltes, M.G. White and B.F. Vansant, Interf. Sci., 5 (1997) 209.

[165] M. Baltes, K. Cassiers, P. Van der Voort, B.M. Weckhuysen, R.A. Schoonheydt and E.F. Vansant, J. Catal., 197 (2001) 160.

[166] B. Solsona, T. Blasco, J.M. Lopez Nieto, M.L. Pena, F. Rey, A. Vidal-Moya, J. Catal., 203 (2001) 443.

[167] Y.M. Liu, Y. Cao, S.R. Yan, W.L. Dai and K.N. Fan, Catal. Lett., 88 (2003) 61.

[168] Y.M. Liu, Y. Cao, N. Yi, W.L. Feng, W.L. Dai, S.R. Yan, H.Y. He and K.N. Fan, J. Catal., 224 (2004) 417.

[169] Hess, M.H. Looi, S.B. Abd Hamid and R. Schlogl, Chem. Commun., 4 (2006) 451.

[170] U.S. Ozkan, T.A. Harris, B.T. Schilf, Catalysis Today, 33 (1997) 57.

[171] Bosch, F. Janssen, Catalysis Today, 2 (1988) 369.

[172] G.C. Bond, S.F. Tahir, Appl. Catal., 71 (1991) 1.

[173] G.A. Du, S. Lim, Y.H. Yang, C. Wang, L. Pfefferle, G.L. Haller, Appl. Catal. A., 302 (2006) 48.

[174] Khodakov, B. Olthof, A.T. Bell, E. Iglesia, J. Catal., 181 (1999) 205.

[175] E. Wachs, B. M. Weckhuysen, Appl. Catal. A., 157 (1997) 67.

[176] Das, H. Eckert, H. C. Hu, I. E. Wachs, J. F. Walzer, F. J. Feher, J. Phys. Chem., 97 (1993) 8240.

[177] S. Irusta, L. M. Cornaglia, E. E. Miro, E. A. Lombardo, J. Catal., 156 (1995) 167.

[178] M. Iwamoto, J. Hirata, K. Matsukami, S. Kagawa, J. Phys. Chem., 87 (1983) 903.

[179] X.T. Gao, S.R. Bare, B. M. Weckhuysen, I. E.Wachs, J. Phys. Chem. B., 102 (1998) 10842.

[180] Busca, G. Centi, L. Marchetti, F. Trifiro, Langmuir, 2 (1986) 568.

[181] Inumaru, M. Misono, T. Okuhara, Appl. Catal. A., 149 (1997) 133.

[182] H. Yang, S. Lim, G. A. Du, Y. Chen, D. Ciuparu, G. L. Haller, J. Phys. Chem. B., 109 (2005) 13237.

[183] M. Stockenhuber, M.J. Hudson, R.W. Joyner, J. Phys. Chem. B., 104 (2000) 3370.

[184] S. Lim, A. Ranade, G. Du, L. D. Pfefferle, G. L. Haller, Chem. Mater., 18 (2006) 5584.

[185] Ciuparu, Y. Chen, S. Lim, G. L. Haller, L. Pfefferle, J. Phys. Chem. B., 108 (2004) 503.

[186] Y. Chen, D. Ciuparu, Y. H. Yang, S. Lim, C. Wang, G. L. Haller, L.D. Pfefferle, Nanotechnology, 16 (2005) S476.

[187] M. Trejda, A. Tuel, J. Kujawa, B. Kilos, M. Ziolek, Microporous and Mesoporous Materials, 110 (2008) 271.

[188] Francois Berube, Abdelkarim Khadhraoui, Michael T. Janicke, Freddy Kleitz, Serge Kaliaguine, Ind. Eng. Chem. Res., 49 (2010) 6977.

[189] T. Blasco, A. Corma, M. T. Navarro, J. Perez-Pariente, J. Catal., 156 (1995) 65.

[190] Daniel A. Ruddy, Richard L. Brutchey, T. Don Tilley, Top Catal.,(2008).

[191] Griselda A. Eimer, Sandra G. Casuscelli, Corina M. Chanquia, Veronica Elıas, Monica E. Crivello, Eduardo R. Herrero, Catalysis Today, (2008) .

[192] C. Berlini, M. Guidotti, G. Moretti, R. Psaro, N. Ravasio, Catalysis Today, 60 (2000) 219.

[193] C. Berlini, G. Ferraris, M. Guidotti, G. Moretti, R. Psaro, N. Ravasio, Microporous and Mesoporous Materials, 595 (2001) 44.

[194] Gallo, I. Paulino, U. Schuchardt, Appl. Catal. A: Gen., 266 (2004) 223.

[195] Guidotti, N. Ravasio, R. Psaro, G. Ferraris, G. Moretti, J. Catal., 214 (2003) 242.

[196] Cagnoli, S. Casuscelli, A. Alvarez, J. Bengoa, N. Gallegos, N. Samaniego, M. Crivello, G. Ghione, C. Perez, E. Herrero, S. Marchetti, Appl. Catal. A: Gen., 287 (2005) 227.

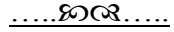

Chapter 2

Materials and Methods

Contents

Catalysis is a complex phenomenon occurring on the active sites present in a catalyst. The knowledge about the physical and chemical structure of the catalyst helps to derive a relationship between the material structure of the catalyst and its catalytic activity in various chemical reactions. Thus the catalyst characterization is a lively and highly relevant discipline in catalysis. A proper utilization of various characterization techniques provides great insight in to the physical and chemical characteristics of the catalysts. In the present chapter, a detailed description of the experimental procedure and chemicals used for the catalyst preparation, characterization and activity studies are given in detail.

2.1 Introduction

Catalysis involves the interaction of the reactant molecules with the active sites of the catalysts. The texture of the catalyst particles and their surface properties largely influence the catalytic activity of the catalyst systems. During the production of catalysts, even a minute change in the condition of preparation can change the quality of the catalyst. Thus a methodological preparation and catalyst characterization becomes highly essential. Various characterization techniques are known today for the characterization of heterogeneous catalysts. Among them ICP-AES, XRD, N_2- adsorption–desorption studies, TG, FT-IR, UV-vis-DRS, NMR, SEM, TEM etc are used to characterize the prepared materials under the present work. Acidity determination was carried out using both adsorption technique and chemical reactions. Activity of the catalysts was tested by conducting various chemical reactions. The detailed experimental procedure for both characterization and activity studies are included in this chapter.

2.2 Catalyst preparation

2.2.1 Chemicals used for the preparation

The chemicals used for the preparation of catalysts are listed below in Table 2.1.

Table 2.1 Chemicals used for the preparation

Sl. No.	Chemicals	Company
1.	TEOS	Sigma Aldrich , Bangalore
2.	P123 poly(ethyleoxide)–poly(propylene oxide)–poly(ethylene oxide), Pluronic P123	Sigma Aldrich , Bangalore
3.	Conc. HCl	Merck
4.	Sodium tungstate	Merck
5.	Titanium isopropoxide	Sigma Aldrich , Bangalore
6.	Ammonium meta vanadate	Merck
7.	Zirconium oxy chloride	Merck
8.	Ammonium hepta molybdate	Merck
9.	Cobalt nitrate	Merck
10.	Chromium nitrate	Merck

2.2.2 Preparation of Mesoporous SBA-15

The SBA-15 was synthesized according to the procedure described by Zhao et al. [1]. In a typical synthesis, 4.0 g of triblock copolymer, poly (ethylene oxide)-poly (propylene oxide)-poly (ethylene oxide) (EO20PO70EO20, P123, Aldrich) was dissolved in 30 g deionised water, and 120.0 g of HCl (2M) was added with stirring. Then 9.0 g tetraethyl orthosilicate (TEOS, 98%, aldrich) was added to the solution at 35^0C. After being stirred for 24 h, the mixture was transferred to an autoclave and placed in an oven at 100^0C for 48 h. The precipitate was filtered and then washed with deionised water and acetone, respectively, before being dried at room temperature (RT) and calcined in air at 540^0C for 6 h.

2.2.3 Preparation of Transition Metal Incorporated SBA-15

In the present work, we have used a novel direct synthetic method for the preparation of transition metal incorporated SBA-15 materials with high metal content , by simply adjusting the molar ratio of hydrochloric acid to silicon (HCl/Si) which can control the local concentration of H^+ ions in the synthesis mixture. It has been found that the amount of metal content in SBA-15 can easily be controlled by the simple adjustment of HCl/Si ratio. [2]

In the preparation of the transition metals (W, Ti, Zr, V, Mo, Co and Cr) included SBA-15, the corresponding metal salt solution were introduced in solution simultaneously with TEOS. The catalysts with Si/M ratio of 10-30 with respect to the content of SiO_2 were prepared [3, 4, 5].

The materials were synthesized following the same procedure of SBA-15. Minor alteration of the typical synthesis was programmed. In typical synthesis procedure, 9 g of tetraethyl orthosilicate (TEOS) and the appropriate amount of metal precursor were added directly to the homogeneous solution of P123, H_2O and HCl. (Proper quantities of 2 M HCl were added to adjust the pH values of

mixture (1-3) to obtain higher metal content). The gel was stirred for 24 h and then maintained in an autoclave at 373 K for another 48 h. The precipitate was filtered and then washed with deionised water and acetone, respectively, before being dried at room temperature (RT) and calcined in air at 540^0C for 6 h. Samples with Si/M ratio 10, 20, 30 were prepared and denoted as SBM1, SBM2, SBM3 respectively, where M denotes the transition metal incorporated.

2.2.4 Catalysts Prepared

The catalysts prepared for the present work with its symbols are listed in Table 2.2

Table 2.2 Catalysts Prepared

Sl. No.	Catalyst	Symbol
1.	Pure SBA-15	SBA15
2.	WSBA-15 with Si/W=10	SBW1
3.	WSBA-15 with Si/W=20	SBW2
4.	WSBA-15 with Si/W=30	SBW3
5.	TiSBA-15 with Si/Ti=10	SBTi1
6.	TiSBA-15 with Si/Ti=20	SBTi2
7.	TiSBA-15 with Si/Ti=30	SBTi3
8.	ZrSBA-15 with Si/Zr=10	SBZr1
9.	ZrSBA-15 with Si/Zr=20	SBZr2
10.	ZrSBA-15 with Si/Zr=30	SBZr3
11.	VSBA-15 with Si/V=10	SBV1
12.	VSBA-15 with Si/V=20	SBV2
13.	VSBA-15 with Si/V=30	SBV3
14.	MoSBA-15 with Si/Mo=10	SBMo1
15.	MoSBA-15 with Si/Mo=20	SBMo2
16.	MoSBA-15 with Si/Mo=30	SBMo3
17.	CoSBA-15 with Si/Co=10	SBCo1
18.	CoSBA-15 with Si/Co=20	SBCo2
19.	CoSBA-15 with Si/Co=30	SBCo3
20.	CrSBA-15 with Si/Cr=10	SBCr1
21.	CrSBA-15 with Si/Cr=20	SBCr2
22.	CrSBA-15 with Si/Cr=30	SBCr3

2.3 Catalyst characterization techniques

Various characterization techniques can be adopted to investigate the designing and structural formation of the prepared catalysts, which helps them to improve catalytic properties. By using the appropriate combination of analysis techniques, the desired characterization on the atomic as well as bulk scale is certainly possible. [6] A brief discussion of each method of characterization adopted with its experimental aspects is presented below.

- Elemental Analysis- ICP-AES
- X-ray Diffraction (XRD)
- Nitrogen Adsorption-Desorption Measurements
- Fourier Transform Infrared (FTIR) Spectroscopy
- Thermal Analysis
- UV-vis Diffused Reflectance Spectroscopy
- Nuclear Magnetic Resonance Spectroscopy (NMR)
- Scanning Electron Microscopy (SEM)
- Transmission Electron Microscopy (TEM)

Chemicals used for the characterization of catalysts are listed in Table 3.3.

Table 2.3 Chemicals used for the characterization of catalysts

Sl. No.	Chemicals	Company
1.	Conc. HNO_3	S.d Fine Chem. Ltd.
2.	Conc.HCl	Merck
3.	Hydrofluoric Acid	Merck
4.	Barium Sulphate	Merck
5.	Liquid Nitrogen	Sterling Gases Pvt. Ltd.
6.	Pottasium Bromide	IR grade-Merck
7.	Cyclohexanol	S.d Fine Chem. Ltd.
8.	Cumene	Sigma Aldrich , Bangalore
9.	2,6-Dimethyl Pyridine	Sigma Aldrich , Bangalore

2.3.1 Elemental Analysis - Inductively Coupled Plasma–Atomic Emission Spectroscopy (ICP-AES)

Inductively Coupled Plasma-Atomic Emission spectrometer is used for the elemental analysis of prepared catalysts. Most of the elements in the periodic table can be analyzed by this technique.. The main advantages of atomic emission spectroscopic techniques such as flame AES or non-flame ICP-AES are some elements can be analyzed with greater sensitivity and several elements can be analyzed simultaneously, which offers a tremendous saving in analysis time. The elemental composition is carried out by analysing the atomic spectrum emitted by a sample and the wavelength at which emission occurs identifies the element, while the intensity of the emitted radiation quantifies its concentration.

High temperature non-flame atomic emission spectroscopy has more advantages because of the greater concentration of emitting atoms. Main high temperature non-flame sources are usually plasmas and can operate at temperatures somewhere between 7000 and 15000K. Thus, the plasma source produces a greater number of excited emitted atoms, especially in the UV region. Plasma is a cloud of highly ionized gas, composed of ions, electrons and neutral particles. In plasma, over one percent of the total atoms in a gas are ionized. In plasma emission spectroscopy the gas, usually Argon is ionized by the influence of a strong electrical field either by a direct current or by radio frequency. Both types of discharge produce plasma, the direct current plasma (DCP) or the inductively coupled plasma (ICP).

The plasma source produces a greater number of excited emitted atoms, especially in the UV region. The plasma source is able to reproduce atomization; conditions with a far greater degree of precision that obtained by classical arc and spark spectroscopy. As a result, spectra are produced for a

large no of elements, which makes the plasma source amenable for simultaneous elemental determination.

ICP source comprises three concentric silica quartz tubes, each is open at the top. The Argon stream that carries the sample in the form of an aerosol passes through the central tube. The excitation is provided by two or three turns of a metal induction tube through which flows a radiofrequency current (freq ≈ 27MHz). The second gas flow of Argon of rate between 10 and 15 $lmin^{-1}$ maintains the plasma. It is this gas stream that is excited by the radiofrequency power. The plasma gas flows in a helical pattern which provides stability and helps to isolate thermally the outside quartz tube. The plasma is initiated by a spark from a Tesla coil probe and is thereafter self-sustaining.

ICP- AES were done on a *Thermo* Electron *IRIS INTREPID II XSP DUO* model. The applications of this instrument are in elemental level analysis of environmental samples, pharmaceuticals, research samples, soil and fertilizers etc. The sample is used to introduce by solution nebulisation. Nebulisation converts the sample in to a form more amenable to rapid atomization. Sample solutions of silica catalysts were prepared by removing silica. For this a known weight of the sample is taken in a platinum crucible, and treated with few drops of 40% HF. The silicates are converted to H_2SiF_6, which can be evaporated leaving other elements of interest. It is then treated with few drops of conc.HCl. The solution is then made up to 50ml in a standard flask using 5% HNO_3.

2.3.2 Powder X-ray diffraction Analysis

X-Ray diffraction analysis is the most frequently employed method for the structural analysis of the mesoporous solids. It helps to identify the crystalline phases present and structural regularity in the analyzed materials.

Analysis of diffraction patterns allows the determination of the XRD detectable phases, the uniqueness of mesoporous structure [7], unit cell parameters [8], degree of structural order, purity of substances, randomness and imperfections in the lattice, compositions of solid solutions etc.

When an X-ray beam passing through a crystal, it undergoes diffraction and produces beams at specific angles depending on the wavelength of the incident ray, the structure and orientation of the crystal etc. The basic principle underlying the X-ray diffraction analysis is that, a radiation of certain wavelength will constructively interfere when partially reflected between surfaces (i.e., the atomic planes) that produce a path difference equal to an integral number of wavelengths. This condition is described by the Bragg's law,

$$n\lambda = 2d\sin\theta$$

where n is an integer called order of reflection, λ is the wavelength of the radiation, d is the inter planar distance and θ is the angle between the radiation and the surfaces (scattering angle).

This relation demonstrates that interference effects are observable only when radiation interacts with physical dimensions that are approximately the same size as the wavelength of radiation.

The distances between atoms or ions are of the order of 10^{-10} m (1Å), so the diffraction methods require radiation in the X-ray region of the electromagnetic spectrum, or beams of electrons or neutrons with similar wavelength. The X-ray spectra widely used to identify and analyse any crystalline matter. The quality of the obtained result depends on the degree of crystallinity or order. An X-ray diffractometer consists of X-ray generator, a goniometer and sample holder and an X-ray detector, such as photographic film or a movable proportional counter. The most usually employed instrument

to generate X-rays is X-ray tubes, which generate X-rays by bombarding a metal target with high energy (10-100 keV) electrons that knock out core electrons. Thus, an electron in an outer shell fills the hole in the inner shell and emits X-ray photons. Two common targets are Mo and Cu, which have strong Kα X-ray emissions at 0.71073 and 1.5418 Å, respectively. Apart from the main line, other accompanying lines appear which have to be eliminated in order to facilitate the interpretation of the spectra. These are partially suppressed by using crystal monochromator.

The most important use of diffraction data is for phase identification [9, 10]. Each crystalline powder gives a unique diffraction diagrams, which is the basis for a qualitative analysis by X-ray diffraction. The X-ray diffraction pattern of a particular phase is characteristic and thus helps to the determination of phase purity and of the degree of crystallinity. Interpretation of the XRD data always accompanied by the systematic comparison of the obtained spectrum with a standard one, taken from any X-ray powder data file catalogues, published by the American Society for Testing Materials (JCPDS).

Powder X-ray diffraction (XRD) studies of mesoporous materials provide direct information about the pore architecture and symmetry of the materials. Crystalline solids show peaks in the 2θ range of $5\text{-}50^0$ whereas the mesoporous materials exhibit characteristic peaks in the low angle region between $1.5\text{-}10^0$ (2θ). Thus, the XRD analysis is not particularly suitable for the quantitative phase composition determination for most ordered surfactant-templated materials because of non crystallinity of their frameworks [11]. In such cases XRD analysis becomes the primary methodology in identifying different mesophases, because each mesophases exhibit distinct “finger print” XRD diffraction patterns.

Structural details of porous materials can be determined from measurements of the small angle (a scale of approximately 1 to 100 nm) scattering (SAS) of both X-rays (SAXS) and neutrons (SANS). Conventional mesoporous materials like MCM-41, MCM-48 or SBA-15 are amorphous. X-ray reflexions are observed at low 2θ angles ($0.5^0 < 2\ \theta < 10^0$). These reflexions represent the long-range order due to the regular arrangement of the pores. Generally the *d*-spaicing of the mesopores are rather big so the X-ray diffraction at low angles observed. Unit cell parameter (a_o) of a hexagonal lattice can be calculated from, $a_o = 2d_{100}/\sqrt{3}$. The frame wall thickness of the channels of the mesoporous materials can also be calculated using the unit cell parameter from XRD analysis and pore diameter from surface area measurements (Frame wall thickness = unit cell parameter-pore diameter).

Small Angle X-ray diffraction studies of the SBA-15 and various transition metal incorporated SBA-15 materials were carried out using a Panalytical Xpert PRO MPD model with Ni filtered Cu K_α radiation (λ= 1.5406 Å) within the 2θ range 0-10° at a speed of 1°/minute.

In order to identify the crystalline nature of the transition metals incorporated SBA-15 materials the wide angle XRD pattern were also recorded using Rigaku D-Max Ni filtered Cu K_α radiation (λ=1.5418A°) diffractometer equipped with a diffracted beam monochromator at a scan rate of 5°/min.

2.3.3 Nitrogen Adsorption-Desorption Analysis

Most of the catalysts with practical importance are highly porous and possess large specific surface areas. It is usually necessary to specify the nature of pore structure since this may control the transport of reactants and products of a catalytic reaction. Gas adsorption is a prominent method to obtain a comprehensive characterization of porous material with respect to the specific

surface area, pore size distribution and porosity. In the case of mesopores (pore widths in the range from 2-50 nm) pore filling occurs by condensation, which reflects a first order gas-liquid phase transition.

Nitrogen physisorption is a commonly applied technique to characterize porous and non-porous materials [12,13,14]. The amount of adsorbed nitrogen is measured as a function of the applied pressure, giving rise to the adsorption isotherm. The shape of the isotherm depends on the porous texture of the measured solid.

To obtain accurate adsorption measurements the amount of adsorbed gas should be high and the temperature constant. Therefore nitrogen physisorption measurements are often performed at liquid nitrogen temperature (-195.8°C = 77.35 K). In this technique, the amount of gas adsorbed onto the solid surface is directly correlated to the material's surface area and pore structure [15].

Isotherms

The nitrogen adsorption desorption isotherms are obtained by measuring the amount of nitrogen adsorbed and desorbed as a function of the applied pressure. IUPAC classified the isotherms into six types (Fig. 2.1) and the shape of the isotherms depend the porous texture of solid materials (Table 2.4) [14].

Table 2.4

Isotherm	Nature of solid
Type I	Microporous solids with relatively small external surfaces.
Type II	Non-porous or macroporous solids.
Type III	Macro- or non-porous material with weak adsorbate-solid interactions
Type IV	Mesoporous material
Type V	Mesoporous material with weak adsorbate –solid interactions
Type VI	Stepwise adsorption at very weak adsorbate-solid interactions.

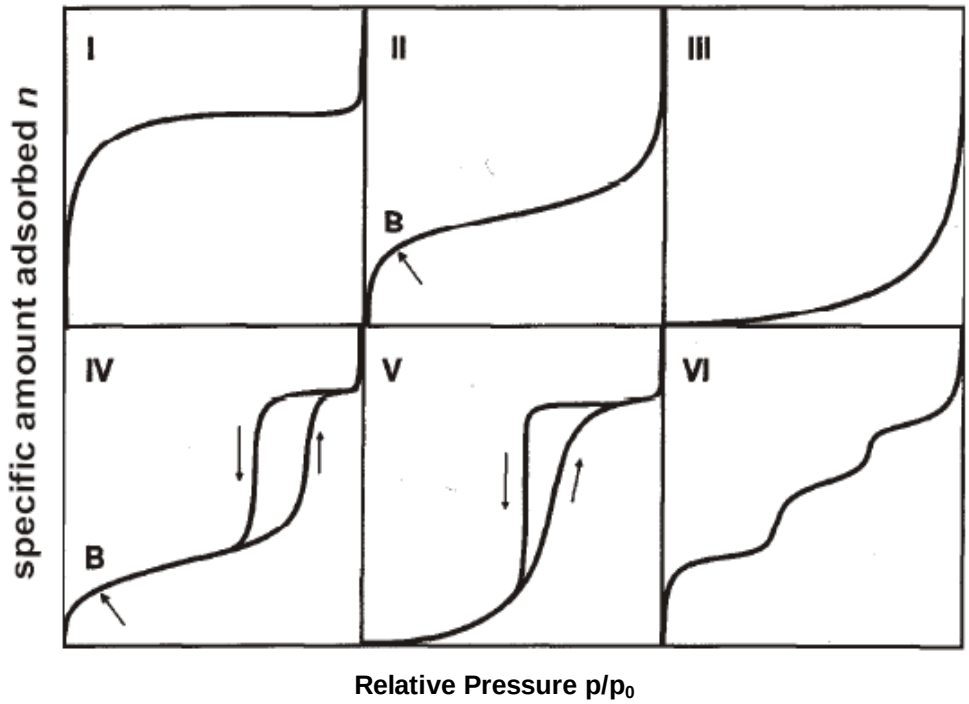

Figure 2.1 Type of physisorption isotherms. Point B, the beginning of the almost linear middle section of the isotherm, is taken to indicate the stage at which monolayer coverage is complete and multilayer adsorption is about to begin [16].

Characteristic features of the *Type IV* isotherm are its hysteresis loop, which is associated with capillary condensation taking place in mesopores. IUPAC classified the various hysteresis loops that are observed experimentally as types H1, H2, H3 and H4 as shown in Figure 2.2 and their interpretation is given as- H1- typical for type IV isotherms, H2- characteristic for "ink-bottle" pores, H3 and H4 - slit pores.

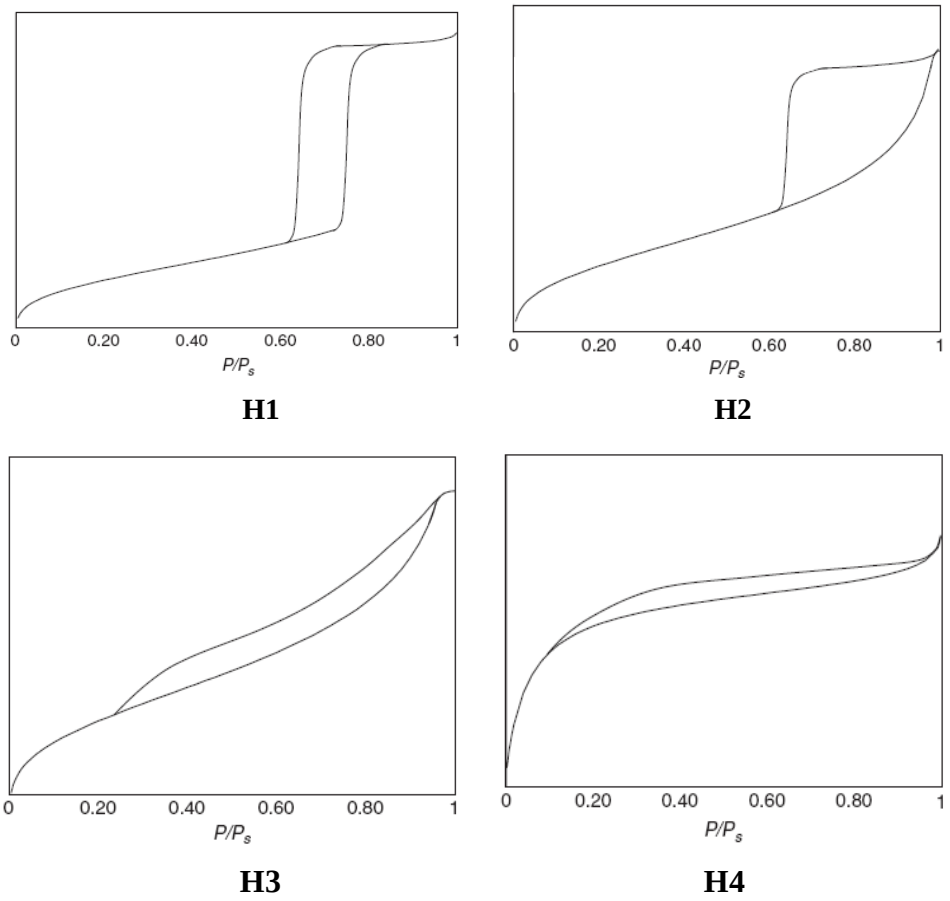

Figure 2.2 IUPAC classification of hysteresis loops

Specific surface area

The standard method for the determination of specific surface area of solid materials is the BET method. This method was established by Brunauer, Emmett and Teller [17]. The model, on which it is based, assumes that the heat of adsorption of the bare surface is different from the heat of adsorption of all successive layers.

$$P/V\ (P_O\text{-}P) = 1/V_MC + (C\text{-}1)\ P/CV_MP_0 \quad \ldots\ldots(1)$$

Where 'V' is the volume of gas adsorbed at equilibrium pressure, 'P' and 'P_0' is the saturated vapour pressure of the adsorbate at liquid nitrogen temperature

and 'C' is a constant for a given system at a given temperature and is related to the heat of adsorption.

A plot of $P/V(P_0-P)$ against P/P_0 is a straight line with slope $(C-1)/V_MC$ and intercept $1/V_MC$. From the slope and the intercept V_M and C can be calculated and the BET surface area of the sample can be calculated using the relation,

$$S_{BET} = V_M A_M N_A / V_{mol} \quad \text{.....(2)}$$

Where N_A is the Avogadro constant and A_M is the cross-sectional area of the adsorbate molecule. Nitrogen (at -196^0C) is generally considered to be the most suitable adsorbate for the determination of surface area of solids. It is usually assumed that the BET nitrogen monolayer is close packed having $A_M = 0.162$ nm^2

In BET method, adsorption of N_2 is carried out at liquid nitrogen temperature. The advantage with nitrogen as adsorbate lies in that the value of C on almost all surfaces is sufficiently small to prevent the localized adsorption and at the same time large enough to prevent the adsorption layer from behaving as a two dimensional gas. The linearity of the plot is normally confined to relative pressures in the range 0.1-0.3.

Pore volumes

The specific pore volumes were determined with two different methods. In the first it is assumed that all pores are filled at a relative pressure $P/P_0 = 0.97$. From the volume adsorbed at that pressure the pore volume was calculated directly. This very simple method gives correct results if (1) the investigated material has a low external surface area and (2) no macropores are present that cause condensation in this pressure range. Since both requirements are fulfilled in ordered mesoporous materials this method was mostly used.

Alternatively, a more sophisticated approach based on the so called t-plot method [18] was used. This method was developed for the characterization of the porosity of a material and in this method measured adsorbed volumes are plotted against the statistical layer thickness t.

Pore diameter distributions and average pore diameters

In ordered mesoporous materials the multilayer adsorption reaches a state where additional adsorptive molecules do not interact with a flat layer of adsorbate any more but with a curved surface. The adsorption on curved surfaces is more favourable. That can be expressed mathematically with the so-called Kelvin equation (eq. 3, P/P_0 is the relative vapour pressure over a curved surface, γ is the surface tension, υ is the molar volume of the liquid and r_k is the radius of curvature. The Kelvin equation shows that the smaller the pore radius, the lower the vapour pressure, P, in the pore

$$\frac{P}{p_0} = \exp\left(-\frac{2\upsilon\gamma}{r_k \times RT}\right) \quad \text{..... (3)}$$

The pore size distribution and pore diameters were calculated using the Barret-Joyner-Halenda (BJH) model based on the Kelvin equation, corrected for multilayer adsorption [16]. The emptying of the filled pores with decreasing relative pressure is incrementally evaluated to obtain a pore diameter distribution. From this value and the volume difference before and after the increment the volume of emptied pores in that increment is calculated. Assuming cylindrical pores, which is the case for most OMS (ordered mesoporous silica), and using parameters developed in 1997 by Jaroniec et al. [19] the pore size distribution can be estimated.

The mesopore size distribution is usually expressed as a plot of $\Delta V_p/\Delta r_p$ versus r_p, where V_p = mesopore volume, and r_p = pore radius. It is assumed that the mesopores volume is completely filled at high P/P_0. This plot will represent the

relative abundance of the pores of various radii in the solid. Specific surface areas S_{BET} were determined by the BET method in the 0.05–0.35 relative pressure range, single-point total pore volume Vp was determined at $p/p_0 = 0.99$ and average pore diameter Dp was calculated on the basis of 4 Vp/S_{BET} [16, 20].

Simultaneous determination of surface area, pore size distribution and total pore volume of the samples were achieved in a *Micromeritics Tristar 3000* surface area and porosity analyzer. Prior to the measurements the samples were degassed at 90^0C for half an hour and then 200^0C for overnight.

2.3.4 Thermal Analysis

Thermal analysis has been used to determine the physical and chemical properties of a variety of substances of interest in materials research. It is useful in both quantitative and qualitative analysis. Samples may be identified and characterized by their thermal behaviour. Thermal stability of a compound depends on the constituent elements present and on the type of linkages between the different elements [21].

Thermal analysis (TG/DTA/DTG) includes a group of techniques in which specific physical properties of a material are measured as a function of temperature. In TGA, the weight of sample is continuously recorded as the temperature is increased. Samples are placed in a crucible that is positioned in a furnace on a quartz beam attached to an automatic recording balance. The horizontal quartz beam is maintained in the null position by the current flowing through the transducer coil of an electromagnetic balance. Any change in the weight of the sample causes a deflection of the beam, which is sensed by one of the photodiodes connected to act as a position sensor to determine the movement of the beam. The beam is then restored to the original null position by a feedback current sent from the photodiodes to the coil of the balance and the current is proportional to the change in weight of the sample. In differential

thermal analysis (DTA), the difference in temperature between the sample and a thermally inert reference material is measured as a function of temperature usually the sample temperature. Any transition that the sample undergoes results in liberation or absorption of energy by the sample with a corresponding deviation of its temperature from that of the reference. A plot of the differential temperature ΔT versus the programmed temperature T indicates the transition temperatures and whether the transition is exothermic or endothermic. When an endothermic change occurs, the sample temperature lags behind the reference temperature because of the heat in the sample. Exothermic behaviour is associated with the decrease in enthalpy of a phase or a chemical system. DTA and thermogravimetric analyses are often run simultaneously on a single sample.

Thermogravimetry or Thermo-Gravimetric Analysis (TGA) provides a quantitative measurement of any weight change associated with thermally induced transitions. TG records the loss in weight as a function of temperature or transitions that involve dehydration or decomposition. TG curves are characteristic of a given compound or transitions and chemical reactions that occur over definite temperature ranges. The changes in weight results from physical and chemical bonds forming and breaking at elevated temperatures. These processes may evolve volatile products or form reaction products that result in a change in weight of the sample. The usual temperature range for TG is from ambient to 1200^0C in either inert or reactive atmospheres. Linear heating rates of 5-10^0C/min are typical.

TG/DTA done on a *Perkin Elmer Pyris Diamond* thermo gravimetric or differential thermal analyzer instrument under nitrogen atmosphere at a heating rate of 10^0C/min from room temperature to 1000^0C with samples mounted on a platinum sample holder.

2.3.5 Scanning Electron Microscopy

Scanning electron microscopy (SEM) has been used to study surface topography of the solid materials. In this technique, a high energy (typically 10 keV) electron beam is scanned across the surface and produce high resolution images of a sample surface by analyzing electrons emitted from a specimen. The interaction of a beam of electrons with the specimen results in the generation of secondary electrons, back scattered electrons, auger electrons, characteristic X-rays and photons of various energies. Secondary electrons and back scattered electrons can form images by attracting them onto a phosphor screen. This screen will glow and the intensity of the light is measured with a photomultiplier [6]. The images obtained provide atomic information about the sample.

In SEM analysis finely powdered sample was applied on to a double sided carbon tape placed on a metal stub. The stub was then inverted in such a manner that the free side of the carbon tapes generally picked up a small amount of the sample, thereby creating a thin coating. It was then sputtered with a thin layer of gold to obtain better contrast and provide improved cohesion [22]. During SEM inspection, a beam of electrons is focused on a spot volume of the specimen, resulting in the transfer of energy to the spot. These bombarding electrons, also referred to as primary electrons, dislodge electrons from the specimen itself. The dislodged electrons, also known as secondary electrons, are attracted and collected by a positively biased grid or detector, and then translated in to a signal. To produce the SEM image, the electron beam is swept across the area being inspected, producing many such signals. These signals are then amplified, analyzed and translated in to images of the topography being inspected. Finally the image is shown on a cathode ray tube.

The combination of higher magnification, larger depth of focus, greater resolution and ease of sample observation makes the SEM one of the most

widely used instruments in research areas today. This makes the technique suitable for producing very impressive, in focus images from a highly irregular structure typical of catalyst specimens. The SEM can be used to measure not only the composition profile of a surface, but also the geometric profile of its magnetic surface.SEM images give a characteristic 3-D appearance and are therefore useful for judging the surface structure of the sample. Beside the emitted electrons, X-rays are also produced by the interaction of electrons with the sample. These can be detected in a SEM equipped with energy dispersive X-ray (EDX) spectroscopy [23]. The chemical compositions of catalysts were determined using energy dispersive X-ray analyzer (EDX). This technique is used in conjunction with SEM. An electron beam strikes the surface of the sample. The energy of the beam is typically in the range 10-20 k eV. This causes X-rays to be emitted from the surface of the material. The energy of the X-rays emitted depends on the material under examination. The X-rays are generated in a region about 2 microns in depth. By moving the electron beam across the material an image of each element in the sample can be acquired.

The scanning electron micrographs of the samples were taken using *JEOL Model JSM-6390LV* scanning electron microscope with a resolution of 1.38ev. The powdered samples were dusted on a double sided carbon tape, placed on a metal stub and was coated with a layer of gold to minimize charge effects.

2.3.6 Transmission Electron Microscopy

The topographic information obtained by TEM in the vicinity of atomic resolution can be utilized for structural characterization and identification of various phases of mesoporous materials, *viz*., hexagonal, cubic or lamellar [24]. TEM also provides real space image on the atomic distribution in the bulk and surface of a nanocrystal [25].

Transmitted electrons form images from small regions of sample that contain contrast, due to several scattering mechanisms associated with interactions between electrons and the atomic constituents of the sample. Analysis of transmitted electron images yields information both about atomic structure and about defects present in the material.

Transmission electron microscopy (TEM) is particularly used for high resolution imaging of thin films of a solid material for microstructural and compositional analysis. Transmission electron microscopy (TEM) is an imaging technique whereby a thin solid specimen (200 nm thick) is bombarded in vacuum with a highly-focused, monoenergetic beam of electrons. Then an image is formed and a series of electromagnetic lenses magnify this transmitted electron signals and direct them either on a fluorescent screen or on a photographic film or to be detected by a sensor such as a CCD camera (charge couple device) [26]. The latter has the advantage that the image may be displayed in real time on a monitor or computer. The transmission electron microscope is an optical analogue to the conventional light microscope. It is based on the fact that electrons can be ascribed a wavelength but at the same time interact with magnetic fields as a point charge. A beam of electrons is applied instead of light, and the glass lenses are replaced by magnetic lenses. The lateral resolution of the best microscopes is down to atomic resolution. TEM also uses an electron gun to produce the primary beam of electrons as in the case of SEM that will be focused by lenses and apertures into a very thin, coherent beam. This beam is then controlled to strike the specimen. A portion of this beam gets transmitted to the other side of the specimen, is collected, and processed to form the image.

The HRTEM of the samples were carried out in ultrahigh resolution analytical electron microscope *JEOL 3010*. The sample was dispersed in

ethanol through sonication and then drop casted on a carbon-coated copper grid.

2.3.7 UV-VIS Diffuse Reflectance Spectroscopy

The UV-VIS Diffuse Reflectance Spectroscopy is known to be a very sensitive probe for the identification and characterization of metal ion co-ordination. It is a non-invasive technique that uses the interaction of light absorption and scattering, to produce a characteristic reflectance spectrum, providing information about the structure and composition of the medium. It gives information regarding electronic transition between orbitals or bands in the case of atoms, ions and molecules in gaseous, liquid or solid state.

In catalysis, the information given by DRS mainly includes the active phase- support interactions. Metal centered transitions and charge transfer transitions can be clearly differentiated by UV-DRS and assignment of these gives a picture about the oxidation state and co-ordination environment of the transition metals [27]. It can also provide the electronic structure of dispersed metal oxides.

UV-VIS DR spectra of the prepared samples were taken in the range 200-800 nm on Labomed UV-VIS DOUBLE BEAM UVD-500 spectrophotometer equipped with an integrating sphere assembly with a charged coupled device detector, using $BaSO_4$ as reflectance standard.

2.3.8 FT-Infrared Spectroscopy

Infrared Spectroscopy has been extensively used for identifying the various functional groups on the catalyst itself, as well as for identifying the adsorbed species and reaction intermediates on the catalyst surface. It is one of the few techniques capable of exploring a catalyst, both in its bulk and its surface and under the actual reaction conditions [6].

The advantages of Infrared Spectroscopy include wide applicability, non-destructiveness, measurement under ambient atmosphere and the capability of providing detailed structural information. Besides these intrinsic advantages the more recent Infrared Spectroscopy by Fourier Transform (FTIR) has additional merits such as: higher sensitivity, higher precision (improved frequency resolution and reproducibility), quickness of measurement and extensive data processing capability. IR spectra originate in transition between two vibrational levels of a molecule in the electronic ground state and are usually observed as absorption spectra in the IR region.

In infrared spectroscopy vibrations in solid lattices are excited by the absorption of photons. Infrared spectroscopic investigations can be widely used to characterize active centres on catalysts surfaces and chemisorbed molecules. It provides information by the careful examination of the twisting, bending, rotating and vibrational motions of atoms in a molecule. Upon interaction with infrared radiation, portions of the incident radiation are absorbed at specific wavelengths. The infrared spectrum of a compound is essentially the superposition of absorption bonds of specific functional groups, yet subtle interactions with the surrounding atom of the molecule impose the stamp individually on the spectrum of each compound [28].

Infrared spectroscopy has a variety of applications in catalysis. FTIR spectroscopy can be used in the determination of bulk structure of the catalyst, this is particularly important for newly synthesized catalysts of unknown structure. This technique also provides information about the peculiarities of the surface such as the presence of surface hydroxyl groups. For porous materials the majority of the hydroxyl groups are on the surface and there is hardly any difference between bulk and surface in this regard. It has application in the study of molecules adsorbed from solution or from the gas phase and their transformation.

The Infrared spectrum can be divided in to two regions, one called the functional group region and the other the finger print region. The functional group region is generally considered to range from 4000 to 1500 cm^{-1} and all frequencies below 1500cm^{-1} are considered characteristic of the finger print region. The finger print region involves molecular vibrations, usually bending motions that are characteristic of the entire molecule or large fragments of the molecule and these are used for identification.

The Infrared induced vibrations of the samples were recorded using *Thermo NICOLET 380 FTIR* Spectrometer by means of KBr pellet procedure. Spectra were taken in the transmission mode and the samples were evacuated before making the pellet and the spectra were taken under atmospheric pressure and room temperature. The changes in the adsorption bands were investigated in the 400-4000cm^{-1}. The resolution and acquisition applied were 4 cm^{-1} and 60 scans respectively.

2.3.9 Magic Angle Spinning Nuclear Magnetic Resonance Spectroscopy -(^{29}Si MAS NMR)

Nuclear magnetic resonance spectroscopy is one of the important spectroscopic aids widely used by the chemists for the structural elucidation. Nuclear magnetic resonance spectroscopy concentrates on the magnetic properties of atomic nuclei. The interaction of the nuclear magnetic moment of a nucleus with an external magnetic field B_o leads to a nuclear energy level diagram, according to the rules of quantum mechanics i.e., the magnetic energy of the nucleus is restricted to certain discrete values E_i, the so-called eigen values. Eigen states associated with the eigen values are the only states in which particle can exist. Through a high frequency transmitter, transitions between eigen states within the energy level diagram can be stimulated. The absorption of energy can be detected, amplified and recorded as a spectral line, the so-called resonance signal. In this way a spectrum can be generated

for a compound containing atoms whose nuclei have non-zero magnetic moments. Several resonance signals are found for various atoms in a molecule because the atoms reside in different chemical environments. The resonance signals are separated by a so-called chemical shift. Empirically determined correlation between the spectral parameters, chemical shift and spin-spin coupling and the structure of chemical compounds forms the basis for the application of nuclear magnetic resonance to the structural determination of unknown samples. In this respect the nuclear magnetic moment has proved itself to be a very sensitive probe with which one can provide extensive information [28, 29].

^{29}Si MAS NMR spectra are very sensitive to the nature and chemical environment of the atoms [30]. ^{29}Si solid-state NMR spectroscopy has been used extensively to elucidate the molecular environment in silicate materials [31].

^{29}Si solid-state NMR spectra of the solids show signals representative of various substructures of the Q^n silane moities. Spectra displaying Q^n ($n < 4$) peaks indicate that the condensation of the silicon alkoxide precursor is incomplete [31]. As the degree of condensation increases, the Q^n peaks are shifted to higher field in the NMR spectrum.

Solid State MAS NMR experiments were carried out over a Bruker DSX-300 spectrometer at a resonance frequency of 75.4MHz. For all measurements a standard 4 mm double- bearing Bruker MAS probe was used. The number of scans collected was 1024. XWIN NMR software was employed to acquire and retrieve data. The standard used for ^{29}Si MAS NMR is tetra methyl silane whose chemical shift is 0 ppm.

2.3.10 Acidity Determination

Surface acidity measurements of catalysts have received very much attention in catalysis research because they can provide significant information

about the behaviour of the catalysts in various catalytic reactions. The nature of active sites as well as its number and strength have decisive role in determining the conversion and selectivity of acid catalyzed reactions. So the determination of the number, nature and strength of the acid sites are necessary to understand the catalytic activity and selectivity. A number of physico-chemical methods have been developed and accepted to evaluate the strength and amount of surface acid sites. A large variety of probe molecules have been utilized to ascertain acidity quantitatively as well as to provide an insight on acid site distribution [32].

2.3.10.1 Thermodesorption studies of 2.6-dimethyl pyridine

The thermo desorption studies of 2, 6-dimethyl pyridine (2, 6-DMP) were used for the selective determination of the Bronsted acid sites. Benesi reported that 2, 6-dimethyl pyridine as a proton specific probe [33]. Due to the steric hindrance of methyl groups, 2, 6-DMP gets selectively adsorbed at the Bronsted acid sites. Previously activated catalyst samples were kept in a desiccator saturated with vapours of 2, 6-dimethyl pyridine for 48 hours for the effective and uniform adsorption. Then the weight loss of the adsorbed sample was measured by thermo gravimetric analysis between 50-600^{0}C under nitrogen atmosphere at a heating rate of 20^{0}C/min. It was observed that the coordinatively adsorbed 2, 6-DMP on Lewis acid sites could be eliminated by purging at a temperature above 300^{0}C [34]. The fraction weight loss in the range of 300-600^{0}C was calculated and taken as a measure of the Bronsted acidity of the sample.

2.3.10.2 Cumene Conversion Reaction

The vapour phase cumene cracking reaction can be used as a model reaction for identifying the Lewis and Bronsted acid sites on a catalyst. Cumene undergo different reactions on different type of acid sites. Cumene cracked to benzene and propene over Bronsted acid sites through dealkylation reactions and dehydrogenated to α-methyl styrene over Lewis acid sites [40]. An idea about the Bronsted and Lewis acid sites possessed by the catalysts can

be derived by comparing the amount of benzene and α-methyl styrene produced during the reaction. This reaction was applied in heterogeneous catalysis for the acidity measurements of various catalysts [41-44].

The vapour phase cumene conversion reaction was carried out at atmospheric pressure in a fixed bed down flow glass reactor at a temperature of 623 K. The previously activated catalyst was packed between silica beads in the reactor with glass wool. The liquid reactant was fed into the reactor with the help of a syringe pump at a flow rate of 5ml/h. The products were analyzed by Chemito GC 1000 gas chromatograph with FID detector using SE30 capillary column. Analysis conditions are specified in Table 2.6.

2.3.10.3 Cyclohexanol Conversion Reaction

Cyclohexanol decomposition reaction has been widely used as a test reaction for acid-base properties of solid catalysts as well as a model reaction to determine the catalytic activity of metal oxides. The dehydration of cyclohexanol to cyclohexene occurs on acid sites, while dehydrogenation to cyclohexanone is associated with both acid/base and redox sites [35, 36]. Acid-base properties of metal oxides are related to a number of variables such as metal salt, method of preparation, precipitation agent, calcination temperature and the effect of promoters. Several reports studied this reaction as a simple test to measure acid sites present in metal oxide catalysts [37-39].

The vapour phase cyclohexanol decomposition reaction was conducted at atmospheric pressure in a fixed bed down flow glass reactor at a temperature of 523 K. About 0.2 mg of the activated catalyst was packed between silica beads in the reactor with glass wool. The liquid reactant was fed into the reactor with the help of an injection pump at a flow rate of 5ml/h. The products were analyzed by Chemito GC 1000 gas chromatograph with FID detector using SE30 capillary column. Analysis conditions are specified in Table 2.6.

2.4 Experimental Procedure for Catalytic Activity Studies

The catalytic efficiency of the prepared catalytic systems were studied by conducting both liquid and vapour phase reactions over the catalysts. A brief description of the experimental procedure for the different types of reactions studied is given below. The catalytic activity was expressed in terms of percentage conversion.

The chemicals used for the catalytic activity studies of prepared catalysts are listed below in Table 2.5 along with the company supplied.

Table 2.5 Chemicals used for the catalytic activity studies

Sl. No.	Chemicals	Company
1.	Cyclohexene	Spectrochem Pvt.Ltd
2.	Cyclopentene	Sigma Aldrich , Bangalore
3.	Cyclooctene	Sigma Aldrich , Bangalore
4.	Benzyl alcohol	Spectrochem Pvt.Ltd
5.	Cyclohexanone	RFCL.Ltd.
6.	Cyclopentanone	Sigma Aldrich , Bangalore
7.	Acetophenone	Merck
8.	Benzophenone	SRL Pvt .Ltd.
9.	Benzaldehyde	Spectrochem Pvt.Ltd
10.	Benzene	Merck
11.	Toluene	Merck
12.	Anisole	Merck
13	Isobutyl benzene	Spectrochem Pvt.Ltd
14.	O-Xylene	Merck
15.	Hydrogen peroxide (30%)	s.d Fine Chem. Ltd.
16.	TBHP	Sigma Aldrich , Bangalore
17.	Acetonitrile	s.d Fine Chem. Ltd.
18.	Acetone	s.d Fine Chem. Ltd.
19.	Methanol	Merck
20.	Isopropanol	Merck
21.	Benzyl chloride	Spectrochem Pvt.Ltd

2.4.1 Liquid Phase Reactions

The liquid phase reactions studied are oxidation of cyclohexene, oxidation of benzyl alcohol, acetalization of cyclohexanone and benzylation of isobutyl benzene.

1. Oxidation of Cyclohexene

The reaction was performed in the liquid-phase using an oil bath in order to make the working temperature constant with acetonitrile as a solvent. The catalytic reaction between cyclohexene and hydrogen peroxide was carried out in a 50 ml round bottom flask equipped with a magnetic stirrer and a reflux condenser. Sufficient amount of calcined catalyst was placed into the flask, and the solvent was added. The oxidation was conducted by efficient stirring of a mixture of a solvent and a catalyst at the reaction temperature. After stirring for 15 min, cyclohexene was added, followed by the drop wise addition of 30% hydrogen peroxide. Samples were withdrawn at regular time intervals and analysed by a gas chromatograph Chemito GC 1000 equipped with a capillary column SE30 attached to a FID detector, operated with a heating program described in table 2.6

2. Oxidation of Benzyl Alcohol

The liquid-phase oxidation of benzyl alcohol was carried out in a 50 ml round bottom flask. The flask was immersed in an oil bath in order to make the working temperature constant, which was connected with a condenser. In a typical run, catalyst, and substrate were added to the solvent. The oxidant, 30% H_2O_2 was added to the system after attaining the reaction temperature. The reaction mixture was stirred using a magnetic stirrer for the indicated reaction time. Then, the reaction products were analyzed by gas chromatograph equipped with flame ionization detector and SE30 capillary column. Conversion rate and selectivity were calculated based on the relative area of each of authentic samples with standard ones.

3. Acetalization of Cyclohexanone

Cyclohexanone was purchased from Aldrich Chemical Company, USA and commercial-grade methanol (available from SD Fine Chemicals, India) was used after distillation. One-pot acetalization reactions of carbonyl compounds were carried out in a 50 ml glass reactor equipped with a magnetic stirrer, thermometer, water condenser and temperature controller. All the experiments were performed under gentle nitrogen flow. In a typical run, 10 ml of a 1:10 mixture of ketone and methanol was stirred with 0.1g of pre-activated catalysts for 3 h under a slow flow of moisture-free nitrogen. Samples were withdrawn every 1 h and at the end of the reaction and were analyzed with a Chemito GC1000 gas chromatograph equipped with a SE-30 capillary column.

4. Benzylation of Isobutyl Benzene

Benzylation reaction of isobutylbenzene was conducted as a liquid phase reaction. The reactants in the required mole ratio and definite amount of catalyst were taken in a 50 ml double necked round bottom flask and refluxed in an oil bath using a condenser. The temperature of the oil bath was adjusted according to the requirement of reaction studies and kept constant by means of a dimmerstat. The reaction mixture was stirred magnetically, and the product analysis was done using Chemito GC1000 gas chromatograph equipped with a SE-30 capillary column.

2.4.2 Vapour Phase Reactions

1. Isopropylation of Benzene

Isopropylation of benzene was carried out in a fixed bed-vertical down flow type reactor made up of a Borosil glass tube at atmospheric pressure. About 0.2g of the activated catalyst is placed in between a glass wool bed packed with silica beads in a glass reactor. The reactor was heated to the requisite temperature with help of a tubular furnace controlled by a digital

temperature controller. Reactants were introduced into the reactor using a syringe pump at controlled flow rate. The catalyst was activated at 500^0C for 3 h in a flow of dry air before the reaction was conducted. The bottom of the reactor was connected to a condenser with ice traps and a receiver to collect the products. The products were collected and analyzed by GC (Chemito GC1000 gas chromatograph equipped with a SE-30 capillary column).

Analysis conditions of various reactions are presented in Table 2.6.

Table 2.6 Analysis conditions of various reactions

Reaction	GC	Analysis Condition		
		Temperature(^{0}C)		Temperature Programme
		Injector	Detector	
Cyclohexanol conversion	GC1000, SE-30 capillary column, FID detector	230	230	60°C -2min-10°C /min -99°C -2min-10°C /min -200°C -2min
Cumene Cracking	GC1000, SE-30 capillary column, FID detector	230	230	70°C -2min-10°C /min -250°C -2min
Oxidation of cyclohexene	GC1000, SE-30 capillary column, FID detector	240	250	65°C -1min-10°C /min -200°C -1min -10°C /min-250°C -1min
Oxidation of Benzyl alcohol	GC1000, SE-30 capillary column, FID detector	240	250	70°C-1min-10°C /min -100°C -1min -10°C/min -250°C -1min
Acetalization of cyclohexanone	GC1000, SE-30 capillary column, FID detector	100	100	75°C-1min-5°C /min -125°C-1min-10°C /min -200°C -1min
Benzylation of isobutyl benzene	GC1000, SE-30 capillary column, FID detector	250	250	70°C-1 min-10°C /min -130°C-1min-10°C /min -225°C -2min
Isopropylation of benzene	GC1000, SE-30 capillary column, FID detector	230	230	60°C-5 min-10°C /min -250°C-2min

References

[1] D. Y. Zhao, Q. S. Huo, J. L. Feng, B.F. Chmelka, G. D. Stucky, J. Am. Chem. Soc., 120 (1998) 6024.

[2] Vinu, P. Srinivasu, D. P. Sawant, S. Alam, T. Mori, K. Ariga, V.V. Balasubramanian, C.Anand, Microporous and Mesoporous Materials, 110 (2008) 422.

[3] Volkan Degirmenci, Ozlen Ferruh Erdem , Orcun Ergun , Aysen Yilmaz , Dieter Michel , Deniz Uner, Top Catal., DOI 10.1007/s11244-008-9078

[4] O. Ergun, O. Karslioglu, A. Yilmaz, D. Uner, Turk , J Chem., 31 (2007) 501.

[5] V. Degirmenci, O. F. Erdem, A. Yilmaz, D. Michel, D. Uner, Catal. Lett., 115 (2007) 79.

[6] W. Niemantsverdriet, Spectroscopy in Catalysis: An Introduction, VCH Publisher, New York (1995) 165.

[7] W. H. Bragg, W. L. Bragg, The Crystalline State, McMillan, New York (1949).

[8] S. Biz, M. Occelli, Catal. Rev. Sci. Eng., 40 (1998) 329.

[9] C. Suryanarayana, M. G. Norton, X-ray Diffraction-A Practical approach, Plenum Press, Newyork (1998).

[10] G. Bergeret, H. Knozinger, Handbook of Heterogeneous Catalysis Eds, Weitkamp. J, 2 (1997) 464.

[11] F. Schüth, U. Ciesla, Microporous and Mesoporous Materials, 27 (1999) 131.

[12] S. J. Gregg, K. S. W. Sing, Adsorption, Surface Area and Porosity, Academic Press, London (1982).

[13] P. A. Webb, C. Orr, Analytical Methods in Fine Particle Technology, Micromeritics (1997).

[14] K. S. W. Sing, D. H. Everett, R. A. W. Haul, L. Moscou, R. A. Pierotti, J. Rouquerol, T. Siemieniewska, Pure Appl. Chem., 57 (1985) 603.

[15] E. P. Joyner, P. P. Halenda, J. Am. Chem. Soc., 73 (1951) 373.

[16] S. Alhir, S. Markajis, R. Chandan, J. Agric. Food Chem., 38 (1990) 598.

[17] S. Brunauer, P. H. Emmett, E. Teller, J. Am. Chem. Soc, 60 (1938) 309.

[18] B. C. Lippens, J. H. de Boer, J. Catal., 4 (1965) 319.

[19] M. Kruk, M. Jaroniec, A. Sayari, Langmuir, 13 (1997) 6267.

[20] D. J. C. Yates, J Phys. Chem., 70 (1966) 3693.

[21] H. H. Willard, L. L. Merrit Jr, J. A. Dean, F. A. Settle Jr, Instrumental Methods Of Analysis, 7th edn, CBS Publishers, New Delhi (1986).

[22] E. Wachs, Characterization of Catalytic Materials, Butterworth Heinemann: Manning (1992).

[23] J. I. Goldstein, Dale E. Newbury, l. Echlin, D. C. Joy, C. Fiori, E. Lifshi, Scanning Microscopy and X-Ray Microanalysis. Plenum Press, New York (1981).

[24] J. M. Thomas, O. Terasaki, P. L. Gai, W. Zhou, J. Gonzalez-Calbet, Acc. Chem. Re., 34. (2001) 583.

[25] Z. L. Wang, Characterization of Nanophase Materials, Ed.in:, Wiley-VCH, Weinheim (2000) 37.

[26] B. Fultz, J. Howe, Transmission Electron Microscopy and Diffractometry of Materials, Springer, 2nd edn. (2002).

[27] M. A. Larrubia, G. Busca, Mater. Chem. Phys., 72 (2001) 337.

[28] X. Yu, S. Cai, Z. Chen, Spectrochimica Acta Part A., 60 (2004) 391.

[29] H. Gunther, NMR Spectroscopy; Basic Principles, Concepts and Applications in Chemistry, 2nd edn. John Wiley and Sons, New York (1998).

[30] E. Lippama, M. Magi, A. Samoson, M. Tarmak, G. Engelhardt, J. Am. Chem. Soc., 103 (1981) 4992.

[31] B. Gorlach, S. S. Hellriegel, H. Yiksel, K. Albert, E. Plies, M. Hanack, J. Mater. Chem., 11 (2001) 3317.

[32] P. A. Jacobs, F. Delanney, Characterization of Heterogeneous Catalysts, (Eds.), Elsevier, Amsterdam, (1985) 311.

[33] H. A Benesi, J. Catal., 28 (1973) 176.

[34] Satsuma, Y. Kamiya, Y. Westi and T. Hattori, Appl. Catal.A. Gen., 194 (2000) 253.

[35] H. J. M. Bosman, E. C. Kruissink, J. van der Spoel, F. van den Brink, J. Catal., 148 (1994) 660.

[36] B. M. Reddy, I. Ganesh, J. Mol. Catal. A., 169 (2001) 207.

[37] J. Babu, K. R. Sunajadevi, S. Sugunan, Indian J. Chem. Sect A., 43 (2004) 473.

[38] C. G. Ramankutty, S. Sugunan, B. Thomas, J. Mol. Catal. A., 187 (2002) 105.

[39] C. Bezouhanava, M. A. Al-Zihari, Catal. Let., 11 (1991) 245.

[40] S. M. Bradley, R. A. Kydd, J. Catal., 141 (1993) 239.

[41] T. Mishra, K. M. Parida, S. B. Rao, Appl. Catal. A., 166 (1998) 115.

[42] M. Hino, M. Kurashige, K. Arata, Catal. Commun., 5 (2004) 107.

[43] K. Wada, K. Tada, N. Itayama, T. Kondo, T. Mistudo, J. Catal., 228 (2004) 374.

[44] K. M. Parida, S. K. Samantaray, H. K. Mishra, J. Colloid Interface Sci., 216 (1999) 127.

Chapter 3

Physico – Chemical Characterization

Contents

Mesoporous SBA-15 has become a promising oxide support for many catalysts owing to its high surface area and silanol concentrations allowing the active sites with high dispersion. . In recent years a considerable interest has been focused on heterogeneous catalysis by mesoporous materials especially modified mesoporous SBA-15 materials, which are new class of solid acid catalysts. The isomorphous substitution of heteroelements in all silica mesoporous SBA-15 could lead to a useful catalyst for the reactions involving bulkier molecules. The degree of frame work substitution has been monitored by means of powder XRD, N_2 adsorption desorption and UV-DRS spectral techniques. The physicochemical characterization of transition metal incorporated SBA-15 materials was carried out and the results obtained are presented in this chapter. The characterization techniques are usually employed to investigate the composition and structure of the catalysts. It also helps to get an insight into the nature of active sites on the catalyst surface. A detailed investigation was performed by different techniques such as powder XRD, ICP-AES, surface area and pore volume measurements, TG-DTA analysis, FT-IR and UV-DRS spectroscopy, Si NMR, SEM, and TEM. Strength and distribution of acid sites were determined by thermo desorption of 2,6-Dimethyl Pyridine and by catalytic test reactions such as cumene conversion and cyclohexanole conversion. Maintaining of structure and ordered arrangement after modifications is important in the case of mesoporous materials. Characterization of the catalysts will give better knowledge about them. An increase in lattice parameter gives an idea about the isomorphous substitution of hetero elements in parent SBA-15. Characterization of catalysts is needed to know the efficiency of the preparation procedure adopted.

3.1 Introduction

Catalytic performance of the catalysts can be better appreciated if one knows as many of its properties as well. Knowledge about the structure, ordering, and exact location of heteroelements and nature of active sites is essential to acquire a better understanding of the improved activity of the catalysts. In an attempt to improve the catalytic efficiency there has been adopted the modification by hetero elements into SBA-15 because these materials are expected to be better catalytic candidates. In the present work the modifications are achieved by the hydrolysis of a number of transition metal cations during the synthesis process of SBA-15. The influence of modification on the structural arrangement, surface area, and morphology and on various other properties was investigated in this chapter. Since solid supported catalysts are well known for its surface acidity, a more detailed investigation of the acidity of the prepared systems is also discussed.

The various properties of the catalysts were investigated by X-ray techniques, electron and nuclear spectroscopies, thermogavimetry, acidity measurements etc. The chemical composition of the catalysts was quantitatively obtained from ICP-AES results. XRD and N_2 adsorption desorption isotherms helps to investigate the well ordered structure of the catalysts. Thermo gravimetric analysis gave an idea about the thermal stability of the catalysts. Spectral analysis were carried out to understand the chemical structure and metal ion coordination. Surface morphology was obtained by SEM. A detailed investigation of structural arrangement was obtained from TEM images.

3.2 Physico Chemical Characterizations

3.2.1 ICP-AES measurements

Various transition metal incorporated SBA-15 materials (MSBA-15) with various Si/M mole ratios were synthesized and elemental analysis was done using ICP-AES after the quantitative separation of SiO_2. The data shown in the

Table 3.1 gives the amount of Si/M mole ratio of the prepared catalysts. The values are very high upon Ti, W and Zr incorporated SBA-15 materials compared with other transition metals. There is no stoichiometric incorporation V, Mo, Co and Cr, and the metal contents that are obtained are quite low in the case of the approach that is proposed. The highly dispersed tetrahedral metal oxides (MO_x) were found to be stabilized in the SBA-15 mesopores even at low metal loading.

Table 3.1

Catalysts	Si/M mole ratio		Catalysts	Si/M mole ratio	
	Theoretical	Obtained		Theoretical	Obtained
SBA15	-	-	SBV2	20	86.72
SBW1	10	22.43	SBV3	30	130.58
SBW2	20	33.20	SBMo1	10	33.24
SBW3	30	44.86	SBMo2	20	48.26
SBTi1	10	17.10	SBMo3	30	80.30
SBTi2	20	49.13	SBCo1	10	31.26
SBTi3	30	59.88	SBCo2	20	46.39
SBZr1	10	28.22	SBCo3	30	94.24
SBZr2	20	48.02	SBCr1	10	43.64
SBZr3	30	62.72	SBCr2	20	68.93
SBV1	10	49.51	SBCr3	30	101.05

The Si/M mole ratio of the samples decreases with decreasing the Si/M ratio in the synthetic gel irrespective of the pH of the solution. However, the elemental analysis by ICP-AES showed that the metal content of the products is much less than that of initial gels, which is possibly due to a portion of the metal that remains in the acidic solution. A similar result has been reported for some mesoporous metal incorporated materials prepared under acidic conditions [1].

The nature of metal species and the solubility of metal hydroxo complexes formed during the synthesis performed at lower HCl/Si ratio would contribute to increase the metal content in MSBA-15 materials [2]. These materials can generally be synthesized under acidic hydrothermal conditions. The hydrolysis of a metal salt is virtually instantaneous, whereas the hydrolysis of silicon precursors is much slower. Lowering the local concentration of H^+ ions in the

solution by reducing the HCl/Si ratio may decrease the hydrolysis rate of the metal precursors to match that of the silicon precursors. These factors may also prevent the formation of charged metal hydroxo complexes and decrease of the pH of the synthesis mixture which may reduce the solubility of metal hydroxo complex formed during the synthesis. This might enhance the interaction between the M–OH and Si–OH species in the synthesis gel resulting in a higher amount of M incorporation at low HCl/Si ratio. The results apparently show that a decrease of the local concentration of the H^+ ions induced a high loading of M in the SBA-15 structure, which was probably caused by suppressed M– O–Si cleavage and moderated hydrolysis of metal precursor [3].

However, the Si/M mole ratio of the materials prepared by incorporating W, Ti and Zr, indicate a successful incorporation of these species added in the synthesis gel into a mesoporous silica framework in a highly acidic medium. The exact reason for the successful incorporation of some cations in the SBA-15 silica framework is not clear at the moment. However, we summarise that the local concentration of H+ ions in the synthesis mixture plays a crucial role in controlling the amount of metal ion incorporation which changes as a function of the HCl/Si ratio. Vinu et al. have recently proposed that the lessened positive-charge on the SiO_2 particle under lower HCl/Si ratio promotes interaction between cationic hydroxo complex of metal cation and the surfactant-silica micelles, resulting in increase of the metal content [4]. Such extremely high heteroatom content was not achieved in VSBA-15, MoSBA-15, CoSBA-15 and CrSBA-15 prepared here. This could be mainly attributed to the fact that these cations have the tendency to form a complex with the chloride ion in the synthesis mixture and form the charged hydroxo complexes which decrease the pH of the synthesis mixture, resulting in a higher solubility of the metal source and reduce the amount of metal incorporation since the acid conditions easily induce the dissociation of the M–O–Si bonds. Another possible explanation for the relatively low

incorporation efficiency of metal species within the framework under these specific conditions could be related to some leaching occurring during template extraction [5]. It has been reported that in the case of aluminium-doped mesoporous materials the heteroatom source has a great influence on degree of insertion [6]. In the case of Zr-containing silica synthesized under acidic conditions; the use of a slowly hydrolysing source of zirconium may lead to a well crystallised SBA-15 framework [7]. Rapid heating and fast supersaturation are believed to enhance the degree of heteroatom insertion [8]. The increase in the overall metal amount inserted seems to disturb the mesoporous framework. It may be argued that the difference in the precursor reactivity and its hydrolysis result in a disordered hydrolysis–condensation, thereby contributing to the overall heterogeneity of the final product. The same explanation can be extended to TiSBA-15 and WSBA-15 materials prepared under the present synthesis approach.

3.2.2 X-ray Diffraction Analysis (XRD)

The low angle XRD patterns of SBA-15 and MSBA-15 materials are shown in figure 3.1. The d_{100} spacing and cell parameter obtained from XRD data and the wall thickness of SBA-15 are listed in Table 3.2. Small angle XRD pattern of mesoporous SBA-15 displays three well resolved peaks, a very intense peak at 2θ=0.96 and two distinct peaks at 2θ=1.59 and 1.85 which confirmed that the samples had an ordered structure. The XRD signals were indexed as (100), (110) and (200), a reflection associated with hexagonal symmetry with space group p6mm which was characteristic of SBA-15 materials. The XRD pattern is similar to those pure siliceous SBA-15 materials as reported by Zhao et al. [9, 10]. The length of the hexagonal unit cell a_o is calculated from the d spacing values using the formula $a_o = 2d_{100}/\sqrt{3}$. The calculated d spacing and unit cell parameters are well-matched with the hexagonal P6mm space group [11].

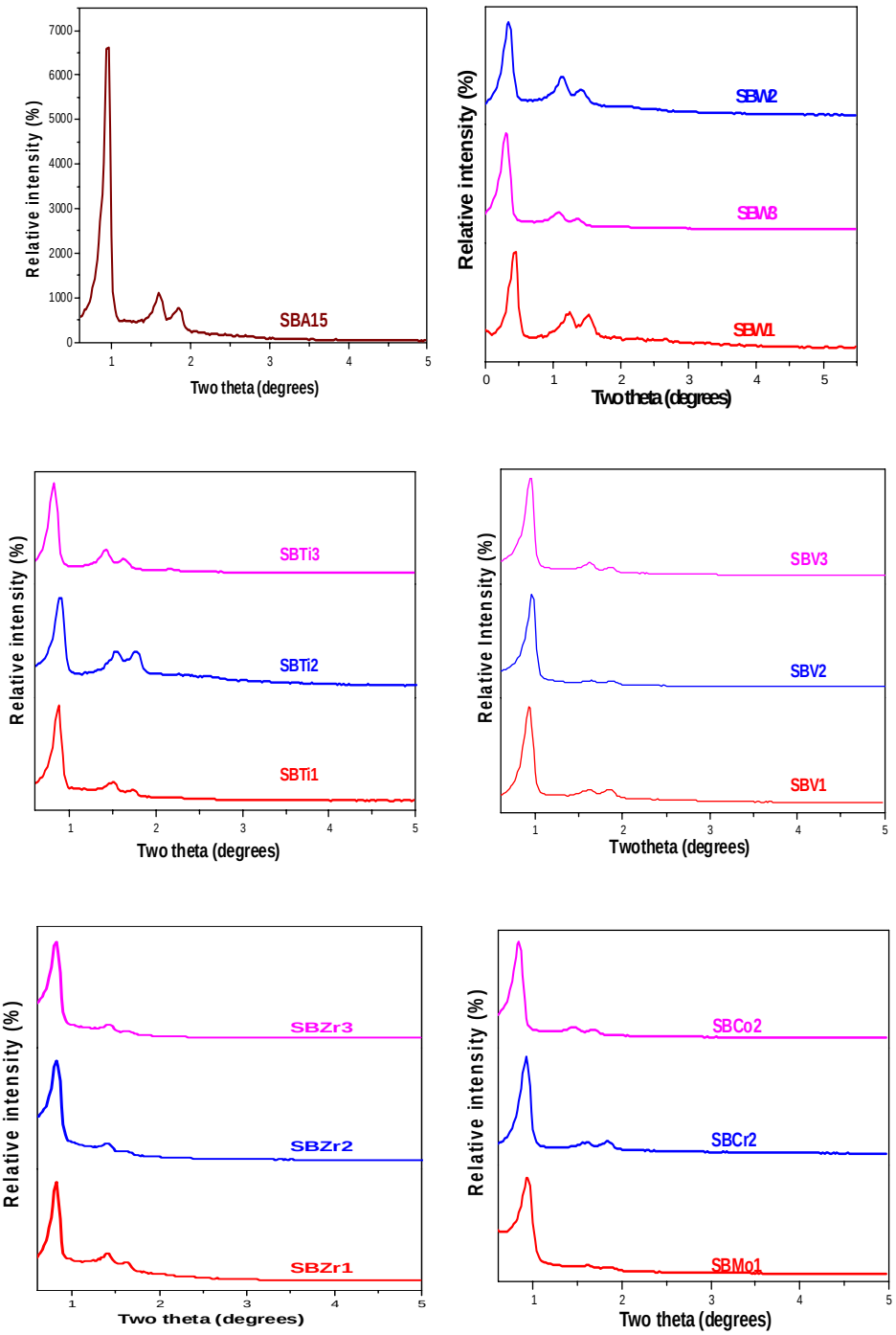
Relative intensity (%)
SBA15
Two theta (degrees)
SBV2
SBV8
SBV1
Two theta (degrees)
Relative intensity (%)
SBTi3
SBTi2
SBTi1
Two theta (degrees)
Relative Intensity (%)
SBV3
SBV2
SBV1
Twotheta (degrees)
Relative intensity (%)
SBZr3
SBZr2
SBZr1
Two theta (degrees)
Relative intensity (%)
SBCo2
SBCr2
SBMo1
Two theta (degrees)

Figure 3.1

No significant changes in the small-angle XRD patterns are observed after the solid state modification with transition metal oxides, demonstrating the preservation of the silica support long-range order. The XRD patterns of MSBA-15 samples also display three well resolved peaks at low angle which can be indexed to (100), (110), and (200) reflections in the hexagonal space group p6mm, which are very similar to those of SBA-15 itself. After metal incorporation, the presence of all the peaks (100, 110, 200) indicate that the addition of metal didn't destroy the characteristic structure of SBA-15. These results indicate that the uniform porous structure of SBA-15 is retained. The d-spacing of the modified samples slightly increase .This shift suggested that the framework of silica host was slightly enlarged during the synthesis process [12].

The unit cell parameter of the MSBA-15 samples is much higher as compared to that of the pure silica sample, which increases with increasing the metal content. This could be mainly due to the fact that the atomic radius of M^{n+} is larger as compared to that of the Si^{4+} (0.40A°) by assuming the coordination number of both the atoms as 4, leading to a longer M–O distance. Moreover, these observations suggest that the transition metal ions are successfully incorporated into the silica framework. However, the unit cell constant of the MSBA-15 materials is higher than that of the pure silica sample and increases with increasing the M content. The change in the unit cell parameter of MSBA-15 could be mainly due to the fact that a large charge mismatching in the surfactant- silica assembly process during the formation of mesophase changes the size of the unit cell as a huge amount of metal ions is involved in the synthesis process [3]. Similar such correlations have been reported as evidence for Ti substitution for Si in the framework of microporous TS-1 and large pore Ti-β molecular sieves [13, 14, 15].

Table 3.2

Catalysts	d_{100} (nm)	Unitcell parameter $a_o=2d_{100}/3^{1/2}$ (nm)	Wall thickness (a_0-pore diameter) (nm)
SBA-15	9.10	10.51	3.86
SBW1	10.53	12.16	6.03
SBW2	10.13	11.70	5.59
SBW3	9.32	10.76	4.66
SBTi1	10.77	12.44	5.85
SBTi2	9.98	11.52	4.60
SBTi3	9.89	11.42	4.04
SBZr1	10.79	12.46	4.73
SBZr2	10.70	12.36	4.46
SBZr3	10.67	12.32	4.07
SBV1	9.49	10.96	4.98
SBV2	9.29	10.73	4.43
SBV3	9.26	10.69	4.23
SBMo1	9.44	10.90	3.95
SBCo2	10.50	12.12	6.62
SBCr2	9.62	11.11	4.87

3.2.3 Wide Angle XRD Analysis

Figure 3.2 illustrates the X-ray diffractions within the range of 3-70^0 of calcined SBA-15 and M-SBA 15. Only the diffuse peaks of noncrystalline silica have been observed for most of the samples and no characteristic peaks belong to metal oxides. It indicates that the crystalline size of metal oxides is below the lower limit for XRD detectability (5nm) or an amorphous metal oxide is formed [16]. All the samples showed a broad reflection ranging from 15-30^o characteristic of amorphous silica. In the wide angle XRD pattern appreciable characteristic peaks of the crystalline metal oxide were observed for the samples having (Si/M=10) but the intensity of peaks were very low. For lower loadings no characteristic peaks were observed. The absence of peaks of MOx indicates that the MOx guest has been highly dispersed in the molecular sieve framework of SBA-15.

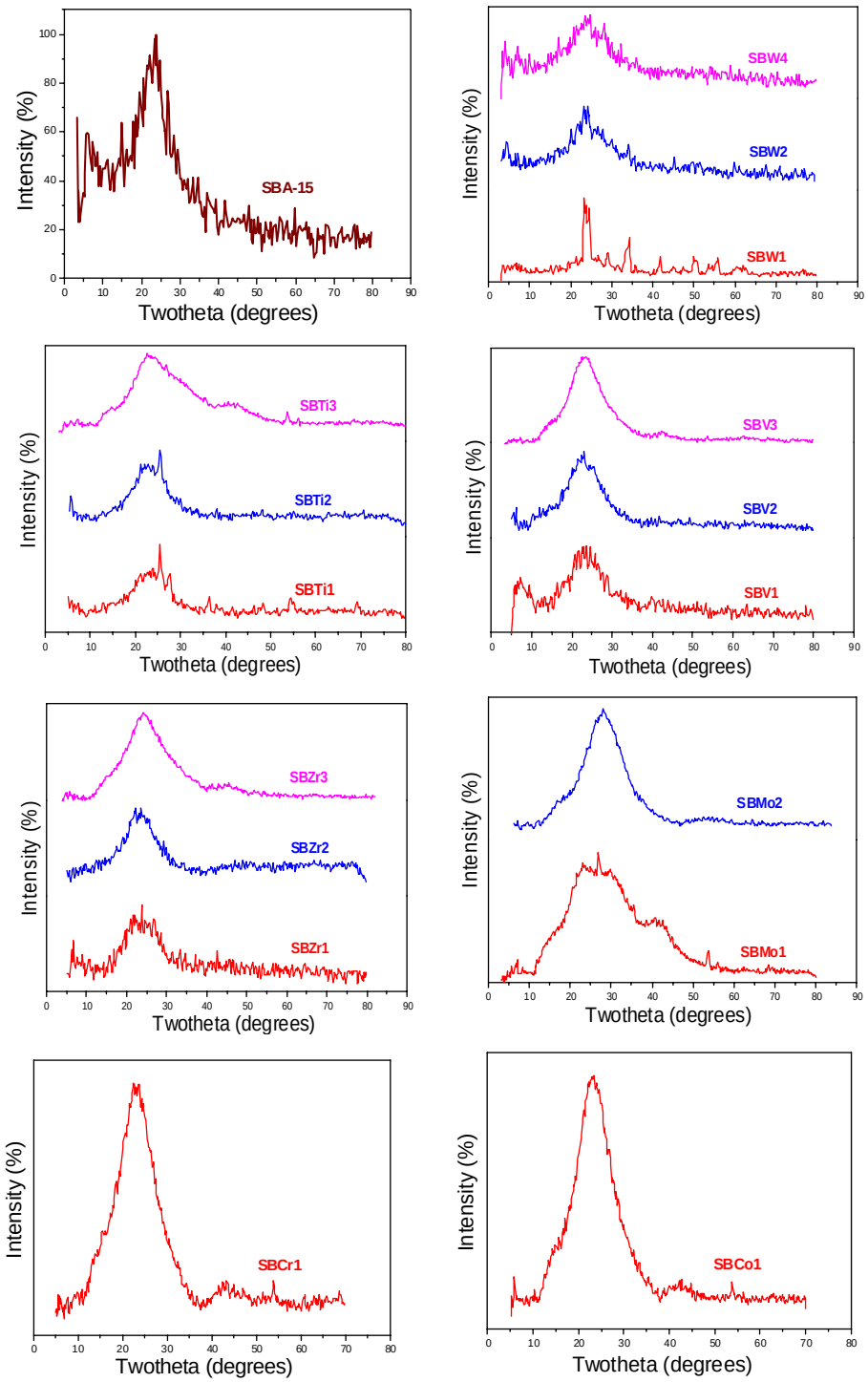
Intensity (%)
Twotheta (degrees)
SBA-15
SBW4
SBW2
SBW1
SBTi3
SBTi2
SBTi1
SBV3
SBV2
SBV1
SBZr3
SBZr2
SBZr1
SBMo2
SBMo1
SBCr1
SBCo1

Figure 3.2

3.2.4 BET Surface Area and Pore Volume Measurements

The metal/SBA-15 composites, together with the calcined SBA-15 silica, were characterized by N_2 adsorption-desorption measurements. The N_2 adsorption-desorption isotherms and the calculated pore size distributions obtained from the desorption braches using the BJH method of calcined SBA-15 mesoporous silica and MSBA-15 with different Si/M mole ratios are shown in Figure 3.3 and Figure 3.4. The main textural properties of different samples are listed in Table 3.3, including BET specific surface area (S_{BET}), total pore volume (V_P), pore diameter (D_{BJH}) from N_2 adsorption-desorption measurements, and are discussed in this section.

Table 3.3

Catalysts	Surface Area (m^2/g)	Total Pore Volume (cm^3/g)	Average Pore Diameter (nm)
SBA15	907	1.449837	6.65
SBTi1	470	1.030485	6.59
SBTi2	479	1.150491	6.92
SBTi3	570	1.230535	7.38
SBW1	679	1.042059	6.13
SBW2	739	1.214384	6.11
SBW3	795	1.205528	6.10
SBV1	548	0.901715	5.98
SBV2	558	0.914544	6.30
SBV3	564	1.053105	6.46
SBZr1	458	1.281061	7.73
SBZr2	506	1.294542	7.90
SBZr3	601	1.423990	8.25
SBMo1	657	1.007491	6.95
SBMo2	748	1.012146	7.05
SBMo3	779	1.203405	7.17
SBCr1	711	0.995818	5.97
SBCr2	722	1.120694	6.24
SBCr3	798	1.287856	6.55
SBCo1	725	0.909297	5.25
SBCo2	786	1.069232	5.50
SBCo3	883	1.359911	7.23

As observed in Figure 3.3, the isotherms of SBA-15 and MSBA-15 with (Si/M) mole ratio 10-30 show typical type IV features and have an H1 hysteresis loop in which the two branches are almost vertical and are nearly parallel over an appreciable range of relative pressure (P/P_0). It was observed that two obvious inflection points in the adsorption isotherms are in the range of relative pressure P/P_0= 0.4–0.8 for all the prepared samples. The volume of adsorbate shows a sharp increase at a P/P_0 of approximately 0.70 arising from capillary condensation of nitrogen within the uniform mesoporous structures. It is typical for the mesoporous materials with 2D-hexagonal structure that has large pore size and narrowed size distribution. This is characteristic of homogeneous distribution channels in highly ordered mesoporous materials. Moreover, the narrow pore size distribution confirms the regularity of the pore diameter. The adsorption–desorption isotherms move slightly to low pressure, presumably because the meso channels shrink after introducing metal oxides into SBA-15 [17]. The sharpness of the inflection step also decreased gradually for Si/M molar ratio down to 10, but decreased significantly there for it can be speculated that the greater heterogeneity of pore size distribution has occurred. The P/P_0 position of the inflection points is clearly related to a diameter in the mesopore range. The textural and structural properties clearly demonstrate that the distribution of metal within SBA-15 is highly dependent on the metal content. For lower metal content, the metal oxides are uniformly distributed within the SBA-15 channels. For higher metal content, the distribution of metal oxides within SBA-15 may not be uniform and may be occurring in the channels and on intrachannel surfaces, and there may be a higher proportion of framework metal atoms. In the present work the shape of the isotherm and pore size distribution curves of the prepared catalysts did not show any sign of the percolation effect. It is reasonable to conclude that present synthesis approach is an efficient method to disperse various transition metal oxides inside the pore channels of SBA-15.

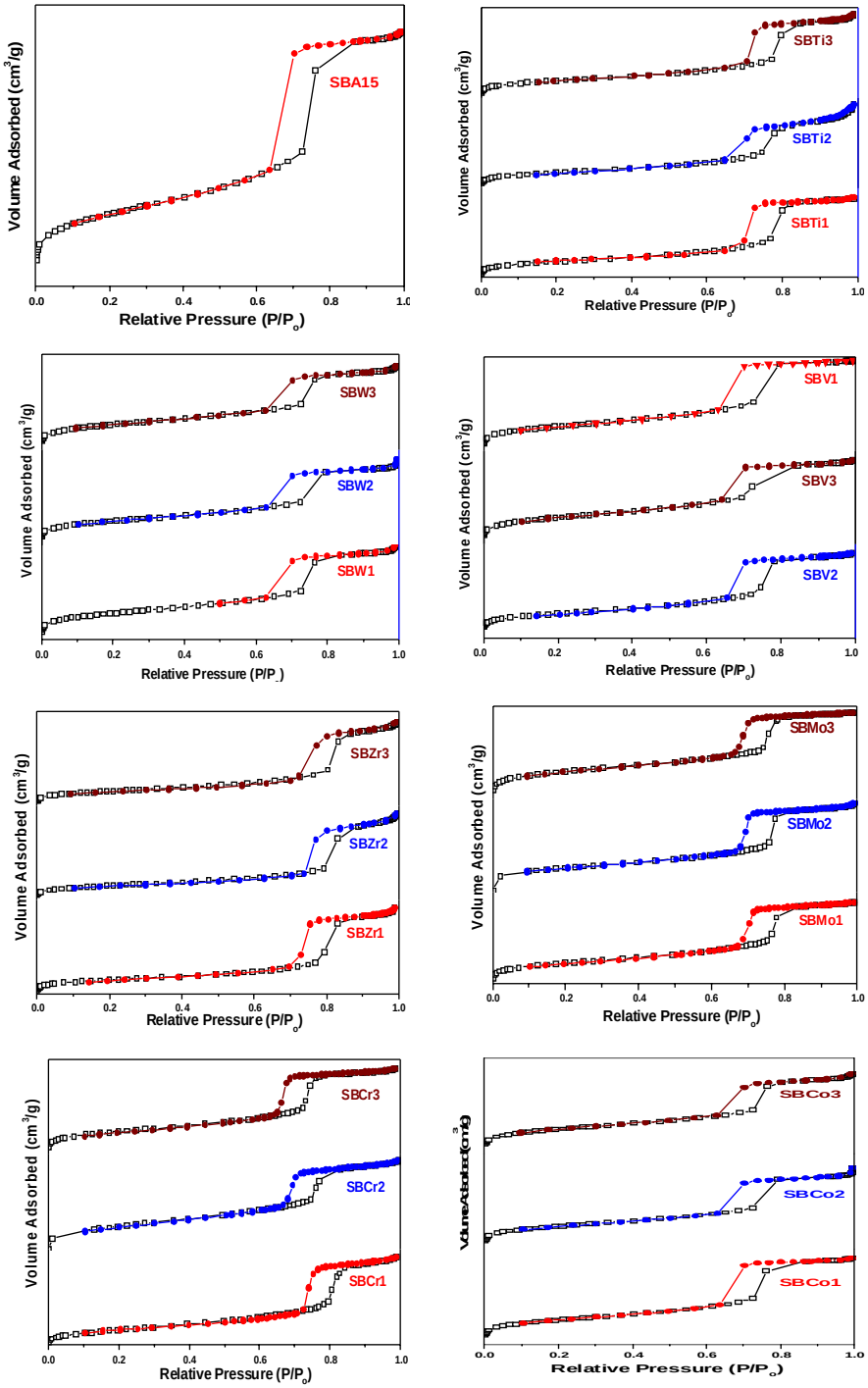
SBA15
SBTi3
SBTi2
SBTi1
SBW3
SBW2
SBW1
SBV1
SBV3
SBV2
SBZr3
SBZr2
SBZr1
SBMo3
SBMo2
SBMo1
SBCr3
SBCr2
SBCr1
SBCo3
SBCo2
SBCo1
Volume Adsorbed (cm3/g)
Relative Pressure (P/Po)

Figure 3.3

SBA-15 exhibited a uniform hexagonal array of mesopores connected by smaller micropores and the broad hysteresis loop in the isotherms for all the studied samples is an indication of long mesopores. The BET surface area of the modified samples decreased compared with that of the bare SBA-15, which suggested the incorporation of metal nanoparticles into the pore channels of SBA-15 [18, 19, 20]. This trend continued with the further increases in metal content on SBA-15.

High surface area and large total pore volume values are obtained for all samples prepared compared with corresponding metal oxide catalysts. Larger surface area and pore volume are probably due to the improved order of the mesoporous SBA-15 structure. These results suggest that the samples possess a highly ordered framework with cylindrical mesoporous channels, in line with the interpretation of the XRD patterns shown in Figure 3.1. Pure SBA-15 possesses high surface area 907 m^2/g, on metal incorporation the surface area decreases due to pore blockage. The values of S_{BET} and V_P both show a monotonic decrease with increasing concentration of transition metals consistent with the formation of metal oxides within the mesoporous structure of SBA-15. Even for the highest metal content, (MSBA-15 (Si/M) 10), the values of S_{BET} and V_P are more than 50% of the corresponding values for the host itself. As shown in Table 3.2, the cell parameter increases with metal content. The increase in the cell parameter is consistent with the incorporation of metal atoms into the framework of SBA-15.

The pore size distributions have been determined by referring to the BJH model applied to the desorption isotherm branch (the desorption branch better meets the requirements of ideal wetting inherent in the model). The quantitatively obtained averaged pore diameters summarized in Table 3.3 showed absence in large deviations of pore diameter after metal oxide incorporation.

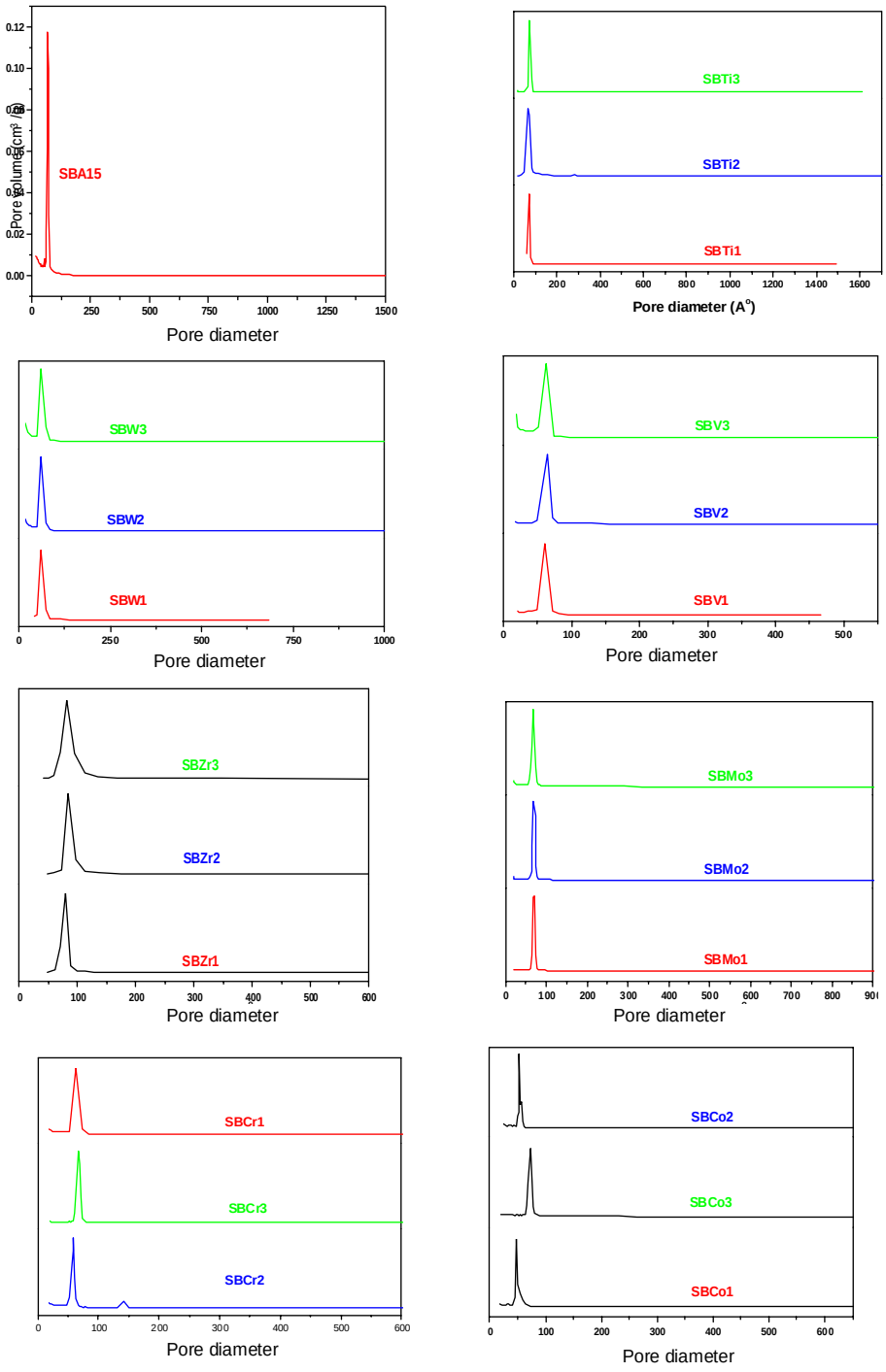
SBA15
Pore volume(cm³/g)
Pore diameter
SBTi3
SBTi2
SBTi1
Pore diameter (A°)
SBW3
SBW2
SBW1
Pore diameter
SBV3
SBV2
SBV1
Pore diameter
SBZr3
SBZr2
SBZr1
Pore diameter
SBMo3
SBMo2
SBMo1
Pore diameter
SBCr1
SBCr3
SBCr2
Pore diameter
SBCo2
SBCo3
SBCo1
Pore diameter

Figure 3.4

However, the BJH pore size distribution of each sample is narrow, suggesting an open mesopore channel. It also implies that the transition metal oxides are well dispersed and are accessible via the open pore channels [21].

3.2.5 FT- IR Spectroscopy

Infrared spectroscopy has been used extensively for the characterization of transition-metal cation modified molecular sieves. A comparative FT-IR study of the prepared calcined materials is presented below. FT-IR spectra of the prepared samples in the infrared region from 400 to 4000 cm^{-1} are shown in Figure 3.5. The bands at about 460 cm^{-1}, 1081 cm^{-1}, and 800 cm^{-1}, were detected for all transition metal substituted SBA-15 samples. The bands at 3745 cm^{-1} can be assigned to the stretching vibration mode of isolated terminal silanol (Si-OH) groups [22], whereas the bands at 3430 cm^{-1} can be assigned to the hydrogen-bonded Si-OH groups because of geminal Si-OH of Q^2 and adjacent Q^3. It is consistent with the FTIR result of previous reports by Zhao et al. [23] who deemed the band at 3222 cm^{-1} to hydrogen-bonded Si-OH groups perturbed by physically adsorbed water.

The FTIR spectra of the parent mesoporous material SBA-15 (Figure-3.5) present bands at about 460, 800, and 1080 cm^{-1}, attributed to the vibration modes of the silica host matrix [24, 25, 26]. The presence of hydroxyl groups, in different amount and coordination is well seen in the region 3200–3600 cm^{-1}. The characteristic band at 3640 cm^{-1}, recorded for SBA-15, is ascribed to the presence of terminal Si–OH groups. The band at 3480 cm^{-1}, with a shoulder in the low frequencies region, observed for SBA-15, is due to the presence of terminal silanol groups and their interaction with the neighboring hydroxyl groups. A small peak of isolated silanol groups, at about 3690 cm^{-1}, is also observed. The existence of silanol groups, situated as silanol nests is verified by the band centered at 960 cm^{-1} [27,28,29].

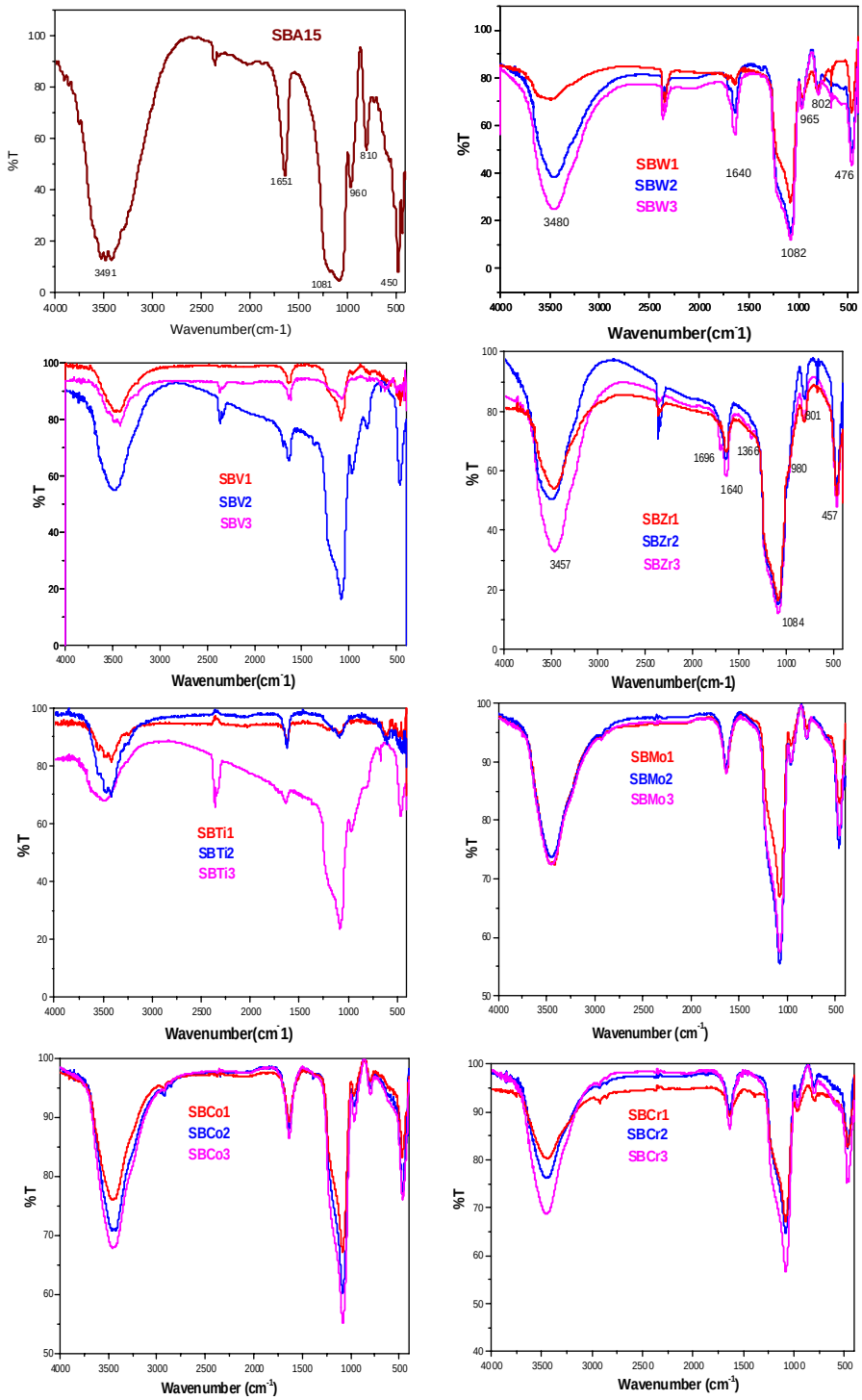
SBA15
%T
Wavenumber(cm-1)
3491
1651
1081
960
810
450
SBW1
SBW2
SBW3
3480
1640
1082
965
802
476
Wavenumber(cm-1)
SBV1
SBV2
SBV3
Wavenumber(cm-1)
SBZr1
SBZr2
SBZr3
3457
1696
1366
1640
1084
980
801
457
Wavenumber(cm-1)
SBTi1
SBTi2
SBTi3
Wavenumber(cm-1)
SBMo1
SBMo2
SBMo3
Wavenumber (cm-1)
SBCo1
SBCo2
SBCo3
Wavenumber (cm-1)
SBCr1
SBCr2
SBCr3
Wavenumber (cm-1)

Figure 3.5

The band area of 3430 cm^{-1} for MOx- SBA-15 samples displays gradual decrease with increasing metal content. This indicates that the amount of the O-H bond in Si-O-H decreases after metal-doped hydrothermal synthesis. It is consistent with the formation of Si-O-M bonds by the combination of metal and hydroxyl groups of Q^3 sites during calcination on the intrachannel surfaces of SBA-15. As shown in Figure 3.5, the bands at 966 cm^{-1} and 810 cm^{-1} correspond to characteristic stretching vibration of nonbridging oxygen atoms ($Si\text{-}O^{\delta-}$) of Si-O-H bonds and symmetric stretching vibration (Si-O-Si) of tetrahedral $SiO4^{4-}$ for SBA-15 [23].

The sharp absorption band at 3740–3745 cm^{-1} due to the O–H stretching vibration of free hydroxyl groups (figure 3.5) was considerably more intense for the blank sample than for the transition metal incorporated samples suggesting that a proportion of the surface silanol groups were utilised for bonds to the transition metal sites. The O–H stretching band was also considerably broadened for the metal-incorporated samples, and slightly displaced, with respect to the blank showing that several different O–H groups were present in addition to free Si–OH groups. The diverse chemical nature of the silanols leading to band broadening for the modified samples may be due to additional H-bonding between hydroxide groups, or to interactions with neighbouring transition metal Lewis centres, increasing the hydroxide group acidity [30]. The silanol groups "consumption" through its interaction with MOx and formation of a SiO_4 unit bonded to a metal ion is well demonstrated by the decrease of the bands at 3400–3600 cm^{-1} [29]. Hence, it could be deduced that, for the MSBA-15 molecular sieves, the change in intensity of silanol groups might be due to the metal species, mostly existed in the framework of SBA-15 [31].

3.2.6 Thermogravimetry

TG analysis of SBA-15 type materials provides information about the mass loss steps of the uncalcined samples. The mass loss steps are located in the following temperature ranges: 1) from 30- 100^0C as thermodesorption of physically adsorbed water; 2) from 100-450^0C as P123 decomposition and 3) from 450-600^0C as residual P123 decomposition and water from silanol condensation [32]. The thermogravimetric monitoring of the P123 removal from the SBA-15 material represents a good technique to preview the temperature and time for calcinations, in order to obtain a high quality material.

The thermogravimetric (TG) plots for the as-synthesized SBA-15 sample are given in Figure 3.6. With an increase in temperature the sample gradually loses weight up to *ca.* 380 K. This could be due to the removal of water molecules present in the external and internal surfaces of the material. From 380 to 723K the sample loses rapidly its weight, which is mainly due to the decomposition of the organic templating molecule P123 [33]. A broad exothermic peak centered at 723K suggested the burning of the template molecules. After that the sample undergoes a slight weight loss steadily till 1073K.

All TG curves of the transition metal modified samples show analogous behaviour, which is characteristic for uncalcined SBA-15 type materials. The TG traces of MOx-SBA-15 with different metal content are also shown in Figure 3.6.

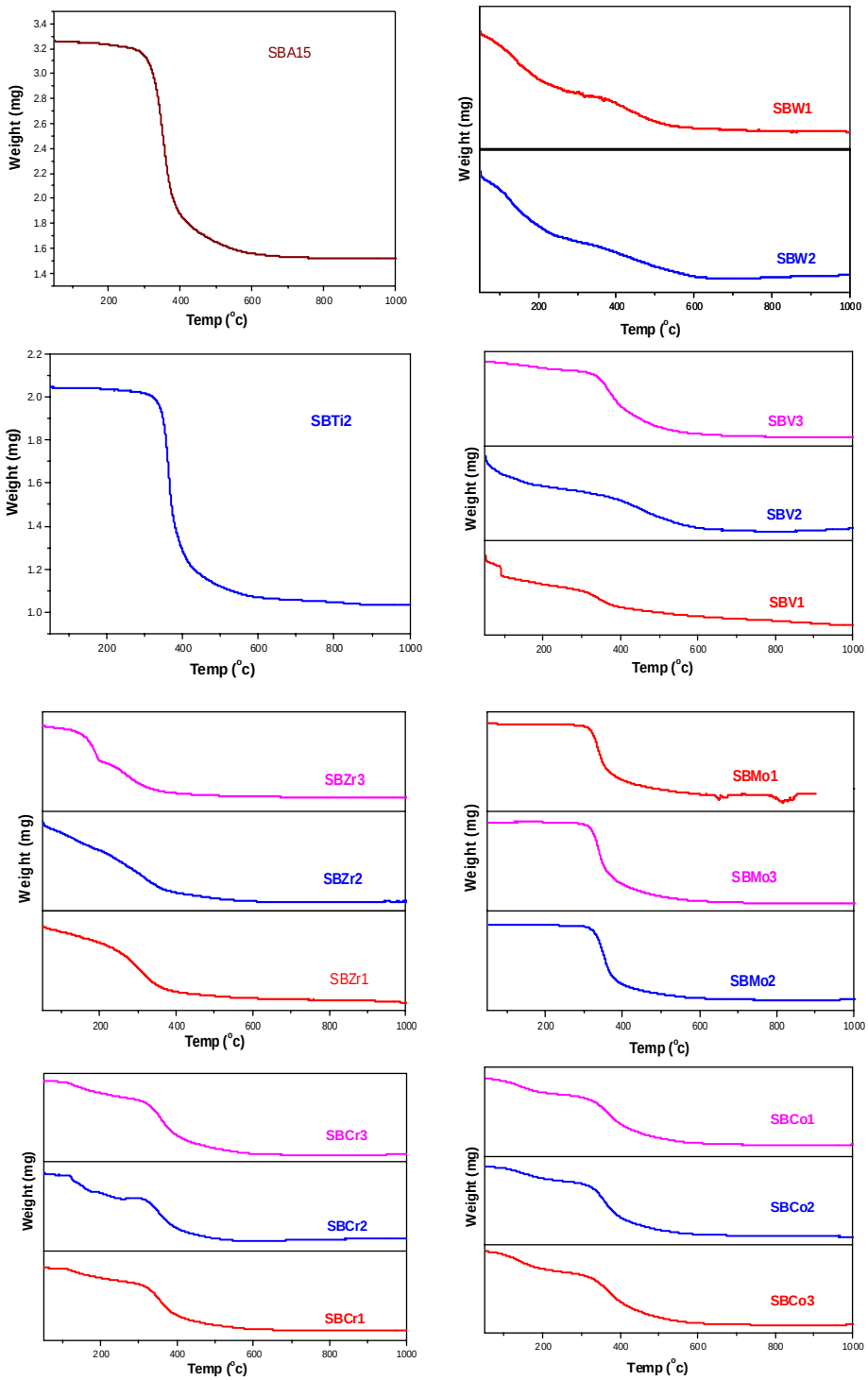
SBA15
Weight (mg)
Temp (°c)
SBW1
SBW2
SBTi2
SBV3
SBV2
SBV1
SBZr3
SBZr2
SBZr1
SBMo1
SBMo3
SBMo2
SBCr3
SBCr2
SBCr1
SBCo1
SBCo2
SBCo3

Figure 3.6

3.2.7 UV-vis DRS Spectroscopy

Electronic spectroscopy in the UV–vis region is a useful technique for studying the local coordination environment and electronic state of isolated transition metal ions as well as aggregated transition metal oxides. In order to obtain information of surrounding environment of incorporated transition metal atoms in the SBA-15 framework, UV–vis diffuse reflectance (UV–vis DRS) spectra were measured. UV-VIS DRS is widely used to detect the presence of framework or extra frame work active species that are incorporated in to the mesoporous materials. Generally the major absorption peaks for mesoporous materials like SBA-15 were found between 200-400nm. Position of adsorption bands gives information regarding surrounding environment of metal atoms in silica framework. A band at lower wavelength (at about 200–240 nm) is assigned to a ligand-to-metal charge-transfer transition in isolated MO_X or $HOMO_{X-1}$ units. This band can be the direct evidence for metal atoms incorporated into the framework of the mesoporous silica. A band at higher wavelength is typical of ligand to metal charge-transfer, from which the presence of bulk metal oxide is indicated. All the samples prepared in the present work exhibit a sharp peak at the UV region around 200 nm with no broad band near the higher wavelength. Thus the heteroatoms introduced by this route locate at mainly tetrahedrally coordinated sites. With increasing metal concenteration, the peak around 200 nm is somewhat broadened with maintaining the same peak wavelength. The UV–vis DRS spectra of the as synthesized and calcined MSBA-15 samples with different Si/M ratios are shown in Figure 3.7 (pure siliceous materials do not present electronic transitions in this spectral region) [34].

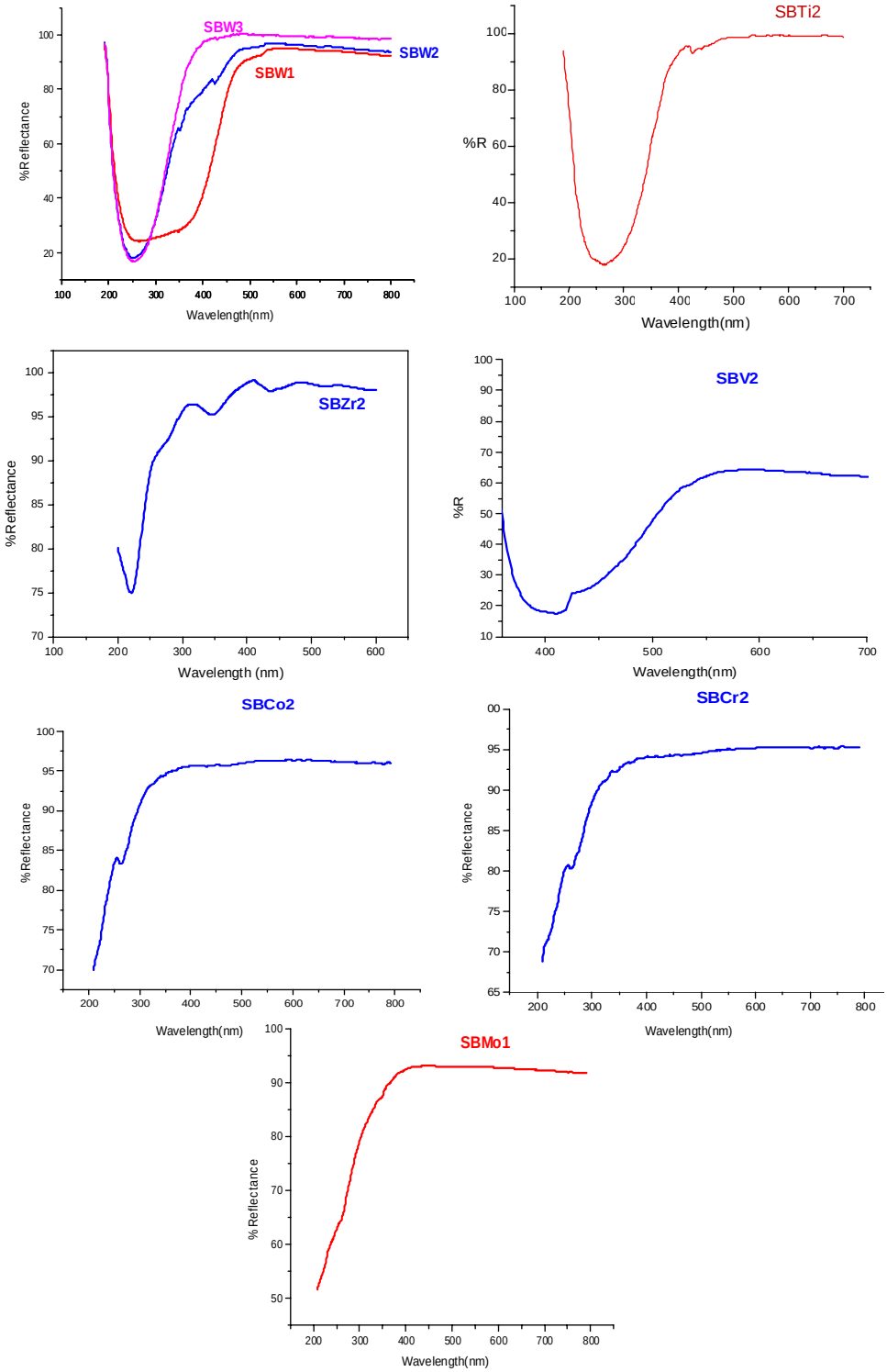
SBW3
SBW2
SBW1
%Reflectance
Wavelength(nm)
SBTi2
%R
Wavelength(nm)
SBZr2
%Reflectance
Wavelength (nm)
SBV2
%R
Wavelength(nm)
SBCo2
%Reflectance
Wavelength(nm)
SBCr2
%Reflectance
Wavelength(nm)
SBMo1
% Reflectance
Wavelength(nm)

Figure 3.7

The WSAB-15 samples were colorless, which indicates the absence of any colored crystalline WOx species on the outside of the framework. The synchrotron radiation XRD analysis also indicated that no significant diffraction patterns corresponding to crystalline WOx appeared during the course of calcinations up to 500^0C. This result is supported by a comparison of the diffuse reflectances of WSBA-15 in the UV–Vis region (Figure 3.7). We assign unambiguously the broad absorption band between 250-300 nm to the (Laporte allowed; sp^3 - sd^3) ligand-to-metal electron transition, which is consistent with tetrahedral sites on silica-based materials. The more-intense absorption band observed for WSBA-15 supports the assumption that the majority of the tungsten atoms remain in tetrahedrally coordinated geometries within the SBA-15 framework [35].

Ultraviolet spectra absorption spectroscopy has been extensively used to characterize the constituents of the local Ti environment. Figure 3.7 shows the UV–vis DR spectra of the as synthesized and calcined TiSBA-15 samples with different Si/Ti ratios. As expected, all spectral features are due to metal charge transfers between the oxygen-ligand and the titanium (IV) ion. At low titanium loading the observed absorption band maximum is at 214 nm, the peak can be assigned to isolated tetrahedral species present within the walls or near the surface [36]. For increasing titanium loading the maximum shifts to near 220 nm in the absorption spectrum and its intensity increases somewhat with increasing titania content. Further increase in titanium loading show an absorption band over the 228 nm range, which is blue shifted from the spectrum of bulk TiO_2 anatase (335 nm) [37]. The absorption maximum at 230 nm has been observed for various zeolite materials that contain tetrahedral titanium like TS-1 and has been assigned to a charge transfer transition between the oxygen ligands and a central Ti^{4+} ion with tetrahedral coordination [38]. Thus, inspection of UV–vis diffuse

reflectance spectra of the TiSBA-15 samples implied that the Ti ions were well dispersed [39]. UV–vis DR spectra of the prepared materials confirmed that Ti atoms are exclusively incorporated within silica framework and occupy the tetrahedral position while the presence of isolated bulk titania could be negligible [3]. These results indicate that most of the Ti species in the TiSBA-15 materials, regardless of the Ti content, are mostly tetrahedrally coordinated in the SBA- 15 silica walls. A slight difference in the adsorption in the samples could be mainly due to the difference in the amount of Ti coordinated in the silica framework. A similar high-energy absorption edge due to tetrahedral coordination of Ti has been observed for other titanium-containing molecular sieves [33, 40-46]. The high-energy absorption band of titanium silicate indicated that the tetrahedral coordination of Ti is predominant in this material.

CoSBA-15 samples are analyzed by UV–vis spectroscopy in order to investigate the local environment of cobalt ions present in the materials. As shown in figure 3.7, the UV –VIS spectra of Co SBA-15 sample display three absorption peaks between 200-400 nm, which can be unambiguously assigned to the $^4A_2(F) \rightarrow {}^4T_1(P)$ transition of Co (II) ions in tetrahedral environments [47-49]. The absence of peaks at around 480 and 506 nm indicates the absence of Co (II) in an octahedral environment [50], and the absence of peak at 410 nm indicates the absence of Co (III) [51]. The long time stirring, subsequently filtrating, and gently washing permit the sufficient reaction between Co^{2+} and SiO^- groups and prevent the excessive Co^{2+} from adsorbing on the surface. Thus at low CoO loading , CoO may be formed in tetrahedral coordination state inside the walls and inner surface of SBA 15 . The abundant silanol and the walls of SBA-15 may stabilize low loading of CoO in tetrahedral coordination [52].

Additional information on the oxidative state of the vanadium species and their environment is seen in the UV–vis spectra. A broad band at about 260 nm and a shoulder at 310 nm could be assigned to a low energy ligand to metal charge transfer (LMCT) of tetrahedral V^{5+} species, coordinated to the mesoporous silica surface [53-55]. A broad band between 200 nm and 350 nm, assigned to low-energy charge transfer transitions between tetrahedral oxygen ligands and central V^{5+} ion, was observed for all samples [53, 56]. Such a tetrahedral environment was typical for framework V^{5+} ions in V-substituted micro and mesoporous molecular sieves [32, 54].

DR UV-vis spectroscopic results for Zr ions dispersed within silica SBA-15 agree with the data published by Moon *et al*. [57], who produced a series of spectra for decreasing Zr content in a mixed zirconium–silicon oxide. The absorption peak is situated below 220 nm for low Zr contents. The electronic transitions of the Zr ions should occur at wavelengths around 200 nm [30].

All the as synthesized CrSBA-15 materials show a very intense band in the 210–220 nm wavelength regions that is shifted toward higher wavelength with increasing the Cr content. This could be due to the electronic transition from oxygen 2p to Cr^{6+} 3d orbital

The molybdnum environment in MoSBA-15 samples was evaluated by means of diffuse reflectance UV-Vis spectroscopy, the spectra being depicted in Figure 3.7. All the samples show DR-UV Vis signals located at 210 nm and are attributed to the presence of Mo^{6+} species in a silica matrix adopting a tetrahedral coordination.

3.2.8 SEM Pictures: morphological characterization

Morphology as well as structural ordering of SBA-15 and MSBA-15 samples were analyzed by electron microscopy studies and are shown in figure 3.8 [52]. Morphologies of SBA-15 material and its metal-doped families have been well characterized. We have successfully prepared SBA-15 materials in well-ordered crystal morphologies through control of synthetic conditions. Morphology depends on the synthesis conditions (silica source; presence of co-surfactant; etc.) Acidity of the synthetic gel is also known as an important factor to determine mesophase of the resulting silica materials. Condensation rate of alkoxy silicate is much influenced by surrounding acidity, which is strongly related to charge density of the formed silica precursor. Charge matching in $S^0H^+X^-I^+$ complex leads to changes in packing and morphology of the template micelle, eventually resulting in control of mesophase and morphologies of mesoporous silica particles. Similarly, factors to modify charge density and morphologies of silica precursor and template micelles are expected to be important in morphological control of SBA-15 materials. Characteristic rod like morphology of SBA-15 was preserved for all the prepared MSBA-15 samples.

The SEM images clearly show that the morphology of the present MSBA-15 samples form fibrous aggregates, the typical shape of SBA-15 type particles [10].This trend has been also previously detected in the case of MCM-41 materials synthesized with high loadings through direct synthesis procedures, but in that case the final materials turn microporous [58] regarding the morphology at the mesoscale. For some samples nanodomains of ordered material are observed and worm-like pore channels are dominant [5].

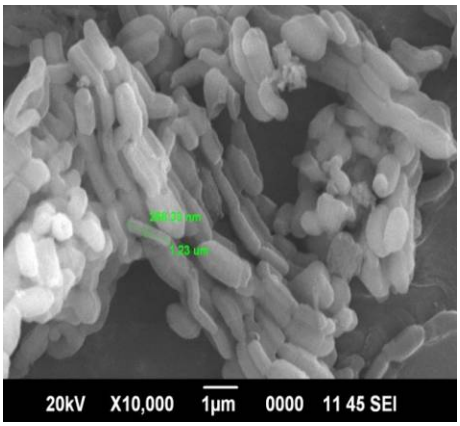

SBA 15

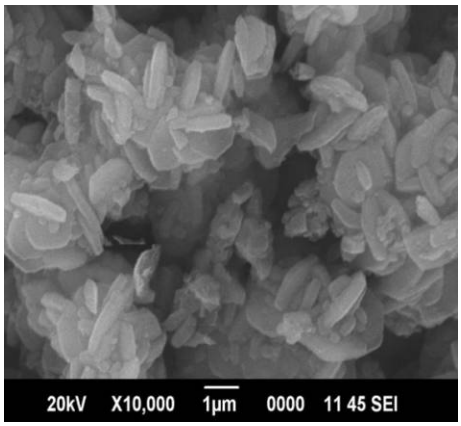

SBZ1

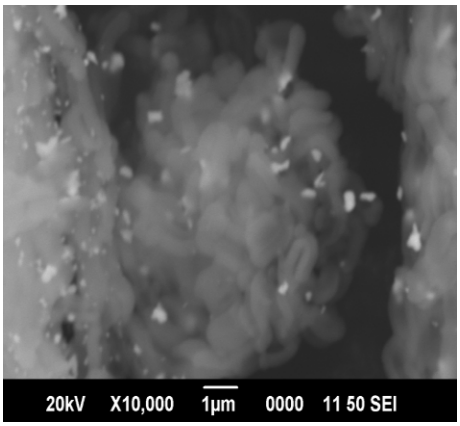

SBW1

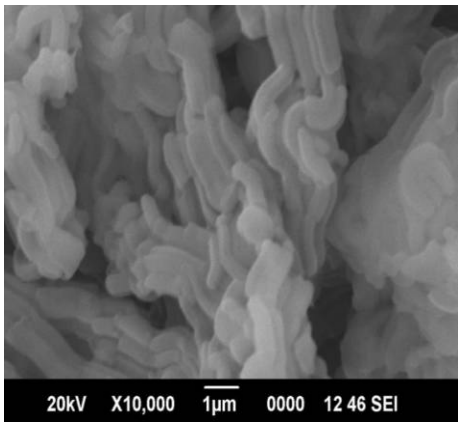

SBMo1

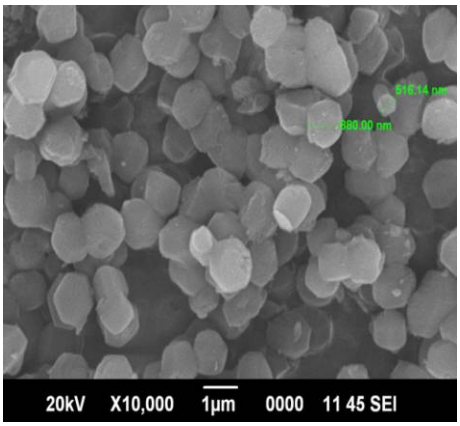

SBTi1

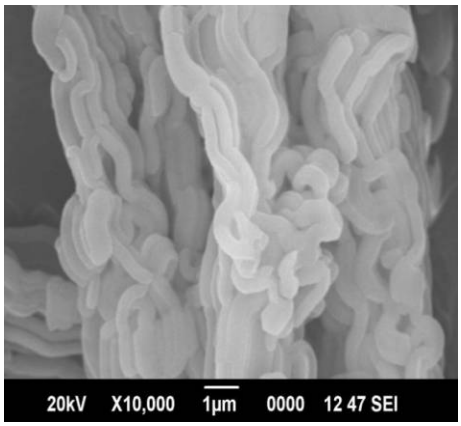

SBMo2

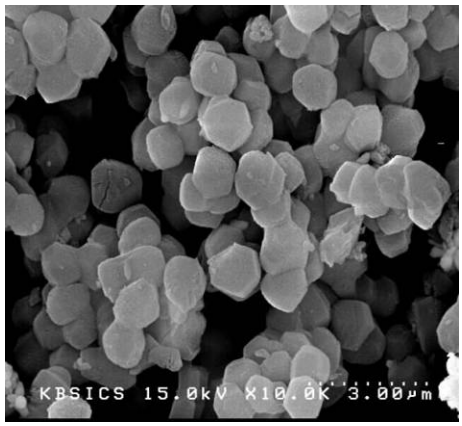

SBTi2

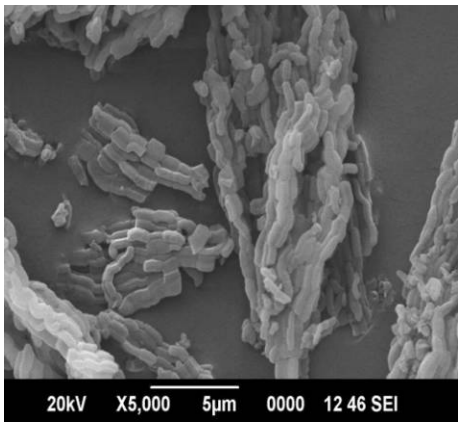

SBCr1

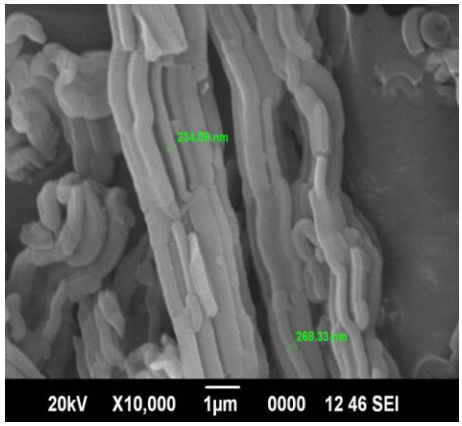

SBTi3

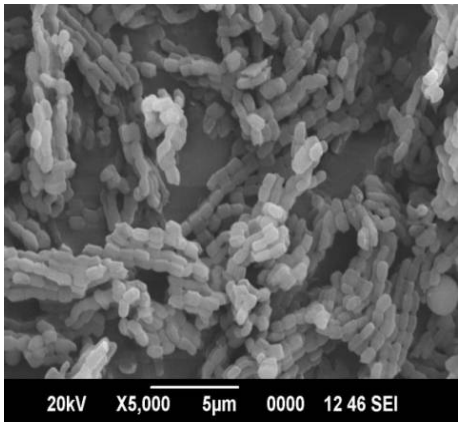

SBCo1

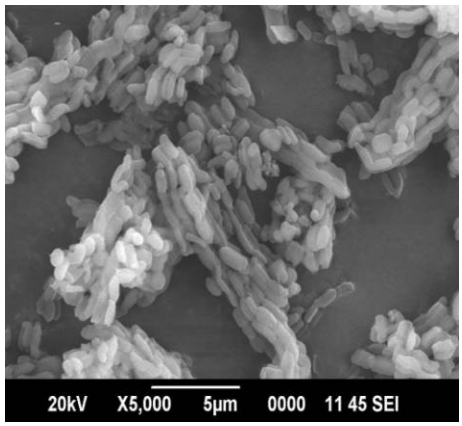

SBV1

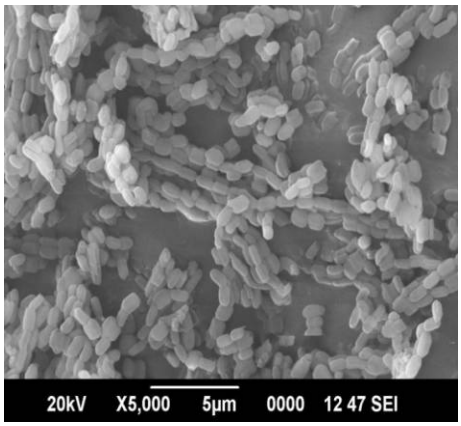

SBV2

Figure 3.8

Majority of TiSBA-15 materials are hexagonal particles where objects of fused particle can also be observed. The morphological control of TiSBA-15 with increasing the Ti content could be due to the fact that the incorporation of Ti atom in SBA-15 silica framework induces mismatches in size and lattice due to difference of atom radius, possibly resulting in large curvature in the TiSBA-15 materials [3]. However, the exact mechanism in the observed morphological control is currently under veil.

The SEM image shows that the curved morphology of the Co-SBA-15 materials, rope like aspect of as long as several hundred micrometers is the enlarged SEM image of this sample. It is observed that many strip-like structures with relatively uniform sizes (the length is about 1.5 lm and the width is around 0.4 lm) are aggregated into rope-like macrostructures [11].

SEM images show that the morphology of MSBA-15 remains the same as that of parent SBA15.

3.2.9 TEM Pictures: morphological characterization

The morphological analysis was also carried out using Transmission electron Microscopy. The micrographs taken with the beam direction perpendicular to the pores evidences that the well- ordered hexagonal arrangement of the SBA-15 framework is maintained after MOx is introduced. On the other hand, taken with the beam direction parallel to the pore direction the hexagonally ordered pore structure can clearly be observed in the micrographs, and no MOx particles have been found on the outside surfaces of samples, indicating that MOx is highly dispersed. It is also consistent with the XRD spectra [52]. The different morphologies of the nano structured metal incorporated materials may be attributed to the intrinsic properties of the different metals, such as surface energy, redox potential, etc. [59, 60]. Further investigation is being conducted for a better understanding. TEM analysis results of SBA-15 and metal/SBA-15 composites

are shown in Figure 3.9. The representative TEM images reveal that the SBA-15 silica materials have a well-ordered mesoporous channel structure, which supports the afore mentioned N_2 sorption and low-angle XRD results and the metal nanoparticles were highly dispersed in the interior of the SBA- 15 channels [18].

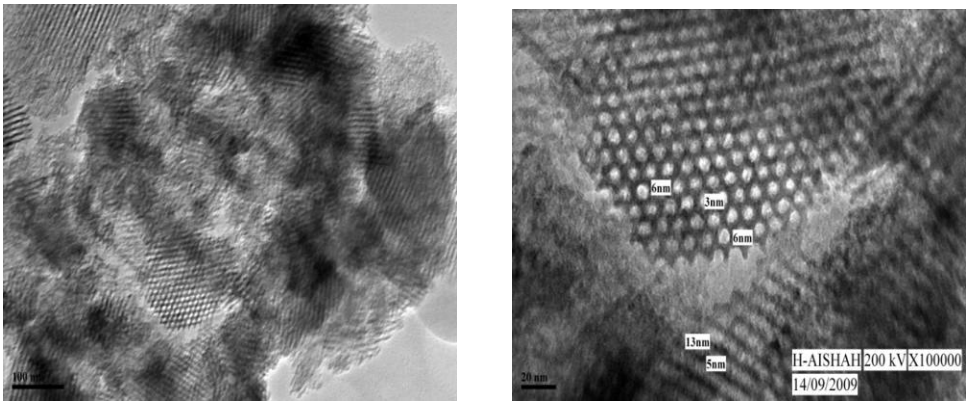

SBA -15

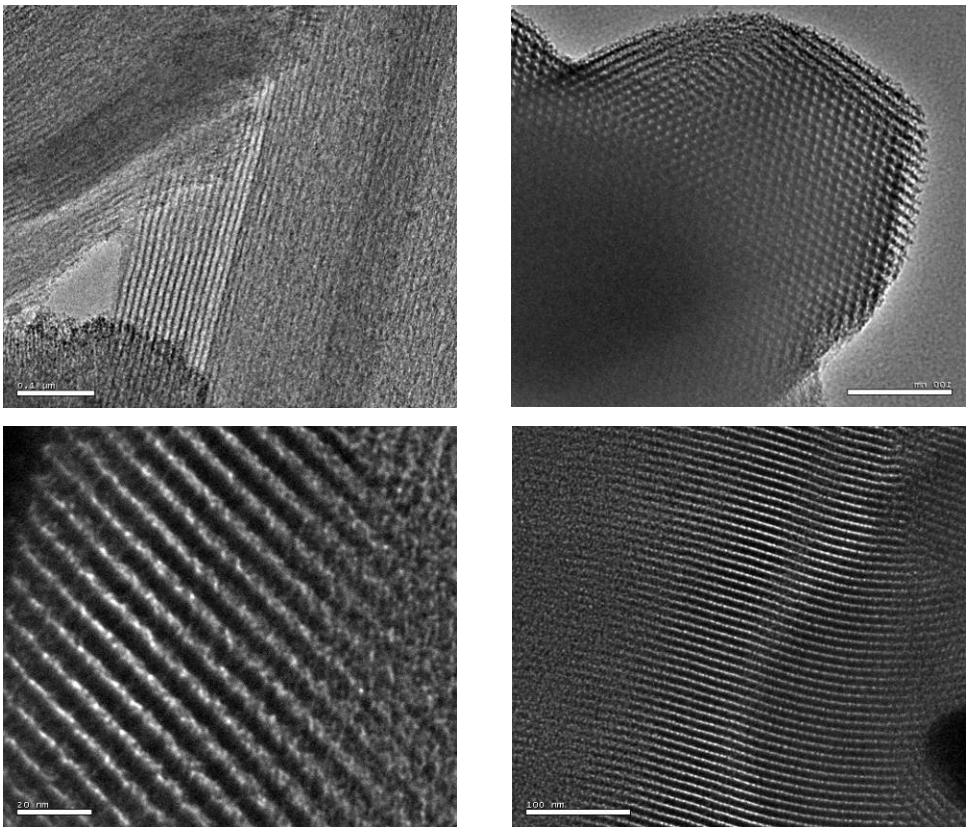

SBW1

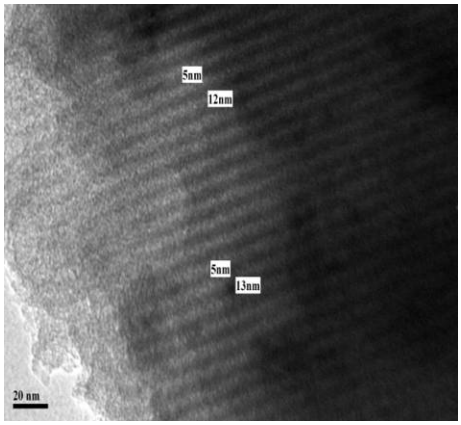
5nm
12nm
5nm
13nm
20 nm

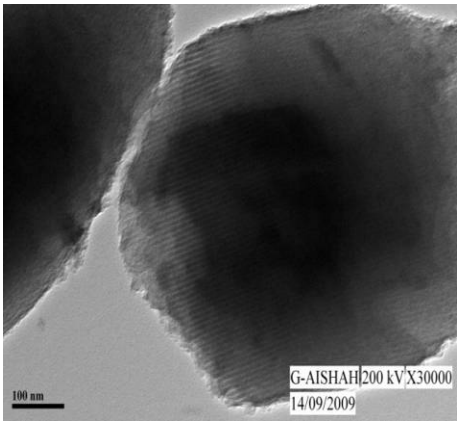
100 nm
G-AISHAH 200 kV X30000
14/09/2009

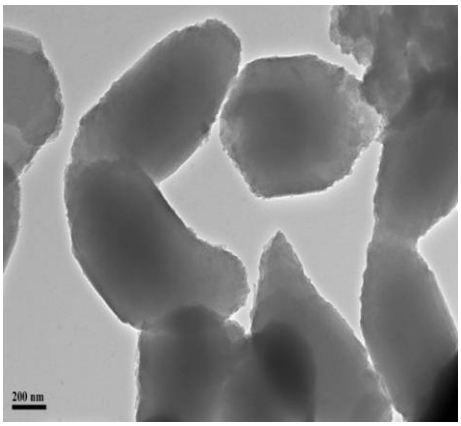
200 nm

SBW2

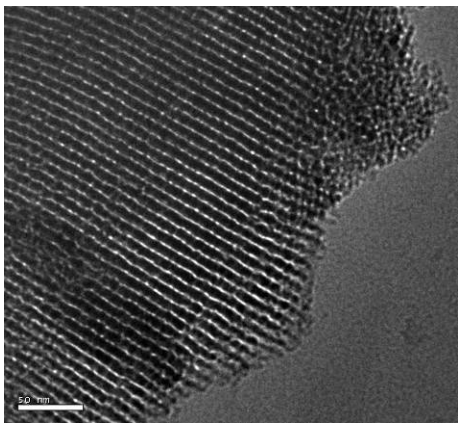

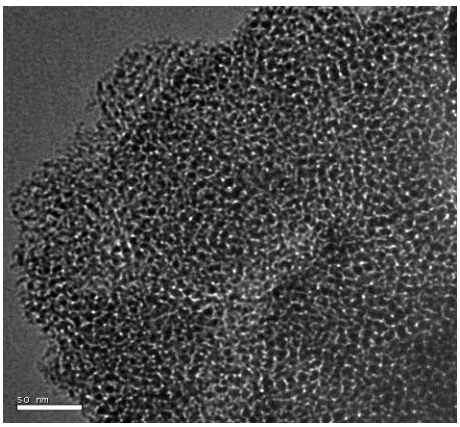

SBTi1

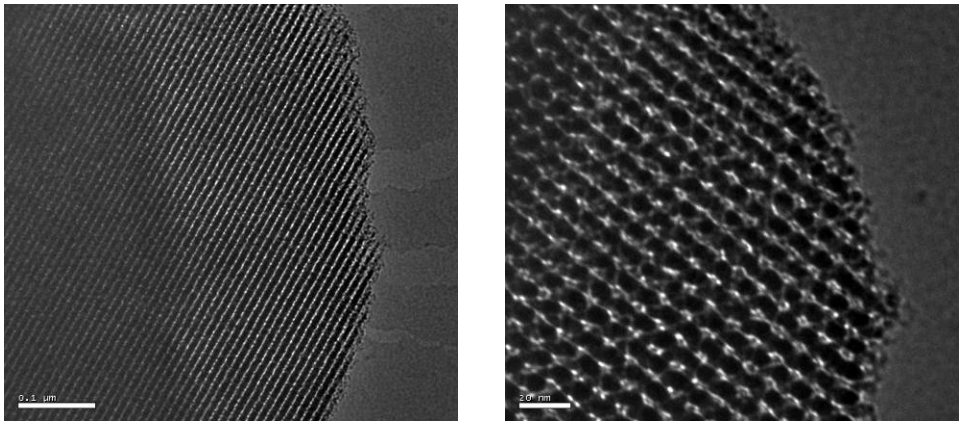

SBZr1

Figure 3.9

The HRTEM images of calcined SBA-15 products prepared show well ordered hexagonal arrays of mesopores with one-dimensional channels, which indicates a P6mm mesostructure (Figure 3.9). These HRTEM observations are consistent with the results of the XRD studies and confirm that our preparation approach is favourable for maintaining the highly ordered mesostructure.

Transmission electron microscopy (TEM) was conducted to confirm the existence of MOx inside SBA-15. Depicted in Figure 3.9 are TEM images of various transition metal modified SBA-15 materials. TEM images of the MOx loaded sample showed the intactness of the ordered mesoporous structure after the modification procedure. HRTEM images display the presence of the hexagonally ordered pore system in MOxSBA-15. Moreover, a linear array of pores with regular intervals is also observed, indicating that the structure of SBA-15 is retained even after the formation of MOx nanoclusters in the mesochannels. The MOx nanoclusters are not seen in the HRTEM images which confirm the metal oxide nano clusters are not deposited in the external surface but are indeed present inside the meso channels of SBA-15. TEM images confirm that the preparation approach is favorable for maintaining the highly ordered meso structure. It failed to discern directly the presence of

MOx in the channels of the SBA- 15 even with the higher amount of MOx (Si/M-10). This can be correlated with the wide angle X-ray diffraction (XRD) results of the composites calcined at 550^0C. Similar phenomena were reported for incorporation of Fe_2O_3, GaN, ZnO and ZnS inside MCM-41 mesoporous materials [61-64]. Zhang et al. considered that this was probably due to a weak contrast between the silica frameworks and the inside nanoparticles. No bulk aggregation of the nanoparticles was observed on the outer surface up to a content of Si/M ratio of 10.

Table 3.4

Catalyst	d Spacing (from XRD Analysis)	d Spacing (from TEM Images)
SBA-15	9.10 nm	9.0 0 nm
SBW1	10.53 nm	10.40 nm
SBW2	10.13 nm	10.00 nm
SBTi1	10.77 nm	10.33 nm
SBZr1	10.79 nm	10.52 nm

3.2.10 ^{29}Si MAS-NMR Spectra

High-resolution solid-state magic angle spinning (MAS) NMR spectroscopy has become a powerful tool for structural characterization of zeolites and other catalytic materials. The high resolution now available allows small structural differences such as those induced by temperature variations or by the presence of crystallographically inequivalent environments among the silicon sites to be detected [65-67]. Mesoporous silicas are generally characterized by the presence of three silicon sites Q^2, Q^3, and Q^4 representing the species Si $(OSi)_2(OH)_2$, Si $(OSi)_3(OH)$, and Si $(OSi)_4$, respectively [68].

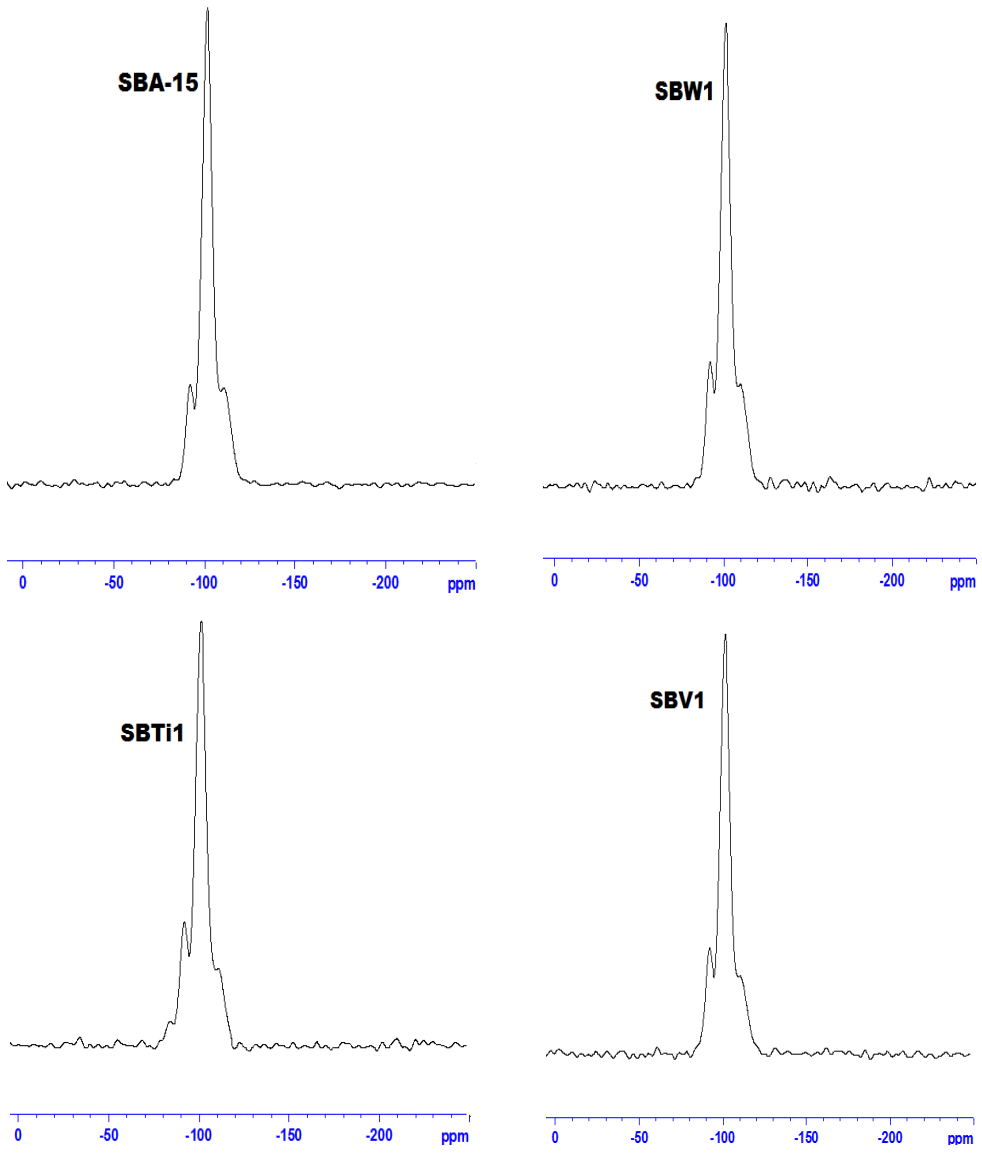

Figure 3.10

High-resolution solid-state magic angle spinning (MAS) NMR spectra of the samples under present study are shown in Figure 3.10. The peaks corresponding to the various Q^n groups were observed [11, 69-71] for all the prepared SBA-15 and MSBA-15 samples.

Q^n = $Si(OSi)_n(OH)_{4-n}$, n = 2-4

Q^4 at δ = -111 ppm

Q^3 at δ = -101 ppm

Q^2 at δ = - 93 ppm can be identified for all the samples.

3.3 Discussion

The results of various characterization techniques demonstrate the nature of metal sites in MSBA-15 samples. The metal atoms inside SBA-15 channels are denoted as α-M; those embedded in the intrachannel surfaces of the SBA-15 are denoted as β-M; and the metal atoms in the framework of SBA-15 are denoted as γ-M [68]. The mechanism of formation and distribution of the different metal sites are discussed in detail in this section. SBA-15 is synthesized by using neutral nonionic surfactants as templates acting through hydrogen bonding and other electrostatic interactions. In acid media, cationic silica species will be present as precursors, and the assembly process can be expected to proceed through an intermediate of the form $S^0H^+X^-I^+$, where S^0 is the neutral nonionic surfactant, X^- is a halide anion, and I^+ is a protonated Si-OH moiety (SiO^+) [9]. The micellar rods are encased in a layer of SiO^+, and subsequent auto-polymerization is expected to form the hexagonal silica structure. When transition metal cations are present in the acidic medium, MOxSBA-15 is expected to form via an intermediate of the form $S^0H^+X^-I^+M^+$, where M^+ is a protonated M-OH moiety (MO^+). The micellar rods are encased in a layer of SiO^+ and MO^+, and subsequent auto-polymerization is expected to form the hexagonal silica structure doped with transition metals. A schematic representation of the complete process from micellar rods to ordered MOxSBA-15 materials is shown in Figure 3.11. Incorporation of α-M, *β*-M, and γ-M has different effects on the structure of SBA-15 because of their different chemical environments. The mesoporous structures of MSBA-15 vary with composition in some respects, such as the gradual decrease in pore

diameter and increase in cell parameter. Formation of MOx involves α-M sites, and the observed decrease in pore diameter can be attributed to the bonding of α-M with Si sites on the internal surfaces of SBA-15. The formation of framework metal sites (γ-M) is responsible for the observed increase in cell parameter since a M-O bond is longer than Si-O (1.60 Å). The presence of *β*-M sites favours the formation of shorter micellar rods and results in a larger number of shorter hexagonal channels.

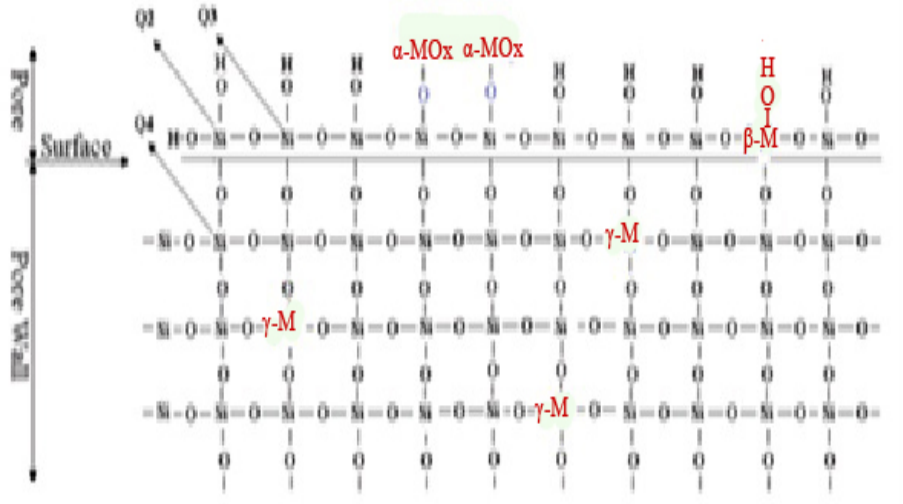

Figure 3.11 Schematic representation of α-M, *β*-M, and γ-M in MSBA-15

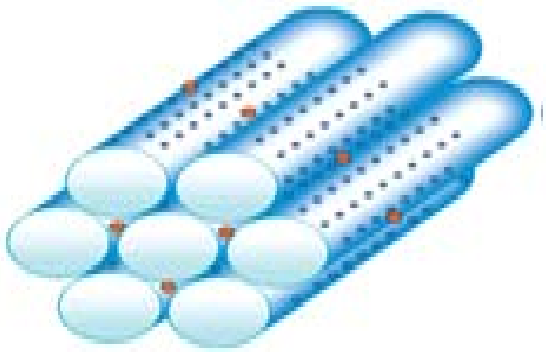

Figure 3.12 Schematic representation of metal in the surface and wall of MSBA-15

In summary, it could be stated that the solid state modification of mesoporous silica with transition metals leads to the formation of grafted metal species to the silica framework, in various state and environment. Small angle XRD patterns, nitrogen physisorption data and FTIR spectra show that the modification process does not affect the silica matrix long-range order, although it is related with a consumption of some surface silanol groups. Based on the UV– vis measurements, we could assume that isolated tetrahedral MOx units are grafted to the silica matrix.

The adsorption–desorption properties of the catalytic centers as well as the easiness of oxygen insertion into the organic intermediate molecules are of considerable importance for oxidation reactions. It is well established that both the adsorption and decomposition ability of the organic molecules are directly related to the acid–basic properties of the catalytically active centers [29, 72, 73]. They could be essentially changed by the type of the metal species and the oxidative state of metal atoms incorporated.

3.4 Acidity Measurements

The nature and strength of various acid sites possessed by heterogeneous catalysts have an important role in determining their catalytic properties. Incorporation of transition metals always result a remarkable increase in acid sites in the case of mesoporous solids. Mesoporous SBA-15 itself possesses Bronsted acid sites and the generation of Lewis acid sites is possible by various types of modifications. Several techniques are available to determine the nature, strength and density of acid sites presented in the prepared transition metal incorporated mesoporous SBA-15 catalysts. The acidic properties of the prepared catalytic systems were investigated with the help of various techniques, which indicated the existence of both Lewis and Brönsted acid sites on the catalysts. The results obtained from various studies are described here in detail.

3.4.1 Thermodesorption studies of 2,6-Dimethyl Pyridine

Thermodesorption study of an adsorbed base molecule is one of the popular methods to determine the acid strength of solid catalysts. Selective determination of Bronsted acid sites is generally carried out by the thermodesorption studies of 2,6-Dimethyl pyridine since it adsorbs strongly on Bronsted acid sites and forms only weak bonds with Lewis acid sites at low temperatures only [74]. A complete elimination of the coordinatively adsorbed 2,6-Dimethylpyridine on Lewis acid sites is possible by employing an appropriate purging temperature [75].

In order to obtain a better understanding of the Bronsted acid sites presented in the prepared mesoporous catalysts, the TG patterns of the samples were recorded after adsorption of 2,6-Dimethyl pyridine on the catalysts. The adsorbed 2,6-Dimethyl Pyridine gets desorbed during the thermal treatment at different temperature ranges depending on the strength of acid sites from which the desorption occurs. In the present study the purging temperature for eliminating the contribution from Lewis acid sites was kept at 300^0C. The amount of 2,6-Dimethyl Pyridine desorbed per gram of the catalyst is calculated in different temperature regions and the results are presented in Table 3.5.

From the results it is clear that almost all catalysts possess comparable amount of Bronsted acid sites. After metal incorporation there is a slight increase in medium strength acid sites are as observed in the case of catalysts prepared with higher metal content (Si/M ratio 10).

Table 3.5

Catalysts	2,6-DMP desorbed (mmol/g)			
	Weak (300-400 °C)	Medium (400-500 °C)	Strong (500-600 °C)	Total (300-600 °C)
SBA-15	0.064	0.049	0.025	0.138
SBW1	0.025	0.064	0.044	0.133
SBW2	0.019	0.057	0.027	0.103
SBW3	0.044	0.024	0.019	0.087
SBTi1	0.019	0.064	0.044	0.127
SBTi2	0.019	0.050	0.019	0.088
SBTi3	0.044	0.057	0.025	0.126
SBZr1	0.063	0.027	0.025	0.115
SBZr2	0.082	0.091	0.025	0.198
SBZr3	0.086	0.095	0.056	0.237
SBV1	0.056	0.019	0.064	0.139
SBV2	0.041	0.019	0.094	0.154
SBV3	0.081	0.082	0.076	0.239
SBMo1	0.094	0.045	0.064	0.203
SBMo2	0.057	0.050	0.113	0.220
SBMo3	0.019	0.094	0.050	0.163
SBCo1	0.069	0.052	0.035	0.156
SBCo2	0.089	0.090	0.077	0.256
SBCo3	0.038	0.054	0.076	0.168
SBCr1	0.037	0.045	0.038	0.120
SBCr2	0.044	0.082	0.120	0.246
SBCr3	0.025	0.025	0.019	0.069

3.4.2 Cumene Conversion Reaction

Cumene conversion reaction is a test reaction for the determination of acid sites present in solid catalysts. It is possible to make a correlation of the acidic properties of the catalysts with the conversion of cumene and with the product distribution of the reaction. During the reaction over the acidic sites cumene either dealkylated or dehydrogenated depending upon the nature of acid site present. Usually dealkylation or cracking occurs over Bronsted acid

sites and the reaction over Lewis acid sites resulted in dehydrogenation. So cumene conversion reaction can be used as a test reaction for the simultaneous determination of Bronsted and Lewis acid sites present in the catalysts. In the present work cumene conversion reaction is carried out in a vapour phase mode. α-methyl styrene and benzene were observed as the major products with small amounts of other dealkylated products. The cracking products are considered together as dealkylated products.

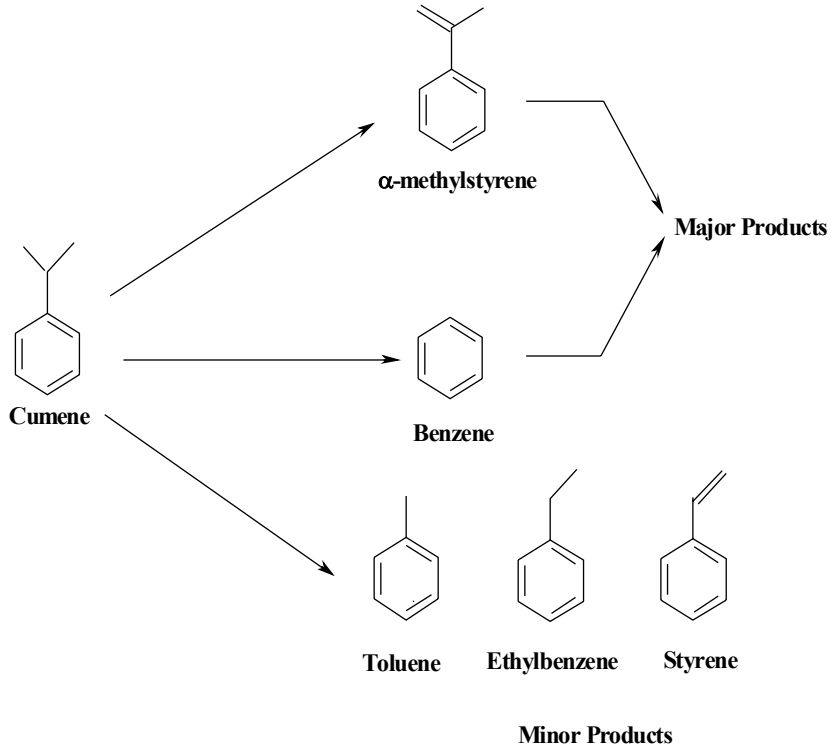

Scheme 3.1

3.4.2.1 Effect of Reaction Conditions

The reaction conditions were optimized by varying the parameters such as reaction temperature and WHSV of the reaction. The results obtained are presented in the following section.

1. Effect of Temperature

To study the effect of temperature, the reaction was carried out in a temperature range from 623 to 723 K. The results are presented in Figure 3.13. From the results it is clear that there was no observable variation in conversion of cumene. The selectivity to α-methyl styrene decreased drastically with increase in temperature. Corresponding increase in the amount of dealkylated products were also observed. At higher temperature the possibility of cracking the alkyl chain is higher. The temperature at which the selectivity of α-methyl styrene is maximum was selected as the optimum temperature for further reaction.

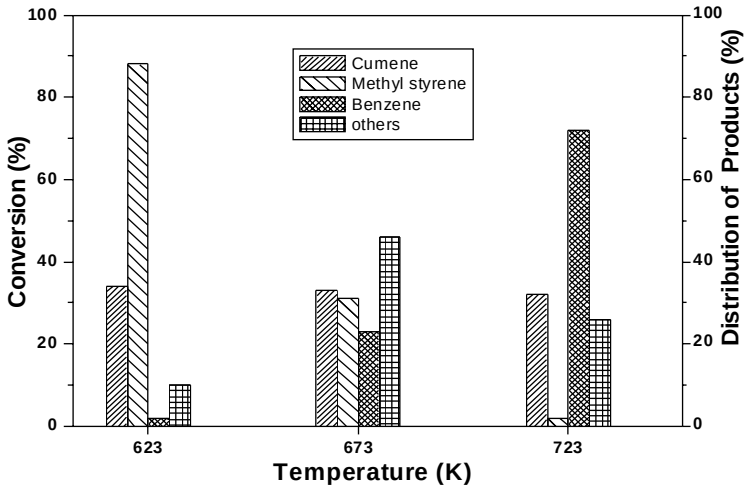

Figure 3.13 Influence of temperature on Cumene Conversion Reaction
Reaction Conditions:SBZr1-0.2g, WHSV-21.55, Time-2h

2. Effect of WHSV

The influence of WHSV on cumene conversion reaction was studied by conducting the reaction with different WHSV values. The results obtained are described in Figure 3.14. Conversion of cumene decreased with increase in WHSV. Decrease in residing time of the reactants on the catalyst surface result

an enhancement in catalytic activity. The selectivity of α-methyl styrene first increased with increase in WHSV up to 21.55. Further increase in WHSV causes a decrease in selectivity of α–methyl styrene. The optimum WHSV selected for further reaction was 21.55.

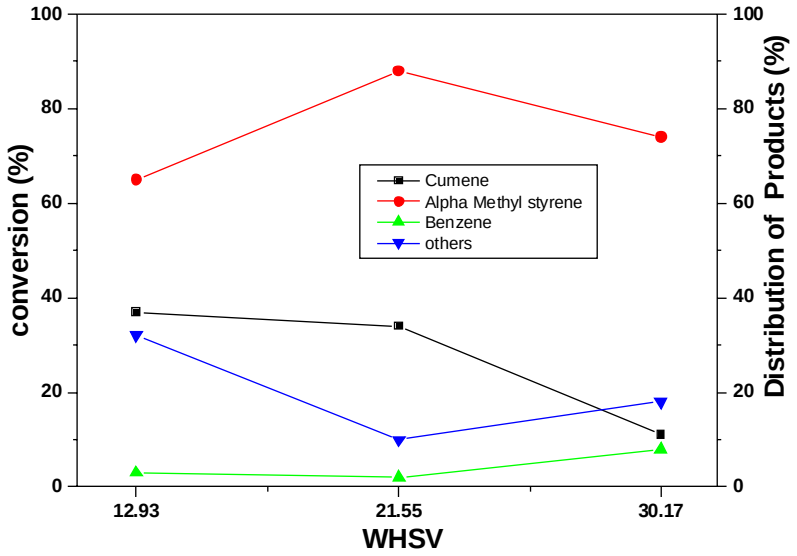

Figure 3.14 Influence of WHSV on Cumene Conversion Reaction Reaction Conditions: SBZr1-0.2g, Temp-623 K, Time-2h

3.4.2.2 Effect of Catalysts

The cumene conversion reaction was carried out over all the prepared catalysts under the optimized reaction conditions described below.

Table 3.6 Optimized reaction condition for cumene conversion reaction

Parameters	Optimized condition
Temperature	623K
WHSV	21.55
Time	2h
Catalyst Amount	0.2g

The catalytic activity of prepared transition metal incorporated SBA-15 catalysts along with the percentage distribution of various products on cumene conversion reaction is illustrated in Table 3.7.

Table 3.7 Influence various catalysts on cumene conversion reaction Reaction conditions: Catalyst Amount-0.2g, Temp-623K, WHSV-21.55, Time-2h

Catalyst	Conversion of Cumene (%)	Distribution of Products (%)	
		α-Methyl styrene	Dealkylated products
SBA-15	7	52	48
SBW1	25	64	36
SBW2	14	70	30
SBW3	17	76	24
SBTi1	18	67	33
SBTi2	20	71	29
SBTi3	33	49	51
SBZr1	34	88	12
SBZr2	24	71	29
SBZr3	29	58	42
SBV1	25	65	35
SBV2	13	62	38
SBV3	19	55	45
SBMo1	17	59	41
SBMo2	15	53	47
SBMo3	25	56	44
SBCo1	14	79	21
SBCo2	18	42	58
SBCo3	23	49	51
SBCr1	23	70	30
SBCr2	19	58	42
SBCr3	13	69	31

α-methyl styrene is the major product obtained over the prepared catalytic systems. Compared with pure SBA-15 the metal incorporated systems showed increased catalytic activity in cumene conversion reaction. The maximum

conversion of 34% with maximum selectivity for α–methyl styrene 88% was observed with SBZr1. Since the dealkylation reaction of cumene occurs over the Bronsted acid sites present we can correlate the dealkylation selectivity with total Bronsted acidity obtained from thermodesorption studies of 2,6-Dimethyl Pyridine. The results are presented in figure 3.15. A correlation was observed between the dealkylation selectivity and the total Bronsted acidity.

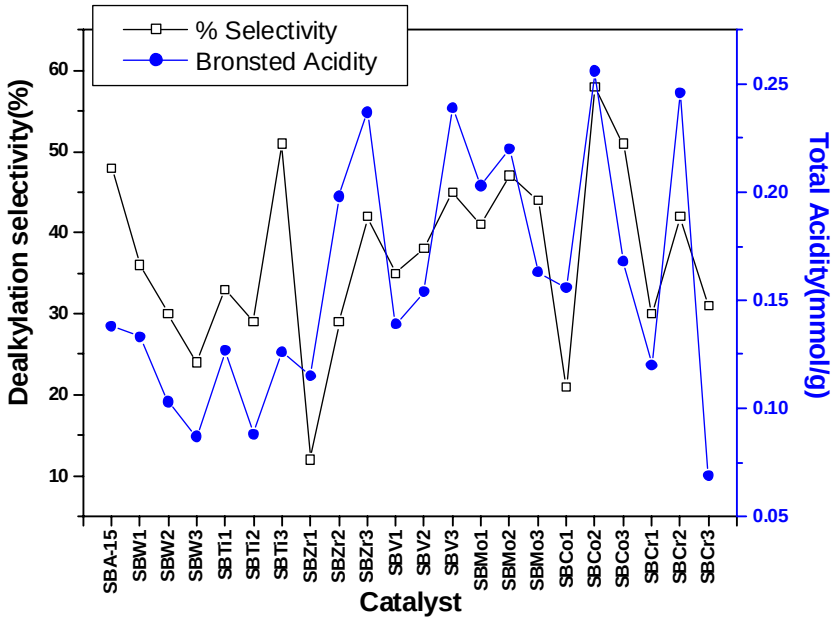

Figure 3.15 Dealkylation Selectivity and Acidity from 2,6-Dimethyl Pyridine

3.4.3 Cyclohexanol conversion

Alcohol decomposition reactions are usually carried out for the determination of both the acidic and basic character of solid catalysts. Alcohols are generally considered as amphoteric in nature, thus it can interact with the acidic and basic sites present in a catalyst. Cyclohexanol decoposition reaction is the most widely studied reaction under the category. Dehydrogenation and dehydration are the most important reactions occuring during the cyclohexanol conversion reaction. Acidic sites are responsible for

the dehydration reaction while the dehydrogenation reaction is linked with both acidic and basic sites.

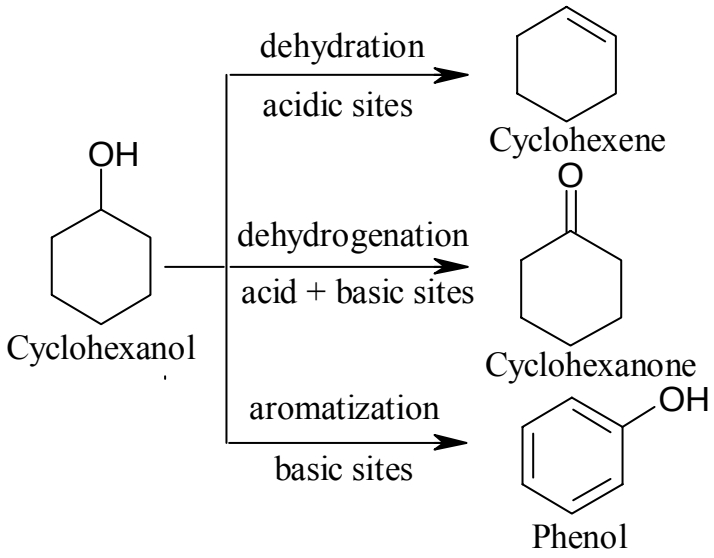

Scheme. 3. 2

3.4.3.1 Effect of Reaction Variables

The optimum parameters for the cyclohexanol conversion reaction were determined by conducting the reaction at various reaction conditions such as temperature and WHSV of the reaction.

1. Effect of Temperature

The reaction was carried out at different temperatures in the range of 523 to 623 K. The results obtained are presented in Figure 3.16. As the temperature is increased from 523 to 573 K the percentage conversion also increases to 100% from 92%. Further increase in temperature to 623 K causes a decrease in conversion to 85%. Cyclohexene is the major product obtained during the reaction. The maximum selectivity is at 523 K. So the temperature 523 K was selected as the optimum temperature for further reaction.

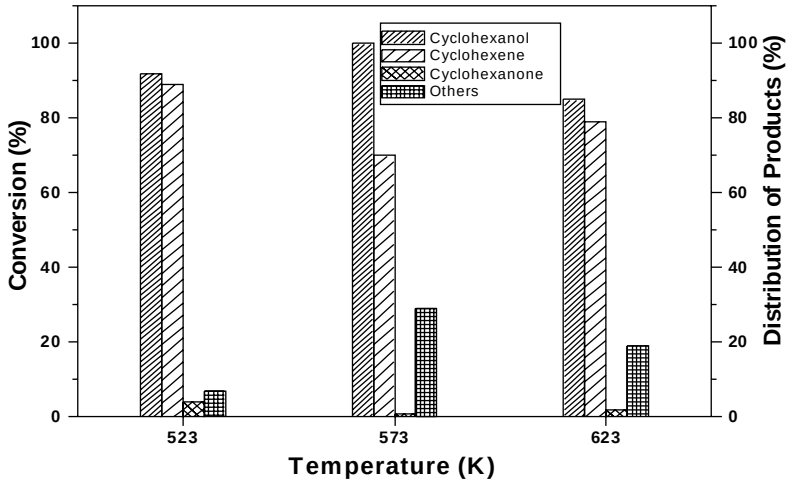

Figure 3.16 Influence of Temperature on Cyclohexanol Conversion Reaction
Reaction conditions: SBZr2-0.2g, WHSV-24.05, Time-2h

2. Effect of WHSV

The effect of WHSV on cyclohexanol conversion reaction was studied and the results obtained are described in Figure 3.17.

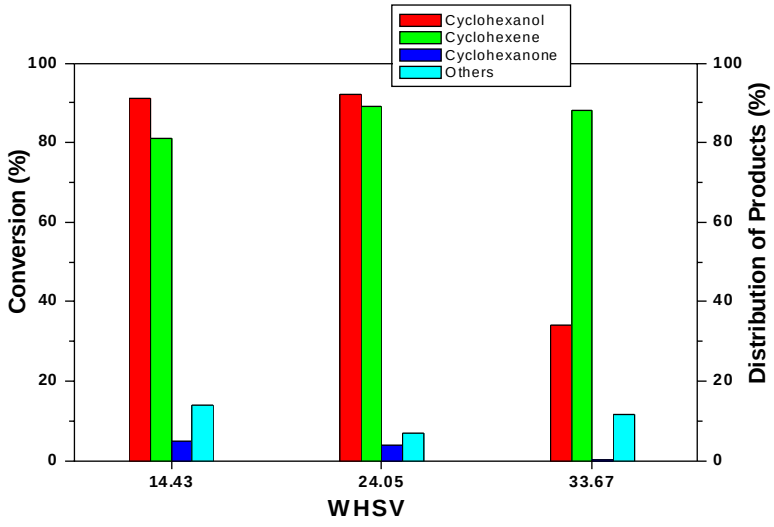

Figure 3.17 Influence of WHSV on Cyclohexanol Conversion Reaction
Reaction conditions: SBZr2-0.2g, Temp-523K, Time-2h

There was not much change in conversion when the WHSV increases from 14.03 to 24.05. Further increase in conversion causes a drastic decrease in conversion. The increase in WHSV did not alter the selectivity of cyclohexene to a considerable extent. About 90% selectivity was observed always. The optimum WHSV selected for further reaction was 24.05 by considering both the conversion and selectivity.

3.4.3.2 Effect of Catalysts

To compare the catalytic performance of the prepared catalytic systems, the cyclohexanol conversion reaction was carried out using the catalysts under the optimized reaction conditions described below.

Table 3.8 Optimized reaction condition for cyclohexanol conversion reaction

Parameters	Optimized condition
Temperature	523K
WHSV	24.05
Time	2h
Catalyst Amount	0.2g

Table 3.9 gives the percentage conversion and the product distribution obtained in the vapour phase cyclohexanol decomposition reaction for transition metal incorporated SBA-15 catalysts prepared under the present study.

Dehydration of cyclohexanol to cyclohexene is the predominant reaction over all the prepared systems. All the transition metal incorporated systems show higher conversion than pure SBA-15. A maximum conversion of 98% was observed with SBZr2. The highest dehydration activity of the systems is related to the acid sites associated with prepared systems. Figure 3.19 and 3.20

describes the correlation graphs of the conversion of cyclohexanol with Bronsted and Lewis acid sites respectively. From the results it is clear that both acidic sites are responsible for the dehydration of cyclohexanol.

Table 3.9 Influence various catalysts on cyclohexanol conversion reaction
Reaction conditions: Catalyst-0.2g, Temp-523K, WHSV-24.05, Time-2 h

Catalyst	Conversion of Cyclohexanol (%)	Distribution of Products (%)		
		cyclohexene	Cyclohexanone	Others
SBA-15	9	94	-	6
SBW1	59	78	-	22
SBW2	44	77	-	23
SBW3	50	74	-	26
SBTi1	26	85	1	14
SBTi2	25	89	2	9
SBTi3	19	95	2	3
SBZr1	73	82	2	16
SBZr2	98	70	1	29
SBZr3	69	87	0.2	12.8
SBV1	27	78	3	19
SBV2	33	84	1	15
SBV3	27	91	2.5	6.5
SBMo1	15	90	2	8
SBMo2	17	88	1	11
SBMo3	31	90	-	10
SBCo1	23	87	2	11
SBCo2	29	90	3	7
SBCo3	26	77	4	19
SBCr1	51	90	3	7
SBCr2	58	94	-	6
SBCr3	22	91	-	9

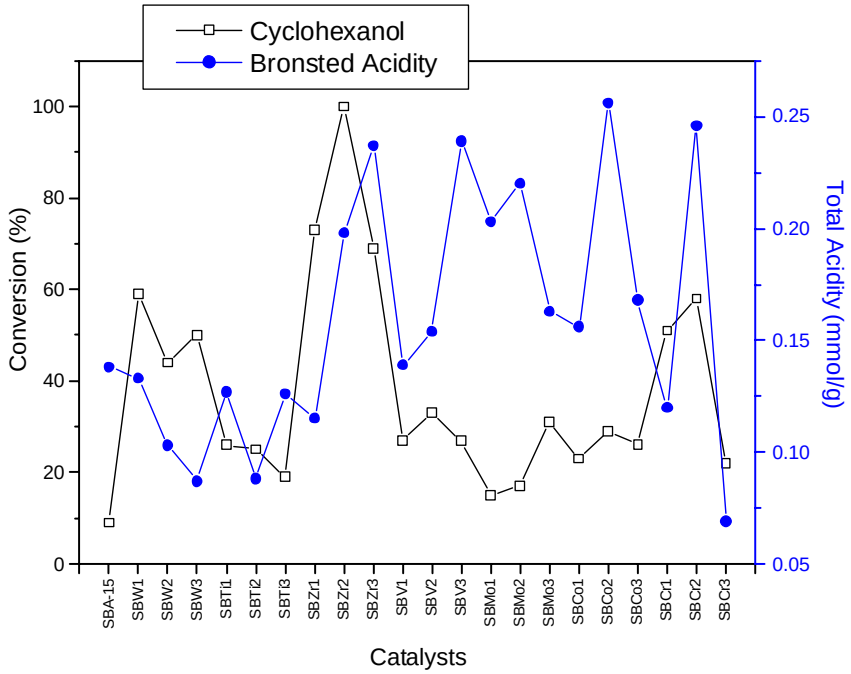

Figure 3.19 Cyclohexanol Conversion and Broansted Acidity

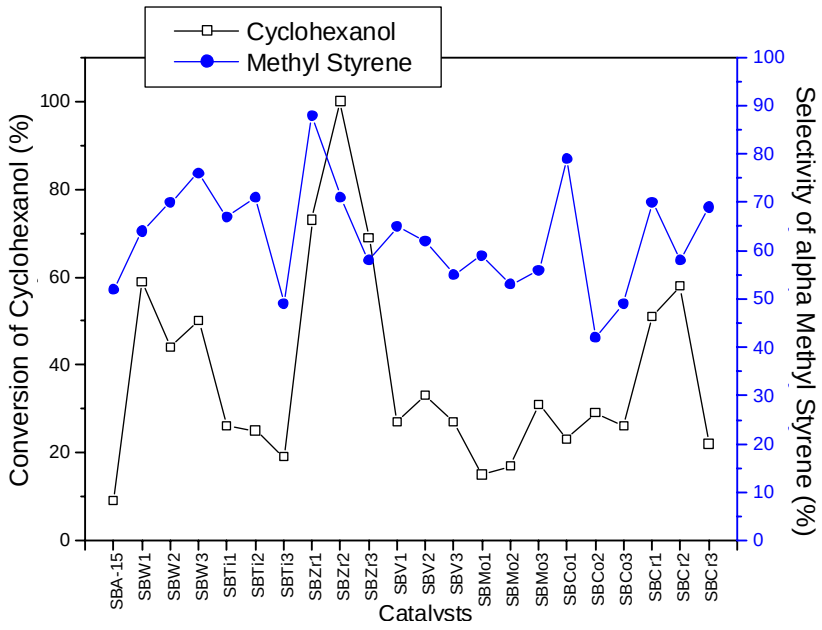

Figure 3.20 Cyclohexanol Conversion and Lewis Acidity

3.5 Conclusions

- Ordered SBA-15 silica containing various transition metals were directly synthesized, and their structures have been investigated in detail. All the prepared samples have an ordered mesoporous structure in which the incorporated metal atoms are highly dispersed within SBA-15.
- The results of various characterization techniques suggest a successful isomorphous substitution of metal species into the siliceous framework of SBA-15 without affecting of structural and textural order.
- Results from XRD, SEM, HRTEM and N_2 physisorption characterizations suggest that this is a good method for the formation of mesoporous silica with highly ordered structures.
- The nitrogen sorption isotherms of SBA-15 and MSBA-15 materials are found to be type IV isotherms and a sharp increase in the adsorbed amount of nitrogen at a relative pressure (P/Po) of 0.6–0.9, confirms typical curves of mesoporous structures which are still maintained in MSBA-15.
- From the results of thermogravimetric analyses, we found that MSBA-15 can be thermally stable up to 1000^0C in air without collapsing the pore structure and that the mesoscale periodicity is completely preserved. These findings provide good evidence that MSBA-15 is a hierarchically ordered porous material in which the embedding metal silica matrix provides enhanced chemical, mechanical, and thermal robustness.
- HRTEM images of MSBA-15 materials show that the materials retain the hexagonally ordered porous structure even after the

formation of MOx nanoclusters in the mesochannels. However, the MOx nanoclusters are not seen in the HRTEM images. This confirms that the MOx nanoclusters are not deposited on the external surface but are indeed present inside the mesochannels of SBA-15.

- The hexagonal arrangement of the pores with a different contrast than that of the pore walls is quite clear from the TEM image of the as-synthesized sample. Average pore diameters measured from this micrograph agree well with that derived from N_2 adsorption isotherms.
- In FTIR spectroscopy all characteristic bands due to the siliceous content in the material are observed.
- From acidic measurements it s clear that both Lewis and Bronsted acid sites are present in the prepared samples.

References

[1] W. Zhang, M. Froba, J. Wang, P. T. Tanev, J.Wong, T. J. Pinnavaia, J. Am. Chem. Soc., 118 (1996) 9164.

[2] Vinu, P. Srinivasu, M. Miyahara, K. Ariga, J. Phys. Chem. B., 110 (2006) 801.

[3] Vinu , P. Srinivasu , D. P. Sawant , S. Alam, T. Mori , K. Ariga , V.V. Balasubramanian , C. Anand, Microporous and Mesoporous Materials, 110 (2008) 422.

[4] Vinu, D. P. Sawant, K. Ariga, K. Z. Hossain, S. B. Halligudi, M. Hartmann, M. Nomura, Chem. Mater., 17 (2005) 5339.

[5] Juan A. Melero, Jose Iglesias, Jesus M. Arsuaga, Javier Sainz-Pardo, Pilar de Frutos, Sandra Blazquez, J. Mater. Chem., 17 (2007) 377.

[6] Vinu, V. Murugesan, W. Bohlmann, M. Hartmann, J. Phys. Chem. B., 108 (2004) 11496.

[7] B.L. Newalkar, J. Olanrewaju, S. Komarneni, J. Phys. Chem. B., 105 (2001) 8356.

[8] Karol Szczodrowski , Benedicte Prelot , Sebastien Lantenois , Jerzy Zajac, Marc Lindheimer, Deborah Jones, Anne Julbe Arie van der Lee, Microporous and Mesoporous Materials, 110 (2008) 111.

[9] D. Zhao, Q. Huo, J. Feng, B.F. Chmelka, G.D. Stucky, J. Am. Chem.Soc., 120 (1998) 6024.

[10] D. Zhao, J. Feng, Q. Huo, N. Melosh, G. Fredrikson, B. Chmelka, G.D. Stucky, Science, 279 (1998) 548.

[11] Zhensong Lou, Ruiheng Wang, Hui Sun, Yuan Chen, Yanhui Yang, Microporous and Mesoporous Materials, 110 (2008) 347.

[12] Anuj Kumar, Darbha Srinivas, Paul Ratnasamy, Chem. Commun., (2009) 6484.

[13] T. Thangaraj, R. Kumar, S. P. Mirajkar and P. Ratnasamy, J. Catal., 130 (1991) 1.

[14] R. Millini, E. Previde Massara, G. Perego and G. Bellussi, J. Catal., 137 (1992) 497.

[15] M. A. Camblor, A. Corma, J. Perez Periante, Zeolites, 13 (1993) 82.

[16] J. Panpranot, S. Kaewkun, P. Praserthdam and J.G. Goodwin, Catal. Lett., 91 (2003) 95.

[17] Xiancai Li, Shaoxiang Huang, Qingrong Xu, Yifeng Yang, Transit.Metal. Chem.

[18] Zhou-jun Wang, Yongbing Xie, Chang-jun Liu, J. Phys. Chem. C., 112 (2008).

[19] Y. Liu, J. Zhang, W. Hou, J. J. Zhu, Nano.Tech., 19 (2008).

[20] S. C. Chang, M. H. Huang, J. Phys. Chem. C., 112 (2008) 2304.

[21] Renyuan Zhang, Wei Ding, Bo Tu, Dongyuan Zhao, Chem. Mater. Commun., (2007).

[22] X. S. Zhao, G. Q. Lu, A. K. Whittaker, G. J. Millar, H. Y. Zhu, J. Phys. Chem. B., 101(1997) 6525.

[23] M. S. Morey, S. OBrien, S. Schwarz, G. D. Stucky, Chem. Mater., 12 (2000) 898.

[24] J. George, S. Shylesh, A.P. Singh, Appl. Catal. A Gen., 290 (2005) 148.

[25] L. J. Burcham, G. Deo, X. Gao, I. E. Wachs, Top. Catal., 85 (2000) 11.

[26] M. S. Marth, A. Wokaun, A. Baiker, J. Catal., 124 (1990) 86.

[27] S. Dzwigaj, P. Massiani, A. Davidson, M. Che, J. Mol. Catal. A. Chem., 155 (2000) 169.

[28] S. Dzwigaj, M. Matsuoka, M. Anpo, M. Che, J. Phys. Chem. B., 104 (2000) 6012.

[29] Tanya Tsoncheva, Ljubomira Ivanova, Rayna Dimitrova, Jessica Rosenholm, J. Colloid. Inter. Sci., 321 (2008) 342.

[30] Enrica Gianotti, Maria E. Raimondi, Leonardo Marchese, Gianmario Martra, Thomas Maschmeyer, John M. Seddon, Salvatore Coluccia, Catal. Lett., 76 (2001)1.

[31] Fei Gao, Yanhua Zhang, Haiqin Wan, Yan Kong, Xingcai Wu, Lin Dong, Baiqin Li, Yi Chen, Microporous and Mesoporous Materials, 110 (2008) 508.

[32] Ana Carla S. L. S. Coutinho, Solange A. Quintella, A. S. Araujo, Joana M. F. Barros, Anne M. G. Pedrosa, V. J. Fernandes, M. J. Souza, J. Therm. Anal. calorim., 87 (2007) 457.

[33] Mahasweta Nandi, Krishanu Sarkar, Asim Bhaumik, Mater. Chem. Phy., 107 (2008) 499.

[34] L. Marchese, E. Gianotti, T. Maschmeyer, G. Martra, S. Coluccia and J. M. Thomas, Nuovo Cimento, 19 (1997) 1707.

[35] M. Boulova, G. Lucazeau, J. Solid State Chem., 167 (2002) 425.

[36] S. Kein, B.M. Weckhuysen, J.A. Martens, W.F. Maier, P.A. Jacobs, J. Catal., 163 (1996) 489.

[37] Z. Luan, E.M. Maes, P.A.W. van der Heide, D. Zhao, R.S. Czernuszewicz, L. Kevan, Chem. Mater., 11 (1999) 3680.

[38] B. J. Aronson, C. F. Blanford, A. Stein, Chem. Mater., 9 (1997) 2842.

[39] Shenmin Zhu, Di Zhang, Xingchen Zhang, Le Zhang, Xiongwei Ma, Yunlu Zhang, Min Cai, Microporous and Mesoporous Materials, (2009).

[40] Corma, Chem. Rev., 97 (1997) 2373.

[41] Bhaumik, R. Kumar, J. Chem. Soc., Chem. Commun., (1995) 349.

[42] M. Taramaso, G. Perego, B. Notari, US Patent 4, 410 (1983)501.

[43] D. R. C. Huybrechts, L. DeBruycker, P. A. Jacobs, Nature, 345 (1990) 240.

[44] L. J. Schofield, O. J.Kerton, P. McMorn, D. Bethell, S. Ellwood, G. J. Hutchings, J. Chem. Soc., Perkin Trans. 2 (2002) 2064.

[45] M. P. Kapoor, A. Bhaumik, S. Inagaki, K. Kuraoka, T. Yazawa, J. Mater. Chem., (2002) 3078.

[46] Bhaumik, S. Inagaki, J. Am. Chem. Soc. 123 (2001) 691.

[47] T. Vralstad, W. R. Glomm, M. Ronning, H. Dathe, A. Jentys, J. A. Lercher, G. Oye, M. Sto cker, J. Sjoblom, J. Phys. Chem.B., 110 (2006) 5386.

[48] S. Lim, D. Ciuparu, C. Pak, F. Dobek, Y. Chen, D. Harding, L. Pfefferle, G. Haller, J. Phys. Chem. B., 107 (2003) 11048.

[49] P. Katsoulidis, D. E. Petrakis, G. S. Armatas, P. N. Trikalitis, P. J. Pomonis, Microporous and Mesoporous Materials, 92 (2006) 71.

[50] J. E. Haskouri, S. Cabrera, C. J. Gomes Garcia, C. Guillem, J. Latorre, A. Beltran, D. Beltran, M.D. Marcos, P. Amoros, Chem. Mater., 16 (2004) 2805.

[51] W. A. Carvalho, P. B. Varaldo, M. Wallau, U. Schuchardt, Zeolites, 18 (1997) 408.

[52] Hong Ma, Jie Xu, Chen Chen, Qiaohong Zhang, Jianbo Ning, Hong Miao, Lipeng Zhou, Xiaoqiang Li, Catal. Lett., 113 (2007).

[53] M. Morey, A. Davidson, H. Eckert, G. D. Stucky, Chem. Mater., 8 (1996) 486.

[54] D. Wei, H. Wang, X. Feng, W. T. Chueh, P. Ravikovitch, M. Lyubovsky, C. Li, T. Takeguchi, G.L. Haller, J. Phys. Chem. B., 103 (1999) 2113.

[55] N. Y. Topsoe, J. A. Dumesic, H. Topsoe, J. Catal., 151 (1995) 241.

[56] Y. Kong, H. Y. Zhu, G. Yang, X. Guo, W. Hou, Q. Yan, M. Gu, Adv. Funct. Mater., 14 (2004) 816.

[57] S. C. Moon, M. Fujino, H. Yamashita, M. Anpo, J. Phys. Chem, B., 101 (1997) 369.

[58] R. A. Garcia, R. van Grieken, J. Iglesias, V. Morales, J. Martin, Stud. Surf. Sci. Catal., 158(2005) 485.

[59] Wang, Z. L. J. Phys. Chem. B., 104 (2000) 1153.

[60] R. C. Weast, Ed. Handbook of Chemistry and Physics, 66th ed.; CRC Press: Boca Raton, FL, (1986)151.

[61] T. Abe, Y. Tachibana, T. Uematsu, M. Iwamoto, Chem. Commun.., (1995) 1617.

[62] H. Wrinkle, A. Birkner, V. Hagen, I. Wolf, R. Schmechel, H. V. Seggern, R. A. Fischer, Adv. Mater. 11 (1999) 1444.

[63] W. Zhang, J. Shi, L. Wang, D. Yan, Chem. Mater. 12 (2000) 1408.

[64] W. Zhang, J. Shi, H. Chen, Z. Hua, D. Yan, Chem. Mater., 13 (2001) 648.

[65] S. Bordiga, R. Buzzoni, F. Geobaldo, C. Lamberti, E. Giamello, A. Zecchina, G. Leofanti, G. Petrini, G. Tozzola, G. Vlaic, J. Catal., 158 (1996) 486.

[66] Y. Q. Wang, C. M. Yang, B. Zibrowius, B. Spliethoff, M. Linden, F. Schuth, Chem. Mater., 15 (2003) 5029.

[67] X. G. Wang, K. S. K. Lin, J. C. C. Chan, S. Cheng, J. Phys. Chem. B., 109 (2005) 1763.

[68] G. Engelhardt, D. Michel, High Resolution Solid State NMR of Silicates and Zeolites; Wiley: New York, (1987) 149.

[69] S. A. Axont, Klinowski, J. Phys. Chem., 98(1994) 1929.

[70] Steel, W. C. Stuart, M. W. Anderson, Chem. Mater., 7 (1996) 1829.

[71] Linhua Hu, Shengfu Ji, Zheng Jiang, Huanling Song, Pingyi Wu, Qianqian Liu, J. Phys. Chem. C.,111(2007) 15173.

[72] S. Lim, G.L. Haller, Appl. Catal. A Gen., 188 (1999) 277.

[73] N. Y. Topsoe, M. Anstrom, J.A. Dumesic, Catal. Lett., 76 (2001) 11.

[74] P. A. Jacobs, C. F. Heylen, J. Catal., 34 (1974) 267.

[75] Satsuma, Y. Kamiya, Y. Westi and T. Hattori, Appl. Catal. A. Gen., 195 (2000) 253.

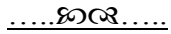

Chapter 4

Oxidation of Cyclohexene

Contents

Many homogeneous catalytic systems have been tried in the title reaction. Since heterogeneous catalysis has a lot of advantages of an easier catalyst separation and recycling, various research groups were focused on the development of a heterogeneous catalyst for cyclohexene oxidation with environmentally friendly oxidants. Heterogeneous catalysis has also found to be very effective in enhancing selectivity. Most of the mesoporous materials have been successfully used in the selective oxidation of various aromatics. Supported, site-isolated metal oxide materials are considered as an important class of heterogeneous, selective oxidation catalysts. High-surface-area supports like SBA-15 afford highly dispersed metal oxide species which are the key parameter in the rather difficult oxidation of cycloalkenes. Cyclohexene oxidation has been the subject of extensive studies as the products obtained are important synthetic intermediates for the production of fine chemicals and can also be utilized in polyether polymer synthesis. In the present chapter the oxidation of cyclohexene was applied to examine the properties of prepared catalysts in liquid phase reactions. Optimization of various reaction conditions leads to the formation of products with high selectivity and yields. The use of present heterogeneous catalysis has afforded good to excellent conversions with good selectivity to cyclohexene oxide and cyclohexane-1, 2-diol .The adopted procedure was simple, greener and more efficient to cyclohexene oxidation. The use of a clean oxidant such as H_2O_2 is an important feature of a green chemical reaction since it produces water, the only by-product. The mesoporous structure of transition metals incorporated SBA-15 materials enabled a better accessibility of active sites to bulky substrate molecules which is reflected in the high conversions of cyclohexene and better selectivity to the epoxide or diol over these novel catalysts.

4.1 Introduction

Olefin oxidation is an important transformation in synthetic organic chemistry because the products obtained are valuable and resourceful commercial intermediates, and undergo further reactions [1, 2]. There are a large number of ways available for the olefin oxidation and most of them are utilizing the peroxide moiety which generally involves the addition of other reagents to activate the peroxide compound. Epoxidation of alkenes using peroxycarboxylic acids was established nearly a century ago [3]. Recently metal-catalyzed epoxidation of olefins has been reported. The systems with high valence compounds such as Mo (VI), W (VI), and Re (VII) complexes were used as epoxidation catalysts in the presence of organic peroxides [4-8]. Studies reveal that the large positive charge of the metals make these compounds capable of accepting electron pairs in vacant d orbitals and form stable complexes with organic peroxides. This complex formation results in, the peroxidic oxygen atom to be more electrophilic and, therefore, readily attacked by an olefinic double bond [4]. Various studies have been conducted on oxidation of olefins using metal oxide based catalysts for both reactivity [5, 9-12] and mechanistic studies.

Specifically, the selective oxidation of cyclohexene is widely used as a possible alternative route for the production of adipic acid, which is a key intermediate in the manufacture of Nylon- 66 polymer [13]. Various oxometal reagents, including permanganate [14] and ruthenium tetroxide [15], were reported as catalysts for this reaction. By the addition of various oxygen donors, such as NaOCl [16], $NaIO_4$ [17] and peracetic acid [18] the activity of these catalysts can be increased. Peroxotungstates were found to be effective catalysts for the selective oxidative cleavage of cyclohexene under phase-transfer conditions with lipophilic quaternary ammonium salts [19, 20]. Adipic acid is traditionally prepared through a two-step process involving cyclohexane oxidation with dioxygen to -ol/-one mixture followed by the

catalytic oxidation with HNO_3 [14, 21–22]. But this process results in the formation of nitrous oxide, a greenhouse gas that has to be decomposed. Thus the heterogeneous oxidation of cyclohexene in the presence of hydroperoxides has much more advantages in the field of synthetic chemistry [23]. The development of green practical procedures for the oxidation of six-carbon feedstock is highly desirable—particularly for the medium and large-scale synthesis of various intermediates and fine chemicals [24].

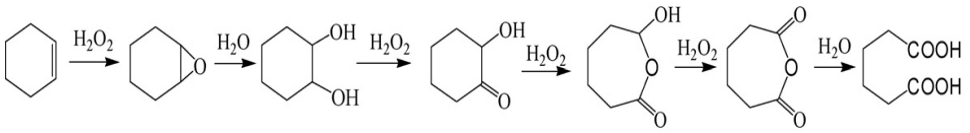

The area of catalytic oxidation of cycloalkenes has been widely investigated but several fundamental problems still remain. A search for a simple procedure to obtain high yield and selectivity, combining favourable economic and environmental concerns among other factors, is still a goal for current research field [25] and the establishment of a more efficient and selective catalyst for these reactions is an active area of research. Many researchers are interested in designing such a catalyst for the oxidation of cycloalkenes and the reaction system involved only the catalyst, substrate, and H_2O_2 [26]. More activated oxygen atoms are required if a direct oxygen transfer mechanism is operative in the oxidation reaction [27]. Aqueous hydrogen peroxide is the most attractive oxidant (after dioxygen) since it is green, quite cheap and easy to handle [14, 22, 28, 29]. Many researchers have reported the cyclohexene epoxidation using H_2O_2 over various micro and mesoporous catalysts [30–35]. Epoxidation catalysts developed and utilizing the H_2O_2 system is constructive for the environment also [27]. The catalytic performance of Ti-MCM-41 catalysts was studied in the oxidation reaction of cyclohexene, but resulting a low catalytic activity and product selectivity [36–40]. In recent years a lot of research was carried out on cyclohexene

oxidation reaction to test the catalytic activity of transition metal modified mesoporous materials [13, 24, 41-50].

The mesoporous materials have attracted considerable attention in the area of catalysis in recent years. Remarkably large surface area and narrow pore size distributions make them ideal candidates for catalysis [51]. The use of high surface area mesoporous SBA-15 materials as a support for transition metals has some beneficial effects in the area of catalysis. The transition metal incorporated SBA-15 materials would give rise to well dispersed metal nano particles and show an improved catalytic efficiency especially in various oxidation reactions. Selectivity control is also a key issue in various chemical reactions and selective processes are always superior to non-selective ones to purify the target compound for its use in further application by minimizing the difficulties in the separation of the product/s from the reaction mixture. Thus the selectivity in oxidation catalysis has been thoroughly reviewed for conventional catalysts employed in oxidations [52-54].

In the present study we have demonstrated that the different physicochemical techniques indicate that the transition metals were incorporated into the silica framework in all the samples prepared and these framework metal species are the effective active sites for the selective oxidation of cyclohexene with aqueous hydrogen peroxide.

Oxidation of cyclohexene was chosen as a model reaction for the present work. In cyclohexene, oxidation of the carbon–carbon double bond undergo oxidation by aq. H_2O_2 yields cyclohexene oxide (epoxide) which upon further reaction with water produces 1,2-cyclohexanediol (diol). Oxidation of the allylic C–H bond results in 2-cyclohexene-1-ol which is further oxidized to 2-cyclohexene-1-one. Selective epoxidations over transition metals incorporated SBA-15 systems occur via heterolytic cleavage of the O–O bond

by hydroperoxo/ superoxo-metal species. Allylic C–H bond oxidations proceed via homolytic O–O bond cleavage. Due to differences in electronic structure, tetrapodal metal in the metallosilicates ($M(OSi)_4$) facilitate heterolytic O–O bond cleavage while the tripodal M sites ($M(OH)(OSi)_3$) facilitate homolytic cleavage of the O–O bond [41].

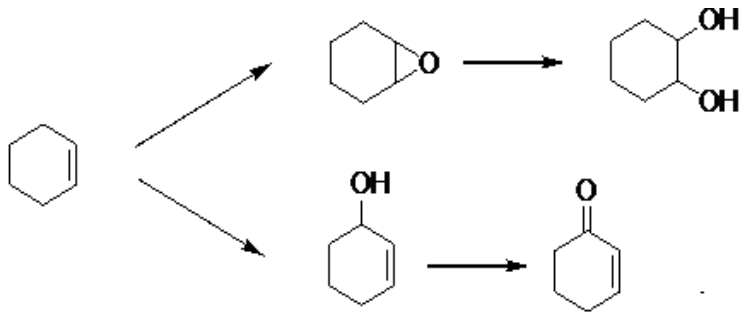

By an appropriate choice of oxidant and solvent, high conversions and, importantly, selectivity in oxidation reactions of bulky molecules over transition metal incorporated mesoporous SBA-15 catalysts could be obtained. The mesoporous structure of the prepared catalysts enabled a better accessibility of active sites to bulky substrate molecules which is reflected in the high conversions of cyclohexene and selectivity to the epoxide /diol over these novel catalysts. Special attention is drawn to the questions of the catalysts stability under the reaction conditions and their recyclability, both crucial for heterogeneous liquid-phase oxidations.

4.2 Influence of Reaction Parameters

The initial screening of the reaction systems provided very good conversions of the starting material with high selectivies to epoxide/diol. Blank reactions of the mesoporous SBA-15 material provided no cyclohexene conversions. We then decided to investigate the different parameters that could influence the conversion and selectivity in the present cyclohexene oxidation reaction.

4.2.1 Effect of Temperature

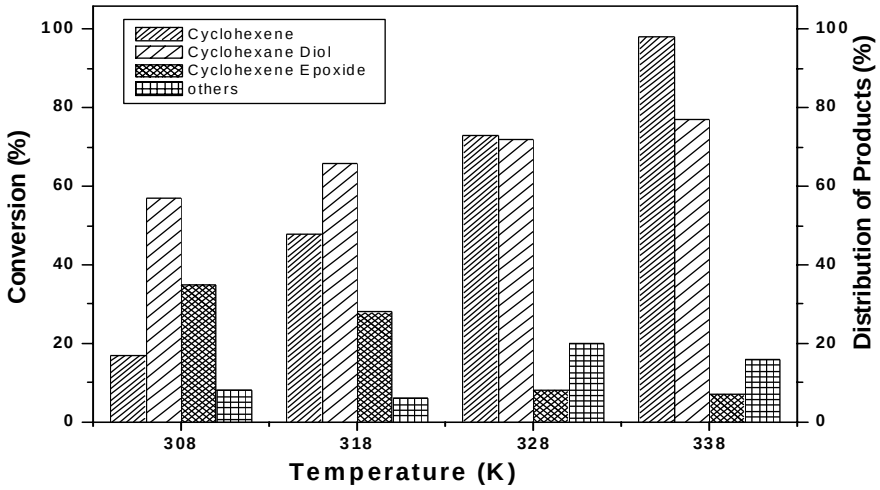

Figure 4.1. Reaction conditions: H_2O_2-45 mmol, SBW2-0.05g, Cyclohexene-40mmol, Acetonitrile-10ml, Time-6h

Effect of temperature in the oxidation of cyclohexene was initially assayed in a non optimized condition with SBW2 as the catalyst. The reaction was carried out in a range of temperatures from 308-338 K. The results obtained are presented in the Figure 4.1. Oxidation of cyclohexene with the catalyst SBW2 using H_2O_2 in acetonitrile produced cyclohexane diol as the major product.Cyclohexene epoxide and small quantities of allylic oxidation products are also formed. The percentage distribution of products varied interestingly with reaction temperature. As the temperature rises there is an increase in conversion. The cyclohexene conversion reached a value of 98% at a temperature of 338 K. The selectivity to diol increases from 57 to 75 % as the temperature rises from 308 to 338 K and that of epoxide decreases from 35 to 7 %. From this it is clear that the oxidation of epoxide to diol ocuurs at higher temperature. To study the effect of other reaction parameters in the oxidation of cyclohexene we chose the temperature 328 K by considering both the conversion and selectivity.

4.2.2 Effect of Catalyst Amount

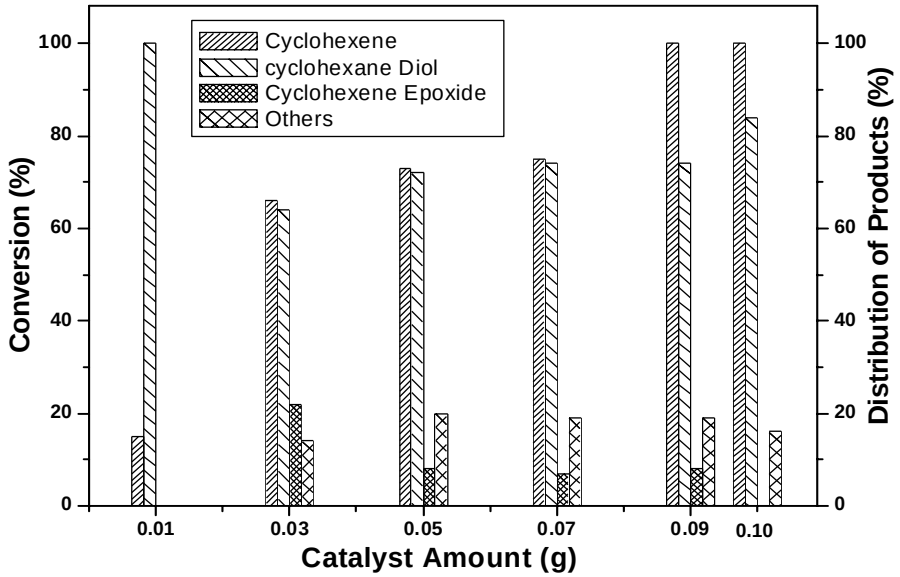

Figure 4.2. Reaction conditions: Temperature-328K, Catalyst-SBW2, Acetonitrile-10ml, Time-6h, Cyclohexene-40mmol, H_2O_2-45mmol,

The present oxidation reaction of cyclohexene was not observed in the absence of catalyst indicating that H_2O_2 alone is unable to oxidize the substrate cyclohexene. The effect of the quantity of the catalyst in the oxidation of cyclohexene was studied by varying the amount of catalyst and the results are presented in Figure 4.2. A gradual increase in conversion was observed with the increase of catalyst amount. It was observed that the conversion rate reaches 100 % when the catalyst amount is 0.09 g. Further increase of catalyst weight to 0.1 g causes an increase in the percentage of diol, which is due to the oxidation of epoxide initially formed. At all catalyst concentration, diol is the major product. A clear correlation of the catalyst weight with the product distribution cannot be established. At moderate conversions only the epoxide formation observed. An optimum catalyst amount of 0.05 g is selected for further reactions.

4.2.3 Effect of Amount of Solvent

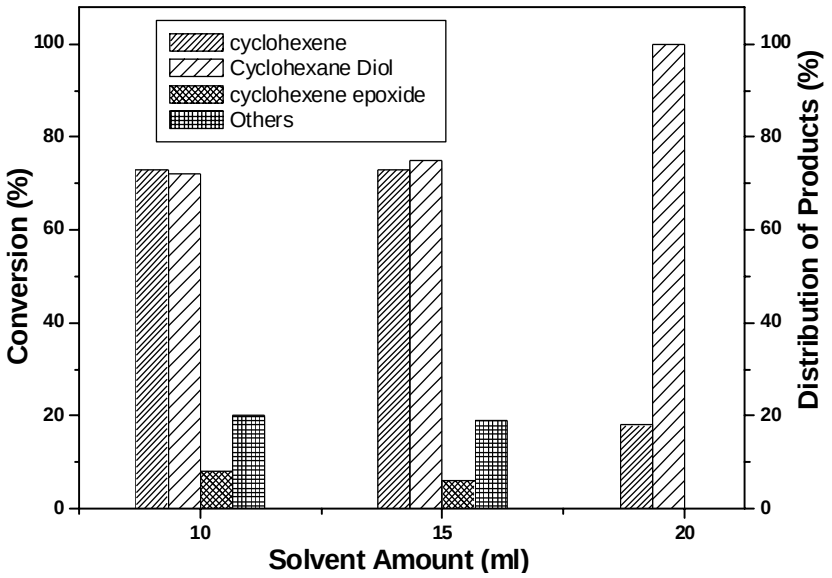

Figure 4.3. Reaction conditions:Temperature-328K, H_2O_2-45mmol, SBW2-0.05g, Cyclohexene-40mmol,Time-6h

The effect of concenteration of the solvent on the oxidation of cyclohexene is shown in Figure 4.3. The reaction conducted with various concenteration of acetonitrile shows that the solvent concenteration affects the conversion and selectivity in the present liquid phase oxidation reaction. No reaction was observed in the absence of solvent and no detectable conversion was observed upto a solvent amount 10 ml. The same conversion of 73% was obtained with sovlent amounts of 10 and 15 ml. Further increase in solvent amount causes a large decrease in conversion. This can be attributed to the fact that excess amount of solvent may cause a reduction in the substrate and catalyst concentration at the interface, which results a decrease in conversion. The selectivity of diol increses with increase in solvent amount. The solvent amount selected was 10 ml for further studies.

4.2.4 Effect of the concentration of H_2O_2

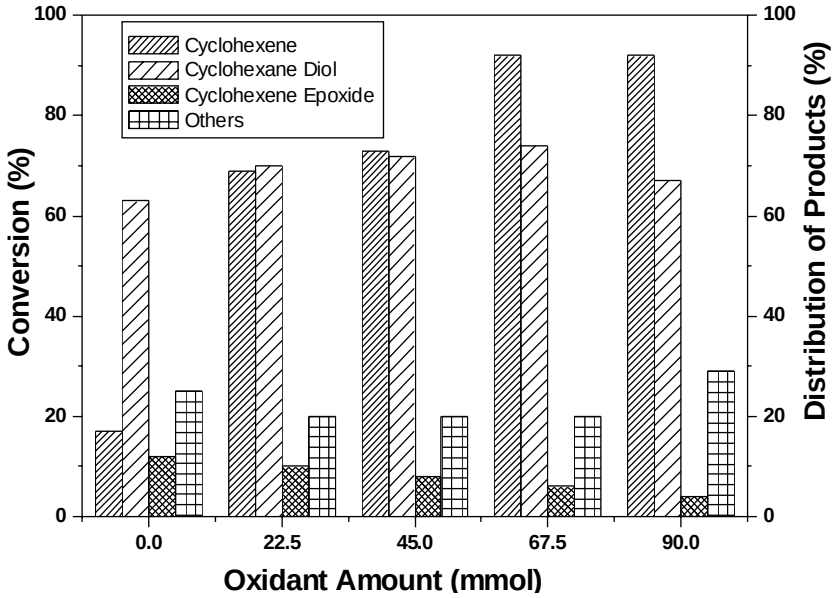

Figure 4.4. Reaction conditions:Temperature-328K, SBW2-0.05g, Cyclohexene-40mmol, Acetonitrile-10ml, Time-6h

The concentration of H_2O_2 has also a critical effect in the reaction. The effect of the amount of H_2O_2 on the oxidation of cyclohexene was investigated and the results are presented in Figure 4.4. Low H_2O_2 concentrations (22.5–45 mmol) gave relatively similar conversion of cyclohexene and selectivity to cyclohexanediol. Higher H_2O_2 concentrations (67.5 mmol) results in an increase in conversion but the selectivity remains the same. Further increase in concentration of H_2O_2 did not lead to a considerable increase of activity and selectivity in the reaction. A 67.5 mmol H_2O_2 concentration is selected as optimum in further oxidation of the cycloalkene. Interestingly, an increase in the H_2O_2 content in the systems did not significantly vary the activity and selectivity of the catalyst under the reaction conditions.

4.2.5 Effect of Substrate Amount

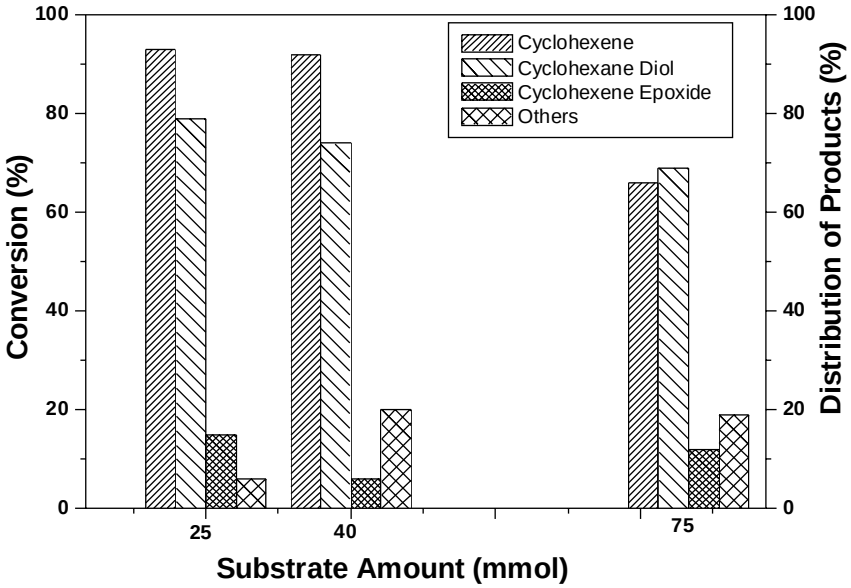

Figure 4.5. Reaction conditions:Temperature-328K, SBW2-0.05g, Acetonitrile-10ml , H_2O_2-67.5mmol, Time-6h

The effect of subsrate concentration in the oxidation of cyclohexene is shown in Figure 4.5. No significant change in conversion and selectivity to diol was observed at 25 and 40 mmol of cyclohexene. The conversion rate and diol selectivity decrease with increase in cyclohexene volume from 40 mmol to 75 mmol. An increase in substrate to catalyst ratio can cause unavailability of active sites for the reaction , which reduces the activity and selectivity [55]. Further reactions were carried out with a substrate amount 25 mmol.

4.2.6 Effect of Oxidants

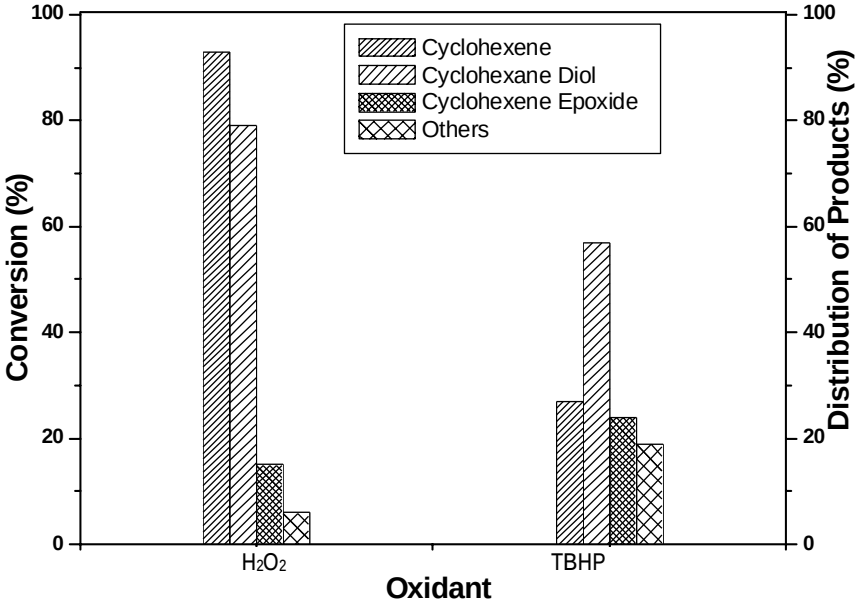

Figure 4.6. Reaction conditions:Temperature-328K, Acetonitrile-10ml, SBW2-0.05g,Cyclohexene-25mmol, Oxidant-67.5mmol, Time-6h

The oxidants tested were H_2O_2 (30% in water) and TBHP for cyclohexene oxidation reaction. The results obtained are presented in Figure 4.6. It was observed that the suitable oxidant for the present oxidation reaction is H_2O_2. Hydrogen peroxide is a very attractive green oxidant [56] for various organic compounds, as H_2O is the by product [57, 58]. The development of oxidation catalysts utilizing the H_2O_2 system is constructive for the environment [27]. H_2O_2 efficiency was also affected by the solvent and the catalyst structure [59].

4.2.7 Effect of Solvents

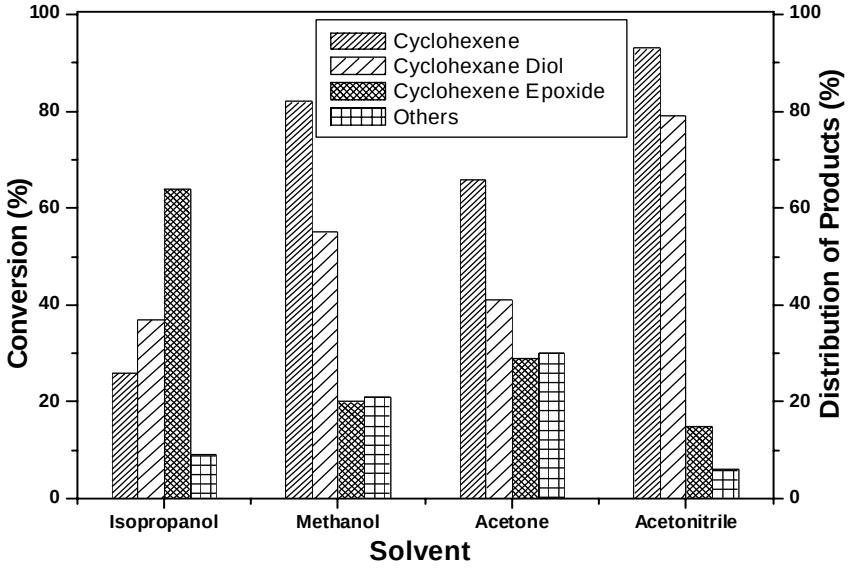

Figure 4.7. Reaction conditions:Temperature-328K, Solvent-10ml, H_2O_2-67.5mmol, Cyclohexene-25mmol, SBW2-0.05g, Time-6h

The effect of solvent on catalytic performance is a quite complicated but important area in studies of heterogeneous catalytic systems involving metallo silicate catalysts. Various solvent systems have been investigated; and acetonitrile is the most suitable solvent for the H_2O_2 system. However, with respect to the oxidation of cyclohexene, a converse solvent effect was observed (Figure 4.7); when acetonitrile was used as the solvent, the conversion was nearly fourfold greater than that obtained with isopropanol as solvent. A major influence of solvents on product selectivity was also observed. Isopropanol favoured the formation of epoxide. Epoxide selectivity of only 15-30 % was observed in solvents acetonitrile, methanol and acetone. However, reactions in acetonitrile showed 93% cyclohexene conversion and 79% diol selectivity.

4.2.8 Effect of Time

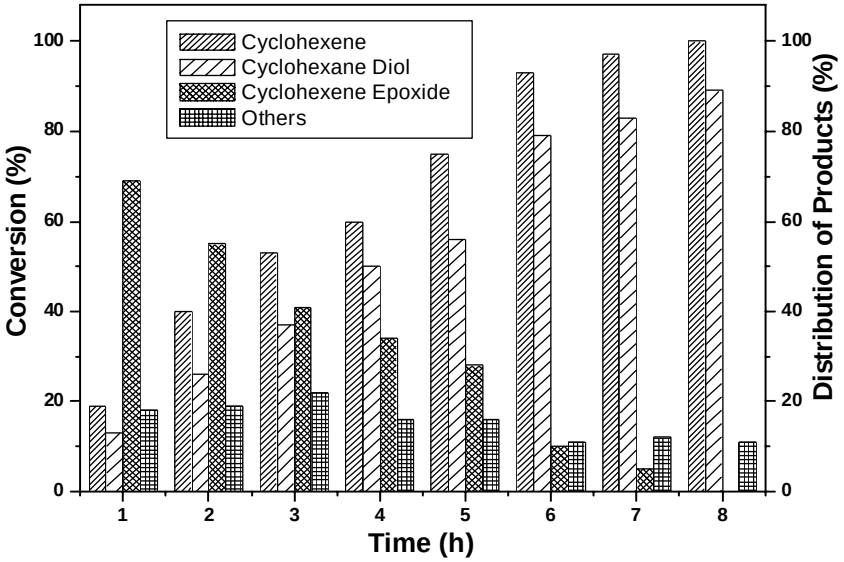

Figure 4.8. Reaction conditions:Temperature-328K, SBW2-0.05g Cyclohexene-25mmol, Acetonitrile-10ml, H_2O_2-67.5mmol.

Figure 4.8 shows the cyclohexene conversion profiles versus the reaction time for the catalyst SBW2. In the cyclohexene oxidation the activity systematically increased with the reaction time and it was accompanied by a significant decrease in epoxide and an increase in diol formation. After 7 h of the reaction, the main product observed was diol. The conversion increased strongly up to 6^{th} hour of the reaction (1-6 h) and then a dramatic slope change was observed. Cyclohexene epoxide was the main product during the initial stages of the reaction. On the other hand, Figure 4.8 shows the amount of H_2O_2 consumed (mmol) as a function of reaction time for the oxidation of cyclohexene.

4.3 Cyclohexene oxidation over prepared systems.

The cyclohexene oxidation reaction was carried out with all the prepared transition metal incorporated SBA-15 materials under the optimized reaction condition shown in Table 4.1

Table 4.1. Optimized reaction condition for cyclohexene oxidation

Parameters	Optimized condition
Temperature	328K
Solvent Amount (Acetonitrile)	10ml
Oxidant Amount (H_2O_2)	67.5mmol
Substrate Amount (Cyclohexene)	25mmol
Catalyst Amount	0.05g
Time	6h

Table 4.2. Effect of catalysts in cyclohexene oxidation reaction Reaction conditions: Temperature-328K, Acetonitrile-10ml, Time-6h, Cyclohexene-25mmol, Oxidant-67.5mmol, Catalyst-0.05g

Catalyst	Conversion of Cyclohexene (%)	Distribution of Products (%)		
		Cyclohexane Diol	Cyclohexene Epoxide	Others
Nil	Nil	-	-	-
SBA-15	19	35	55	10
SBW1	99	83	8	9
SBW2	93	79	10	11
SBW3	85	58	30	12
SBTi1	86	59	31	10
SBTi2	64	54	39	7
SBTi3	49	29	57	14
SBZr1	94	6	87	7
SBZr2	89	2	94	6
SBZr3	84	-	99	1
SBV1	90	10	76	14
SBV2	78	9	81	10
SBV3	69	3	90	7
SBMo1	94	9	75	16
SBMo2	79	7	83	10
SBMo3	69	4	85	11
SBCo1	80	13	59	28
SBCo2	52	7	77	16
SBCo3	41	3	82	15
SBCr1	89	28	48	24
SBCr2	73	11	74	15
SBCr3	42	8	78	14

The oxidation of cyclohexene using hydrogen peroxide is frequently used as a test reaction for the catalytic evaluation of different transition metal incorporated SBA-15 materials. The cyclohexene oxide generated by the heterolytic epoxidation of the cyclohexene double bond, and the 1,2-cyclohexanediol side product, formed by hydrolysis of the epoxide ring. The allylic oxidation side products, 2- cyclohexen-1-one and 2-cyclohexen-1-ol are often ascribed to a homolytic radical pathway and are presented here as others. The oxidation products were identified by comparison with authentic samples (retention times in GC). The blank reaction conducted in the absence of catalyst did not result any reaction and the mesostructured silica support has a little activity. The modified catalysts synthesized here showed a very good activity for the oxidation of cyclohexene. Cyclohexene epoxide was the main reaction product in almost the whole range of metal incorporated SBA-15 catalysts studied. The formation of 1, 2- cyclohexane diol was observed from epoxide ring opening in the case of W and Ti incorporated catalysts. The tungsten analogues displayed very high catalytic activity. The conversion of cyclohexene is in direct relation with the concentration of the active metal sites in the materials. For the present catalytic systems, the major product was cyclohexene oxide or diol and the secondary products were mostly 2-cyclohexene-1-ol and possibly 2-cyclohexene-1-one. In all cases, the selectivity for major product was around 90%. A maximum conversion of 99% was obtained for SBW1. For samples synthesized by varying the metal content, decreasing cyclohexene conversions was observed with decrease in metal content. This result indicates a decrease in the density of metal species that are active for the oxidation of cyclohexene. As reported in Table 4.2, the W and Ti based catalysts were more selective towards cyclohexane diol however the other catalysts produced epoxide. A maximum selectivity value of 99 % epoxide was observed using the

SBZr3. The Zr incorporated SBA15 catalysts exhibited an inherently higher selectivity for epoxide. The results show acceptable catalytic activity and selectivity compared to reported literatures [60, 61]. The epoxide formation did not depend only on the metal species in the samples but also on the surface acidity. In the presence of acid centres, epoxide can react further with another molecule of hydrogen peroxide or water to form a diol. Therefore, this factor is also important for considering the catalyst selectivity [62].

4.4 Cyclohexene Conversion and Si/M mole ratio

As expected, the activity decreased with decreasing metal content because of the number of active sites decreased. Figure 4.9 illustrates the role of active metal sites in the oxidation of cyclohexene. From the figure it is clear that the conversion increases with decrease in Si/M mole ratio of each transition metal incorporated SBA-15 systems.

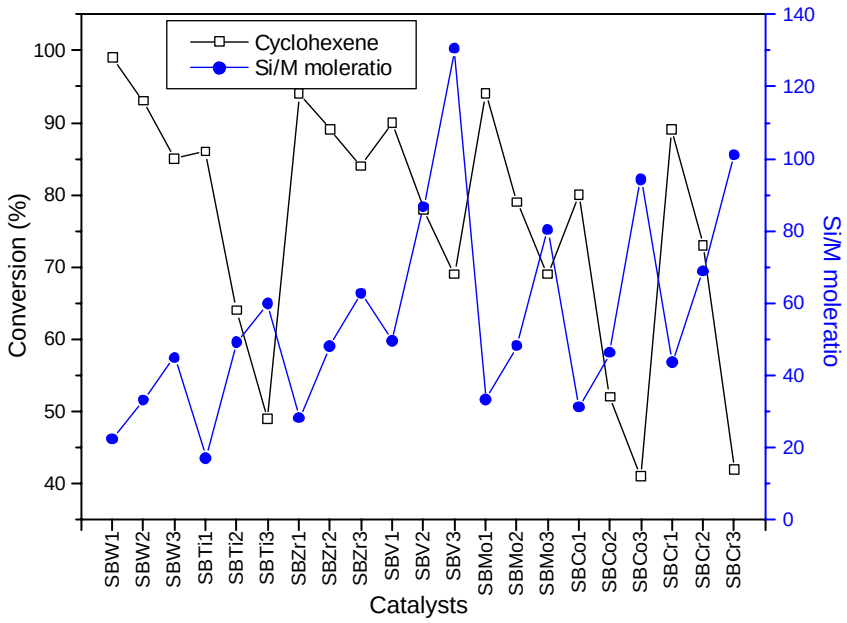

Figure 4.9 Cyclohexene Conversion and Si/M mole ratio

4.5 Effect of Substrates

The oxidation reaction was also carried out for various cyclo alkenes using the catalyst SBW2 under the optimized reaction condition of cyclohexene for comparative studies. The results obtained are presented in Table 4.3.

Table 4.3. Effect of substrates
Reaction conditions: Temperature-328K, Acetonitrile-10ml, Time-6h, Substrate-2.5ml, Oxidant-67.5mmol, SBW2-0.05g

Cyclopentene	Conversion (%)		96
	Distribution of Products (%)	Glutaraldehyde	56
		Diol	31
		Epoxide	9
		Others	4
Cyclohexene	Conversion (%)		93
	Distribution of Products (%)	Diol	79
		Epoxide	10
		Others	11
Cyclooctene	Conversion (%)		90
	Distribution of Products (%)	Epoxide	93
		Others	7

Oxidation of cyclopentene occurs with a high conversion of 96%. The major products obtained are glutaraldehyde (56%) and diol (31%). Cyclooctene, an even bulkier substrate, was converted (90%) to epoxide with 93% selectivity, over SBW2 under similar conditions using aq. H_2O_2 as the oxidant. All the substrates were converted above 90 % but there is a difference in product distribution observed.

4.6 Leaching Studies

Table 4.4. Temperature-328K, Acetonitrile-10ml, Catalyst-0.05g, Cyclohexene-25mmol, Oxidant-67.5mmol.

catalyst	Time (h)	Conversion of cyclohexene (%)	Distribution of Products (%)		
			Cyclohexane Diol	Cyclohexene Epoxide	Others
SBW2	1	24.00	43	57	-
	6	25.20	56	39	4
SBZr2	1	22.64	51	31	18
	6	23.27	58	26	16
SBT2	1	11.32	41	46	13
	6	11.73	47	38	15

A very important factor in processes carried out in liquid phase is the stability of the catalyst, i.e. their resistance to leaching of the active species. The catalyst was filtered out after one hour of the reaction while hot and analysed. The filtrate was kept under the same condition for 6h and then subjected to GC analysis. It was found that the conversion of cyclohexene remain practically constant within experimental error. There was no significant oxidation of cyclohexene after the hot filtration, suggesting that leaching of catalytically active, soluble titanium species was limited under these experimental conditions. Elemental analysis after the test confirm that the metal concentrations in the catalyst vary little; proving that leaching of these atoms is negligible, due to the strong anchoring of metal species in the lattice of SBA-15. The mixture was heterogeneous before and after the reaction and the catalysis nature was also proved to be true heterogeneous.

4.7 Recycling Studies

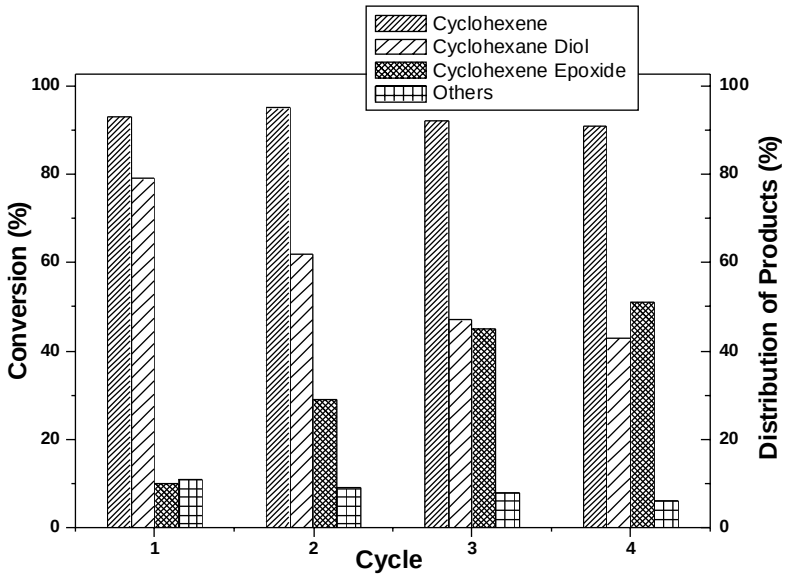

Figure 4.10. Reaction conditions:Temperature-328K, SBW2-0.05g Cyclohexene-25mmol, Acetonitrile-10ml, H_2O_2-67.5mmol.

The stability of the materials was also tested. In the case of materials possessing the highest amount of metal, the oxidation of cyclohexene was also carried out after catalyst regeneration under the same experimental conditions. The results of these experiments are shown in Figure 4.10. Special tests were performed to assess the catalyst stability and activity after recycling. After each operation cycle, the catalyst was separated, washed with H_2O/MeOH, dried, calcined at 540^0C for 6h and used in the next run. Moreover, recycling of the material showed that the activity is maintained over four runs, proving there is no leaching of active metal species. The material was therefore found to be highly reusable, preserving up to 95% of its initial catalytic activity after four reuses. It was established that the catalytic activity with respect to diol formation decreased significantly after each run although the conversion of cyclohexene was still attained. The formation of epoxide was faster after regeneration of the catalyst, which was attributed to the modification of the

catalyst surface during the first run of the process. Interestingly, the second run of the reaction gave rise to a higher initial activity.

4.8 Discussions

Cyclohexene oxidation catalysts are of particular interest, due to the potential uses of the products that can be obtained, including cyclohexene oxide, cyclohexane diol and 2-cyclohexene-1-one. From the product distribution it was observed that the oxidation of cyclohexene seems to proceed via two different and competitive reaction pathways. The substrate can be oxidised to the epoxide and ring cleavage takes place to give cyclohexanediol in the case of some prepared catalysts. A competitive reaction gives the 2-cyclohexene-1-ol which then undergoes further oxidation to 2-cyclohexen-1-one. The mesoporous structure of transition metals incorporated SBA-15 materials enabled a better accessibility of active sites to bulky substrate molecules which is reflected in the high conversions of cycloalkenes and better selectivity to the epoxide over these novel catalysts [41, 63].

The proposed mechanism suggests that the oxygen atom (from a metal-bonded peroxo activated entity) is transferred to the olefin through a direct pathway [64]. According to recent theoretical predictions for the epoxidation mechanism of olefins with supported metal oxide catalysts, an electron-poor metal center would increase the electrophilicity of the activated oxygen in the M-OOH hydroperoxy complex, thereby making the catalyst a more efficient oxygen-transfer agent. [65-67]. A more active oxygen transfer reaction would increase the amount of epoxide formed relative to allylic oxidation. The observed increase in selectivity for epoxidation over allylic oxidation is not sufficiently explained, however, by the hydrophilicity/ hydrophobicity of the surface [68]. Additionally, not a lot of research has gone into understanding this observation from a mechanistic standpoint [69].

The nucleophilic attack of the double bond of the alkene on an oxygen atom of hydroperoxy complex leads to the epoxide formation. For higher metal content, the epoxide selectivity decreases steadily due to an opening of side reaction of epoxide ring with water, probably catalyzed by the acid character of the metallosilicates. It should be taken into account that, as it has been observed by the broadening of the main UV–vis band of the catalyst at higher metal contents [70], H_2O has a strong tendency to coordinate with the four coordinated metal species. Moreover, the Lewis acid sites of catalyst, being the active species for the epoxidation [70], can also coordinate to water molecules which may react with the formed epoxide via epoxide ring-opening reactions leading to the formation of 1, 2-cyclohexanediol as side product [36].

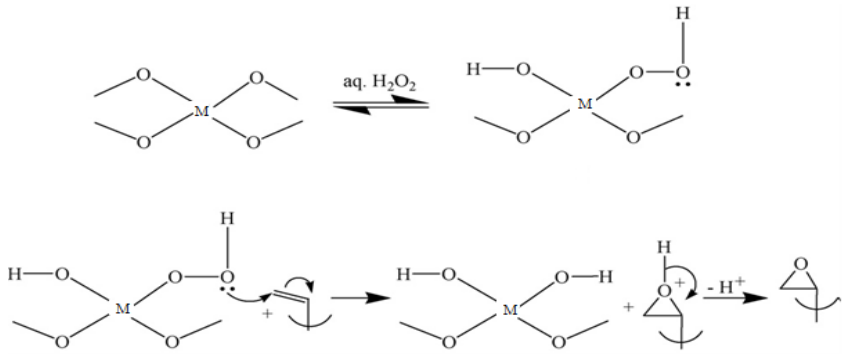

Scheme of the epoxidation reaction.

It is possible to suggest that the metal sites remain active and available even though high contents of the metals are incorporated into SBA-15. The main oxidation product was the cyclohexene oxide for almost of the prepared catalysts, indicating that the direct epoxidation mechanism which takes place through the formation of the metal-hydroperoxo intermediate is being favoured [36]. It was believed that the homogeneous distribution of tetrahedral transition metal entities within the channel walls is vital for the success of this catalytic process. Different metal loadings in the catalyst may induce changes in the surface species and may modify, sometimes noticeably, the catalytic features.

Little research has been done for elucidating the effect of varying the metal content on the catalytic effectiveness of the active sites [36].

The catalysts synthesized here showed a very good activity for the oxidation of cyclohexene, the cyclohexene oxide being the main reaction product in most of the catalysts studied. The formation of 1, 2- cyclohexanediol as by-product arising from epoxide ring opening was also observed for some catalysts. The density of silanol groups on the support greatly influences the retention and coordination number of the grafted metal species. This characteristic of the mesoporous silica supports also has an influence on the catalytic activity of the resulting metallosilicate materials. The metal center is able to activate the oxidant and then to control the oxygen atom transfer from the metal-oxo species to the substrate [71–74].

4.9 Conclusions

- As a catalytic test reaction, the activity, selectivity, and catalyst regenerability were studied in the oxidation of cyclohexene.
- Reaction parameters such as temperature, catalyst weight, time, amount of substrate, H_2O_2 and solvent, effect of various solvents and oxidants were studied in detail and reaction conditions were optimized.
- By an appropriate choice of oxidant and solvent, high conversions and, importantly, selectivity in oxidation reaction of cyclohexene over the prepared transition metals incorporated SBA-15 catalysts could be obtained.
- It was demonstrated that these catalysts do not significantly leach under the reaction conditions.

- Highly dispersed tetrahedrally coordinated metal species evidenced by various spectroscopic techniques are highly active and selective for the oxidation reactions.
- The catalytic activity of the different grafted metal-SBA-15 materials was mainly influenced by the accessibility of the reactants to the active sites.

References

[1] S. Bhaduri, D. Mukesh, Homogeneous Catalysis: Mechanisms and Industrial Applications; Wiley-Interscience: New York, 2000.

[2] B. Cornils, W. A. Herrmann. Eds. Applied Homogeneous Catalysis with Organometallic Compounds, 2nd ed.; Wiley-VCH: Weinheim, 2002.

[3] N. Prilezhaev, Ber. 1910, 42, 4811-4815., D. Swern, Organic Peroxide; Wiley-Interscience, New York, 1971.

[4] R. A. Sheldon, J. A. Van Doorn, J. Catal., 31 (1973) 427.

[5] K. A. Jørgensen, Chem. Rev., 89 (1989) 431.

[6] F. E. Kuhn, A. M. Santos, I. S. Goncualves, C. C. Romao, A. D. Lopes, Appl. Organomet. Chem., 15 (2001) 43.

[7] F. E. Kuhn, A. M. Santos, M. Abrantes, Chem. Rev., 106 (2006) 2455.

[8] F. E. Kuhn, A. M. Santos, W. A. Herrmann, Dalton Trans., 15 (2005) 2483.

[9] P. Chaumette, H. Mimoun, L. Saussine, J. Fischer, A. Mitschler, J. Organomet. Chem., 250 (1983) 291.

[10] M. K. Trost, R. G. Bergman, Organomet. Chem., 10 (1991) 1172.

[11] S. W. Park, K. J. Kim, S. Y. Seung, Bull. Korean Chem. Soc., 21 (2000) 446.

[12] Y. L. Wang, D. K. P. Ng, H. K. Lee, Inorg. Chem., 41 (2002) 5276.

[13] N. Timofeeva, O. A. Kholdeeva, S. H. Jhung, J. S. Chang, Appl. Catal. A., 345 (2008) 195.

[14] R. A. Sheldon, J. Kochi, Metal-Catalyzed Oxidation of Organic Compounds, Academic Press, New York, 1981.

[15] D. G. Lee, M. van der Engh, in: W.S. Trahanovsky (Ed.), Oxidation in Organic Chemistry, Academic Press, New York (1973) p. 186.

[16] S. Wolfe, S. K. Hasan, J. R. Campbell, J. Chem. Soc., Chem. Commun., (1970) 1420

[17] H. J. Carlsen, T. Katsuki, V. S. Martin, K. B. Sharpless, J. Org. Chem., 46 (1981) 3936.

[18] W. Merk, G. Schreyer, W. Weigert, Ger. Offen. 2,106,307, Degussa (1972); W. Merk, G. Schreyer, W. Weigert, Chem. Abstr. 77 (1972) 151485.

[19] K. Sato, M. Aoki, R. Noyori, Science, 281 (1998) 1646.

[20] C. Venturello, R. D. Aloisio, J. Org. Chem., 53 (1988) 1553.

[21] J. P. Oppenheim, G. L. Dickerson, 5th ed., Kirk-Othmer Encyclopedia of Chemical Technology, Vol. 2, John Wiley & Sons, New York (2003).

[22] P. Arpentinier, F. Cavani, F. Trifiro, The Technology of Catalytic Oxidations, Editions TECHNIP, Paris (2001).

[23] G. Lapisardi, F. Chiker, F. Launay, J. P. Nogier, J. L. Bonardet, Microporous and Mesoporous Materials, 78 (2005) 289.

[24] C.Y. Cheng, K. J. Lin, M. R. Prasad, S. J. Fu a, S.Y. Chang, S. G. Shyu, H. S. Sheu, C. H. Chen, C. H. Chuang, M. T. Lin, Catal. Commun., 8 (2007) 1060.

[25] K. Sato, M. Aoki, M. Ogawa, T. Hashimoto, R. Noyori, J. Org. Chem., 61(1996) 8310.

[26] T. J. Collins, Acc. Chem. Res., 35 (2002) 782.

[27] Jimtaisong, R. L. Luck, Inorganic Chemistry, 45 (2006) 25.

[28] J. M. Bregeault, Dalton Trans., (2003) 3289.

[29] R. A. Sheldon, J. Dakka, Catal. Today., 19 (1994) 215.

[30] M. A. Camblor, A. Corma, J. Perez-Pariente, Zeolites, 13 (1993) 82.

[31] M. H. Zahedi-Niaki, M. P. Kapoor, S. Kaliaguine, J. Catal., 177 (1998) 231.

[32] T. Blasco, A. Corma, M. T. Navarro, J. P. Pariente, J. Catal., 156 (1995) 65.

[33] M. Besson, M. C. Bonnet, P. Gallezot, I. Tkatchenko, A. Tuel, Catalysis Today,51 (1999) 547.

[34] L. Y. Chen, G. K. Chuah, S. Jaenicke, Catal. Lett., 50 (1998) 107.

[35] T. Tatsumi, K. K. Koyano, N. Igarashi, Chem. Commun., (1998) 325.

[36] G. A. Eimer, S. G. Casuscelli, C. M. Chanquia, V. E. Monica, E. Crivello, E. R. Herrero, Catalysis Today, 133 (2008) 891.

[37] R. Sever, R. Alcala, J. Dumesic, T. Root, Microporous and Mesoporous Materials, 66 (2003) 53.

[38] A. Hagen, K. Schueler, F. Roessner, Microporous and Mesoporous Materials, 51 (2002) 23.

[39] L. Chen, G. Chuah, S. Jaenicke, Catal. Lett., 50 (1998) 107.

[40] S. Laha, R. Kumar Microporous and Mesoporous Materials, 53 (2002) 163.

[41] A. Kumar, D. Srinivas, P. Ratnasamy, Chem. Commun., (2009) 6484.

[42] M. A. Camblor, A. Corma, J. Perez-Pariente, Zeolites, 13 (1993) 82.

[43] N. N. Trukhan, A.Yu. Derevyankin, A. N. Shmakov, E. A. Paukshtis, O. A. Kholdeeva, V. N. Romannikov, Microporous and Mesoporous Materials, 44 (2001) 603.

[44] O. A. Kholdeeva, A.Yu. Derevyankin, A. N. Shmakov, E. A. N. N. Trukhan, A. Paukshtis, V. N. Tuel, Romannikov, J. Mol. Catal. A: Chem., 158 (2000) 417.

[45] O. A. Kholdeeva, M. S. Melgunov, A. N. Shmakov, N. N. Trukhan, V.V. Kriventsov, V. I. Zaikovskii, M. E. Malyshev, V. N. Romannikov, Catalysis Today, 91 (2004) 205.

[46] O. A. Kholdeeva, O.V. Zalomaeva, A. N. Shmakov, M. S. Melgunov, A. B. Sorokin, J. Catal., 236 (2005) 62.

[47] N. N. Trukhan, V. N. Romannikov, E. A. Paukshtis, A. N. Shmakov, O. A. Kholdeeva, J. Catal., 202 (2001) 110.

[48] O. A. Kholdeeva, N. N. Trukhan, Russ. Chem. Rev., 75 (2006) 411.

[49] S. O. Lee, R. Raja, K. D. M. Harris, J. M. Thomas, B. F. G. Johnson, G. Sankar, Angew. Chem., Int. Ed., 42 (2003) 1520.

[50] H. Chen, W. L. Dai, J. F. Deng, K. Fan, Catal. Lett., 81 (2002) 131.

[51] D. Trong On, D. Desplantier-Giscard, C. Danumah, S. Kaliaguine, Appl. Catal. A., 222 (2001) 299.

[52] R. Luque, K. S. Badamali, J. H. Clard, M. Fleming, D. J. Macquarrie, Appl. Catal. A., 341 (2008) 154.

[53] E. M. McGarrigle, D. G. Gilheany, Chem. Rev., 105 (2005) 1563.

[54] B. S. Lane, K. Burguess, Chem. Rev., 103 (2003) 2457.

[55] D. Rohan, C. Canaff, E. Romeafin, M. Guismet, J. Catal., 177 (1998) 2743.

[56] R. Noyori, M. Aoki, K. Sato, Chem. Commun., 16 (2003) 1977.

[57] C. W. Jones, In Applications of Hydrogen Peroxide and Derivatives; Clark, J. H., Ed.; Royal Society of Chemistry, Thomas Graham House, Cambridge (1999).

[58] G. Centi, F. Cavani, F. Trifiro, Selective oxidation by Heterogeneous Catalysis; Kluwer Academic/Plenum Publishers: New York (2001).

[59] W. Fan, Peng W.T. Tatsumi, J. Catal., 256 (2008) 62.

[60] S. Mohebb, A. H. Sarvestani, Transition Met. Chem., 31 (2006)749.

[61] D. M. Boghaei, S. Mohebi, J. Mol. Catal. A: Chem., 41 (2002) 179.

[62] M. Trejda, A. Tuel, J. Kujawa, B. Kilos, M. Ziolek, Microporous Mesoporous Mater., 110 (2008) 271.

[63] P. Ratnasamy, D. Srinivas,H. Knozinger, Adv. Catal., 48 (2004) 1.

[64] J. M. Mitchell, N. S. Finney, J. Chem. Am. Soc., 123. (2001) 862.

[65] P. E. Sinclair, R. A. Catlow, J. Phys. Chem. B., 103 (1999) 1084.

[66] D. H. Wells, W. N. Delgass, K. T. Thomson, J. Am. Chem. Soc., 126 (2004) 5.

[67] A. Urakawa, T. Burgi, P. Skrabal, F. Bangerter, A. Baiker, J. Phys. Chem., 109 (2005) 2212.

[68] S. A. Holmes, F. Quignard, A. Choplin, R. Teissier, J. Kervennal, J. Catal., 176 (1998) 182.

[69] R. L. Brutchey, D. A. Ruddy, L. K. Andersen, T. Don Tilley, Langmuir, 21(2005) 9576.

[70] G. A. Eimer, S. G. Casuscelli, C. M. Chanquia, V. Elias, M. E. Crivello, E. R. Herrero, Catalysis Today, 133 (2008) 639.

[71] S. Mohebbi, A. H. Sarvestani, Transit. Metal. Chem., 31 (2006)749.

[72] J. Bernadou, B. Meunier, Chem. Commun., 2167 (1998).

[73] K. A. Lee, W. J. Nam, J. Am. Chem. Soc., 119, 1916 (1997).

[74] S. Shaik, M. Filatov, D. Schrder, H. Schwarz, Chem. Eur. J., 4 (1998) 193.

…..ꕥ…..

Chapter 5

Oxidation of Benzyl Alcohol

Contents

Oxidation of 1^o and 2^o alcohols to the corresponding carbonyl compounds is a fundamental and important transformation in organic chemistry as the products are valuable synthetic intermediates. In recent years the development of heterogeneous catalysts for selective oxidation of alcohols has been studied extensively. Several studies have suggested that metal nanoparticles may function as active species in various organic reactions. Recent reports have revealed that supported metal nanoparticles show attractive catalytic performances for the oxidation of alcohols. It is an important transformation from the viewpoint of establishing a green process for the synthesis of carbonyl compounds to replace the conventional stoichiometric oxidation process using dichromate or permanganate. In this chapter the liquid phase oxidation reaction of benzyl alcohol over various transition metals incorporated mesoporous SBA-15 materials were analysed in detail. The influence of various reaction parameters were investigated thoroughly.

5.1 Introduction

For a liquid phase reaction which contains both oil and water phases, vigorous stirring and a co-solvent, or a phase transfer catalyst is required to promote the reaction, of which using a phase transfer catalyst is the most efficient method. To reuse the expensive and sometimes toxic phase transfer reagents for the consideration of economy and environment, the phase transfer catalyst tends to be immobilized onto a solid support to obtain a heterogeneous catalyst, which is more suitable for industrial fabrications. Such a concept of liquid-liquid-solid "triphase catalysis" has been well adopted in many cases [1-4].

Present work demonstrated the use of the ordered mesoporous silica (SBA-15) as a nanoreactor for liquid-liquid biphase reaction with high activity. It is expected that the amphiphilic surface of the mesoporous silica provide a suitable accommodation for both hydrophilic and hydrophobic molecules [1].

Transition metal incorporated SBA-15 systems appear as promising catalysts which are active and selective in various types of oxidation reactions of organic compounds. Catalytic oxidation of primary alcohols to aldehydes is essential for the preparation of fragrances and food additives as well as many organic intermediates. The formation of benzaldehyde with high yields will have great advantages economically and energetically. Hydrogen peroxide is found to be a superior oxidising agent for the oxidation of alcohols as it is efficient and yields water and oxygen only on decomposition.

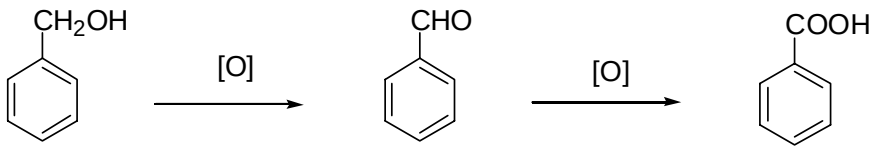

Various metal oxides were found to be effective in catalytic oxidation of benzyl alcohol. Pd nanoparticles supported on magnesia or entrapped in aluminum hydroxide were found to be efficient catalysts for the aerobic oxidation of alcohols [5-7]. Changli Li et. al studied the possibility of Pd/SBA-15 catalysts for the aerobic oxidation of benzyl alcohol under solvent-free conditions in the absence of any additives [5]. Oxidation over supported gold catalysts using molecular oxygen has gained much attention recently and microwave heating was employed and H_2O_2 was used as an oxidant, since the catalytic performance was not sufficiently high under aerobic conditions at ambient temperature [8-15]. Under N_2 atmosphere or airtight conditions, the benzyl alcohols can be selectively oxidized to aldehydes [1]. When MCM-41 with small pore size (2.4 nm) was used as the support, a relatively low yield (71%) was obtained. It may arise from the difficulty for both the substrates and the products to enter and escape from the mesochannels [1].

In the present study liquid phase oxidation of benzyl alcohol has been attempted under a variety of reaction conditions over various transition metal incorporated SBA-15 catalysts. It was suggested that the relatively larger pore size of SBA-15 can accelerate the diffusion of alcohol molecules and which is highly beneficial to the oxidation reaction [5]. The enhanced selectivity of benzaldehyde even at higher substrate conversions achieved over the prepared catalysts is attributed to the unique facile discharge of the desired products from the channels of the catalyst at the reaction temperature and atmospheric pressure [11]. It was found that the catalysts are recyclable without much loss of activity. This strategy could be used for similar chemical transformations to use in an ecofriendly manner [16]. To examine the heterogeneity of the reaction, the catalyst was removed from the reaction by hot-filtration and the reaction was continued

with the filtrate and without catalyst. The results clearly proved that the reaction was a heterogeneous process [17-20].

The experiments were done and the products were analysed by the procedure given in section 2.4.1(2) of chapter 2. The reaction was carried out at different reaction temperatures and with different substrate to H_2O_2 mole ratios and in a variety of solvents and oxidants in order to optimize the reaction conditions. Furthermore the reaction was performed by varying the concentration of solvent acetonitrile. The effect of time on the reaction was also studied by running the reaction in a 8h period. The major product identified was benzaldehyde for all the catalytic systems. A slight amount of benzoic acid was also observed. The catalytic activity was expressed as the % conversion of benzyl alcohol. Comparison of the reactivity results with literature data reveals that a better catalytic performance can be obtained over transition metal oxides supported on mesoporous silica SBA-15 material [21-23]. The result may be thought of as the proof that the performance of the metal containing SBA-15 catalysts may arise from the active metal sites in the prepared catalysts. We also obtained a possible correlation between the metal content and the catalytic activity regarding the oxidation of benzyl alcohol.

The observations of the present investigations and the possible explanation of the results are presented here.

5.2 Effect of Reaction Variables

An attempt has been made to optimize the reaction variables such as temperature, catalyst amount, time, substrate to oxidant mole ratio, amount of solvent etc in order to study the effect of various parameters on the conversion and selectivity. It also helps to know the condition for getting maximum conversion and product yields. Since the reaction conditions play an important role in deciding the catalytic activity and selectivity for products, it is essential

to study the influence reaction condition for a chemical reaction. Oxidation of benzyl alcohol using H_2O_2 was carried out initially in non optimized conditions with SBW1 as the catalyst.

5.2.1 Effect of Temperature

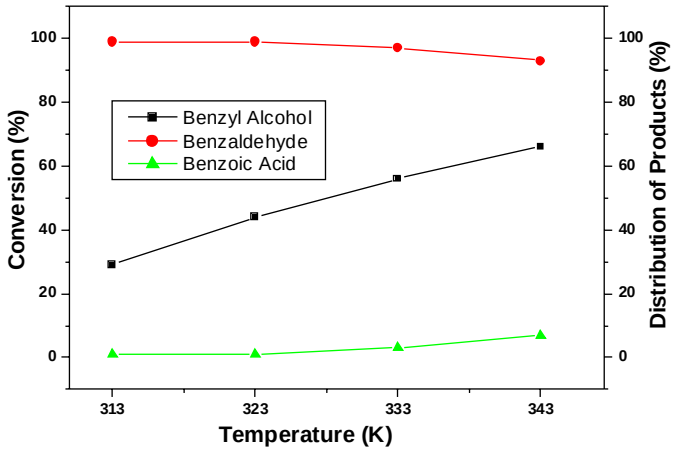

Figure 5.1. Influence of temperature on benzyl alcohol oxidation Reaction conditions: Acetonitrile-10ml, SBW1-0.05g, H_2O_2-45mmol, Benzyl Alcohol-19mmol, Time-6h.

The effect of temperature on the oxidation of benzyl alcohol was studied in a temperature range 313 K to 343 K while all other reaction parameters were kept constant. The results are given in Figure 5.1. When temperature was increased from 313 to 343 K, conversion rate increased drastically with benzaldehyde selectivity greater than 90%. Further increase in temperature may cause a decrease in conversion. At higher temperature, the self decomposition of H_2O_2 to molecular oxygen proceeds faster and it could not participate efficiently for the oxidation processes [24]. Evaporation of the solvent at higher temperature may also result in reduced conversion. Literature reports also support this. So we did not conduct the reaction at higher temperature than 343 K. For the present reaction the temperature selected was 343 K in order to get high conversion. From the Figure it is clear that a very

small decrease in selectivity of benzaldehyde was observed by raising the temperature from 313 K to 343 K.

5.2.2 Effect of Time

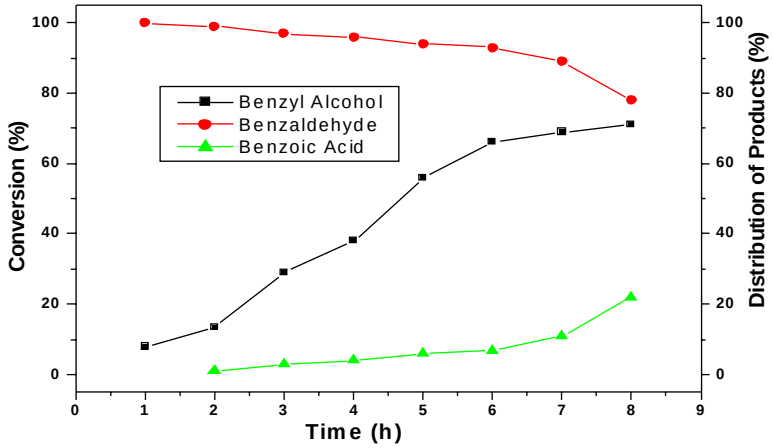

Figure 5.2. Influence of time on benzyl alcohol oxidation
Reaction conditions: Acetonitrile-10ml, SBW1-0.05 g, Benzyl Alcohol-19mmol, H_2O_2-45mmol, Temp-343K

Effect of time on the oxidation of benzyl alcohol is illustrated in Figure 5.2. An appropriate reaction time is the main assurance for a perfect reaction. In the present study the reaction mixture was analyzed at various time intervals in order to study the effect of reaction time on the oxidation of benzyl alcohol. An increase in the conversion was observed as the time proceeds. But the selectivity toward benzaldehyde decreased continuously. This is due to the consecutive oxidation of the product benzaldehyde, which was favored with increasing time. The maximum conversion of 71% is reached at 8h of reaction time with selectivity of benzaldehyde 78%. For further studies of the present reaction a reaction time of 6h was selected in order to achieve an appreciable conversion of benzyl alcohol and selectivity of benzaldehyde.

5.2.3 Effect of Catalyst Amount

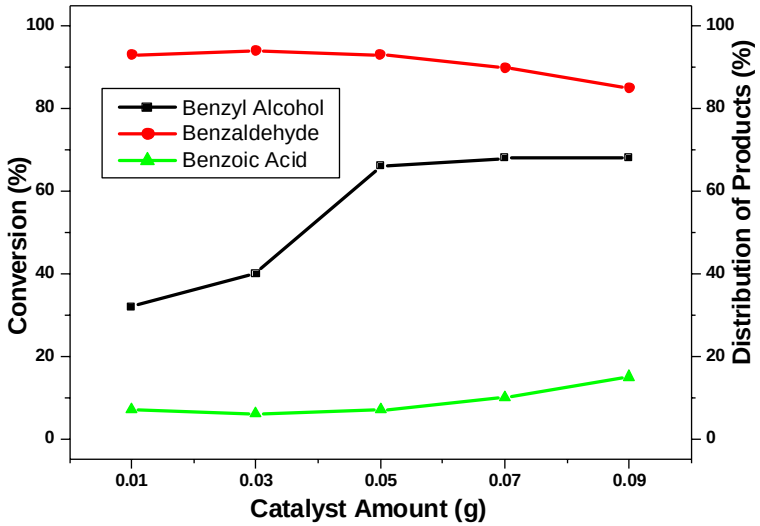

Figure 5.3. Influence of catalyst amount on benzyl alcohol oxidation Reaction conditions: Acetonitrile-10ml, Temp-343K, Benzyl Alcohol-19mmol, H_2O_2-45mmol, Time-6h

The dependence of the amount of catalyst on the production of benzaldehyde by the oxidation of benzyl alcohol is presented in Figure5.3. Here the influence of catalyst amount was studied by taking different weight of the catalyst SBW1 while keeping the other parameters constant. The oxidation rate sharply increased from 40 to 66% as the amount of catalyst increased from 0.03g to 0.05g. Benzyl alcohol conversion remained steady with further increase of catalyst amount but there is a lowering in selectivity of benzaldehyde. This lowering in selectivity is attributed to the oxidation of benzaldehyde to benzoic acid. The optimized catalyst amount for further reaction was 0.05g. The results of this study indicate that an appropriate conversion and selectivity was obtained even with the small amount of catalyst 0.05g.

5.2.4 Effect of Solvent Amount

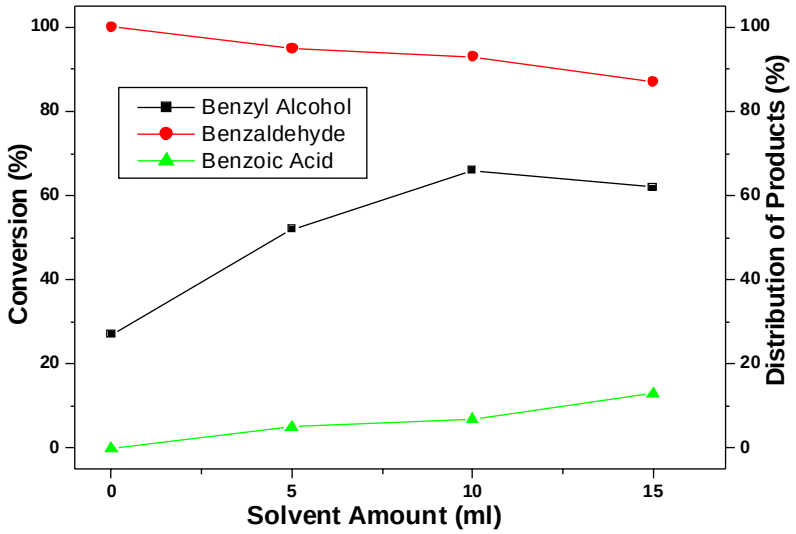

Figure 5.4. Influence of solvent amount on benzyl alcohol oxidation Reaction conditions: Benzyl Alcohol-19mmol, SBW1-0.05 g, H_2O_2-45mmol, Temp-343K, Time-6h

The effect of volume of acetonitrile on the benzyl alcohol oxidation reaction is presented in Figure 5.4. The present oxidation was conducted as a function of acetonitrile concentration in order to study the effect of solvent amount in the reaction. Benzaldehyde selectivity was found to be 100% in the absence of solvent with a minimum conversion of 27%. The conversion of benzyl alcohol increased with an increase in the concentration of acetonitrile up to 10 ml. Further increase in acetonitrile volume causes a reduction in conversion. The selectivity of benzaldehyde decreases with increase in acetonitrile volume. The acetonitrile volume of 10 ml was found to be an optimum solvent amount to achieve high conversion and selectivity. When the solvent was excess, the substrate or catalyst concentration at the interface may be lower, thus resulting a decrease in conversion.

5.2.5 Effect of Oxidant Amount

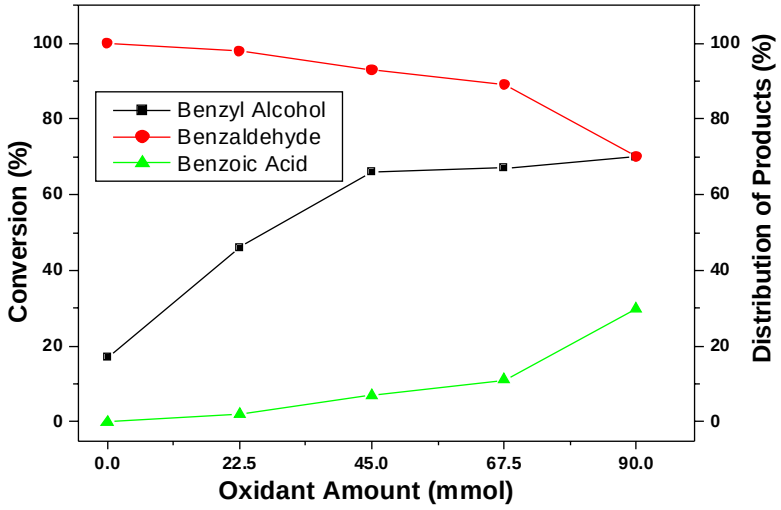

Figure 5.5 Influence of oxidant amount on benzyl alcohol oxidation Reaction conditions: Acetonitrile-10ml, SBW1-0.05g, Benzyl Alcohol-19mmol, Temp-343K, Time-6h

Figure 5.5 depicts the influence of oxidant amount in the present oxidation reaction. The reactions were carried out under previously optimized condition and changing the volume of H_2O_2 from 22.5 to 90 mmol while keeping the substrate constant. Without oxidant only 17 % conversion was observed with 100% benzaldehyde selectivity. In the presence of oxidant higher conversion was observed. The conversion increases from 46 to 66 % upon changing the H_2O_2 amount from 22.5 to 45 mmol. A small increase in conversion was noticed with further increase of oxidant amount. The selectivity of benzaldehyde decreased drastically with 90 mmol of oxidant. The presence of excess oxidant favoured further oxidation of the initially formed product benzaldehyde. A volume of H_2O_2 45 mmol was found to be the optimum for further studies.

5.2.6 Effect of Solvents

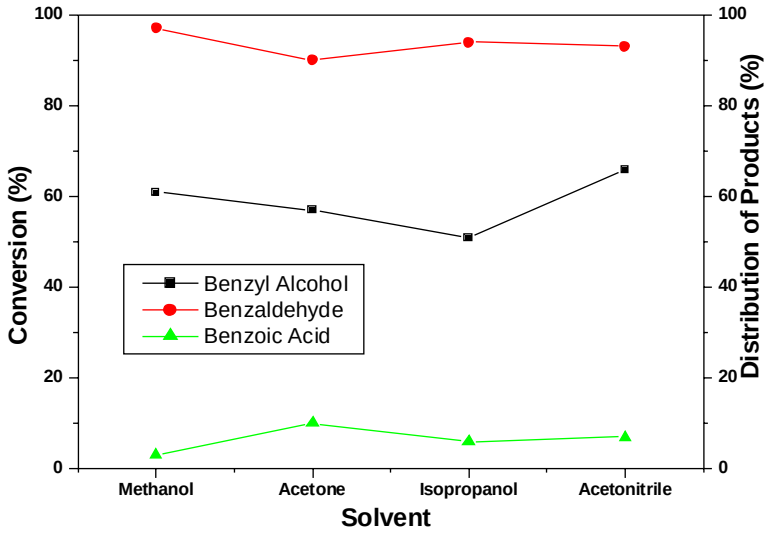

Figure 5.6. Influence of various solvents on benzyl alcohol oxidation Reaction conditions: Solvent-10ml, Benzyl Alcohol-19mmol, H_2O_2-45mmol, SBW1-0.05 g, Temp-343K, Time-6h

It has been reported in several articles that the liquid phase oxidation of alcohols are sensitive to the solvents used [25-27]. Therefore we carried out the reaction with different solvents such as methanol, acetone, isopropanol, and acetonitrile in order to investigate the role of solvents. The results are illustrated in Figure 5.6. The choice of solvent is important in the case of liquid phase oxidation reaction because the solvent had a great influence on the catalytic activity and in the percentage distribution of products. They can affect the mass transfer and diffusion rates with heterogeneous solid acid catalysts. The maximum conversion was observed with acetonitrile as solvent. The conversion decreases as the solvent is changed from acetonitrile to others. Among acetone, isopropanol and methanol, better results were observed in the case of methanol. Selectivity of benzaldehyde did not change much with different solvents. Acetonitrile is found to be the best solvent for the present reaction system and it could be due to its high polarity. Comparatively good solubility power of acetonitrile for both the organic

substrate and the aqueous H_2O_2 make it as a good solvent. The activity of catalyst increased in acetonitrile since the phase separation between the aromatic substrate and the aqueous oxidant is greatly reduced which enables easy transport of the active oxygen species for the oxidation [28]. It is evident that for this reaction the hydrophobic/ hydrophilic properties of the catalyst should be of paramount importance.

5.2.7 Effect of Oxidants

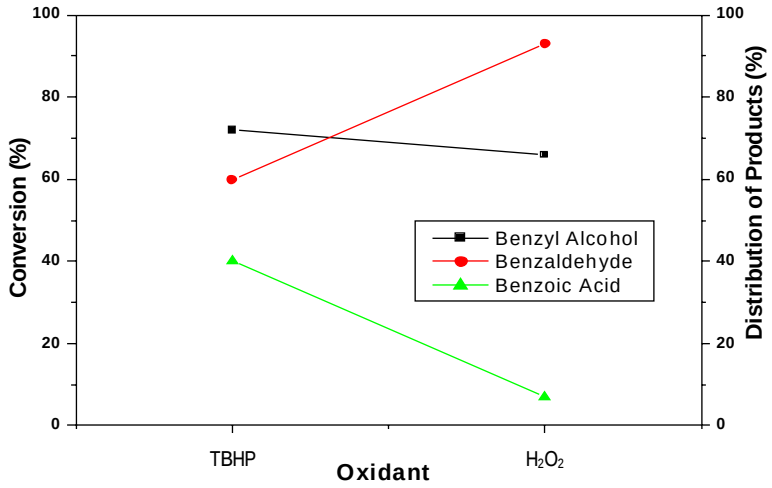

Figure 5.7. Influence of oxidants on benzyl alcohol oxidation
Reaction conditions: Acetonitrile-10ml, Oxidant-45mmol, Benzyl Alcohol-19mmol, SBW1-0.05 g, Temp-343K, Time-6h

To study the effect of oxidants on the oxidation of benzyl alcohol, the reaction was carried out with the oxidants H_2O_2 and TBHP. The results are presented in Figure 5.7. The conversion decreased from 72 to 66 % as the oxidant changed from TBHP to H_2O_2. But the selectivity of benzaldehyde is higher in the case of H_2O_2. So we selected H_2O_2 as an oxidant for further oxidation studies of benzyl alcohol. Oxidations using environmental friendly oxidants like H_2O_2 are more desirable in these days since it is efficient and yields water and oxygen only on decomposition

5.3 Performance of Different Catalyst Systems on Benzyl Alcohol Oxidation.

The above observations and results clearly reveal that the reaction parameters play an important role in determining the conversion and selectivity of the liquid phase oxidation of benzyl alcohol. The present oxidation reaction was carried out over all the prepared systems under the optimized reaction conditions in order to produce higher conversion and selectivity of products. The optimized reaction parameters are summarized in Table 5.1

Table 5.1 Optimized reaction condition for benzyl alcohol oxidation

Parameters	Optimized condition
Temperature	343K
Solvent Amount (Acetonitrile)	10ml
Oxidant Amount (H_2O_2)	45.0mmol
Substrate Amount (benzyl Alcohol)	19.0mmol
Catalyst Amount	0.05g
Time	6h

Catalytic activities of all the prepared systems on benzyl alcohol oxidation reaction were evaluated under the optimized reaction condition. The results obtained are presented in Table 5.2.

Table 5.2 Influence various catalysts on benzyl alcohol oxidation. Reaction conditions: Acetonitrile-10ml, Benzyl Alcohol-19mmol, Oxidant-45mmol, Temp-343K, Time-6h, Catalyst Amount-0.05 g

Catalyst	Conversion of Benzyl Alcohol (%)	Distribution of Products (%)	
		Benzaldehyde	Benzoic Acid
SBA-15	11	94	6
SBW1	66	93	7
SBW2	59	95	5
SBW3	52	99	1
SBTi1	49	88	12
SBTi2	42	93	7
SBTi3	37	99	1
SBZr1	54	89	11
SBZr2	43	90	10
SBZr3	40	94	6
SBV1	49	78	22
SBV2	40	89	11
SBV3	36	97	7
SBMo1	45	86	14
SBMo2	42	88	12
SBMo3	36	91	9
SBCo1	46	89	11
SBCo2	41	91	9
SBCo3	33	95	5
SBCr1	43	91	9
SBCr2	36	92	8
SBCr3	30	98	2

Pure SBA-15 gave very low conversion under the specified reaction condition. From the results it is clear that the catalytic oxidation of benzyl alcohol to benzaldehyde can be accelerated to a greater extent by the incorporation of transition metals into SBA-15. Among the various transition metals incorporated SBA-15 systems an enhanced activity was observed in the case of tungsten incorporated systems. Maximum benzyl alcohol conversion was observed for the system SBW1 and the highest conversion is found to be 66% with a selectivity of benzaldehyde 93%. Small amount of benzoic acid was also detected for all the systems. All the other transition metal incorporated SBA-15 systems show comparable activity in the present reaction. Examinations of the data (Table 5.2) reveal that the percentage of metal incorporation can significantly affect the activity of the prepared catalysts. So an attempt is made to correlate the catalytic activity with Si/M mole ratio of transition metal incorporated SBA-15 catalysts. Figure 5.8 shows the correlation of conversion of benzyl alcohol with Si/M mole ratio in benzyl alcohol oxidation reaction. From the Figure 5.8 it was observed that the conversion increases with decrease in Si/M mole ratio of each transition metal incorporated SBA-15 systems. It was concluded that among the prepared catalysts, which possess higher fraction of isolated tetrahedral metal oxide species in silica framework have higher activity in benzyl alcohol oxidation reaction. But the presence of crystalline metal oxides was detected at higher metal concentration, which will result a decrease in activity. This will limit the metal incorporation into silica framework also.

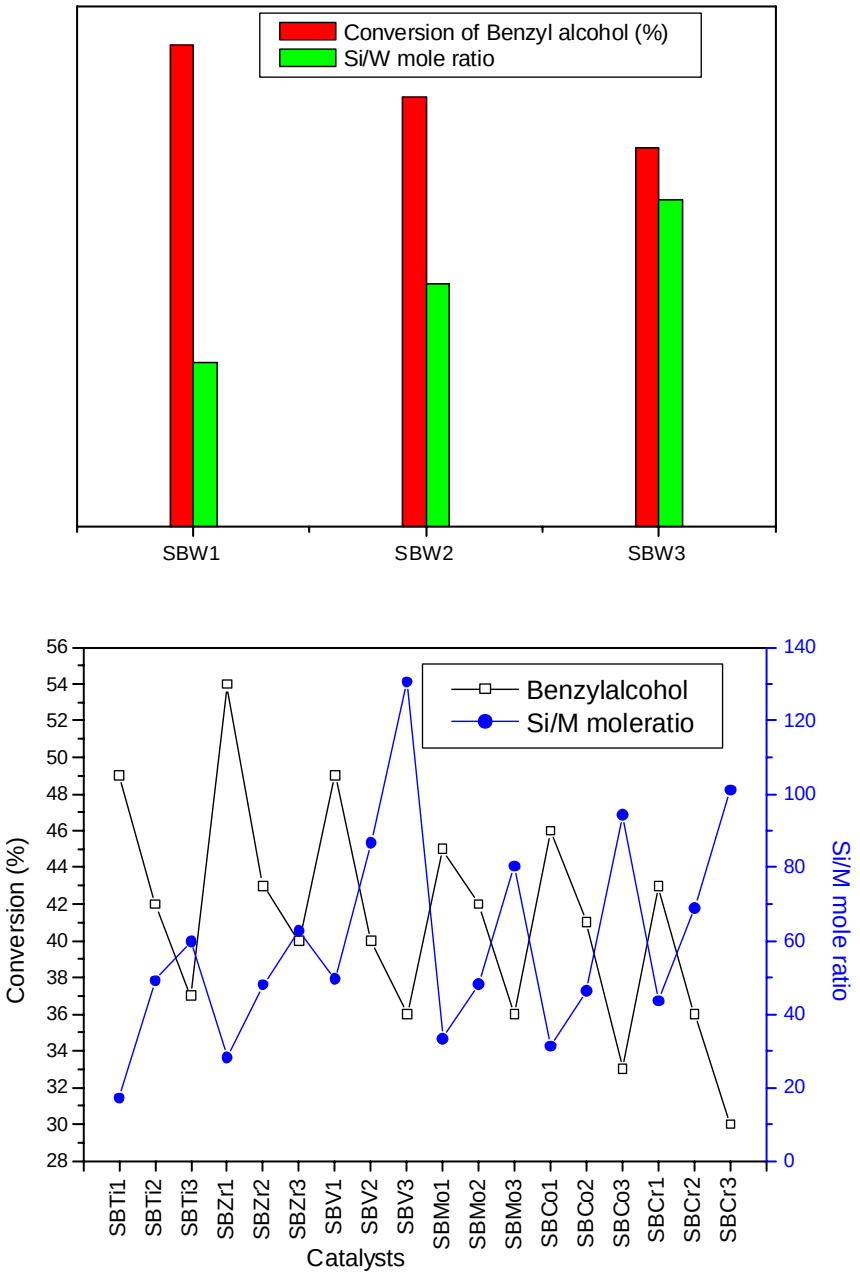

Figure 5.8. Dependence of activity with Si/M mole ratio

5.4 Recycling Studies

One of the major objectives guiding the development of solid heterogeneous catalysts includes the easy separation of final products from the reaction mixture and efficient catalyst recovery. Regeneration studies were done by removing the catalyst by filtration from the reaction solution after completing the reaction, washed thoroughly with acetone and then dried and activated at 540^0C for 6h. The same catalyst was again used for carrying out the subsequent runs under similar reaction conditions. The recycling of the SBW1 catalyst was examined for the oxidation of benzyl alcohol under the same reaction conditions. Figure 5.9 displays the conversion of benzyl alcohol and selectivity of the products obtained for benzyl alcohol oxidation reaction using regenerated catalyst SBW1.

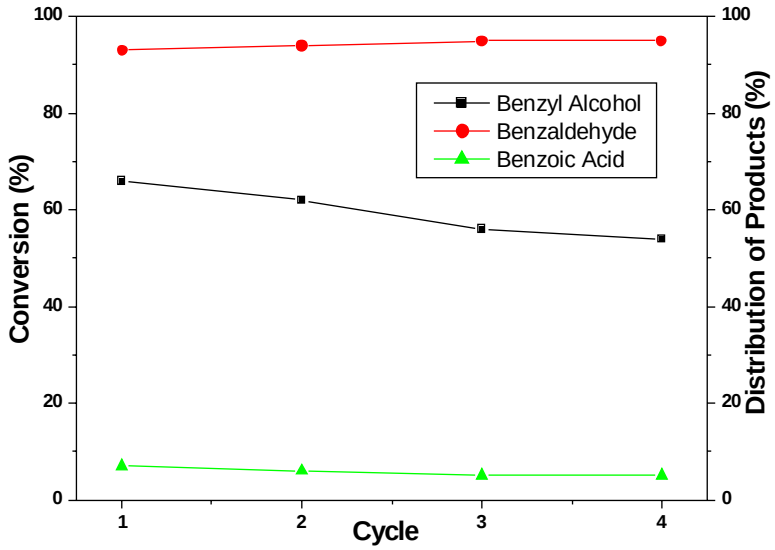

Figure 5.9. Recycling study of catalyst on benzyl alcohol oxidation Reaction conditions: Acetonitrile-10ml, Oxidant-45mmol, Benzyl Alcohol-19mmol, SBW1-0.05 g, Temp-343K, Time-6h

The result suggests that the catalyst can be recycled at least four times without much loss in activity. Benzyl alcohol conversion showed a decrease of 4% at the end of 2nd cycle and a marked decrease of 12% was observed after fourth cycle of use. There is no significant variation in benzaldehyde selectivity during the recycling process. These suggest the resistance to rapid deactivation in this oxidation reaction of benzyl alcohol using transition metal incorporated SBA-15 catalysts.

5.5 Leaching Studies

In addition to thermal stability, chemical stability is also an essential requirement for heterogeneous catalysts. Leaching of the metal ions can occur during a catalyzed reaction without an induction period and the nature of the reaction may gradually change from heterogeneous to homogeneous without any indication in the reaction profile [29]. Metal leaching studies give an idea about the nature of the reaction. For this the solid catalyst was removed from the reaction mixture after one hour by filtration and subsequently the catalytic activity of the filtrate was tested. The results obtained are presented in Table 5.3. The filtrate was further subjected to qualitative analysis for testing the presence of leached metal ions. Qualitative analysis of the filtrate also confirmed the absence of any metal ions in the filtrate.

Table 5.3. Leaching studies of catalysts on benzyl alcohol oxidation. Reaction conditions: Acetonitrile-10ml, Benzyl Alcohol-19mmol, Oxidant-45mmol, Catalyst amount-0.05 g, Temp-343K.

catalyst	Time (h)	Conversion of Benzyl Alcohol	% Distribution of Products	
			Benzaldehyde	Benzoic Acid
SBW1	1	35.00	81.42	18.68
	6	35.89	80.97	19.03
SBV2	1	2.63	82.4	17.6
	6	3.30	73.6	26.4
SBTi2	1	9.68	80.14	19.86
	6	10.67	80.11	19.89

According to Table 5.3, the conversion of benzyl alcohol at the time of filtration is 35% for SBW1. After the removal of the catalyst, though the reaction is continued up to six hour, no noticeable change in conversion was observed. The same trend was observed in the case of SBV2 and SBTi2. From these results it is clear that the metal ions are not leached out from the catalyst during the reaction. This reveals the heterogeneous nature of the reaction.

5.6 Discussion

Mesoporous silica SBA-15 with large pore size and high surface area was used as supports for the present oxidation reaction. The catalytic properties of the W, Ti, Zr, V, Mo, Co and Cr incorporated SBA-15 catalysts were studied using the oxidation of benzyl alcohol in acetonitrile as a model reaction. Gas Chromatographic (GC) analysis showed that benzaldehyde and benzoic acid were obtained as reaction products. The recovery of benzyl alcohol and yields of products were determined by the external standard method and are listed in Table 5.2.

The oxidation of benzyl alcohol to benzoic acid by hydrogen peroxide was chosen as a probe liquid-liquid biphase reaction. The oxidation reactions were carried out under the solvent acetonitrile with 30 wt % H_2O_2 at 70 °C. As shown in Table 5.2, a high conversion of 66 % was obtained when SBW1 was used as a catalyst. It was also detected that mesoporous silica SBA-15 showed little catalytic activity. However, when transition metal incorporated SBA-15 materials were employed; higher conversion for benzyl alcohol oxidation was obtained. It is believed that the large mesochannels of SBA-15 can accommodate the metal oxides and water from aqueous H_2O_2 which promoted the oxidation reaction [1]. The improved activity could be attributed to the rich concentration of active sites in the mesochannels. The recovery of the catalyst could be easily realized through a filtration or centrifugation process.

The results reveal that the oxidation that occurred in the mesochannels is quite similar to that reported by Noyori and co-workers [30, 31]. In the present work, the loading of catalysts is much lower than that of the conventional metal oxide catalysts used for primary alcohols, implying that the mesochannels as a nanoreactor can enrich the substrate and make the oxidation be more efficient [1].

The amphiphilic mesochannels of SBA-15 can provide a suitable accommodation for both hydrophilic hydrogen peroxide and hydrophobic alcohols. High conversion was obtained with a low catalyst loading for the oxidation of benzyl alcohol with hydrogen peroxide, which can be attributed to the enrichment effect of the mesochannels. It is a green and economical process for the oxidation industry. The mesoporous silica materials may have potential applications in various liquid-liquid biphase reactions by controlling the hydrophobic/hydrophilic properties of the mesochannels [1].

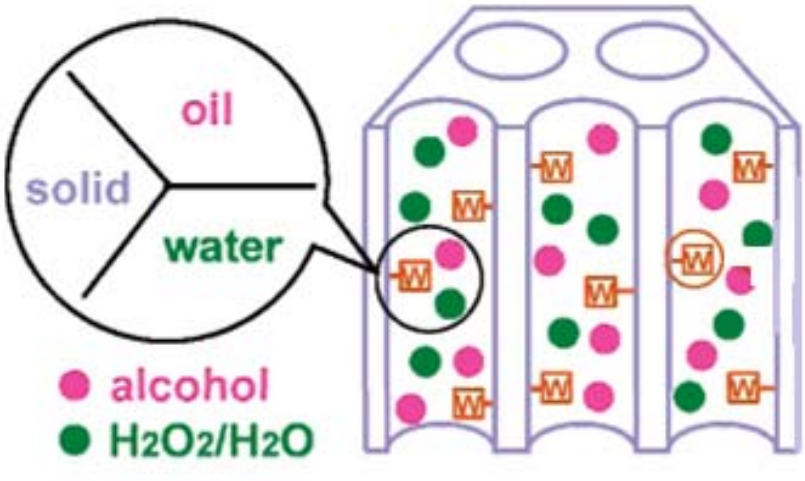

Scheme 1. Reaction of Alcohol Oxidation Using M-SBA-15- as a Catalyst

5.7 Conclusions

- Various transition metals (W, Ti, Zr, V, Mo, Co and Cr) incorporated SBA-15 catalysts has been successfully utilized for the catalytic oxidation of benzyl alcohol with ecofriendly hydrogen peroxide as an oxidant.
- The imperative role played by various reaction parameters in deciding the catalytic efficiency is well established and each parameter has an optimum value in order to acquire maximum activity.
- Metal leaching studies prove the true heterogeneous nature of the reaction.
- Catalysts are found to be reusable and resistant to rapid deactivation.
- Structural characterization results of the presently developed systems confirm the active site to be tetrahedrally coordinated metal ions in the frame work of SBA-15.
- A correlation is found between the conversion of benzyl alcohol and Si/M mole ratio of the prepared catalysts.

References

[1] Renyuan Zhang, Wei Ding, Bo Tu, and Dongyuan Zhao, Chem. Mater., 18 (2006) 5279.

[2] S. L. Regen, J. Am. Chem. Soc., 97 (1975) 5956.

[3] T. Balakrishnan, S. H. Babu, A. Perumal, J. Polym. Sci., Part A: Polym. Chem., 28 (1990) 1421.

[4] M. L. Wang, Z. F. Lee, F. S. Wang, Ind. Eng. Chem. Res., 44 (2005) 5417.

[5] C. Li, Q. Zhang, Y. Wang, H. Wan, Catal Lett., 120 (2008)126.

[6] U. R. Pillai, E. Sahle-Demessie, Green Chem., 6 (2004) 161.

[7] M. S. Kwon, N. Kim, C. M. Park, J. S. Lee, K.Y. Kang, J. Park, Org Lett.,7 (2005) 1077.

[8] Y. Liu, H. Tsunoyama, T. Akita, T. Tsukuda, J. Phys. Chem. C, 113 (2009) 31.

[9] M. Haruta, Chem. Rec., 3 (2003) 75.

[10] S. K. Hashmi, G. J. Hutchings, Angew. Chem., 45 (2006) 7896.

[11] Corma, H. Garcia , Chem. Soc. ReV., 37 (2008) 2096.

[12] D. Pina, E. Falletta, L. Prati, M. Rossi, Chem. Soc. ReV., 37 (2008) 2077.

[13] G. J. Hutchings, S. Carrettin, P. London, J. K. Edwards, D. I. Enache, D. W. Knight, Y. J. Xu, A. F. Carley, Top. Catal., 38 (2006) 223.

[14] Z. Su, Y. M. Liu, L. C. Wang, Y. Cao, H. Y. He, K. N. Fan, Angew. Chem., 47 (2008) 334.

[15] S. Kanaoka, N. Yagi, Y. Fukuyama, S. Aoshima, H. Tsunoyama, T. Tsukuda, H. Sakurai, J. Am. Chem. Soc., 129 (2007) 12061.

[16] Bordoloi, A. Vinu, S. B. Halligudi, Chem. Commun., 45 (2007) 4806.

[17] Ma, J. Xu, C. Chen, Q. Zhang, J. Ning, H. Miao, L. Zhou, X. Li, Catal. Lett., 113 (2007) 3.

[18] R. Anand, M. S. Hamdy, U. Hanefeld, T. Maschmeyer, Catal. Lett., 95 (2004) 113.

[19] R. A. Sheldon, I. W. C. E. Arends, H. E. B. Lempers, Catalysis Today, 41 (1998) 387.

[20] R. Anand, M. S. Hamdy, P. Gkourgkoulas, T. Maschmeyer, J. C. Jansen, U. Hanefeld, Catalysis Today, 117 (2006) 279.

[21] Hessa, I. Drake, J. D. Hoefelmeyera, T. Don Tilleya, A. T Bella, Catal. Lett ., 105 (2005) 1.

[22] J. Li, Y. Shi, L. Xu, G. Lu, Ind. Eng. Chem. Res., 49 (2010) 5392.

[23] Z. Zhiqing, B. Wei, Chin. J. Chem. Eng., 16(6) (2008) 895.

[24] Strukul, Angew. Chem., Int. Ed. Engll., 37 (1998) 1199.

[25] R. Yu, F. Xiao, D. Wang, T. Sun, Y. Liu, G. Pang, S. Feng, S. Qui, R Xu, C. Fang, Catalysis Today, 51 (1999) 39.

[26] Tuel, M. Khouzami, B. Tarrit, Naccache, J. Mol. Catal., 68 (1991) 45.

[27] R. Neumann, M. Levin-Elad, Appl. Catal. A. Gen., 122 (1995) 85.

[28] S. Shylesh, A. P. Singh, J. Catal., 228 (2004) 333.

[29] Z. H. Fu, Y. Ono, Catal. Lett., 21 (1993) 43.

[30] K. Sato, M. Aoki, J. Takagi , R. Noyori, J. Am. Chem. Soc., 119 (1997) 12386.

[31] R. Noyori, M. Aoki, K. Sato, Chem. Commun., 16 (2003) 1977.

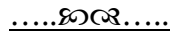

Chapter 6

Acetalization of Cyclohexanone

Contents

Acetalization is a widely used synthetic method for protecting aldehydes and ketones and is of current interest in preparation of a variety of multifunctional complex organic molecules. Carbonyl compounds need to be stabilized by converting them to corresponding acetal because they are used in the fragrance industry and are unstable under the alkali conditions. They also undergo chemical attack by oxygen, resulting in change in properties of the product. The diacetal of carbonyl compounds give no reaction in alkali media. The chemical reaction pathway for the acetalization of cyclohexanone can be depicted as ketones react with methanol under well optimized reaction conditions and at ambient temperatures in presence of acid catalysts to produce dimethyl acetal. The choice of the catalyst has great importance in these environmentally conscious days. Green chemistry demands the replacement of commonly used highly corrosive, hazardous and polluting acid catalysts with eco-friendly and reusable solid acid catalysts. Various transition metal incorporated SBA-15 mesoporous materials prepared for the present work provide a convenient catalytic route for protecting the carbonyl groups during organic synthesis. The effects of the parameters, such as reactant molar ratio, temperature, and amount of catalyst on the reaction rate were studied. It is also stated that the deactivation was insignificant in the period of the reaction time. Based on the results it is concluded that the acidic properties of the materials have a major role in deciding catalytic activity.

6.1 Introduction

Acetalization of aldehydes and ketones are widely accepted and highly effective method for protecting the carbonyl group in the field of synthetic organic chemistry since dimethyl acetals display higher stability towards organic reagents, strong oxidants, strong bases, and esterification reagents than corresponding carbonyl compounds [1, 2]. 1, 2-Diacetals are found to be efficient protecting groups for 1, 2-diol units in carbohydrates [3–5]. Monosaccharide units can be protected as cyclohexanone 1, 2-diacetal through acetalization, which offer rapid access to important building blocks for oligosaccharide synthesis [5, 6]. Grice et al. have reported the preparation and structure of cyclohexanone diacetal protected carbohydrates [7, 8]. The synthesis of large, complex oligosaccharides presents significant importance in synthetic chemistry. Presently used synthesis routes to such molecules involved large number of steps owing to unavoidable protecting group manipulation and activation protocols. Tetrasacchrides, pentasaccharides etc. can be prepared by one-pot sequential glycosidation of four or five components. Acetalization reactions have extensive applications in the synthesis of enantiomerically pure compounds [9, 10] and in the fields of synthetic carbohydrates [11, 12]. They have found practical application for the synthesis of steroids [13], and as fragrance [14, 15] cosmetics [6], food and beverage additives [7, 8], and pharmaceuticals [9]. So the development of efficient catalysts for acetalization reaction of carbonyl compounds is of considerable interest.

According to S. Arctander Perfumary and Flavour Chemicals the methyl and ethyl acetals of n-octanal and n-decanal exhibit widespread applications in perfume and flavour industries [16]. The conversion of a carbonyl compound to its acetal alters its vapour pressure, solubility and aroma characteristics, and often results in flavour attenuation. For example, the propylenedioxy

derivative of vanillin is commonly used as a vanilla flavour since it causes flavour attenuation [17]. Bejoy et al. compared the catalytic applications of Montmorillonite clay, Zeolites, Silica and alumina in protecting the carbonyl groups through acetalization [18]. Acetals have found applications as an additive that increase the cetane number of the fuel and help in the combustion of the resulting mixture [19, 20] and as intermediates for the synthesis of various industrial chemicals and organic solvents [21, 22, 23]. Mehmet and co workers found benzaldehyde dimethyl acetal has sweet-green and warm odor remotely reminiscent of nuts and bitter almonds. It is also in flavour compositions for the imitation cherry, fruit, almond, nut, etc. [16]. Many researchers reported the synthesis of acetals using heterogeneous catalysts. The reaction between ethanol and acetaldehyde using the acid resin Amberlyst 18 as a catalyst in a batch reactor was studied and found that the experimental data verify the model based on a Langmuir- Hinshelwood rate expression [24]. A heterogeneous kinetic model related to the acetal formation from *n*-octanal and methanol has been developed by Yadav and Pujari to observe that the Eley-Rideal type of mechanism prevails with chemisorption of the aldehyde on the active sites [25]. The heterogeneous catalytic acetalization reaction has been studied in batch mode, in semibatch reactive distillation mode, and in a continuous reactive distillation column by using various types of heterogeneous catalysts. The data obtained from the batch reactor can be explained with pseudo-homogeneous model [26, 27].

Acetals are synthesized by the reaction of alcohol with carbonyl compounds in the presence of acid catalysts. Acetalizations of aldehydes and ketones are generally employed using trimethyl orthofomate in the presence of an acid catalyst such as HCl, H_2SO_4, p-toluenesulphonic acid, or iron(III) chloride [28,29]. Eco-friendly solid acid catalysts such as

SO_4^{2-}/ZrO_2, SO_4^{2-}/TiO_2 [30], Ce exchanged montmorillonite [31], acidic zeolites [15, 32, 33], and siliceous mesoporous material [34] etc. are also widely used for the acetalization reactions of various carbonyl compounds. Several Lewis acid complexes such as $[(dppe)M(H_2O)_2]$, where M is Pt or Pd (dppe is 1,2-bis(diphenylphosphino)ethane) have also been employed successfully for acetalization reactions in homogeneous reaction medium [35,36].

The basic structural requirements of the catalysts to achieve better activity of the catalysts in various acetalization reactions are described by Gorla and Venanzi [37]. However, in currently used acetalization procedures the neutralization of the strongly acidic media leading to the production of harmful wastes and also requires expensive reagents, tedious work-up procedure. Furthermore, the formation of dimethyl acetals in homogeneous phase is often carried out by using trimethyl orthoformate as the reagent. Though methanol is found to be more desirable for the acetalization reaction, many kinds of by-products are often produced when methanol/acid system is employed [18].

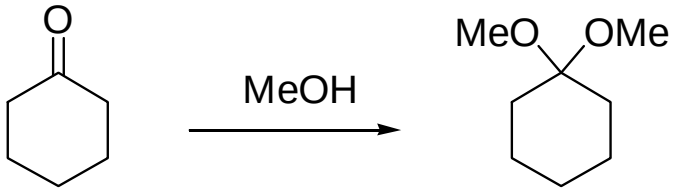

Heterogeneous catalysts have inherent advantages in catalysis research since they eliminate the corrosive environment and can be easily recovered from the reaction mixture by decantation and filtration. The heterogeneous catalysts also avoid unnecessary side reaction and leading to the production of highly purified product [38, 39].

In this present work, a simple, efficient, and highly eco-friendly protocol is described for the acetalization of cyclohexanone using transition metal

(W, Ti, Zr, V, Mo, Co, Cr) incorporated mesoporous SBA-15 materials. Acetalization of cyclohexanone with methanol produced the corresponding diacetals as the only product

6.2 Effect of Reaction Parameters

The effects of temperature, time, molar ratio of cyclohexanone to methanol and amount of catalyst on the acetalization reaction were investigated in detail.

6.2.1 Effect of Time

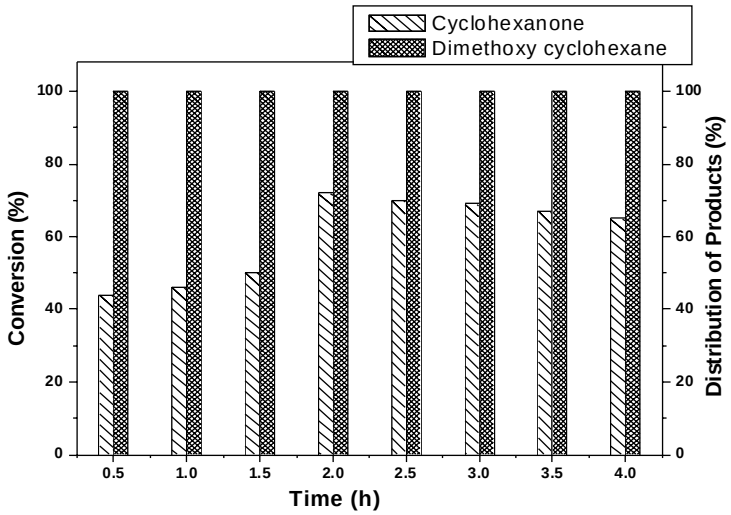

Figure 6.1 Reaction conditions: Temperature-301K, SBW1-0.1g, Cy/Methanol-1:10

The dependence of cyclohexanone conversion on the reaction time was studied and the results are presented in Figure 6.1. For this the reaction was carried out at room temperature for 4h. It is seen that during the initial stages of the reaction the percentage conversion increases up to 2h. After that a small decrease in conversion was observed. It appears that the acetalization products themselves adsorb to the catalysts and thereby block the active sites leading to the loss of catalytic activity. Reaction time of 2h was selected for further studies.

6.2.2 Effect of Mole ratio of Cyclohexanone:methanol

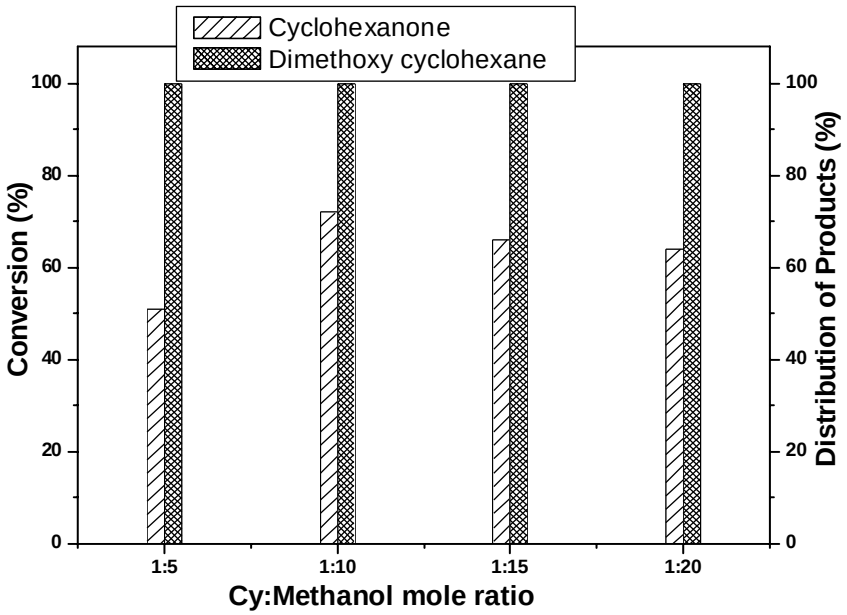

Figure 6.2 Reaction conditions: Temperature-301K, SBW1-0.1g, Time-2h

In a set of experiments the catalytic activity for SBW1 was scanned by taking different molar ratios of cyclohexanone to methanol with already optimized condition of reaction time. Figure 6.2 reveals the effect of mole ratio of cyclohexanone to methanol on the acetalization reaction. From the Figure it is clear that the mole ratio has a profound influence on the catalytic activity. The percentage conversion increases with increase in methanol concentration up to 1:10 mole ratio. Further increase in mole ratio causes a small decrease in conversion.

6.2.3 Effect of Temperature

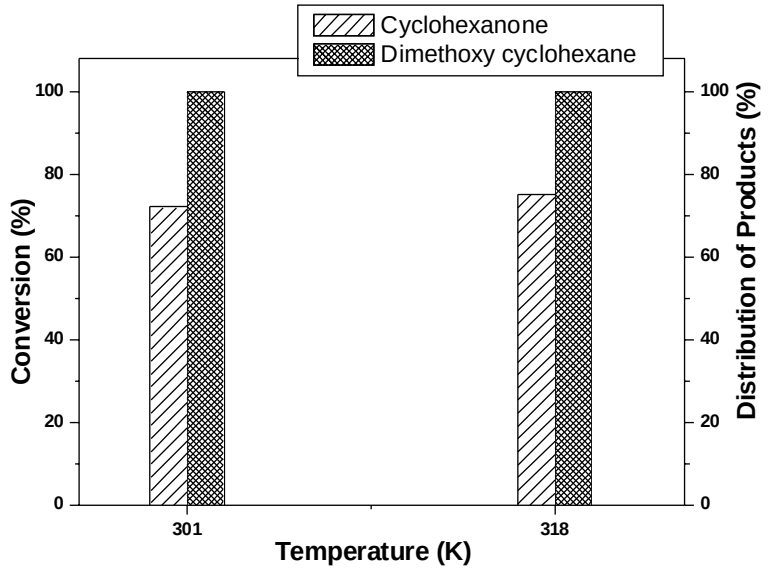

Figure 6.3 Reaction conditions: SBW1-0.1g, Cy/Methanol-1:10, Time-2h

In order to understand an optimum temperature for the acetalization reaction, experiments were performed at room temperature and 318 K. Figure 6.3 displays the results obtained. There was no predominant increase in the percentage conversion with increase of temperature. From this it is clear that temperature does not have much influence in deciding the catalytic activity.

6.2.4 Effect of Catalyst Amount

Figure 6.4 illustrates the influence of catalyst weight on acetalization of cyclohexanone with methanol. Cyclohexanone conversion increases with increasing catalyst amount. As the amount of catalyst increase from 0.05 to 0.1g the percentage conversion increases from 47 to72%. Further increase of catalyst amount to 0.15g results only a slight increase (4%) in conversion. A catalyst amount of 0.1g was selected for further studies.

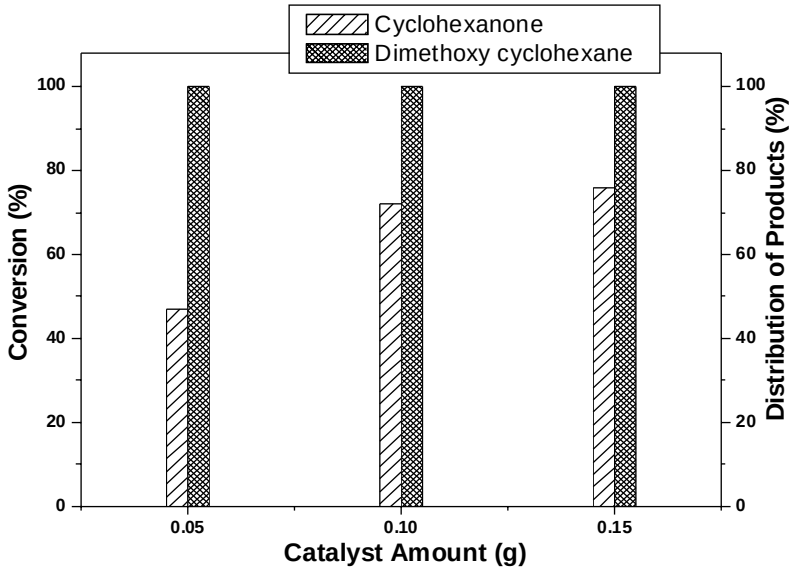

Figure 6.4 Reaction conditions: SBW1, Temperature-301K, Cy/Methanol-1:10, Time-2h

6.3 Catalytic Activity of Prepared Catalyst Systems

Acetalization of cyclohexanone was carried out using methanol over the prepared catalysts under the optimized reaction condition. In all the cases the corresponding dimethylacetal was obtained as a single product with high yield.

Table 6.1 Optimized reaction conditions for acetalization of cyclohexanone

Parameters	Optimized condition
Temperature	301K
Cy/Methanol mole ratio	1:10
Catalyst Amount	0.1g
Time	2h

A comparative evaluation of the catalytic activity of various transition metal incorporated SBA-15 materials on acetalization of cyclohexanone is presented in Table 6.2.

Table 6.2 Catalytic Activity of the prepared systems
Temperature 301K, Catalyst-0.1g, Cy/Methanol-1:10, Time-2h

Catalyst	Conversion of Cyclohexanone (%)	Selectivity of Dimethoxy cyclohexane (%)
Blank	4	100
SBA-15	12	100
SBW1	72	100
SBW2	51	100
SBW3	45	100
SBTi1	64	100
SBTi2	52	100
SBTi3	59	100
SBZr1	40	100
SBZr2	50	100
SBZr3	52	100
SBV1	46	100
SBV2	51	100
SBV3	61	100
SBMo1	52	100
SBMo2	66	100
SBMo3	61	100
SBCo1	51	100
SBCo2	56	100
SBCo3	51	100
SBCr1	67	100
SBCr2	59	100
SBCr3	53	100

Acetalization was studied both in presence of pure and transition metal incorporated SBA-15 catalysts and without catalyst. From the reaction mechanism, it appears that the reaction proceeds with the formation of very bulky intermediates and the mesoporous materials are expected to be highly active. Highly porous SBA-15 materials favoured the diffusion of the reactants, bulky intermediates and products during the reaction. A negligible conversion was observed in the blank run (without catalyst). Pure SBA-15 gave very low

conversion under the specified reaction condition. Incorporation of the various transition metals enhances the activity in the acetalization reaction. All the prepared catalysts exclusively produced the corresponding dimethyl acetal. Among the catalytic systems studied, SBW1 showed highest activity. All other catalyst systems have comparable activity towards the presently studied acetalization of cyclohexanone with methanol.

6.4 Conversion of Cyclohexanone and Acidity of Catalysts

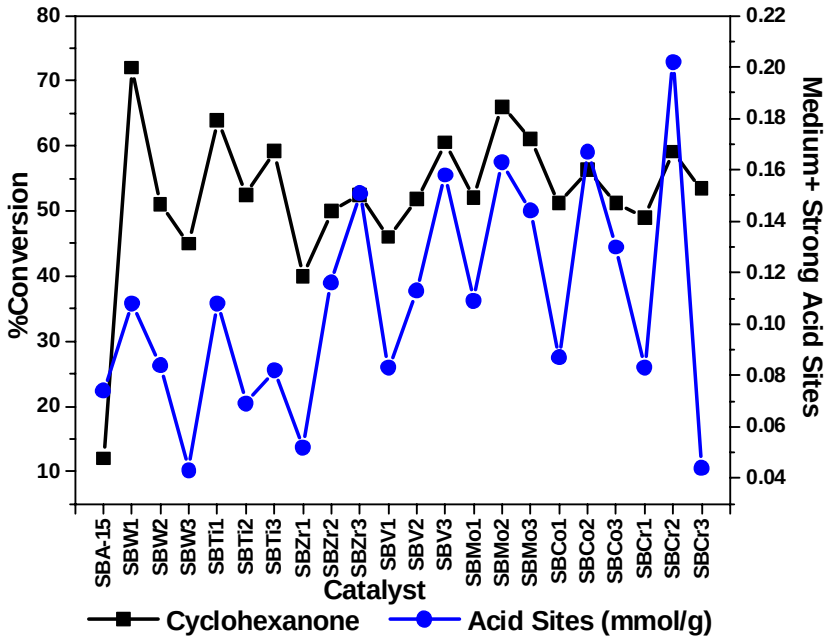

Figure 6.5 Conversion of Cyclohexanone and Acidity of Catalysts

Since acetalization is an acid-catalyzed reaction, it is logical to correlate the catalytic activity with the acid structural properties of the materials. Figure 6.5 reveals that the percentage conversion for different systems is in agreement with the sum of medium and strong acid sites as measured by the thermal desorption studies of 2, 6-dimethyl pyridine. Transition metal incorporated SBA-15 materials possess some amounts of medium plus strong acid sites and an assembly of these acid sites may act as an effective acid site for the present reaction. The strong influence of the textural properties of the catalysts such as

acid amount and adsorption properties (surface area and pore volume) determine the catalytic activity. The reaction requires active sites with considerable acid strength. In addition to the acid strength the pore volume, pore sizes and their distribution in the catalyst are also responsible for their activity in the acetalization reaction.

6.5 Recycling Studies

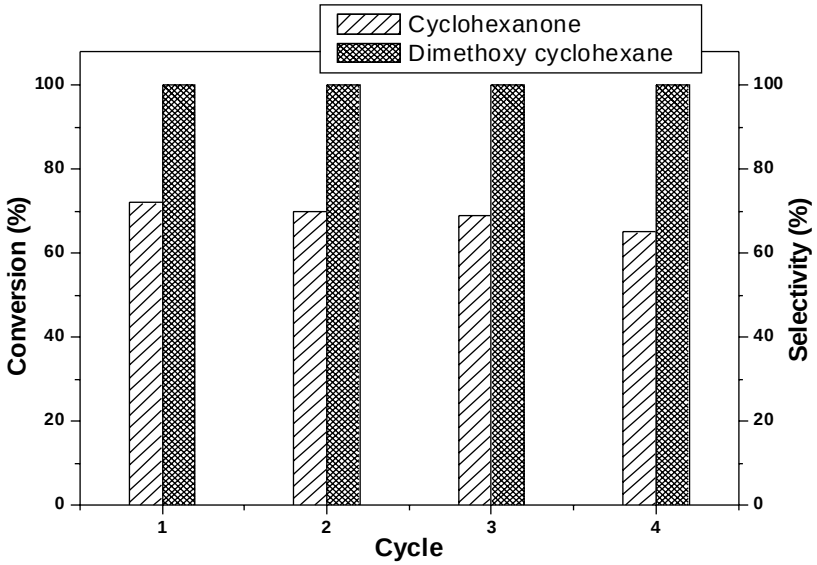

Figure 6.6 Temperature-301K, SBW1-0.1g, Cy/Methanol-1:10, Time-2h

The stability of the catalysts were tested by conducting the experiments with regenerated catalysts. For this the catalyst was recovered by filtration after the reaction, washed several times with water/acetone ,dried and calcined at 540^0C for 5h.Then the reaction was conducted with the recovered catalyst under the same reaction condition. The process continued to four cycles. Figure 6.6 displays the conversion of cyclohexanone obtained with the regenerated catalyst. The activity of the regenerated catalysts was found to be slightly lower than the fresh catalyst and only 7% decrease in conversion was

observed at the end of fourth cycle. It was concluded that the catalyst was stable up to four cycles

6.6 Leaching Studies

Table 6.3 Temperature-301K, Catalyst-0.1g, Cy/Methanol-1:10

catalyst	Time (h)	Conversion (%)	Selectivity of Dimethoxy cyclohexane (%)
SBW1	1	46	100
	2	47	100
SBMo1	1	38	100
	2	42	100

By checking the complete heterogeneity of the reaction it is possible to attain a better insight in to the behaviour of the catalyst. After 1h of the reaction, the catalyst was removed by filtration and the filtrate obtained was used to examine the catalytic activity of the possible dissolved components of the catalyst. The filtrate was further subjected to acetalization reaction for 2 h. The results are presented in Table 6.3. A slight increase in conversion of ketone to acetal was observed in the case of SBMo1. From this it is clear that leaching of the active metal sites may occur during the reaction. In the case of SBW1 no noticeable increase in conversion is observed, which reveals the true heterogeneous nature of the reaction with this catalyst.

6.7 Effect of Substrates

The acetalization reaction was also carried out with various carbonyl compounds using the catalyst SBW2 under the specified reaction condition for comparative studies. The results obtained are presented in Figure 6.7. The activity of the catalyst in acetalization reaction of various substrates with methanol is in the order cyclopentanone>cyclohexanone>benzaldehyde>acetophenone>benzophenone.

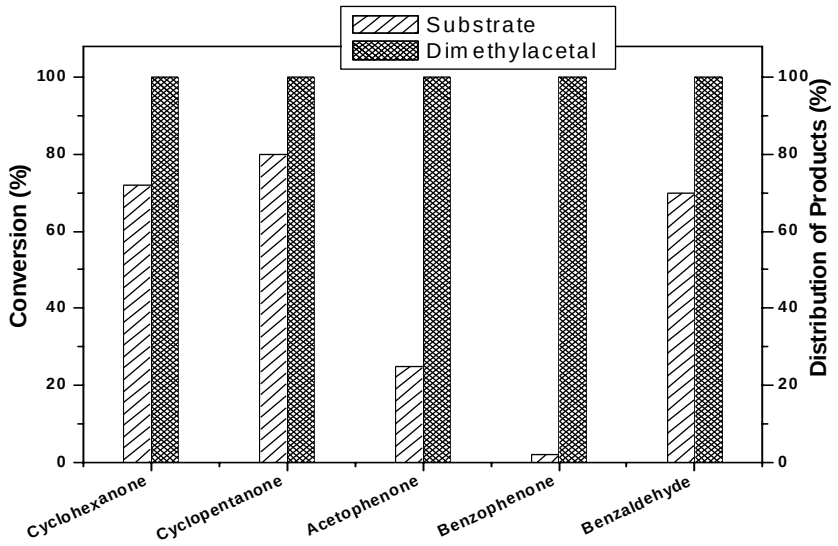

Figure 6.7 Temperature-301K, SBW1-0.1g, Cy/Methanol-1:10, Time-2h

A comparatively low activity was observed in the case of acetophenone and benzophenone. It is known that cyclohexanone is more reactive towards nucleophiles than both acetophenone and benzophenone. This may also be due to the bulkiness of hemiacetals which prevent the attack of the CH_3OH on the carbonyl carbon atom and the electron withdrawing power of phenyl group in acetophenone and benzophenone reduces the easy release of the pair of electron on the carbonyl carbon during the reaction. Lin and co-workers compared the activity of these substrates in the acetalization with trimethoxy orthoformate and proposed a similar explanation in their work [40]. Further studies needed the extension of this reaction to other types of substituted ketones to examine the exact reason for the difference in the reactivity.

6.8 Discussion

The successful direct preparation of cyclohexanone dimethyl acetal was employed in the present work using transition metal incorporated SBA-15 materials, probably results from the fact that the *exo* double bond in cyclohexanone is unstable relative to tetrahedral bonding for each of the six

carbons. This is sufficient to place the equilibrium on the side of the ketal. The less hindered carbonyl group of the cyclic ketone also contributes to the ease of acetalization reaction [41].

The activity difference could be due to two important properties acid structural properties (amount and strength of the acidic sites) and diffusional properties, which are determined by the pore structure of the materials. Enhancement in the total pore volume in the prepared catalysts could provide a better diffusional pathway for the bulky acetals. The activity of catalyst towards the acetalization reaction cannot be explained with acidic sites only [42, 18]. Corma and co-workers pointed out that the pore diffusion limitation imposed by larger molecular sizes of the reactant played an important role during the acetalization reaction using porous catalysts [43, 33].

Acetal formation is a reversible reaction, which proceeds by a two-step mechanism. Their formation is strongly affected by electronic and steric factors. The first step is the formation of hemiacetal, followed by the removal of a molecule of water. Formation of a cation from the protonated hemiacetal is the rate determining the step of acetalization reactions. However, the protonation of hemiacetal is also a slow step and the reaction medium has to be sufficiently acidic to promote required protons [18, 44, 45]. Scheme 1 envisages the exact mechanism of the acetalization of cyclohexanone with methanol. cyclohexanone is first protonated by the Bronsted acid sites (H^+ ions of the catalyst) to produce an intermediate which then combine with methanol to form the hemiacetal . Another intermediate is formed by the protonation of the hemiacetal which undergo subsequent dehydration and reaction with another molecule of methanol. Finally the removal of a proton from the resulting intermediate leads to the formation of the cyclohexanone dimethyl acetal [18]

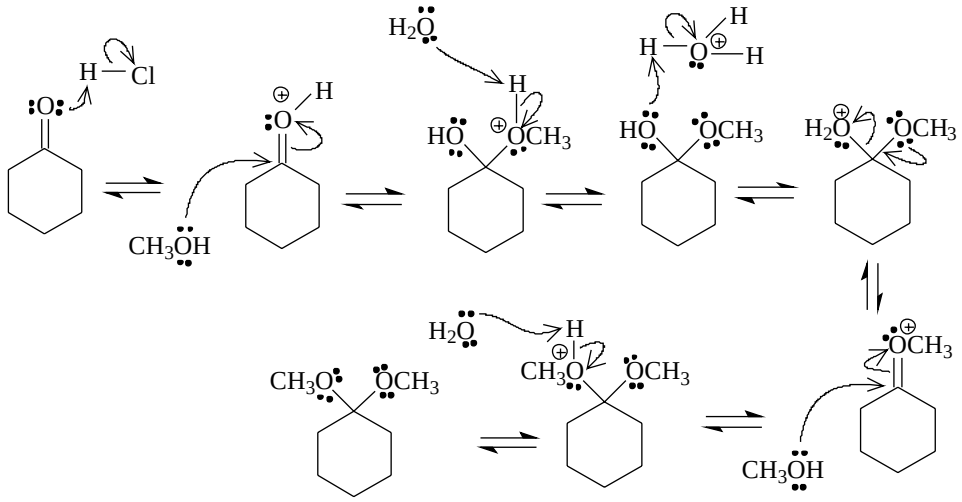

Scheme 1

6.9 Conclusions

- The transition metal (W, Ti, Zr, V, Mo, Co, and Cr) incorporated mesoporous SBA-15 catalysts offer a mild, efficient and environmentally benign protocol for the preparation of acetals of carbonyl compounds
- The reaction of acetalization of cyclohexanone with methanol always results the formation of dimethoxy cyclohexane
- The enhancement in catalytic activity could be explained in terms of improvement in textural and structural properties
- The mesoporous structure of the catalysts promotes the rate of diffusion of the bulky products through the channels.
- The catalysts can be recycled without loss of activity.
- The prepared catalysts are attractive alternative for the protection of carbonyl compounds.

References

[1] B. Thomas, S. Sugunan, J. Porous. Mater., 13 (2006) 99.

[2] T. W. Greene, Protective Groups in Organic Synthesis, Wiley- Interscience, New York (1981) p. 178.

[3] P. Grice, S. V. Ley, J. Pietruszka, H. W. M. Priepke, Angew. Chem. Int. Ed. Engl., 35 (1996) 197.

[4] S. V. Ley, R. Downham, P. J. Edwards, J. E. Innes, M. Woods, Contemp. Org. Synth. 2 (1995) 365.

[5] S. V. Ley, H.W.M. Priepke, S.L.Warriner, Angew. Chem. Int. Ed. Engl., 33 (1994) 2290.

[6] S. V. Ley, H. W. M. Priepke, Angew. Chem. Int. Ed. Engl., 33 (1994) 2292.

[7] P. Grice, S. V. Ley, J. Pietruszka, H. W. M. Priepke, S. L. Warriner, J. Chem. Soc., Perkin Trans., 1 (1997) 351,

[8] P. Grice, S. V. Ley, J. Pietruszka, H. W. M. Priepke, E. P. E. Walther, Synletter., (1995) 781.

[9] M. K. Cheung, N. L. Douglas, B. Hinzen, S. V. Ley, X. Pannecoucke, Synletter.,(1997) 257.

[10] K. Narasaka, M. Inone, T. Yamada, J. Sugiomori, N. Iwasawa, Chem. Lett., (1987) 2409.

[11] D. M. Clode, Chem. Rev., 79 (1979) 224.

[12] S.V. Ley, H. W. M. Priepke, Angew. Chem., 106 (1994) 2412.

[13] J. R. Bull, J. Floor, G. J. Kruger, J. Chem. Res. Synop., (1979) 224.

[14] K. Bruns, J. Conard, A. Steigel, Tetrahedron, 35 (1979) 2523.

[15] M. J. Climent, A. Velty, A. Corma, Green Chem., 4 (2002) 565.

[16] S. ArctanderPerfumary and Flavour Chemicals, vols. I and II, Allured Publishing, New York (1969).

[17] G. A. BurdockFenarolis Handbook of Flavour Ingradients, vol. 2, CRC, New York (1995).

[18] B. Thomas, S. Prathapan, S. Sugunan, Microporous and Mesoporous Materials, 80 (2005) 65.

[19] K. Bonnhoff, Obenaus, F. Dieselkraftstoff., DE2911411, 1980.

[20] K. Oppenlaender, F. Merger, R. Strickler, F. Hovemann, H. Schmidt, K. Starke, K. Stork, W. Vodrazka, EP0014922, 1980.

[21] M. Kaufhold, M. El-Chahawi, Process for preparing acetaldehyde diethyl acetal. U.S. Patent 5527969 (1996).

[22] T. Aizawa, H. Nakamura, K. Wakabayashi, T. Kudo, Hasegawa, H. Process for producing acetaldehyde dimethylacetal. U.S. Patent 5362918 (1994).

[23] M. R. Altıokka, H. L. Hosügu1n, Ind. Eng. Chem. Res., 46 (2007) 1058.

[24] V. M. T. M. Silva, A. E. Rodrigues, Chem. Eng. Sci. 56 (2001) 1255.

[25] G. D. Yadav, A. A. Pujari, Can. J. Chem. Eng., 77 (1999) 489.

[26] S. P. Chopeda, M. M. Sharma, React. Funct. Polym., 32 (1997) 53.

[27] S. P. Chopeda, M. M. Sharma, React. Funct. Polym., 34 (1997) 37.

[28] C. A. Mcckinzie, J. H. Stocker, J. Org. Chem., 20 (1655) 1695.

[29] J. Bornstein, S. F. Bedell, P. E. Drummond, C. F. Kosoloski, J. Am. Chem. Soc., 78 (1956) 83.

[30] C. H. Lin, S. D. Lin, Y. H. Yang, T. P. Lin, Catal. Lett., 75 (2–4) (2001) 121.

[31] J. I. Tateiwa, H. Horiochi, S. Uemora, J. Org. Chem., 60 (1995) 4039.

[32] F. Algarre, A. Corma, H. Garcia, J. Primo, Appl. Catal. A: Gen., 128 (1995) 119.

[33] M. J. Climent, A. Corma, S. Iborra, M. C. Navarro, J. Primo, J. Catal., 161 (1996) 161.

[34] Y. Tanaka, N. Sawamara, M. Iwamoto, Tetrahedron Lett., 39 (1998) 9457.

[35] E. Nieddu, M. Cataldo, F. Pinna, G. Strukul, Tetrahedron Lett., 40 (1999) 6987.

[36] G. Strukul, Top. Catal. 19 (1) (2002).

[37] F. Gorla, L.M. Venanzi, Helv. Chim. Acta., 73 (1990) 690.

[38] M. R. Altıokka, A. Citak, Appl. Catal., A., 239 (2003) 141.

[39] M. R. Altıokka, H. L. Hosügu1n, Ind. Eng. Chem. Res,. 46 (2007) 1058.

[40] C. H. Lin, S. D. Lin, Y. H. Yang, T. P. Lin, Catal. Lett., 73 (2–4) (2001) 121.

[41] Robert. E. McCOY, Alvin. W. Baker, Roland. S. Gohlke, Presented in part at the 129th meeting of the American Chemical Society, Allas, Tex., April 1956.

[42] Corma, M. J. Climent, H. Garcia, J. Primo, Appl. Catal. A: Gen., 59 (1990) 333.

[43] R. Ballini, G. Bosica, B. Frullanti, R. Maggi, G. Sartori, F. Schroer, Tetrahedron Lett., 39 (1998) 1615.

[44] J. March, Advanced organic Chemistry- Reactions, Mechanism and Structure, John Wiley sons, Ed. 4 (1992) 889.

[45] T. H Fife, Acc. Chem. Res., 5 (1972) 264.

…..ൟ…..

Chapter 7

Isopropylation of Benzene

Contents

Friedel–Crafts alkylation reaction with heterogeneous mesoporous catalysts have provided insight into the trends in which activity and selectivity are mostly considered. The isopropylation of benzene catalyzed by solid acids is of significant industrial and pharmaceutical interests. The corrosive nature of traditional Friedel-Crafts catalysts provide some environmental problems due to the formation of large amount of harmful wastes. Mesoporous solid acid catalysts will be effectively catalyze various Friedel-Crafts reactions since they have been shown to exhibit outstanding catalytic behaviour in several acid-catalyzed reactions. The present study has undertaken the isopropylation of benzene over various transition metal incorporated SBA-15 mesoporous catalysts. The investigations revealed that the catalytic activity and product distribution are sensitive to various reaction parameters and can be related to the acidity of the systems. Another possible reason of the increased activity may be attributed to the porous structure of the molecular sieve made it possible for the diffusion of reactants to active sites.

7.1 Introduction

Friedal–Crafts alkylation reactions are found to be an important reaction for attaching alkyl chains to aromatic ring. Friedel– Crafts alkylation reaction of aromatics is of substantial industrial and pharmaceutical significance [1]. Alkylation reactions have been usually carried out in the presence of Lewis acids or organometallic reagents using alkyl halides as alkylating agents. In the presence of strong acids, alcohols and alkenes can also serve as sources of electrophiles in Friedel–Crafts reactions. Recent reports reveal that solid phosphoric acid and Friedel–Crafts catalysts like $AlCl_3$ and BF_3 can be used in the synthesis of many fine chemicals and pharmaceutical intermediates [2]. But more than stoichiometric amount of $AlCl_3$ is required in many cases and giving poor selectivity because of degradation, polymerization and isomerization. The traditionally used Lewis acids are not easily separable after reaction and causes large amount of acid waste generation [3, 4]. Solid acid catalyst, are important candidates for Friedel-Crafts alkylation reactions since various industrially important reactions are reported using solid acids [2, 5– 8].

The use of environmental friendly catalysis involving the use of solid catalyst should lead to minimum pollution and waste. In recent years the preparation of solid acid catalysts is extended to mesoporous molecular sieves, which minimize the diffusion limitation with small zeolite pores. Mesoporous molecular sieves after incorporation of various metals as active sites have become promising catalysts and have been shown to exhibit outstanding catalytic behaviour in several acid-catalyzed reactions [9–11]. Large pore diameter with less diffusion constraint of these mesoporous solids eliminates further alkylation and deactivation by coke formation. Moreover, the mesoprous catalysts can provide spatial environment for the reactants in

the channels as that in the homogenous solution phase which leads to the formation of products.

A variety of solid acid catalysts have been examined and few have been employed for alkylation of various aromatics since 1960. Olah et al. studied isopropylation of benzene and toluene with isopropylbromide as alkylating agent and $AlCl_3$ as catalyst [12]. Many researchers reported the production of aromatics and petrochemicals such as xylene, ethylbenzene, cumene and linear alkylbenzenes using solid acids like zeolitic materials through Friedel-Crafts alkylation reactions [13–16]. A recent work by Cheng et al claimed a Mobil patent for cumene production over MCM-56 and MCM-22 [17]. Clark et al. found that montmorillonites supporting zinc and nickel catalysts are active towards Friedal– Crafts alkylation reaction [18–20]. Intensive research in the field revealed Zeolites X and Y are more active for alkylation of benzene with olefins than amorphous silica-alumina [21, 22]. The advantages of some other solid catalysts, which make them applicable for alkylation, have been reported extensively [23–26]. Qiaoxia Guo and coworkers investigated the synergetic effects of the $MoCl_5$ and molecular sieve (HZSM-5 and TS-1), and the Lewis acidity of $FeCl_3$, $ZnCl_2$, or $AlCl_3$ using the alkylation reaction of benzene derivatives [27].

The Friedel-Crafts alkylation of aromatics catalyzed by solid mesoporous acids is of significant interest in the fields of organic chemistry. Acidic mesoporous heterogeneous catalysts, having Brønsted or Lewis acid centers have substantial acid strengths and are capable of replacing homogenous bulk acids. Here we studied vapour-phase isopropylation of benzene using 2-propanol as alkylating agent over transition metals (W, Ti, Zr, V, Mo, Co, Cr) incorporated mesoporous SBA-15 catalysts. The product cumene serves as precursors for the coproduction of phenol and acetone. The results concerning the optimization of the reaction conditions are presented here.

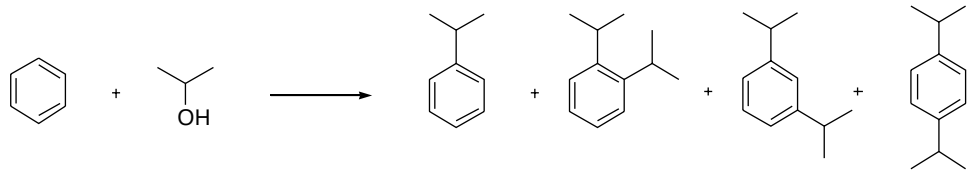

Scheme 7.1 Isoprpylation of Benzene

In the isopropylation reaction isopropanol gets chemisorbed on the Bronsted acid sites of the catalyst to yield isopropyl cation. Electrophilic reaction between isopropyl cation and benzene yields the observed reaction products.

7.2 Influence of reaction parameters

Generally in any reaction, the yield and selectivity to a desired product depends on various reaction parameters such as temperature, mole ratio of the reactants, flow rate etc. Before testing the catalytic activity of various systems prepared, it is essential to optimize the reaction parameters.

7.2.1 Effect of Temperature

The vapour phase reaction of benzene with isopropanol was studied at 423, 473 and 523 K over SBW3 catalyst.

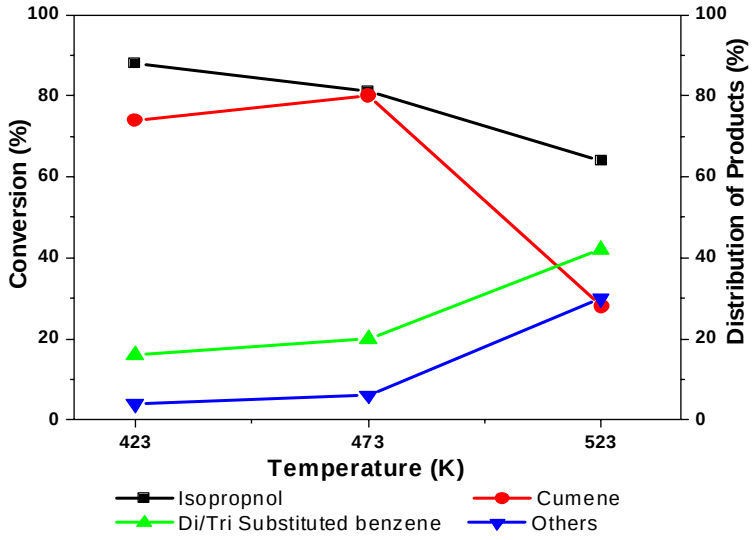

Figure 7.1 Reaction conditions: SBW3-0.2g, mole ratio-7:1, WHSV-21.6, Time-2h

The reaction was investigated by co-feeding benzene and isopropanol in the ratio 7:1, WHSV 21.6 and the results are presented in Figure 7.1. The major products were found to be cumene and di/tri isopropyl benzene.

The isopropyl conversion decreased slightly with increase in temperature. The selectivity to cumene was high at low temperatures but decreases gradually with the increase in temperature to 523 K. This may be due to subsequent alkylation to di/tri isopropyl benzene, which takes place at high temperature. It was observed that the selectivity to di/tri isopropyl benzene increases with increase in temperature in this study. Maximum cumene selectivity with good conversion of isopropanol is obtained at a temperature 423 K. The selected temperature for further reaction is 423 K.

7.2.2 Effect of Mole ratio of Benzene/isopropanol

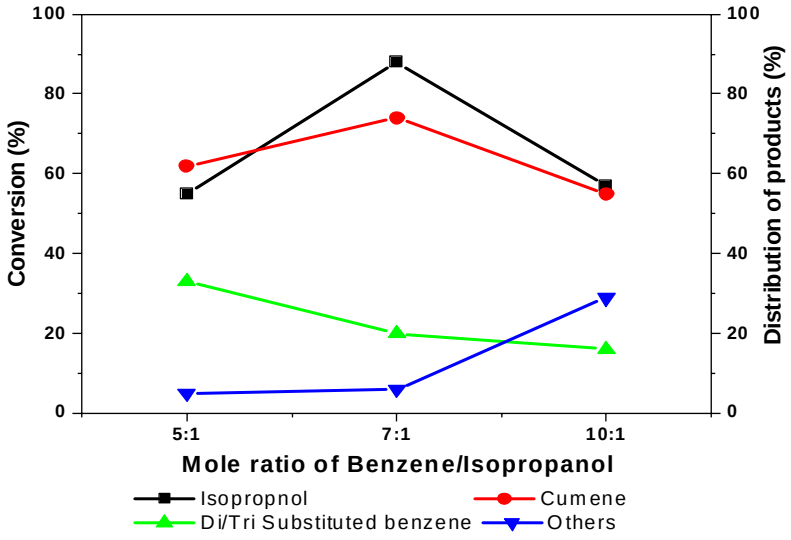

Figure 7.2 Reaction conditions: SBW3-0.2g, WHSV-21.6, Temp-423K, Time-2h

The effect of feed ratio on conversion and product selectivity were studied at a temperature 423 K and WHSV 21.6 over SBW3. The feed ratios employed were (B: IPA) 5:1, 7:1, and 10:1. The results are shown in Figure 7.2. It was

observed that the conversion of isopropanol increases with increasing mole ratio in the feed up to 7:1. Further increase causes reduction in conversion. The selectivity to product cumene also increases from 62 to 74 % with increase in the mole ratio from 5:1 to 7:1 and then decreases to 55% with further increase of mole ratio to 10:1. The selectivity of di/triisopropyl benzene decreases with the change in feed ratio from 5:1 to 10:1 and the decrease in the selectivity of di/tri isopropyl benzene is due to the fact that trans alkylation of these products is more favoured with increased benzene. Mole ratio 7:1 was selected for further studies.

7.2.3 Effect of WHSV

Contact time is an important parameter, as it not only influences the conversion of a reactant; it also leads to change in selectivity of various products. Desired selectivity to a particular product can be achieved by choosing right space velocity. The effect of WHSV on isopropanol conversion and product selectivity was studied over SBW3; feed ratio 7:1 (B: IPA) at 423 K. The WHSV was varied as 12.9, 21.6, and 30.3 h^{-1} and the results are shown in Figure 7.3.

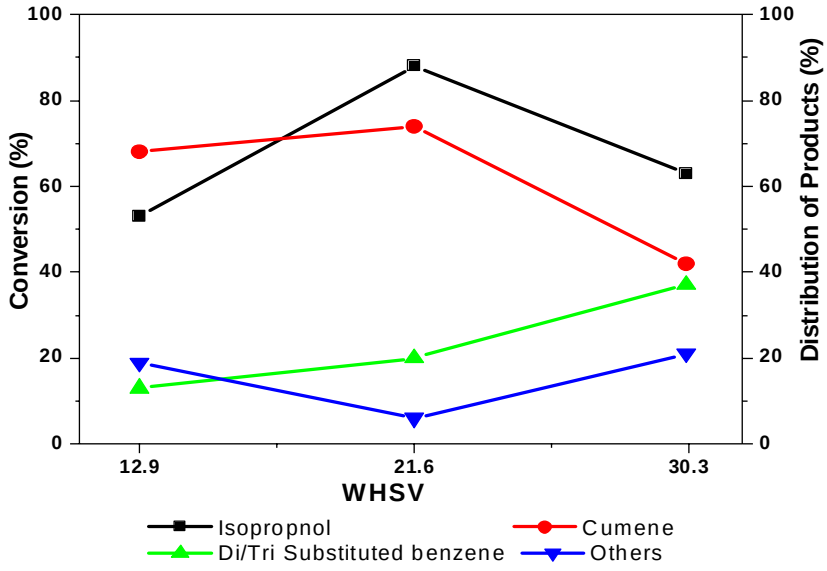

Figure 7.3 Reaction conditions: SBW3-0.2g, Mole Ratio-7:1, Temp-423K, Time-2h

The conversion increased with increase in WHSV up to 21.6 and then decreases to 63%. The reduction in the conversion may simply be due to high diffusion when the WHSV is increased from 21.6 to 30.3. It was observed that the selectivity of di/tri isopropyl benzene increases with increase in WHSV. The selectivity to cumene increases with an increase if WHSV 12.9 to 21.6 and the increase is only about 6%. Further increase in WHSV to 30.3 causes a decrease in selectivity to cumene and it could be suggested that with increase in the WHSV there might be less concentration of isopropyl cation on the catalyst surface.

7.3 Comparison of different catalytic systems

The catalytic activity of all the prepared catalysts on isopropylation of benzene was evaluated under the optimized reaction condition.

Table 7.1 Optimized reaction condition

Parameters	Optimized condition
Temperature	423K
WHSV	21.6
Time	2h
Mole ratio	7:1
Catalyst	0.2g

Very low conversion with comparatively poor cumene selectivity was obtained for the isopropylation of benzene over parent SBA-15. Among the different transition metal incorporated SBA-15 materials SBCo1 gives maximum conversion. Cumene is the major product over all the catalytic systems. The conversion was found to be very low in chromia incorporated systems which may be due to their low Bronsted acidity values. It was found that most of the prepared catalysts effectively catalyze the isopropylation of benzene at relatively low temperature and catalyst weight.

Table 7.2. Catalytic activity of the prepared systems
Reaction conditions: Mole ratio-7:1, WHSV-21.6, Temp-423K, Time-2h, Catalyst weight-0.2g

Catalyst	Conversion of Isopropanol (%)	Distribution of Products (%)		
		Cumene	Di/Tri Substituted benzene	Others
SBA-15	7	64	21	15
SBW1	68	84	15	1
SBW2	51	66	29	5
SBW3	88	74	16	10
SBTi1	78	84	7	9
SBTi2	69	65	24	11
SBTi3	88	51	37	12
SBZr1	66	44	40	16
SBZr2	74	51	36	13
SBZr3	94	30	56	14
SBV1	98	86	10	4
SBV2	89	88	10	2
SBV3	83	89	9	2
SBMo1	82	71	16	13
SBMo2	60	55	33	12
SBMo3	62	99.5	-	0.5
SBCo1	99	80	12	8
SBCo2	92	78	14	8
SBCo3	86	69	21	10
SBCr1	15	63	27	10
SBCr2	15	67	12	21
SBCr3	11	72	13	15

7.4 Conversion of Isopropanol and Acidity of Catalysts

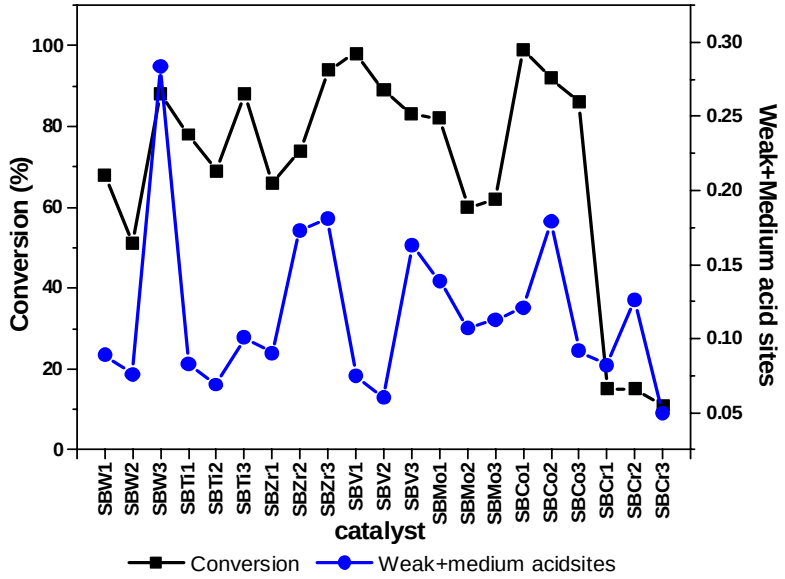

Figure 7.4 Activity and Acidity relationship

Since isopropylation of benzene occurs over Bronsted acid sites, an attempt is made to correlate the catalytic activity with acidic characteristics of the prepared catalysts. Figure 7.6 shows the correlation of isopropanol conversion with the Bronsted (weak +medium) acid sites.

7.5 Recycling studies

One of the major objectives guiding the development of heterogeneous solid acid catalysts includes the easy separation of reaction products from the final reaction mixture and efficient catalyst regeneration. Remarkable results were obtained when SBW3 was reused for the 2nd run directly after filtration, subsequent drying and calcination. The results given in Figure 7.5 shows that highest selectivity is to cumene. The same catalyst was used for carrying out subsequent runs under similar conditions. Recycling studies (four times) of the catalyst confirmed that the catalysts retained its activity and impart higher product selectivity with respect to the fresh catalyst.

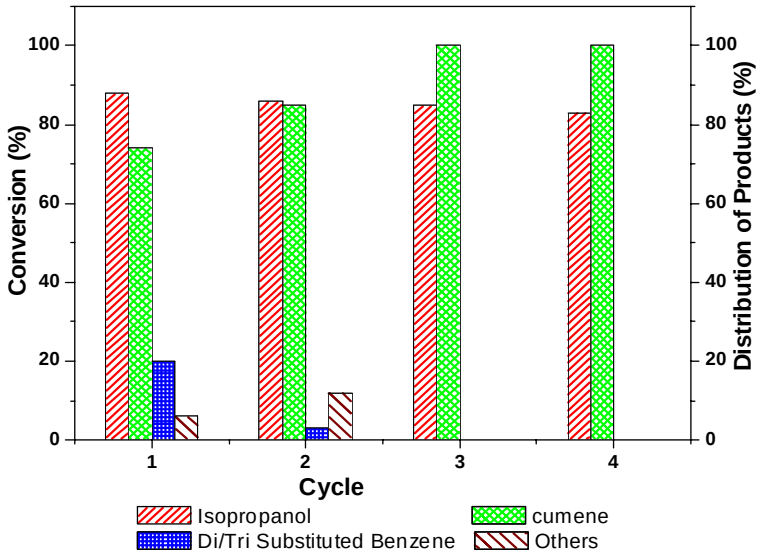

Figure 7.5 Reaction conditions: SBW3-0.2g, mole ratio-7:1, WHSV-21.6, Temp-423K, Time-2h

7.6 Effect of Substrates

Figure 7.6 Reaction conditions: SBW3-0.2g, mole ratio-7:1, WHSV-21.6, Temp-423Kfor benzene and Temp-473K for others, Time-2h

Benzene	Conversion of Isopropanol (%)		88
	Distribution of Products (%)	Cumene	74
		Di/Tri Substituted benzene	20
		Others	6
Toluene	Conversionof Isopropanol (%)		83
	Distribution of Products (%)	Para isomer	67
		Ortho isomer	18
		others	15
Anisole	Conversionof Isopropanol (%)		95
	Distribution of Products (%)	Para isomer	90
		Ortho isomer	10
Isobutyl Benzene	Conversionof Isopropanol (%)		94
	Distribution of Products (%)	Para isomer	74
		Ortho/meta isomer	11
		others	15

Catalytic activity of the prepared systems is largely dependent on the substrate used. Variation of reactivity with substrate was studied by carrying out the reaction using benzene, toluene, anisole, and isobutyl benzene over the same catalyst Table 7.3 illustrates the influence of substrate on the catalytic activity for isopropylation reaction. The isopropylation of toluene and anisole with lower catalyst concentrations under mild conditions shows predominant ortho/para directing effect. When the substrate is isobutyl benzene, 74% para isomer is produced in the isopropylation reaction. A slight amount of meta isomer is also present in the reaction mixture. An electron donating group will increase the electron density on the aromatic ring and make it more flexible to the attack by an electrophile. Thus it is worth mentioning that the reactivity of aromatic nucleus increases with the number and strength of electron donating groups attached to the aromatic ring.

7.7 Discussion

The isopropylation of aromatics with isopropanol involve a complex reaction network. Alkylation of benzene with propene is the major reaction that occurs under the reaction scheme of isopropyaltion of benzene. This reaction is sometimes associated with several side reactions which results in the formation of various products through transalkylation, dispropotionation, dealkylation etc. The formation of n-propylbenzene is always accompanied with the production of cumene, which is formed either by the isomerisation reaction of cumene or from the primary n-propyl cation formation before isopropylation of benzene. According to Kaeding and Holland the formation of n-propylbenzene is not a favourable reaction at low temperatures due to the wide variation in thermodynamic equilibrium ratios. Similar observations are also made by some other researchers [28, 29]. From the mechanism suggested it is clear that the isopropylation reaction takeplace over Bronsted acid sites. The isopropanol is converted into propene by dehydration followed by the

proton abstraction from Bronsted acid sites which results in the formation of carbocation. Isopropyl substitution on aromatic ring is possible by the attack of the carbocation after the removal of H^+ back to the catalyst.

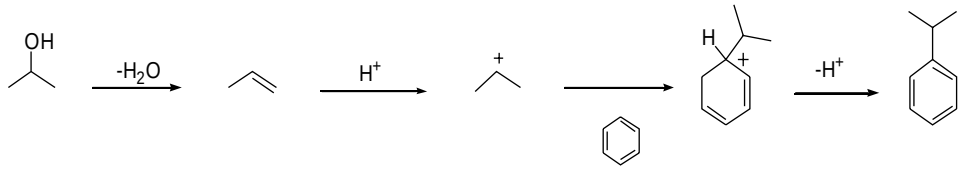

Scheme 7.2. Benzene isopropylation over Bronsted acid sites

From the results obtained it is clear that the prepared catalysts are highly adequate for the reaction and producing better results.

7.8 Conclusions

- All the transition metal incorporated mesoporous SBA-15 catalysts prepared in the present work effectively catalyze the isopropylation reaction of benzene.
- Comparatively low activity was observed in the case of chromia incorporated systems.
- The present method offers an alternative method for the selective cumene preparation with low temperature and low catalyst weight.
- The critical role played by various reaction parameters on the catalytic activity and percentage distribution of products is well established.
- Bronsted acidity of the catalysts plays an important role in the present reaction.
- The reaction is found to be clean with negligible formation of polyalkylated products in comparison with monoalkylated product.
- The prepared catalytic systems are found to be reusable and resistant to rapid deactivation in the present isopropylation reaction.

References

[1] G. A. Olah and S. J. Kuhn, in: Friedel–Crafts and Related Reactions; Vol. II, ed. Interscience., New York, 1964

[2] G. A. Olah, S. Kobayashi, M. Tashiro, J. Am. Chem. Soc., 94 (1972) 7448.

[3] P. Kamala, A. Pandurangan, Catal. Commun .,9 (2008) 605–611

[4] S. Jun, R. Ryoo, J. Catal. 195 (2000) 237.

[5] K. Tanabe and W. F. Holderich, Appl. Catal. A: General., 181 (1999) 399.

[6] A. V. Ramaswamy, in: Petrotech-99, Third Int. Petrol. Conf., Vol. III, New Delhi.

[7] D. N. Mazzone, D. O. Marler, K. M. Keville and L. A. Green, US Patent., 5900520 (1999)

[8] (a) G. J. Gajda, R. T. Gajek, US Patent 5907073, 1999.

(b) C. Flego, G. Pazzuconi, E. Bencini and C. Perego, Stud. Surf. Sci. Catal., 126 (1999) 461.

[9] K. Shanmugapriya, M. Palaniswamy, Banumathi Arabindoo, V. Murugesan, J. Catal., 224 (2004) 347.

[10] Q. N. Le, C. Hill, US patent 117153192; Q.N. Le, C. Hill, Chem. Abstr., 118 (1992) 894.

[11] Jorge Medina-Valtierra, Octavio Zaldivar, A. Miguel, J.A. Sanchez, Montoya Juan Navarrete, J.A. delos Reyes, Appl. Catal, A., 166 (1998) 387.

[12] G. A. Olah, S. H. Flood, S. J. Kuhn, M. E. Moffatt, N. A. Overchuck, J. Am. Chem. Soc., 86 (1964) 1046.

[13] S. Nojima, A. Yasutake, Y. Tanaka, Japanese Patent 10298117, 1998.

[14] A. K. Ghosh, US Patent 5907073, (1999).

[15] R. A. Grigoresa, I. Cojocaru, P. Obloja, C. Papuzu, G. Pop, R. Boeru, G. Ignatescu, S. Ichim, G. Ivanus, T. Stan, RO 11093., (1996).

[16] H. Ming Yuan, L. Zhoghui, M. Enze, Catalysis Today, 2 (1988) 321.

[17] J. C. Cheng et al., US Patent 5453554, (1995).

[18] J. H. Clark, S. R. Cullen, S. J. Barlow, T. W. Bastock, J. Chem. Soc., Perkin Trans, 2 (1994) 1117.

[19] J. H. Clark, A. P. Kybett, D. J. Macquarrie, S. J. Barlow, P. Landon, J. Chem. Soc. Chem. Commun., (1989) 1353

[20] S. J. Barlow, J. H. Clark, M. R. Darby, A. P. Kybett, P. Landon, K. Martin, J. Chem. Res. (s)., (1991) 74.

[21] P. B Venuto, L. A. Hamilton, P. S. Landdis, J. J. Wise, J. Catal., 5 (1966) 81.

[22] O. Kelley, A. A. Kellett, J. Plucker, Ind. Eng. Chem.., 39 (1947) 154.

[23] B. D. Flockhart, K.Y. Liew, R. C. Pink, J. Catal.., 72 (1981) 314.

[24] P. A. Parikh, N. Subramanyam, Y. S. Bhat, A. B. Halgeri, Appl. Catal. A., 90 (1992) 1.

[25] K. S. Reddy, B. S. Rao, V. P. Shiralkar, Appl. Catal. A., 121 (1995) 191.

[26] J. Ceika, G. A. Kapustin, B. Witchterlova, Appl. Catal. A., 108 (1994) 187.

[27] Qiaoxia Guo, Lianshan Li, Liwei Chen, Yanqing Wang, Shenyong Ren, Baojian Shen, Energy & Fuels., 23 (2009),51.

[28] W. W. Kaeding, R. E. Holland, J. Catal., 109 (1988) 212.

[29] J. Panming, W. Qiuying, Z. Chao, X. Yanhe, Appl. Catal. A: Gen., 91 (1992) 125.

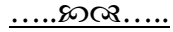

Chapter 8

Benzylation of Isobutyl Benzene

Contents

Catalyzed aromatic Friedel-Crafts benzylation reactions are of great interest due to their importance and widespread use in synthetic and industrial chemistry. In recent years active research has been directed at substituting the traditionally homogeneous catalysts, which have many environmental and technological problems with new green heterogeneous acid catalysts having higher catalytic efficiency and more ecofriendlyness. One of the most important challenges for green catalytic processes is to control the diffusion of the reactants and products from active sites to minimize the on-site coke-formation due to subsequent acid-catalyzed transformations. The use of mesoporous solid acid catalysts, like metal incorporated SBA-15 with confined meso and micropores reduces the difficulty of deactivation due to coke-formation on the active sites of the catalysts. This chapter deals with benzylation reaction of isobutyl benzene with benzyl chloride over various transition metal incorporated mesoporous SBA-15 catalysts. The present study offer a very clean and ecofriendly process for the benzylation reaction to produce the desired mono-alkylated product with very high yield.

8.1 Introduction

Benzylation of aromatic compounds is one of the important reaction used in the chemical industry. The benzylated derivatives of various aromatic compounds are valuable intermediates for the manufacture of pharmaceuticals, antioxidant, and they are usually produced by Friedel-Crafts alkylation reactions. Usually the Friedel-Crafts alkylation reactions are catalyzed by strong mineral acids or Lewis acids [1-7] and leads to the formation of complex reaction mixtures. Under normal reaction conditions polyalkylation, dealkylation, transalkylation, polymerization and isomerization reactions etc. may also occur [1]. Aromatic ring become more activated toward eletrophilic substitution reactions in the presence of alkyl groups. Friedel-Crafts alkylation reaction is always associated with the formation of polyalkylated products in addition to monoalkylated products, leading to decreased yields, laborious separation procedures, and energy-consuming processes [8]. The usual workup will cause additional environmental problems in the disposal of the reaction residue that was generated during the reaction. Thus, the development of new method to increase the selectivity of the desired product is still attractive for chemists. To avoid the above mentioned problems, many efforts have been devoted to the search of solid acid catalysts [9-21]. Based on previous studies it is revealed that the major factor influencing the activity of the solid acid catalysts is the acidity and channel size.

Cation exchanged K-10 was effectively used for the benzylation of benzene and toluene [22, 23]. Benzylation of benzene, toluene and m-xylene using benzyl alcohol over Al impregnated MCM-41 and MCM-48 was reported [24]. Ga_2O_3 and In_2O_3 supported on mesoporous MCM-41 are found to be active for the benzylation and acylation of benzene and other aromatic compounds [25]. He et al. investigated the catalytic performance of iron supported mesoporous materials for the alkylation of benzene with benzyl

chloride [26]. Catalytic activity of HCl gas treated Ga-Mg hydrotalcite anioinc clay for the benzylation and acylation of toluene and benzene was also reported [27]. Sugunan et al. studied the catalytic performance of H-ZSM-5, H-beta, H-mordentite, H-Y, etc. for the benzylation of o-xylene with benzyl chloride [28, 29].Titania and its sulphated analogues [30], various spinel catalysts [31], sulphated zirconia [32], some rare earth oxides [33] were also used for various alkylation reactions. The alkylation of anisole by benzyl bromide was investigated by using the $MoCl_5$/HZSM-5 or $MoCl_5$/TS-1 catalyst system [8].

The inherent disadvantages in the use of conventional Lewis acid metal chlorides for Friedel-Crafts benzylation are that they are non-regenerable and require more than stoichiometric amounts because of complexation with the product formed. Work-up to decompose the resultant intermediate complex by hydrolysis forms a large amount of waste product and separation is lengthy and expensive. There was therefore a need for a catalyst for benzylation reactions which is simple to operate and can be carried out in a media which are not toxic and corrosive. Moreover the solid acid catalyst should be simple to separate and reusable. The use of solid mesoporous acid catalysts relates to an ecofriendly process for benzylation reactions using benzyl chloride as a benzylating agent dispensing the use of stoichiometric amounts of corrosive, toxic aluminium chloride and hydrogen fluoride as Friedel- Crafts reagents.

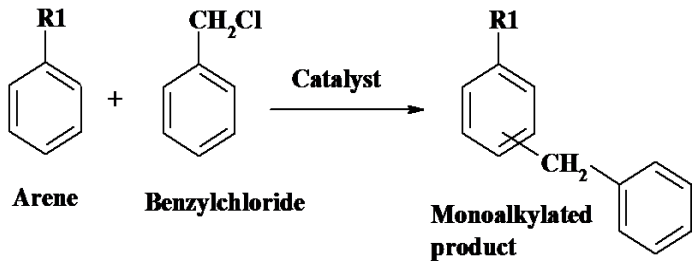

R1= $-CH_2-CH-(CH_3)_2$

Scheme 8.1 Benzylation of Arenes

The present invention relates to a process for isobutyl diphenyl methane (mono benzyl isobutyl benzene) by Friedel-Crafts benzylation of isobutylbenzene using benzyl chloride as an alkylating agent in the presence of various transition metal incorporated mesoporous SBA-15 catalysts. The higher density of acidic sites eventually increases number of benzyl cations generated in the reaction in the electrophilic substitution of the Freidel-Crafts benzylation and thus enhances activity of the reaction. Thus the higher density of acid sites present in metal incorporated SBA-15 are responsible for the Friedel-Crafts benzylation of isobutyl benzene and the isobutyl diphenyl methane is obtained by a simple process involving filtration of the catalyst from the reaction mixture and recovering the product by conventional methods.

8.2 Effect of reaction parameters

In the present work benzylation of isobutyl benzene is done using the prepared catalysts. The reaction always yielded a single major product, which is identified as the monobenzylated product. (It is difficult to identify the product as ortho, meta or para). Before testing the catalytic activity of the various catalytic systems prepared, it is essential to optimize the reaction parameters such as temperature, mole ratio of substrates, time, and catalyst weight. So the influence of various reaction parameters on the benzylation reaction was studied here and results are discussed.

8.2.1 Effect of Temperature

The influence of temperature on the benzylation of IBB with SBW1 studied over a range of temperatures. The variation of conversion of benzyl alcohol and product distribution as a function of reaction temperature is shown in Figure 8.1. An increase in the conversion is achieved with an increase in reaction temperature. The conversion increased from 18 to 88 % when the temperature increased from 363 to 373 K. A further increase in the reaction

temperature gave only a slight increase in conversion. So the temperature 373K was selected for further studies.

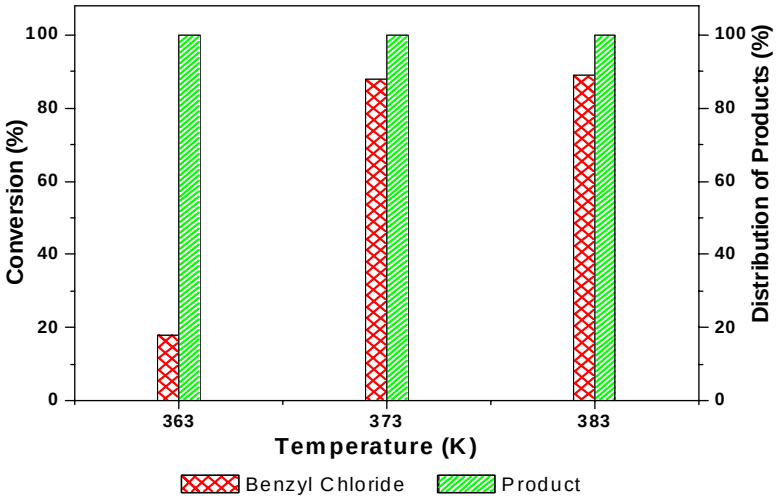

Figure 8.1 Effect of Temperature
Reaction Conditions: IBB: BC Mole ratio-10:1, SBW1-0.1g, Time-3h

8.2.2 Effect of Time

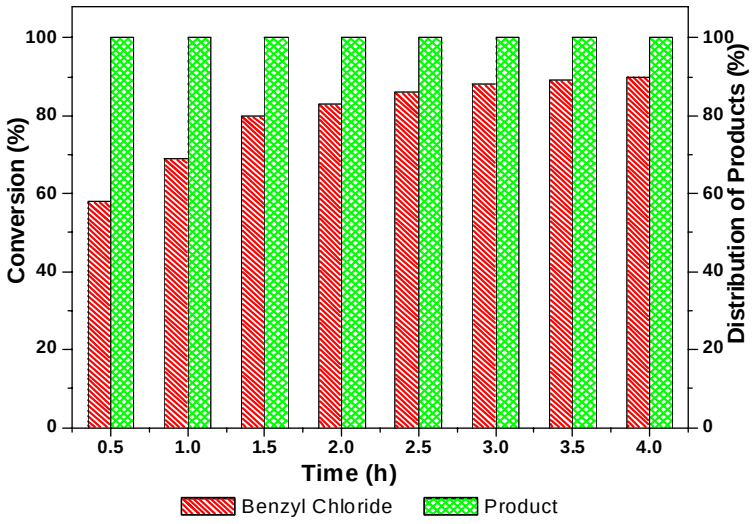

Figure 8.2 Effect of Time
Reaction Conditions: IBB: BC Mole ratio-10:1, SBW1-0.1g, Temp-373K

The influence of the reaction time on the benzylation of IBB with benzyl chloride at 373 K over SBW1 is shown in Figure 8.2. The BC conversion increased with reaction period. The conversion reaches to 90% with 100% selectivity of monoalkylated product after 4h. The continuation of the reaction resulted in saturation of the BC conversion. Only 2% increase was observed in between 3h and 4h.The optimum temperature selected for further reaction was 3h.

8.2.3 Effect of Mole ratio of IBB/BC

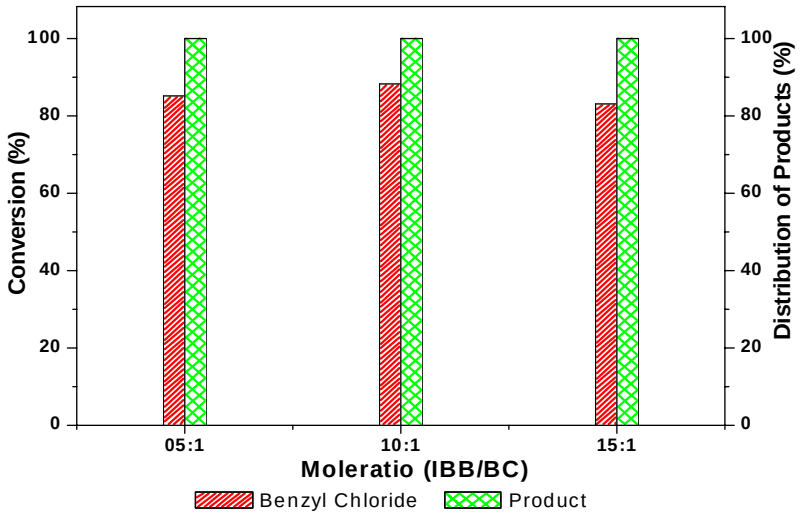

Figure 8.3 Effect of Mole ratio of IBB/BC
Reaction Conditions: SBW1-0.1g, Temp-373K, Time-3h

The effect of molar ratios of reactants on the conversion of BC was studied by changing the alkylating agent concentration and keeping the IBB concentration constant. Three different combinations of molar ratio of IBB/BC were studied and the results presented in Figure 8.3. As the molar ratio of IBB/BC increases from 5 to 10 the conversion increases slightly and then decrease with further increase of mole ratio. Almost 88.0% of BC was consumed at the molar ratio (IBB/BC) of 10. The mono benzylated product concenteration remains the same in all the cases. Mole ratio of 10:1 was selected for further reactions.

8.2.4 Effect of Catalyst Amount

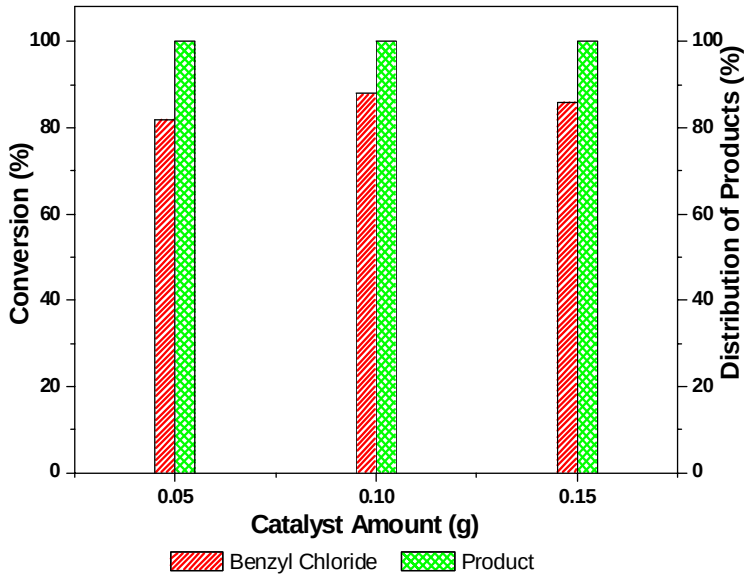

Figure 8.4 Effect of Catalyst Amount
Reaction Conditions: IBB: BC Mole ratio-10:1, Temp-373K, Time-3h

The amount of catalyst plays an important role in deciding the conversion and the percentage distribution of products in heterogeneous catalyzed reactions. Figure 8.4 displays the conversion of benzyl chloride as a function of catalyst amount in the benzylation reaction of isobutyl benzene. As the amount of catalyst increased from 0.05 to 0.1g, an increase in percentage conversion was observed. Increase in the catalyst loading provides higher surface area with higher acid site concentration for reactant molecules to adsorb. Further increase in catalyst weight shows only negligible influence in conversion of benzyl chloride. The optimum catalyst amount for the effective performance of the catalyst in the benzylation reaction is 0.1g.

8.3 Effect of Catalysts

Table 8.2 listed the reaction results of isobutyl benzene with benzyl chloride under the optimized reaction condition.

Table 8.1 Optimized reaction Conditions

Parameters	Optimized condition
Temperature	373K
IBB: BC moleratio	10:1
Catalyst Amount	0.1g
Time	3h

Table 8.2 Reaction Conditions: IBB: BC Mole ratio-10:1, Temp-373K, Catalyst-0.1g

Catalyst	Conversion of Benzyl Chlorid (%)	Distribution of mono alkylated product (%)
Blank	No reaction	
SBA-15	29	100
SBW1	88	100
SBW2	90	100
SBW3	90	100
SBTi1	42	100
SBTi2	92	100
SBTi3	67	100
SBZr1	95	100
SBZr2	97	100
SBZr3	96	100
SBV1	68	100
SBV2	65	100
SBV3	54	100
SBMo1	72	100
SBMo2	67	100
SBMo3	78	100
SBCo1	80	100
SBCo2	69	100
SBCo3	74	100
SBCr1	88	100
SBCr2	46	100
SBCr3	52	100

From the Table 8.2 it was observed that no reaction occurs in the absence of catalyst. Experimental results indicated that pure SBA-15 itself had very low observed reactivity on this alkylation reaction. Remarkable enhancement in the catalytic activity and selectivity for the formation of monobenzylated product was observed in the benzylation of isobutylbenzene (IBB) with benzyl chloride over various transition metals incorporated SBA-15 catalysts. An interesting observation is that only monobenzylated product was obtained in all cases. Among the various transition metals incorporated SBA-15 systems the Zr incorporated systems show higher conversion of benzyl chloride about 95%.

8.4 Conversion of Benzyl Chloride and Lewis Acidity

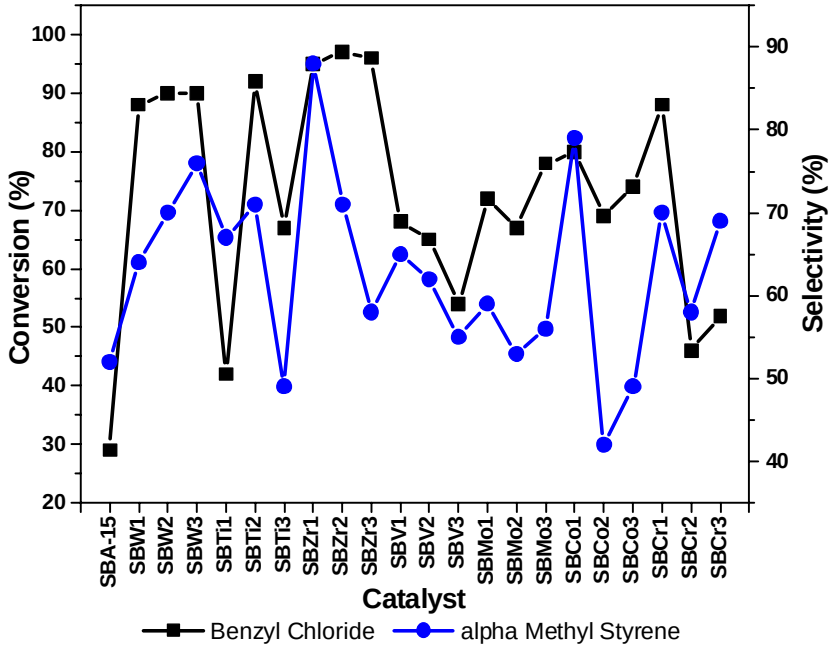

Figure 8.5 Conversion of Benzyl Chloride and Lewis Acidity

The acidic properties of metal oxide based catalysts can significantly affect the catalytic activity of heterogeneous catalysts in alkylation reactions. So an attempt is made to correlate the catalytic activity with the acidic properties of the prepared catalysts. Figure 8.5 shows the correlation

of benzyl chloride conversion over the prepared catalyst systems with the acidity of the corresponding catalysts. From the Figure it is clear that the percentage conversion is in agreement with the Lewis acidity of the catalysts measured as the methyl styrene selectivity from cumene conversion reaction.

8.5 Conversion of Benzyl Chloride and Total Acidity of Catalysts

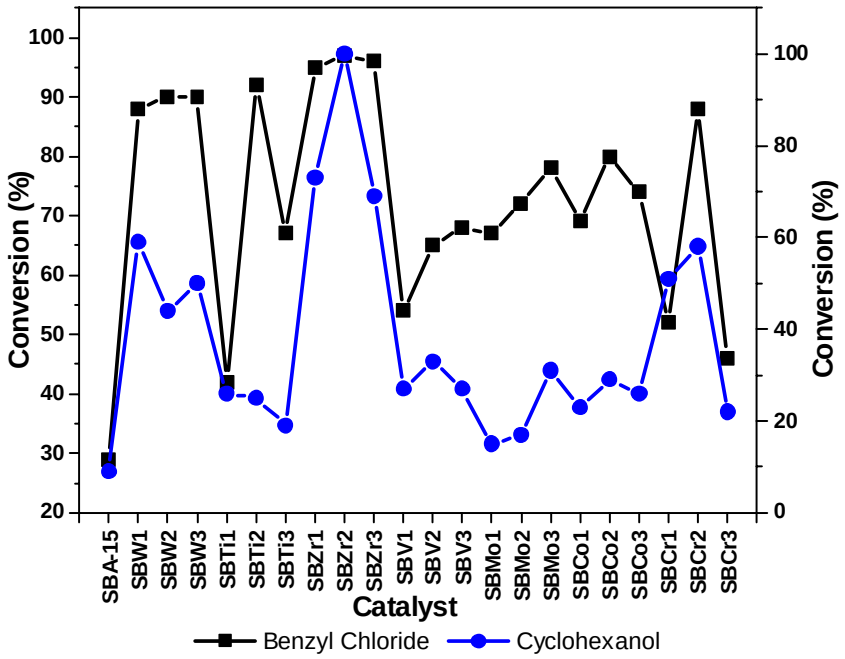

Figure 8.6 Conversion of Benzyl Chloride and Total Acidity of Catalysts

The supported metal oxide contains both Bronsted and Lewis acid sites. Figure 8.6 displays the correlation graph between the conversion of benzyl chloride over the prepared catalysts and the total acidity of the catalyst systems obtained from the cyclohexanol conversion reaction. By comparing Figures 8.5 and 8.6 a dominating impact of Lewis acid sites on the benzylation reaction of isobutyl benzene with benzyl chloride over the prepared catalyst systems was observed.

8.6 Recycling Studies

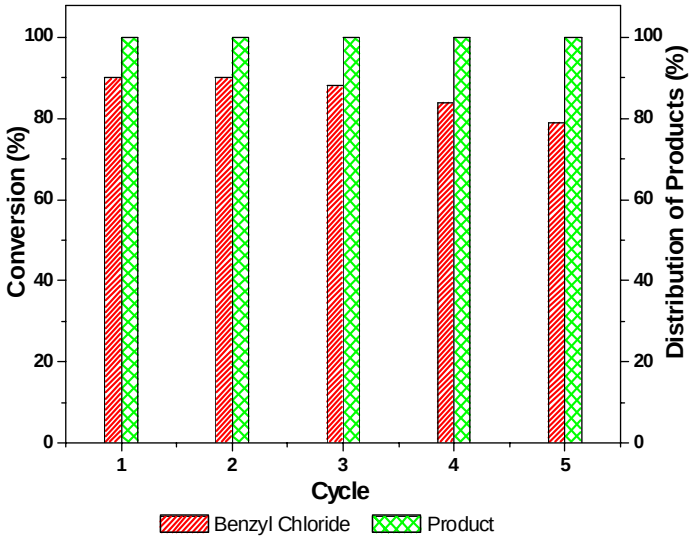

Figure 8.7 Recycling Studies
Reaction Conditions: SBW2-0.1g, Temp-373K,
IBB: BC Mole ratio-10:1, Time-3h

In order to check the stability and catalytic activity of the prepared catalytic systems in the benzylation of IBB, five cycles (fresh and four cycles) were carried out using the same catalyst. The results are presented in Figure 8.7. After workup of the reaction mixture, the catalyst was separated by filtration, washed with acetone and calcined for 6 h at 540^0C in the presence of air. The activity of SBW2 decreases slightly after each recycle. The conversion of BC decreases from 90.0 to79.0% when the catalyst was recycled from fresh to the fifth cycle, respectively, in the benzylation of IBB. The hydrogen chloride produced in the electrophilic benzylation reaction is responsible for the deactivation of the catalyst.

8.7 Leaching Studies

Table 8.3 Reaction Conditions: Catalyst-0.1g, IBB: BC Mole ratio-10:1, Temp-373K, Time-3h

Catalyst		Conversion of Benzyl Chloride (%)	Distribution of mono alkylated product (%)
SBW1	1h	58	100
	3h	60	100
SBTi1	1h	54	100
	3h	55	100
SBZr1	1h	72	100
	3h	75	100
SBV1	1h	37	100
	3h	38	100
SBMo1	1h	34	100
	3h	37	100
SBCo1	1h	42	100
	3h	51	100
SBCr1	1h	35	100
	3h	37	100

To prove the heterogeneous character of the reactions, the catalyst was removed from the reaction mixture after one hour and the filtrate was allowed to react under the same conditions for 2h. No noticeable change in conversion is obtained in all cases except in the case SBCo1 after the removal of the catalyst. Thus it is observed that the active metal ions are not leached from the catalyst during the benzylation reaction. The results reveal the heterogeneous nature of the present reaction. In the case of SBCo1 an increase in conversion occurs after the removal of the catalyst, which implies slight leaching of the cobalt ions from the catalyst.

8.8 Effect of Substrates

Table 8.4 Effect of Substrates
Reaction Conditions: SBW1-0.1g, IBB: BC Mole ratio-10:1, Temp-373K, Time-3h

Isobutyl benzene	Conversion of Benzyl Chloride (%)		88
	Distribution of Products (%)	Monoalkylated product	100
Anisole	Conversion of Benzyl Chloride (%)		94
	Distribution of Products (%)	Para isomer	86
		Ortho isomer	14
O-Xylene	Conversion of Benzyl Chloride (%)		29
	Distribution of Products (%)	Monoalkylated product	100
Toluene	Conversion of Benzyl Chloride (%)		23
	Distribution of Products (%)	Monoalkylated product	100

Variation of reactivity with substrate was studied by carrying out the reaction using isobutyl benzene, anisole, o-xylene and toluene over the same catalyst under the same reaction condition. The benzylation reaction yields of benzyl chloride to the substrates with different substituents are listed in Table 8.3. The reactivity is in the order anisole>isobutyl benzene>o-xylene>toluene, which is related to the electron releasing nature of the substituent present. The results indicated that toluene and anisole were benzylated with benzyl chloride to give benzyl toluene and benzyl anisole. The benzylation reaction activity (yield) sequence of anisole > isobutyl benzene > o-xylene > toluene can be easily understood according to a classical Friedel-Crafts-type acid catalyzed benzene alkylation mechanism, where the benzylation of an aromatic compound is easier if the electron-donating groups are present in the aromatic ring and difficult if an electron-withdrawing group appears [1]. Here, anisole (with an electron-donating group MeO-) showed the highest yield among the four substrates, and toluene has less activity. Kocovsky et al. [7] also reported that increasing the electron density of the aromatic ring had a beneficial effect

on the reactivity. Similar effects have also been reported in the niobium acid and niobium phosphate on the benzylation of anisole and toluene with benzyl alcohol [4, 5, 8, 34]. As the barrier for isomerization in the benzenium ion intermediates of the alkylations is higher in the case of OCH_3^- than CH_3^- substituted systems, anisole tends to give the kinetically controlled ortho-para alkylation products and the amount of meta isomer is low.

8.9 Discussion

Many approaches have been reported in the literature to explain the origin of active sites in solid acid catalysts for the benzylation reactions. Rhodes et al. and Ghorpade et al. [8] reported that the increased accessibility of the Lewis sites to the reactant molecule is responsible for the enhanced catalytic activity of solid acid catalysts. Lachter et al. [4] investigated that the Bronsted acid sites (NbOH or POH) in the niobium phosphate are capable of generating a carbenium ion intermediate (allylic cation) from allylic alcohol under the conditions employed and readily undergo electrophilic substitution with the aromatics. The initial carbenium ion intermediates are generated by protonation of the alcohol under appropriate reaction conditions. The coordination of the allylic alcohol with the Lewis acid sites of the catalysts also leads to electrophilic substitution of the aromatic compounds. Choudhary and Jana [35] suggested a redox mechanism by considering redox properties of the metal chloride species present in the catalysts, which are expected to play important roles in the benzylation reaction over various metal chlorides, supported on commercial clays or on high silica mesoporous MCM-41 catalysts [8]. A mechanism of anisole benzylation over $MoCl_5$ was proposed, which was different from the traditional Friedel-Crafts alkylation mechanism [8].

Mechanism operating in a particular reaction depends mainly on the catalyst used. The catalytic activity studies of different transition metal incorporated SBA-15 systems on the benzylation of isobutyl benzene studied

under the present work suggest the involvement of Lewis acid sites in the reaction. Electrophilic alkylation of aromatics catalyzed by Lewis acid is commonly considered as proceeding via a carbenium-ion-type mechanism. The reaction proceeds through an electrophile, which is obtained by the reaction of benzyl chloride with the acidic metal active site. The corresponding benzylated derivative is produced by the attack of the generated electrophile to the aromatic ring.

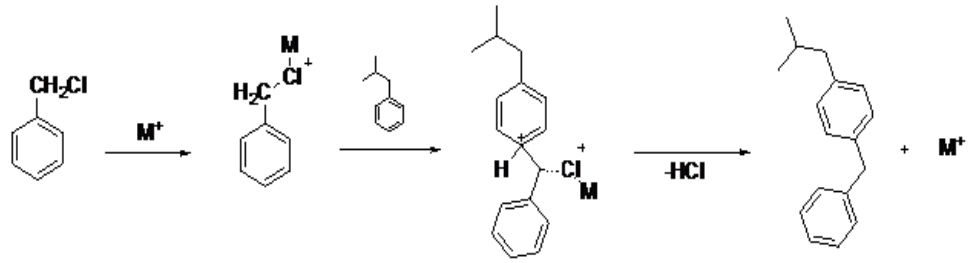

Scheme 8.2 Benzylation of Isobutyl Benzene with Benzyl Chloride.

The faster diffusion of reactants/ products and efficient removal of coke precursors from the mesoporous channels are the main feature for higher IBB conversion and selectivity for monobenzylated product. The results demonstrate that the adopted procedure can prevent deactivation of the catalyst by severe coking and improve selectivity of the desired product(s), resulting in opening new aspects of green catalysis. Further investigations on these aspects are currently ongoing and will be reported in due course.

Transition metal incorporated SBA-15 catalysts prepared in the present work were found to be active in the benzylation of IBB to monobenzyl isobutyl benzene with benzyl chloride. The formation of the meta-isomer may also be possibly followed by the para-isomer due to its lower strain energy compared with the ortho-isomer. Large pore size and strong acid sites promote the catalytic activity of isopropylation of IBB to para, ortho and meta-alkylated products. The high benzylation activity of various transition metal

incorporated SBA-15 catalysts may be attributed to the presence of framework metal oxide species in combination with the strong acid sites.

8.10 Conclusions

- It can be concluded that liquid phase benzylation of IBB is readily catalyzed by various transition metals incorporated SBA-15 mesoporous molecular sieves.
- The present approach is significant for the mono benzylation of various aromatic compounds.
- Lewis acid sites of the catalysts are mainly responsible for the good catalytic performance in the benzylation reaction.
- Recycling of the catalyst does not affect the activity of the catalyst significantly.
- The present process eliminates the use of corrosive and stoichiometric quantities of aluminium chloride and the work-up procedure is simple.
- The present process is environmentally safe since there is no disposal problem and also economical.

References

[1] G. A. Olah, Friedel-Crafts Chemistry, Wiley: New York (1973).

[2] W. H. Du, Zh.W. An, M. L. Xu, Zh. B. Li, D. H. Ma, F. Sh. Wang, F. L. Kong, Chin. J. Synth. Chem., 5 (2) (1997) 205.

[3] R. Commandeur, N. Berger, P. Jay, J. Kervenal, U.S. Patent 5, 186 (1993) 864.

[4] C. C. M. Pereira, E. R. Lachter, Appl. Catal. A., 226 (2004) 67.

[5] De la Cruz, M. H. C, Da Silva, J. F. C,Lachter, E. R. Catalysis Today, 118 (2006) 379.

[6] Z. E. Berrichi, B. Louis, J. P. Tessonnier, O. Ersen, L. Cherif, M. J. Ledoux, C. Pham Huu , Appl. Catal. A., 316(2007) 219.

[7] V. Malkov, S. L. Davis, W. L. Mitchell, P. Kocovsky, Tetrahedron. Lett.,38(27) (1997) 4899.

[8] Qiaoxia Guo, Lianshan Li, Liwei Chen, Yanqing Wang, Shenyong Ren, Baojian Shen, Energy & Fuels., 23(2009) 51.

[9] B. Coq, V. Gourves, V. Figueras, Appl. Catal. A., 100 (1993) 69.

[10] J. Aguilar, F. V. Melo, E. Sastre, Appl. Catal. A., 175 (1998) 181.

[11] A. Corma, V. Martınez-Soria, E. J. Schnoeveld, Catal., 192 (2000) 163.

[12] A. Vinu, D. P. Sawant, K. Ariga, M. Hartmann, S. B. Halligudi, Microporous and Mesoporous Materials,80(2005)195.

[13] J. H. Clark, G. L. Monks, D. J. Nightingale, P. M. Price, J. F. White, J. Catal.,193 (2000) 348.

[14] M. Brown, S. J. Barlow, D. J. McQuarrie, J. H. Clark, A. P. Kybett, European Patent 0 352 878 A1 (1990).

[15] T. Cseri, S. Bekassy, F. Figueras, S. J. Rizner, Mol. Catal. A: Chem., 98 (1995) 101.

[16] C. Cativiela, J. I. Garcia, M. Garcia-Matres, J. A. Mayoral, F. Figueras, J. M. Fraile, T. Cseri, B. Chiche, Appl. Catal.A., 123(1995) 273.

[17] S. R. Chitnis, M. M. Sharma, React. Funct. Polym., 33 (1997)1.

[18] G. A. Sereda, Tetrahedron. Lett., 45 (2004) 7265.

[19] J. E. Chateauneuf, K. Nie, Adv. Environ. Res., 4 (2000) 307.

[20] K. Okumura, K. Yamashita, M. Hirano, M. J. Niwa, Catal., 234 (2005) 300.

[21] Castro, A. Corma, J. J. Primo, Mol. Catal. A: Chem., 177 (2002) 273.

[22] P. Laszlo, A. Mathy, Helv. Chem. Acta., 70 (1987) 577.

[23] T. Cseri, S. Bekassy, F. Figueras, S. Rizner, J. Mol. Catal. A: Chem., 98 (1995) 101.

[24] S. Jun, R. Ryoo, J. Catal., 197 (2000) 237.

[25] V. R. Choudhary, S. K. Jana, B. P. Kiran, j. Catal., 192 (2000) 257.

[26] N. He, S. Bao, Q.Xu, Appl. Vatal. A: Gen., 169 (1998) 29.

[27] V. R. Choudhary, S. K. Jana, A. B. Mandale, Catal. Lett., 74, 1-2 (2001) 95.

[28] B. Jacob, S. Sugunan, A. P. Singh, J. Mol. Catal. A: Chem., 139 (1999) 43.

[29] P. Singh, B. Jacob, S. Sugunan, Appl. Catal A: Gen., 174 (1998) 51.

[30] K. R. Sunajadevi, S. Sugunan, React. Kinet. Catal. Lett., 82 (2004) 11.

[31] S. P. Ghorpade, V. S. Dharsane, S. G. Dixit, Appl. Catal. AGen., 166 (1998) 135.

[32] S. N. Koyande, R. G. Jaiswal, R. V. Jayaram, Ind. Eng. Chem. Res., 37 (1998) 98.

[33] K. B. Sherly, V. T. Bhatt, React. Kinet, Catal. Lett., 75 (2002) 239.

[34] M. Moraes, W. Pinto, S. F. de, W. A. Gonzalez, L. M. P. M Carmo, N. M. R. Pastura, E. R. Lachter, Appl. Catal. A., 138 (1996) 7.

[35] V. R. Choudhary, S. K. Jana, J. Mol. Catal. A: Chem., 180 (2002) 267.

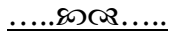

Chapter 9

Summary and Conclusions

Contents

To meet the challenges related to the chemical industry, development of efficient catalysts is necessary. The mesoporous materials like SBA-15 are considered as good catalyst candidates of 21st century. SBA-15 mesoporous materials are catalytically inactive, but allow the dispersion of catalytically active phases into the framework. So these materials can be considered as an interesting alternative for preparing catalytically active metal nanoparticles in-situ into it. In the present work various transition metals are incorporated to improve the catalytic activity of SBA-15 material. The fundamental aspects of the preparation, characterization and the activity studies are briefly viewed in this thesis. Systematic investigation of the physico-chemical properties and catalytic activity studies of the prepared materials were carried out and presented in previous chapters. The present chapter deals with the summary and conclusion of the results described in the preceding chapters of the thesis.

9.1 Introduction

Among the mesoporous materials, SBA-15 is regarded as one of the most promising materials because of its higher surface area, large pore size and higher hydrothermal and thermal stability. It is well known that pure silica SBA-15 is inert in catalytic reactions due to the absence of heteroatom active sites. Therefore many scientists have attempted to incorporate various atoms into the framework or disperse them onto the surface of siliceous materials as metal or metal oxides which can introduce catalytic sites into mesoporous materials. The ordered mesoporous structure and large pore size of SBA-15 are likely more favourable to the diffusion of reactants and products.

The present work describes the synthesis of pure and transition metal modified SBA-15 catalysts. Transition metal incorporation leads to an increase in catalytic activity. Various characterization techniques have been used to evaluate the structural and textural properties of the prepared catalysts. Finally the catalytic activities of the materials in various industrially important reactions are investigated.

9.2 Summary

The present thesis comprises of 9 chapters including introduction, experimental, characterization and activity studies.

Chapter 1 deals with introduction about mesoporous materials. The general principles and mechanism involved in the preparation of ordered mesoporous silica are also discussed in detail. This chapter also presents a brief literature review on the topic and on reactions studied in the present thesis.

Chapter 2 focuses on the building block chemicals and the method adopted for the preparation of catalyst systems. It also gives a brief description

about the various techniques used for the physico-chemical characterization. This also includes the detailed procedure for the preparation of materials. SBA-15 type materials were prepared by using tetraethylorthosilicate (TEOS) as the silicon precursor. Non ionic triblock copolymer surfactant (P123) was used as the structure directing agent. Concentrated HCl solution was used as the acid source. Transition metal modified materials were prepared by in-situ addition of corresponding precursors. Prepared catalysts are characterized by XRD, UV- Visible DRS, BET surface area, EDX, IR, Elemental analysis, TG, SEM, TEM etc. The experimental procedures used to analyze the catalytic activity along with gas chromatographic analysis conditions are also presented in the same chapter.

Chapter 3 describes the results of physico-chemical characterization of the prepared systems. XRD results showed that prepared catalysts have typical highly ordered hexagonal structure, indicating that the addition of transition metals into SBA-15 does not destroy the characteristic structure of SBA-15. In the wide angle XRD pattern appreciable characteristic peaks of the crystalline metal oxides were observed for the samples having Si/M=10 but the intensity of the peaks were very low. For samples with lower amount of incorporation no characteristic peaks are observed. N_2 adsorption desorption experiments indicated that the surface area of SBA-15 decreased upon addition of transition metals. If we compare the pore volume of the catalysts it is seen that the decrease in surface area was followed by a decrease in pore volume. Nitrogen adsorption-desorption isotherms of all the samples show representative type IV curves which are characteristic of

mesoporous materials with uniform pore structure. In UV-DRS spectra the absorption peaks were found for all the samples between 200nm-500nm. This indicates the incorporation of metals into SBA-15. In the frame work region (400-1300cm^{-1}) of the IR spectra of the prepared samples the vibration band at 1082cm^{-1} is assigned to as (Si-O-Si). A band at 965cm^{-1} is also observed in the pure SBA-15. This band can be assigned to the Si-O stretching vibrations of Si-O-R^+ groups as R^+=H^+ groups present in the calcined state. In all spectra a band at 800cm^{-1} is assigned to the symmetric (Si-O-Si) stretching vibration. In the hydroxyl region (3000-4000cm^{-1}) ,the absorption band at 3420$cm^{-1}$for all the samples is attributed to the stretching vibrations of the silanol groups interacting through hydrogen bonding. SEM and TEM micrographs were performed to determine the particle morphology of calcined samples. SEM image of the samples show aggregates of regular ordered rod shaped particles. TEM images reveal that the SBA-15 silica materials have well ordered hexagonal arrays of mesopores with one dimensional channel which indicates a p6mm meso structure. Thermal stability of the samples was revealed by Thermogravimetric analysis and the elemental composition of the prepared catalysts was obtained from ICP-AES results. Acidic properties of the prepared systems were examined by TGA of adsorbed 2,6-Dimethyl Pyridine and also by catalytic test reactions like cumene cracking and cyclohexanol decomposition reaction.

Chapter 4 deals with the activity of prepared catalysts tested towards liquid phase cyclohexene oxidation reaction. The reaction was carried out under the optimized condition after checking the influence of various reaction parameters such as temperature, catalyst weight,

solvents, oxidants, and volumes of substrate, solvent, oxidant in order to get maximum activity.

Chapter 5 focuses on the application of catalytic systems for the liquid phase oxidation of benzyl alcohol. The influence of various reaction conditions on the catalytic activity and product distribution is subjected to investigation.

Chapter 6 discusses the application of the catalytic systems towards acetalization reaction of cyclohexanone with methanol. Reaction was conducted in a selected condition after verifying the influence of reaction parameters in detail. Metal leaching studies are also performed to have an idea about the nature of the reaction. Attempt has been made to correlate the catalytic activity with the acidic properties of the catalytic systems.

Chapter 7 illustrates the catalytic activity of the prepared systems towards the isopropylation of benzene. The influence of reaction variables such as temperature, arene/alkylating agent mole ratio and WHSV (weight hourly space velocity) is studied in detail. The attempt of correlation reveals the role of acidic sites on isopropanol conversion.

Chapter 8 focuses the activity measurements for Friedel-Crafts benzylation of Isobutyl benzene. Benzylation is achieved using benzyl chloride in liquid phase. The influence of various reaction parameters on the catalytic activity is subjected to investigation. The reusability of some representative samples is also checked. Attempt has been made to the catalytic activity with the acidic properties of the catalysts.

Chapter 9 presents the summary and major conclusions of the present work.

9.3 Conclusions

- A direct and simple hydrothermal route for the synthesis of heteroatom incorporated mesoporous materials has been demonstrated.
- The acid synthesis route is an important development because the synthesis is very simple and the morphology is easy to control compared to the basic synthesis route.
- A good compromise is attained by resorting to triblock copolymers, which leads well defined and organized large pores, thick walls and hence an excellent thermal stability
- The proposed synthesis affords the SBA-15 samples with large pore volume, high surface area, good structural ordering and narrow pore size distribution.
- Ordered mesoporous materials with high selectivity and catalytic activity would be potentially important for industrial applications
- The interaction between the inorganic precursor and the template is the key factor for controlling the mesostructure of the materials.
- The XRD results indicated the shift in d-spacing after metal incorporation.
- The Nitrogen adsorption desorption isotherms were Type IV with sharp H1 hysteresis which confirmed the ordered mesoporous structure of synthesized materials.
- The narrow pore size distribution also confirmed the ordered structure of the mesoporous materials.
- The SEM and TEM reflect that a very good control of experimental conditions is required to control the morphology.

- The acidity measurements suggest an enhancement in surface acidity especially Lewis acidity upon incorporation of transition metal oxides.
- All the prepared catalysts are successfully studied for oxidation reactions and show higher selectivity toward desired products.
- The prepared catalysts effectively catalyze the acetalization of cyclohexanone with methanol.
- The efficiency of the prepared catalysts in isopropylation of benzene was proved from the correlation of activity with Bronsted sites.
- The prepared catalysts were successfully used for the benzylation reactions and leading to the formation of monoalkylated products.
- The importance of texture/structure properties of heterogeneous catalysts were evidenced from both liquid phase and vapour phase reactions carried out in the present study.

9.4 Future outlook

Since the discovery of transition metal incorporated mesoporous SBA-15 materials have been attracting much attention, because these materials are capable of serving as highly efficient catalysts for the transformation of various organic substrates (i.e., alkanes, alkenes, alcohols, aromatics) under mild conditions. However, the nature of the active intermediate metal oxide species formed during the reaction process is not yet fully understood. In addition, the factors that determine the activity and selectivity of various metallo silicates in specific reactions are not yet clear, although considerable progress toward this has been made. A full understanding of these factors will be favourable for the development of new potential catalysts and design of optimum oxidation conditions.

…..ꕥ…..